Pure

Bangor University

DOCTOR OF PHILOSOPHY

# Development of a novel integrated system for bioremediating and recovering transition metals from acid mine drainage

Araujo Santos, Ana

*Award date:*
2018

*Awarding institution:*
Bangor University

Link to publication

**General rights**
Copyright and moral rights for the publications made accessible in the public portal are retained by the authors and/or other copyright owners and it is a condition of accessing publications that users recognise and abide by the legal requirements associated with these rights.

- Users may download and print one copy of any publication from the public portal for the purpose of private study or research.
- You may not further distribute the material or use it for any profit-making activity or commercial gain
- You may freely distribute the URL identifying the publication in the public portal ?

**Take down policy**
If you believe that this document breaches copyright please contact us providing details, and we will remove access to the work immediately and investigate your claim.

Download date: 20. Apr. 2024

# Development of a novel integrated system for bioremediating and recovering transition metals from acid mine drainage

*A thesis submitted to Bangor University in candidature for the degree of Philosophiae Doctor*

by

Ana Laura Araujo Santos

B.Sc., M.Sc.

School of Natural Sciences

Bangor University

Bangor, Gwynedd, LL57 2UW

United Kingdom

2018

## Abstract

Mine-impacted water bodies are considered to be one of the most serious threats to the environment. These can be highly acidic and often contain elevated concentrations of sulfate and soluble metals. The microbial generation of $H_2S$ by reduction of more oxidized sulfur species, and consequent precipitation of metal sulfides, known as biosulfidogenesis, is a promising technology for remediating acid mine drainage (AMD).

The objective of this work was to develop an integrated system for remediating a target AMD at an operating mine in northern Brazil using a single low pH anaerobic sulfidogenic bioreactor (aSRBR) and an aerobic manganese-oxidizing bioreactor. A synthetic version of the mine water, which contained 7.5 mM copper and lower concentrations (< 0.25 mM) of other transition metals (Zn, Ni, Co and Mn) was used in the experimental work. In the first stage, $H_2S$ generated in the aSRBR was delivered to an off-line vessel containing synthetic AMD, which removed > 99% copper (as CuS) while no co-precipitation of other metals was apparent. The partly-processed AMD was then dosed with glycerol and fed into the aSRBR where zinc, nickel and cobalt were precipitated. The effect of varying the pH and temperature of the bioreactor was examined, and > 99% of Ni, Zn and Co were precipitated in the aSRBR when it was maintained at pH 5.0 and 35ºC. The bacterial communities, which were included 4 species of acidophilic sulfate-reducing bacteria, varied in composition depending on how the bioreactor was operated, but were both robust and adaptable, and changes in temperature or pH had only short-term impact on its performance.

Manganese was subsequently removed from the partly-remediated synthetic AMD using upflow bioreactors packed with Mn(IV)-coated pebbles from a freshwater stream which contained Mn(II)-oxidizers, such as the bacterium *Leptothrix discosphora* and a fungal isolate belonging to the order *Pleosporales*. This caused soluble Mn (II) to be oxidised to Mn (IV) and the precipitation of solid-phase Mn (IV) oxides. Under optimised conditions, over 99% manganese in the processed AMD was removed.

Metal sulfides (ZnS, CoS and NiS) that had accumulated in the aSRBR over 2 years of operation were solubilised by oxidative (bio)leaching at low pH. With this, ~ 99% Zn, ~ 98% Ni and ~ 92% Co were re-solubilised, generating a concentrated lixiviant from which metals could be selectively recovered in further downstream processes.

The use of methanol and ethanol either alone or in combination with glycerol were evaluated as alternative electron donors for biosulfidogenesis. Methanol was not consumed in the bioreactor, though sulfate reduction was not inhibited in the presence of up to 12 mM methanol. In contrast, ethanol was readily metabolised by the bacterial community and sulfate reduction rates were relatively high compared to glycerol. Two acidophilic algae were

characterised and their potential to act as providers of electron donors for biosulfidogenesis was also evaluated. Although algal biomass was able to fuel sulfate reduction in pure cultures of aSRB and in the aSRBR, rates were much lower than when either glycerol or ethanol were used.

## Acknowledgments

What an adventure these last four years has been! I have met so many incredible people whilst also missing some valued ones back home. Most importantly, each and every one, at some point has helped me bring this work to completion. It would be incredibly difficult to name every single one of them and in fact, would be easy to generate a PhD thesis just in names alone of those people that have been following and supporting my professional achievements.

First, I would like to thank God for my life, and for my family. Without His protection and love I would not have gone this far. My family (mum, dad and 'sistas'), for their constant support during such a long journey, even when, deep down, they just wanted me to be there, close to them. If I am where I am now it is because of their encouragement and for believing that I could make it. My friends from Brazil, who encouraged me to come to a foreign country and make my dream of living abroad (and learning English) come true, even when they thought I was being too ambitious to get a PhD degree in another language (I made it. yay!).

I am very grateful to my former supervisor Denise Bevilaqua for having given me the opportunity and for having chosen me to live this incredible experience. Thank you for all the support, friendship and precious pieces of advice. Special thanks to the Brazilian National Council for Scientific and Technological Development (CNPq) and the Science without Borders program for sponsoring my studies here at Bangor University.

I would like to express my sincere gratitude to Barrie Johnson for sharing his experience and knowledge (in science and gardening!), for all help, advice and patience. I feel honoured and privileged to be one of his last PhD students and for having had the time to learn so much from him. Also, thank you for having inspired me to enter the world of gardening and for being a great landlord. Yes! Supervisor, landlord and garden whisperer! I cannot forget to mention my dear Jan! Thank you for all your support, and for having taken me as your Brazilian daughter.

I cannot thank Barry Grail enough! For four years this man had to put up with me asking thousands of questions (mostly silly questions) about science, English language and basically how to become British. He has seen me changing over the years and I have learnt so much from him. I will never forget our countless jokes at work, lessons on how to fix a washing machine or explaining how the heating system works. Thank you, Barry, for being such an incredible person, for your friendship and support, and for constantly repeating: "Everything is going to be fine". And guess what? Everything **is** fine!

The girls. What a lovely research group! Years of friendship, teamwork, and lovely time out of work as well (usually talking about work). Carmen, Eva, Roseanne, Sarah, Rose Jones and Laura, thank you for your attention, help, patience and for teaching me so much. Most of

you already left the team before the completion of this project, but your long-distance support and friendship have been so important and helpful. Miss you all.

The guys. Bangor has its flaws (we all know that), but if there is a place in the world where you could meet the most extraordinary group of people, that place is Bangor. It is hard to put down in words how grateful I am to have met so many amazing people. The Brazilians who lived here in my first year, Bangor University staff members, that became very close friends (particularly Wendy and Shila), will always have a special place in my heart. The Bangor Crew! Love, happiness and friendship are the best words to summarise this group. We are all completely different from each other, from more than 10 different countries around the globe, different cultures, aims, lifestyles and yet one, when we are together! You all made this experience unforgettable and I have grown so much, learned so much with our differences. I am definitely a better person now, four years on.

Lastly, I would like to express my love, admiration and respect for Wales itself. I had heard very little about this country when I was living in Brazil however, family and friends now struggle to hear about anything else. Such a small country and yet so big, the passion of the Welsh people for their culture and their past is fantastic, it is so strong that it has become impossible not to be encapsulated. Wales and its remarkable landscapes, the mountains, the sea, the lakes and castles and you can have all of these in the same picture. I do not know what the future has prepared for me, but I am sure that everything I have lived in this place will always be part of me.

*In memory of my grandmothers*
*Maria Antonia dos Santos and Eurides Benjamim de Araujo*

## Content

**Chapter 1**

**Introduction** ..... **1**

**1.1 The sulfur cycle** ..... **1**

**1.2 Dissimilatory reduction of oxidized sulfur compounds** ..... **3**

*1.2.1 Sulfate reduction pathways* ..... *3*

*1.2.2 Sulfate-reducing prokaryotes* ..... *5*

1.2.2.1 Physiology ..... 5

1.2.2.2 Distribution and ecology ..... 6

1.2.2.3 Diversity of sulfate-reducing prokaryotes ..... 7

**1.3 Mining activity and its waste products** ..... **8**

*1.3.1 Generation of acid mine drainage* ..... *9*

*1.3.2 The microbiology of acidic mine wastes* ..... *10*

1.3.2.1 Indigenous acidophilic prokaryotes ..... 10

1.3.2.2 Biosulfidogenesis in low pH environments and laboratory cultures ..... 17

1.3.2.3 Acidophilic eukaryotes indigenous to mine-impacted environments ..... 19

*1.3.3 Effects of acid mine drainage on animal, plant and microbial life* ..... *23*

**1.4 Prevention of acid mine drainage** ..... **25**

**1.5 Remediation of acid mine drainage** ..... **26**

*1.5.1 Abiotic treatment* ..... *26*

*1.5.2 Biological treatments* ..... *28*

1.5.2.1 Passive systems ..... 28

1.5.2.2 Active systems: sulfidogenic bioreactors ..... 29

*1.5.3 Remediation of manganese-rich wastewaters* ..... *33*

**1.6 Acid mine drainage as a resource** ..... **35**

**1.7 Scope of the current project** ..... **36**

**Chapter 2**

**Materials and methods** ..... **37**

**2.1 Microorganisms** ..... **37**

**2.2 Cultivation techniques** ..... **37**

*2.2.1 Sterilization* ..... *37*

*2.2.2 Microbial growth media* ..... *38*

2.2.2.1 Basal salts and trace elements solution ..... 38

2.2.2.2 Liquid media ..... 39
2.2.2.3 Overlay solid media ..... 39
*2.2.3 Incubation under anaerobic atmosphere ..... 40*
**2.3 Mine water composition ..... 40**
**2.4 Sulfidogenic bioreactor ..... 40**
**2.5 Analytical methods ..... 42**
*2.5.1 Electrochemical analyses ..... 42*
*2.5.2 Colorimetric analyses ..... 42*
2.5.2.1 Determination of soluble copper concentrations ..... 42
2.5.2.2 Determination of soluble ferrous and ferric iron concentrations ..... 43
2.5.2.3 Determination of soluble manganese concentrations ..... 43
**2.6 Ion chromatography ..... 44**
*2.6.1 Determination of anions ..... 44*
*2.6.2 Determination of organic compounds ..... 44*
*2.6.3 Determination of transition metals concentrations ..... 45*
**2.7 Atomic Absorption Spectroscopy (AAS) ..... 45**
**2.8 Dissolved organic carbon ..... 45**
**2.9 Biomolecular techniques ..... 46**
*2.9.1 Preparation of DNA template ..... 46*
2.9.1.1 Lysates ..... 46
2.9.1.2 DNA extraction kit ..... 46
*2.9.2 Polymerase chain reaction (PCR) ..... 46*
*2.9.3 Agarose gel electrophoresis ..... 47*
*2.9.4 Terminal Restriction Enzyme Fragment Length Polymorphism (T-RFLP) analyses ..... 48*
*2.9.5 Clone libraries ..... 49*
2.9.5.1 Ligation reaction ..... 49
2.9.5.2 Transformation into *Escherichia coli* ..... 49
2.9.5.3 Screening and purification of plasmids ..... 49
2.9.5.4 Sequencing analyses ..... 50
*2.9.6 Phylogenetic analyses ..... 50*
**2.10 Microscopy ..... 50**
2.10.1 Stereo-scan microscopy ..... 50
2.10.2 Phase-contrast microscopy ..... 50
2.10.2.1 Cell counts ..... 51
*2.10.3 Scanning Electron Microscopy (SEM) with Energy Dispersive Analysis of X-rays (EDAX) ..... 51*

2.10.3.1 Dehydration and fixation ..... 51
2.10.3.2 Analysing samples with SEM/EDAX ..... 51

**Chapter 3**

**Combined recovery of copper and mitigation of pollution of a metal-rich stream draining a copper mine in Brazil ..... 53**

**3.1 Introduction ..... 53**

*3.1.1 Mine site: Sossego copper mine ..... 54*

**3.2 Materials and methods ..... 57**

*3.2.1 Composition of actual and synthetic mine water ..... 57*

*3.2.2 Phases of the experiment ..... 58*

**3.3 Results ..... 61**

*3.3.1 Priming phase: Phase 1 ..... 61*

*3.3.2 Mine water treatment: Phase 2 and 3 ..... 62*

*3.3.3 Microbial community in the sulfidogenic bioreactor ..... 68*

**3.4 Discussion ..... 69**

**Chapter 4**

**Effects of variations in chemical and operational parameters on the kinetics of an acidophilic sulfidogenic bioreactor and indigenous microbial communities ..... 75**

**4.1 Introduction ..... 75**

**4.2 Materials and methods ..... 76**

*4.2.1 Sulfidogenic bioreactor ..... 76*

4.2.1.1 Performance of the aSRBR when maintained at different pH values and temperatures ..... 77

4.1.1.2 Variations in yeast extract concentration in the feed liquor ..... 77

4.1.1.3 Variations in salt (NaCl) concentration in the feed liquor ..... 77

*4.1.2 Compositions of the community structure of immobilised bacteria in the aSRBR. 78*

**4.3 Results ..... 79**

*4.3.1 Performance of the aSRBR as impacted by variations in pH and temperature .... 79*

*4.3.2 Performance of the aSRBR as impacted by variations in yeast extract concentrations ..... 84*

*4.3.3 Performance of the aSRBR as impacted by variations in salt (NaCl) concentrations ..... 89*

*4.3.4 pH values and bacterial communities within the aSRBR biofilm bed ..... 95*

*4.3.5 Scanning electron microscopy and elemental composition analysis of the aSRBR biofilm bed* ..... *96*
**4.4 Discussion** ..... **99**

**Chapter 5**
**Solubilisation of metal sulfide concentrates generated from an acidophilic sulfidogenic bioreactor used to remediate acidic mine water** ..... **107**
**5.1 Introduction** ..... **107**
**5.2 Preliminary tests for recovering metals from sulfide precipitates** ..... **108**
*5.2.1 Materials and methods* ..... *108*
*5.2.2 Results* ..... *109*
**5.3 Conversion of the aSRB reactor to a bioleaching reactor to extract metals from accumulated sulfides** ..... **111**
*5.3.1 Materials and methods* ..... *111*
*5.3.2 Results* ..... *113*
**5.4 Second phase bioleaching of the porous beads/precipitates mixture** ..... **118**
*5.4.1* Agua regia *digestion of the porous beads/precipitates mixture* ..... *119*
*5.4.2 Effect of temperature and pulp density on bioleaching of the porous beads/precipitates mixture* ..... *119*
5.4.2.1 Materials and methods ..... 119
5.4.2.2 Results ..... 120
**5.5 Tests for the presence of viable microorganisms in the bioleaching reactor and the second phase bioleaching experiment** ..... **125**
*5.5.1 Materials and methods* ..... *125*
*5.5.2 Results* ..... *125*
**5.6 Discussion** ..... **127**

**Chapter 6**
**Biological Mn (II) oxidation and precipitation of Mn (IV) as part of an integrated bioremediation process for mitigating a moderately acidic metal-rich stream** ..... **133**
**6.1 Introduction** ..... **133**
**6.2 Materials and methods** ..... **135**
*6.2.1 Mn (IV) biofilm-colonised pebbles* ..... *135*
*6.2.2 Manganese oxidation and precipitation: batch tests* ..... *136*
*6.2.3 Commissioning and operation of the Mn (II) oxidizing bioreactor (MnOB)* ..... *136*

6.2.3.1 Variations in operational and set up conditions ..... 136
*6.2.4 Microbial populations in the Mn (IV) biofilm-colonised pebbles ..... 138*
*6.2.5 Isolation and cultivation of Mn (II)-oxidizing microorganisms ..... 138*
*6.2.6 Identification and characterisation of a Mn (II)-oxidizing fungal isolate ..... 139*
6.2.6.1 Effects of pH and temperature on the growth of isolate MnI1 ..... 139
6.2.6.2 Mn (II) oxidation tests ..... 139
6.2.6.3 Growth on different organic substrates ..... 139
**6.3 Results ..... 140**
*6.3.1 Assessing the removal of soluble manganese using Mn (IV) biofilm-colonised pebbles ..... 140*
*6.3.2 Commissioning and performance of the Mn (II) oxidation bioreactor (MnOB) ..... 141*
*6.3.3 Indigenous microbial population of the Mn (IV) biofilm-colonised pebbles ..... 147*
*6.3.4 Characterisation of the Mn (II)-oxidizing fungal isolate MnI1 ..... 154*
6.3.4.1 Physiological and morphological characterisation of isolate MnI1 ..... 154
6.3.4.2 Phylogenetic analysis ..... 160
**6.4 Discussion ..... 161**

**Chapter 7**

**The use of alternative substrates to sustain low pH sulfidogenic bioreactors for remediating acidic and moderately acidic mine drainage ..... 167**
**7.1 Introduction ..... 167**
**7.2 Materials and methods ..... 168**
*7.2.1 Sulfidogenic bioreactor ..... 168*
*7.2.2 Operational set up of the aSRBR using combined methanol and glycerol as electron donors ..... 169*
7.2.2.1 Enzymatic assay for methanol determination in (moderately) acidic liquors ..... 170
7.2.2.1.1 Reagents ..... 170
7.2.2.1.2 Assay protocol ..... 171
7.2.2.2 Clone library analysis of the planktonic bacterial population in the bioreactor ..... 172
*7.2.3 Ethanol as an alternative electron donor for sustaining low pH biosulfidogenesis 173*
7.2.3.1 Enzymatic assay for ethanol determination in (moderately) acidic liquors ..... 174
7.2.3.1.1 Reagents ..... 174
7.2.3.1.2 Assay protocol ..... 175
**7.3 Results ..... 175**
*7.3.1 Effects of combinations of methanol and glycerol on the performance of an acidophilic sulfidogenic bioreactor ..... 175*

7.3.1.1 Clone library analysis ..... 180
*7.3.2 Effects of combinations of ethanol and glycerol on the performance of an acidophilic sulfidogenic bioreactor ..... 181*
*7.3.3 Ethanol as an alternative electron donor for sustaining low pH sulfidogenic bioreactors ..... 184*
*7.3.4 Visual examination of the bioreactor population and isolation of* Dv. desulfuricans *..... 188*
**7.4 Discussion ..... 189**

**Chapter 8**
**Characterisation of two acidophilic microalgae and their potential use as feedstock for sulfidogenic bioreactors ..... 193**
**8.1 Introduction ..... 193**
**8.2 Physiological characterisation of acidophilic algal isolates AC1 and ITV ..... 194**
*8.2.1 Materials and methods ..... 194*
8.2.1.1 Isolation and cultivation of the algal cultures ..... 194
8.2.1.2 Effects of pH and temperature on growth rates of the algal isolate ..... 195
8.2.1.3 Determination of tolerance to transition metals, aluminium and sodium chloride . 195
8.2.1.4 Effect of osmotic stress on growth rates of isolates AC1 and ITV and assessment of osmo-protectant production ..... 196
8.2.1.5 Identification and phylogenetic analysis of algal isolates AC1 and ITV ..... 196
*8.2.2 Results ..... 197*
**8.3 Preliminary tests on low pH biosulfidogenesis sustained by algal biomass . 202**
*8.3.1 Materials and methods ..... 202*
*8.3.2 Results ..... 203*
**8.4 Potential use of algal biomass to fuel sulfidogenesis in bioreactor systems at low pH ..... 208**
*8.4.1 Materials and methods ..... 208*
8.4.1.1 Preparation of algal biomass slurry ..... 208
8.4.1.2 Commissioning and operation of the sulfidogenic bioreactor ..... 209
*8.4.2 Results ..... 210*
**8.5 Discussion ..... 214**

**Chapter 9**
**General discussion ..... 219**

**References ..... 227**

**Appendix 1 ..... 254**

**Appendix 2 ..... 257**

## List of Figures

### Chapter 1

**Fig. 1.1.** Pourbaix diagram for aqueous sulfur cycle. The distribution of $E_H$-pH in natural systems is shaded.

**Fig. 1.2.** The biological sulfur cycle.

**Fig. 1.3.** Schematic representation of the (a) *Rees* pathway and (b) trithionate pathway.

**Fig. 1.4.** Schematic representation of the revised model for sulfate reduction network proposed by Bradley et al. (2011).

**Fig. 1.5.** Pit lakes and streams of acidic waters draining some abandoned mines and mine spoils. (a) AMD draining Cae Coch mine, an underground pyrite mine in north-west Wales, UK, (b) acidic lagoons draining São Domingos copper mine in South-east Portugal, (c) pit lake at San Telmo copper mine, Huelva, Spain, and (d) AMD draining Cantareras copper mine, South-west Spain.

**Fig. 1.6.** Acid streamer growths (dominated by '*Ferrovum'*-like bacteria) in an abandoned copper mine in Spain (left) and microbial stalactites in an abandoned pyrite mine (Cae Coch, Wales) (right).

**Fig. 1.7.** Surface algal growth on a microbial mat in a stream draining abandoned copper mines in the Iberian pyrite belt (a) San Telmo, Spain, (b) São Domingos, Portugal and (c) Cantareras, Spain.

**Fig. 1.8.** Stratification of an acidic stream draining the abandoned Cantareras mine in Spain (top) and model of the biogeochemical cycling of iron and sulfur at the abandoned Cantareras mine proposed by Rowe et al. (2007) (bottom).

**Fig. 1.9.** Abiotic and biological strategies for remediating metal-contaminated mine waters.

**Fig. 1.10.** Schematic representation of the BioSulfide® process.

**Fig. 1.11.** Schematic representation of the SULFATEQ™/THIOTEQ™ processes.

**Fig. 1.12.** Schematic representation of the integrated system designed to remediate AMD at the Maurliden mine, Sweden.

**Chapter 2**

**Fig. 2.1.** Schematic representation of the low pH sulfidogenic bioreactor (aSRBR). The arrows indicate the direction of liquid/gas flow.

**Chapter 3**

**Fig. 3.1.** Aerial (a) and satellite (b) view of Sossego copper mine, Sossego copper complex: Sossego and Sequeirinho open-pits (c) and Sossego open-pit (d).

**Fig. 3.2.** Images of the moderately acidic stream draining the active copper mine in the State of Pará, Brazil, which has been remediated using limestone treatment.

**Fig. 3.3.** Tailings pond at the Sossego mine that receives the residues generated in the copper concentrate processing.

**Fig. 3.4.** Schematic representation of the low pH sulfidogenic bioreactor (aSRBR). The excess of hydrogen sulfide produced in the aSRBR was delivered to an off-line precipitation vessel, containing synthetic mine water in order to mediate selective removal of copper (Phase 2). After copper precipitation, the partly-processed water was used as feed liquor for the bioreactor (Phase 3).

**Fig. 3.5.** Changes in pH (▲) values and HRT (●) in the priming phase of the aSRBR.

**Fig. 3.6.** Images of different stages of copper mineralisation in the off-line vessel. Stage 1: SMW at pH 5.0 (7.5 mM $Cu^{2+}$), Stage 2: SMW at pH 3.4 (7.0 mM $Cu^{2+}$), Stage 3: SMW at pH 2.5 (4.5 mM $Cu^{2+}$), Stage 4: SMW at pH 2.1 (0.7 mM $Cu^{2+}$) and lastly the dried CuS precipitate.

**Fig. 3.7.** Changes in HRTs (■) and copper precipitation rates (●) of the aSRBR during phases 2 and 3 of the experiment.

**Fig. 3.8.** Box plot representation of sulfate reduction rates in Phases 2 (blue) and Phase 3 (green). The single green circle represents an outlier, which did not fall into the inner fences of the box.

**Fig. 3.9.** Changes in concentrations of glycerol consumed (▲) and acetic acid produced (■) in the bioreactor in Phases 2 (day 1 to day 20) and 3 (day 21 to day 84). The downward-pointing arrows indicate times when an active culture of *Acidocella aromatica*$^{T}$ was added to the sulfidogenic bioreactor.

**Fig. 3.10.** Changes in concentrations of transition metals in the bioreactor effluent liquor throughout the time course of the experiment (Phase 3). Key: nickel (▲), zinc (♦), cobalt (■) and manganese (●).

**Fig. 3.11.** Terminal restriction enzyme fragment length polymorphism (T-RFLP) profiles of bacterial 16S rRNA genes (digested with HaeIII) of planktonic samples taken from the sulfidogenic bioreactor with different feed liquor composition: “standard SRB medium” and partly-processed mine water. Shades of orange represent sulfate-reducing bacteria and shades of green represent non-sulfidogens. The digested fragments were identified as corresponding to: 137 nt, *Peptococcaceae* CEB3; 215 nt, *D. acididurans*; 219 nt, *C. acididurans*; 230 nt, actinobacterium AR3 and 253 nt, *At. ferrooxidans*.

**Chapter 4**

**Fig. 4.1.** Schematic representation of the biofilm bed sampling. Liquid samples were withdrawn using sterile glass pipettes in two different depths (0 and 3 cm) and samples of the biofilm bed were withdrawn at 6, 9 and 12 cm using a sterile core sampler. The total depth of the working volume of the bioreactor (biofilm bed plus surface liquor) was 15 cm.

**Fig. 4.2.** Changes in HRTs (●) and pH values (■) in the aSRBR. The bioreactor was maintained at 30°C for the first 229 days of the experiment, and the upward-pointing arrows indicate when it was subsequently changed.

**Fig. 4.3.** Box plot representation of variations in rates of sulfate reduction with changing operational (pH and temperature) parameters. Key: pH 4.0 (red), pH 4.5 (green), pH 5.0 (blue). The open circles represent outlier data points which did not fall into the inner fences of the box.

**Fig. 4.4.** Changes in concentrations of transition metals, Ni (▲), Mn (■), Zn (♦) and Co (●) in the bioreactor effluent liquor.

**Fig. 4.5.** Changes in concentrations of glycerol consumed (●) and acetic acid produced (■) in the sulfidogenic bioreactor. The downward-pointing arrows indicate times when an active culture of *Acidocella aromatica*$^{T}$ was added to the sulfidogenic bioreactor.

**Fig. 4.6.** Terminal restriction enzyme fragment length polymorphism (T-RFLP) analysis (HaeIII digests of amplified 16S rRNA genes) of planktonic bacterial communities in the aSRB reactor operated at different temperatures and pH values. Shades of blue represent sulfate-reducing bacteria and shades of red represent non-sulfidogens. 138 nt: *Peptococcaceae* CEB3; 215 nt: *D. acididurans*; 230 nt: *Actinobacterium* AR3 and 253 nt: *At. ferrooxidans*.

**Fig. 4.7.** Changes in planktonic cell numbers (▲) and HRTs (●) in the aSRBR with different concentrations of yeast extract (0, 0.1 and 0.05 g $L^{-1}$) added to the feed liquor.

**Fig. 4.8**. Changes in concentrations of transition metals in the bioreactor effluent liquor using different concentration of yeast extract (0, 0.05 and 0.1 g $L^{-1}$ YE) in the feed liquor. Key: nickel (▲), zinc (♦), cobalt (■) and manganese (●).

**Fig. 4.9.** Changes in concentrations of glycerol consumed (■) and acetic acid produced (▲) in the bioreactor using different concentration of yeast extract (0, 0.05 and 0.1 g $L^{-1}$ YE) in the feed liquor.

**Fig. 4.10.** Changes in rates of sulfate reduction in the bioreactor using different concentration of yeast extract (0, 0.05 and 0.1 g $L^{-1}$ YE) added to the feed liquor.

**Fig. 4.11.** Terminal restriction enzyme fragment length polymorphism (T-RFLP) analysis (HaeIII digests of amplified 16S rRNA genes) of planktonic bacterial communities in the aSRB reactor operated with different concentrations of yeast extract in the feed liquor. Shades of blue represent sulfate-reducing bacteria and shades of red represent non-sulfidogens 138 nt: *Peptococcaceae* CEB3; 215 nt: *D. acididurans*; 230 nt: *Actinobacterium* AR3 and 253 nt: *At. ferrooxidans*.

**Fig. 4.12.** Changes in planktonic cell numbers (♦) and HRTs (■) in the aSRBR using different concentrations of NaCl (0, 50 and 100 mM) added to the feed liquor. Gaps within data points (day 27 to day 46) represent no generation of effluent liquor and from day 85 to day 114 represent no sample collection.

**Fig. 4.13.** Changes in concentrations of glycerol consumed (■) and acetic acid produced (▲) in the aSRBR using different concentrations of NaCl (0, 50 and 100 mM) added to the feed liquor. Samples were not collected on intervals from day 27 to day 46 and from day 85 to day 114.

**Fig. 4.14.** Changes in rates of sulfate reduction in the bioreactor using different concentration of NaCl (0, 50 and 100 mM) in the feed liquor. Samples were not collected on intervals from day 27 to day 46 and from day 85 to day 114.

**Fig. 4.15.** Changes in concentrations of transition metals in bioreactor effluent liquors using different concentrations of NaCl (0, 50 and 100 mM) in the feed liquor. Samples were not collected on intervals from day 27 to day 46 and from day 85 to day 114. Key: nickel (▲), zinc (♦), cobalt (■) and manganese (●).

**Fig. 4.16.** Terminal restriction enzyme fragment length polymorphism (T-RFLP) analysis (HaeIII digests of amplified 16S rRNA genes) of planktonic bacterial communities in the aSRB reactor operated using different concentrations of NaCl in the feed liquor. Shades of blue represent sulfate-reducing bacteria and shades of red represent non-sulfidogens 137 nt: *Peptococcaceae* CEB3; 215 nt: *D. acididurans*; 230 nt: *Actinobacterium* AR3 and 254 nt: *At. ferrooxidans*; 148 and 226 nt: unknown.

**Fig. 4.17.** Depth-related variations in pH (left) and T-RFLP profiles of the bacterial community (HaeIII digests of amplified 16S rRNA genes) of planktonic cells (liquid phase) and colonised beads (top, mid, bottom layers) (right) within the aSRB reactor, at pH 5.0 and 35ºC. 138 nt: *Peptococcaceae* CEB3; 215 nt: *D. acididurans*; 230 nt: *Actinobacterium* AR3 and 253 nt: *At. ferrooxidans.*

**Fig. 4.18.** Scanning electron micrographs of colonised Poraver beads combined from different depths within the biofilm bed in the aSRBR.

**Fig. 4.19.** Micro-analysis of biofilm-colonised glass beads by electron dispersive analysis of X-ray. (A) SEM image displaying selected area (red square) and (B) EDX spectra of the selected area plus elemental semi-quantitative analysis.

**Chapter 5**

**Fig. 5.1.** Changes in pH values during the preliminary metal dissolution experiment carried out with porous beads and liquid samples taken from the aSRBR reactor: (▲) the inoculated and (●) the non-inoculated flask. The arrow indicates where pH values were adjusted by adding 100 µL of sterile $H_2SO_4$.

**Fig. 5.2.** Metals leached during the preliminary metal dissolution experiment carried out with porous beads and liquid samples taken from the aSRBR reactor: (A), Ni (♦) and Zn (■); (B), Co (●) and Mn (▲). Data from the inoculated flask are represented by filled symbols and those from the non-inoculated flask by open symbols.

**Fig. 5.3.** Schematic representation of the bioleaching reactor (left) and image of the actual system (right).

**Fig. 5.4.** Volume of accumulated sulfuric acid consumed in the bioleaching reactor to drop to and maintain at pH 1.8 (red bars) and pH 1.5 (blue bars).

**Fig. 5.5.** Changes in iron concentrations and redox potential in the bioleaching reactor. Key: $Fe^{2+}$ (■), $Fe^{3+}$ (▲), total Fe (●) and $E_H$ (**X**). The red arrows indicate the points at which additional microorganisms were added to the bioreactor.

**Fig. 5.6.** Changes in sulfate concentrations in the bioleaching reactor at pH 1.5 and pH 1.8. Arrows indicate the points at which additional microorganisms were added to the bioreactor.

**Fig. 5.7.** Changes in concentration of metals in the leaching liquor of the bioreactor at pH 1.8 and pH 1.5: (A) Co (▲), Mn (●), Cu (♦); (B) Ni (■) and Zn (●).

**Fig. 5.8.** Changes in pH in the bioleaching experiment at (A) 30ºC and (B) 45ºC. Key: 5% (▲), 10% (●) and 20% (■).The experiment was carried out in duplicate and differences in ranges between replicates are occluded by the symbols.

**Fig. 5.9.** Changes in redox potential in the bioleaching experiment at (A) 30ºC and (B) 45ºC. Key: 5% (▲), 10% (●) and 20% (■). The experiment was carried out in duplicate and differences in ranges between replicates are occluded by the symbols.

**Fig. 5.10.** Changes in sulfate concentrations in the bioleaching experiment at (A) 30ºC and (B) 45ºC. Key: 5% (▲), 10% (●) and 20% (■). The experiment was carried out in duplicate and differences in ranges between replicates are occluded by the symbols.

**Fig. 5.11.** Changes in metals concentration in the leaching liquor at 30ºC (▲, ●, ■) and 45ºC (▲, ●, ■). Key: 5% (▲,▲), 10% (●,●) and 20% (■, ■).

**Fig. 5.12.** Metal recovery from shake flasks experiment at different temperatures and pulp density. Nickel (blue), zinc (red), cobalt (green). The bars depict mean values and the error bars the range between replicate samples ($n$ = 2).

**Fig. 5.13.** Images from the second-phase bioleaching shake flask experiment set-up at 30ºC. (A) bioreactor filtered leachate; (B) porous beads/precipitates mixture in liquid media at pH 1.5; (C) $FeS_o$ overlay plates inoculated with samples from a shake flask on day 0 (left) and day 5 (right) of the experiment. Similar results were obtained with shake flasks incubated at 45ºC. Plates were incubated for 7 days at their respective temperatures.

**Chapter 6**

**Fig. 6.1.** Pourbaix diagram for manganese (Tekerlekopoulou et al., 2013).

**Fig. 6.2.** Sampling site location at Snowdonia National Park, UK. (A) Location at Waen Wen (Source: Digimap; www.edina.ac.uk/digimap); (B) Location within the UK and (C) Catchment stream. Red stars represent sampling point. Images: Mariner, 2008 (Thesis).

**Fig. 6.3.** Schematic representation of the Mn (II) oxidation bioreactor (MnOB). (A) 1-column system and (B) in-line 2-column system. Effluent liquor from column 1 was pumped upwards through column 2 and collected into an effluent bottle. Sampling devices were added to the top of each column and analysis were carried out on both sampling points.

**Fig. 6.4.** Changes in soluble manganese concentrations in systems containing inert pebbles (●) and Mn (IV)-biofilm-colonised pebbles (▲). The symbols are mean values and the error bars represents standard deviation (*n* = 3).

**Fig 6.5.** Average initial and final pH measured in the inert gravel and Mn (IV)-biofilm-colonised pebbles systems.

**Fig. 6.6.** Fixed bed bioreactor, packed with Mn (IV) biofilm-colonised pebbles. (a) 1-column system (C1: pH 5.0 and HRT 12h), (b) 1-column system (C2: pH 6.5 and HRT 12h and C3: pH 6.5 and HRT 24h), where a thin layer of inert gravel was added to the bioreactor to monitor manganese precipitation, and (c) 2-column system (C4: pH 6.5 and HRT 48h).

**Fig. 6.7.** Variations in the percentage of manganese removed during the time course of the experiment. Key: phase etc C1 (green): 1 column-system pH 5.0, HRT 12h; C2 (yellow): 1 column-system pH 6.5, HRT 12h; C3 (red) 1 column-system pH 6.5, HRT 24h and C4 (blue): 2 column-system pH 6.5, HRT 48h. The arrow indicates where yeast extract (final concentration 0.1 g $L^{-1}$) was added to both columns.

**Fig. 6.8.** Changes in pH in the feed liquor (■) and effluent liquor (●) of the MnOB. Phases C1-C3: 1-column-system; Phase C4: in-line 2-column-system. The pH values of the effluent in phase C4 are those of liquors draining the second in-line column 2.

**Fig. 6.9.** Cell numbers in the feed liquor (blue) and effluent liquor (magenta) of the MnOB. Phases C1-C3: 1-column-system; C4-1 represents column 1 and C4-2 represents column 2 of the in-line 2-column-system. The bars depict mean values and the error bars standard deviations (*n* = 20).

**Fig. 6.10.** Concentrations of manganese in effluent liquors from the two connected MnOB columns used in phase C4 of the experiment. Key: (●) water draining column 1; (♦) water draining column 2.

**Fig. 6.11.** Relative abundance of microbial taxonomy (order) of the clones obtained from the Mn(IV) biofilm-colonised pebbles collected from a stream in Snowdonia, UK, based on the archaea and bacteria 16S and eukaryote 18S rRNA genes.

**Fig. 6.12.** Terminal restriction enzyme fragment length polymorphism (T-RFLP) analysis (HaeIII digests) of amplified 16S rRNA bacterial genes from the biofilm-colonised pebbles collected from the stream (C0) and at different phases (C1, C2 and C4) of operating the MnOB. The T-RFs are stacked upwards in each column in increasing fragment lengths.

**Fig. 6.13.** Terminal restriction enzyme fragment length polymorphism (T-RFLP) analysis (HaeIII digests) of amplified 18S rRNA eukaryotic genes from the biofilm-colonised pebbles collected from the stream (C0) and at different phases (C1, C2 and C4) of operating the MnOB. The T-RFs are stacked upwards in each column in increasing fragment lengths.

**Fig. 6.14.** Evolution of pigmentation of gravel samples at different times.

**Fig. 6.15.** Terminal restriction enzyme fragment length polymorphism (T-RFLP) analysis (HaeIII digests) of amplified 16S rRNA bacterial genes from the gravel samples collected in week 2 and week 5. The T-RFs are stacked upwards in each column in increasing fragment lengths.

**Fig. 6.16.** Terminal restriction enzyme fragment length polymorphism (T-RFLP) analysis (HaeIII digests) of amplified 18S rRNA eukaryotic genes from the gravel samples collected on week 2 and week 5. The T-RFs are stacked upwards in each column in increasing fragment lengths.

**Fig. 6.17.** Images of isolate MnI1 grown on solid media. (A and B) rhizoidal colonies on Mn-containing plates with dark brown-coloured hyphae; (C and D) colonies grown on Mn-free solid medium with dark-coloured centres and non-pigmented hyphae; (E) colonies growing on solid media at nominal pH 6.5 containing 0.5 mM Mn (II) (left) and no added Mn (II) (right).

**Fig. 6.18.** Micrographs of the isolated MnI1. (A-B) potential Mn oxides deposited onto the hyphae and (C-D) growth on Mn-free plates. Bars 10 µm.

**Fig. 6.19.** Changes in soluble manganese concentrations (▲,▲) and pH (●, ●) in shake flasks cultures inoculated with isolate MnI1 (▲, ●) and non-inoculated controls (▲, ●) with isolate MnI1. The experiment was carried out in duplicate and different values between replicates are occluded by the symbols.

**Fig. 6.20.** Phylogenetic tree showing the relationship of the fungal isolate MnI1 to other micro-organisms based on 18S rRNA sequence homology (values in brackets are NCBI accession numbers). Scale bar is number of nucleotides substituted per base pair. Bootstrap values are given at the respective nodes. The tree was rooted with the 18S rRNA gene sequence of *Saccharomyces cerevisiae* (J01353.1).

**Chapter 7**

**Fig. 7.1.** Reaction progress curves for enzymatic oxidation of methanol, monitored by the production of NADH (A) and calibration curve for methanol determination (B).

**Fig. 7.2.** Changes in HRTs (●) with varying relative percentages of methanol (■) used in the feed liquor of the aSRBR.

**Fig. 7.3.** Variations in rates of sulfate reduction (orange bars) and hydrogen sulfide generation (blue bars) for each combination of methanol and glycerol studied.

**Fig. 7.4.** Concentrations of methanol in the influent (▲) and effluent (●) liquors of the aSRBR.

**Fig. 7.5.** Changes in concentrations of glycerol consumed (■) and acetate produced (●) in the sulfidogenic bioreactor, during tests carried out with mixtures of glycerol and methanol in the feed liquor. Concentrations of glycerol in the influent liquor in each phase are indicated by the red lines.

**Fig. 7.6.** Terminal restriction enzyme fragment length polymorphism (T-RFLP) analysis (HaeIII digests) of amplified 16S rRNA genes of planktonic bacterial communities in the aSRB reactor fed with different combinations of methanol and glycerol. Shades of blue represent known sulfate-reducing *Firmicutes* (138 nt, *Peptococcaceae* CEB3; 215 nt, *D. acididurans*), shades of yellow/orange represent non-sulfidogens (230 nt, *Actinobacterium* AR3; 253 nt, *At. ferrooxidans*), shades of green represent bacterial clones identified as probable non-sulfidogens, while the magenta bars represent clone SRB7, which was positively identified as a strain of the sulfate-reducer *Desulfovibrio desulfuricans*.

**Fig. 7.7.** Changes in HRTs (♦) with different relative percentages of ethanol (■) present in the feed liquor of the sulfidogenic bioreactor. Samples were not analysed in the interval between day 66 and day 90.

**Fig. 7.8.** Variations in rates of sulfate reduction (orange bars) and hydrogen sulfide generation (blue bars) in each combination of ethanol and glycerol studied.

**Fig. 7.9.** Concentrations of ethanol in the influent (▲) and effluent (●) liquors of the sulfidogenic bioreactor. Samples were not analysed in the interval between day 66 and day 90.

**Fig. 7.10.** Changes in concentrations of ethanol (●) and glycerol (■) consumed and acetate produced (▲) in the sulfidogenic bioreactor. Concentrations of ethanol and glycerol in the influent liquor in each phase are indicated by the green and red lines, respectively. Samples were not analysed in the interval between day 66 and day 90.

**Fig. 7.11.** Terminal restriction enzyme fragment length polymorphism (T-RFLP) analysis (HaeIII digests) of amplified 16S rRNA genes of planktonic bacterial communities in the aSRB reactor fed with different combinations of ethanol and glycerol. Shades of blue represent known sulfate-reducing *Firmicutes* (215 nt, *D. acididurans*), shades of yellow/orange represent non-sulfidogens (230 nt, *Actinobacterium* AR3; 253 nt, *At. ferrooxidans*), shades of green represent bacterial clones identified as probable non-sulfidogens and the magenta bars represent clone SRB7 (201 nt; *Dv. desulfuricans*).

**Fig. 7.12.** Variations in HRTs (♦) at different operational pH values (■) of the sulfidogenic bioreactor.

**Fig. 7.13.** Variations in rates of sulfate reduction (orange bars) and hydrogen sulfide generation (blue bars) in the aSRBR when fed with ethanol alone and varying operational pH.

**Fig. 7.14.** Changes in pH (■) and concentrations of ethanol in the influent (▲) and effluent (●) liquors of the sulfidogenic bioreactor.

**Fig. 7.15.** Changes in concentrations of ethanol consumed (●) and acetate produced (♦) in the sulfidogenic bioreactor. The concentration of ethanol in the feed liquors remained at 8 mM throughout the experiment.

**Fig. 7.16.** Terminal restriction enzyme fragment length polymorphism (T-RFLP) analysis (HaeIII digests) of amplified 16S rRNA genes of planktonic bacterial communities in the aSRB reactor fed with 100% ethanol, at different pH values. Shades of blue represent known sulfate-reducing *Firmicutes* (215 nt, *D. acididurans*), shades of yellow/orange represent non-sulfidogens (230 nt, *Actinobacterium* AR3; 253 nt, *At. ferrooxidans*), shades of green represent bacterial clones identified as probable non-sulfidogens and the magenta bars represent clone SRB7 (201 nt; *Dv. desulfuricans*).

**Chapter 8**

**Fig. 8.1.** Schematic representation of the acidophilic algae bioreactor (left) and image of the actual system (right). Arrows indicate the direction of liquid/gas flow.

**Fig. 8.2.** Phase contrast microscopy of isolates AC1 (left) and ITV (right). The scale bar represents 10 µm in both images.

**Fig. 8.3.** Effect of temperature (left) and pH (right) on culture doubling times of algal isolates AC1 (●) and ITV (▲) in a bioreactor. The line shown is the best fit based on polynomial analysis of the data.

**Fig. 8.4.** Effect of presence of magnesium sulfate on culture doubling times of algal isolates AC1 (●) and ITV (▲) grown in temperature- and pH-controlled bioreactors. The line shown is the best fit based on polynomial analysis of the data.

**Fig. 8.5.** Changes in concentrations of dissolved organic carbon in harvested biomass suspended in ultra-pure water of algae grown in medium with (● AC1; ■ ITV) and without (● AC1; ■ ITV) additional 600 mM $MgSO_4$ for isolate AC1 and 200 mM $MgSO_4$ for isolate ITV. Data points depict mean values and error bars standard deviations of triplicated analyses of each sample.

**Fig. 8.6.** Phylogenetic tree showing the relationship of algal isolates AC1 and ITV to other green algae based on 18S rRNA sequence homology (values in brackets are NCBI accession numbers). The scale bar is the number of nucleotides substituted per base pair. Bootstrap values are given at the respective nodes. The tree was rooted with the 18S rRNA gene sequence of *Ulospora bilgramii* (DQ384071.1).

**Fig. 8.7.** Image of the experiment set up using the sulfate-reducer *Peptococcaceae* CEB3. Positive control bottle (glycerol and YE; left) and algae/aSRB bottles in duplicate (centre and right). The negative control bottle is not shown.

**Fig. 8.8.** Changes in concentrations of zinc in anaerobic serum bottles containing different species of aSRB, (a) *D. acididurans*$^T$; (b) "*Db. acidavidus*" CL4, (c) *Peptococcaceae* CEB3, (d) *Firmicute* C5, and amended with either AC1 biomass (left) or ITV biomass (right). Key: Negative control (green bars); positive control (blue bars); algae/aSRB (red bars). The bars depict mean values and the error bars the range between replicate samples ($n$ = 2).

**Fig. 8.9.** Comparison between DOC concentrations at the start (2 h after setting up) and end of the experiment. Key: *D. acididurans*$^T$ (blue bars), *Peptococcaceae* CEB3 (red bars), "*Db. acidavidus*" CL4 (green bars) and *Firmicute* C5 (yellow bars). Bars indicate mean values and the error bars the range between replicate samples ($n$ = 2).

**Fig. 8.10.** Percentage of small molecular weight organic carbon compounds in cell-free liquors of positive (glycerol and YE) and negative controls (AC1 and ITV biomass alone) 2 hours after the start of the experiment.

**Fig. 8.11.** Schematic representation of the biosulfidogenic reactor showing the algal injection system (left) and image of the actual bioreactor (right).

**Fig. 8.12.** Changes in hydraulic retention times (HRT) of the aSRBR during the three phases of the experiment: bioreactor fed with 5 mM glycerol + 0.1 g $L^{-1}$ yeast extract (●) (phase 1); algal biomass slurry AC1a (■) (phase 2), and algal biomass slurry AC1b (▲) (phase 3).

**Fig. 8.13.** Changes in rates of hydrogen sulfide production of the aSRBR during the three phases of the experiment: bioreactor fed with 5 mM glycerol + 0.1 g $L^{-1}$ yeast extract (●) (phase 1); algal biomass slurry AC1a (■) (phase 2), and algal biomass slurry AC1b (▲) (phase 3). The time interval between day 20 and day 40 represent the period where the aSRBR did not generate effluent liquor. The arrow indicates the time at which 200 mL of AC1b biomass slurry was injected.

**Fig. 8.14.** Changes in concentrations of DOC for AC1a (phase 2; left) and AC1b (phase 3; right) biomass slurries. Arrows indicate the times of each injection. The first injection of AC1a biomass had a volume of 20 mL while all others were 10 mL. Algal slurry AC1b injected to the aSRBR had a volume of 20 mL on days 2 and 7, followed by 200 mL on day 10 and 80 mL on day 21. DOC was measured 2 - 4 h after each injection of biomass.

**Fig. 8.15.** Terminal restriction enzyme fragment length polymorphism (T-RFLP) analysis (HaeIII digests of amplified 16S rRNA genes) of planktonic bacterial communities in the aSRB reactor operated using different feed stocks. Shades of blue represent sulfate-reducing bacteria (138 nt, *Peptococcaceae* CEB3; 215 nt, *D. acididurans*), shades of green represent non-sulfidogens (221 nt, *Clostridium* sp.; 230 nt, *Actinobacterium* AR3; 253 nt, *At. ferrooxidans*).

**Chapter 9**

**Fig. 9.1.** Summary of the integrated system protocol developed in the current research project. The synthetic AMD remediation process involves: (a) biosulfidogenesis, as (i) off-line precipitation of copper and recovery of CuS, (ii) in-line precipitation and accumulation of most other transition metals ($Me^{2+}$) within the bioreactor, and (b) aerobic oxidation of soluble Mn (II) to Mn (IV) and precipitation of solid-phase Mn (IV) oxides. Subsequently, metal sulfides are re-solubilised, facilitating the downstream recovery of these metals.

# List of Tables

## Chapter 1

**Table 1.1.** Inorganic sulfur compounds and its biological formation.

**Table 1.2.** Physiological properties of some acidophilic bacteria.

**Table 1.3.** Physiological properties of archaeal isolates of the family *Sulfolobaceae* and order *Thermoplasmatales*.

## Chapter 2

**Table 2.1.** Composition of the 50x concentrate basal salt solution.

**Table 2.2.** Composition of the trace elements solution. This mixture is 1000x concentrate.

**Table 2.3** Solid media composition and microorganisms used in the overlay plate technique.

**Table 2.4.** Chemical composition of the synthetic AMD used in experimental work.

**Table 2.5.** Reagents used for PCR Master Mix.

**Table 2.6.** Description of primer pairs used in this study. R = reverse, F = forward.

**Table 2.7.** List of PCR programs and settings used in this study.

**Table 2.8.** List of restriction enzymes and their respective recognition sites. Arrows indicate where the enzymes cleave DNA.

## Chapter 3

**Table 3.1.** Physico-chemical composition of mine water draining the Sossego copper mine.

**Table 3.2.** Chemical composition of the actual Sossego mine water and its correspondent synthetic version. Concentrations are expressed in mM.

**Table 3.3.** Phases of the experiment using the sulfidogenic bioreactor to remediate the synthetic mine water from Sossego copper mine.

**Table 3.4.** Average rates of HRT and copper precipitation rates during the period where the pH of the influent liquor was gradually lowered from 2.5 to 2.2. Intervals shown in brackets represent minimum and maximum figures obtained in each pH experiment.

**Table 3.5.** Composition of the synthetic mine water at different stages of treatment (average concentrations, mM).

**Table 3.6.** Economics of the synthetic mine water treatment.

**Chapter 4**

**Table 4.1.** Chemical composition of the partly processed mine water used in experimental work.

**Table 4.2.** Average percentage (and standard deviation) of metal removal (Ni, Zn, Co) using different concentrations of sodium chloride in the feed liquor.

**Table 4.3.** Maximum rates of $H_2S$ production for the laboratory-scale system, equivalent rates for a 10 $m^3$ aSRBR and the correspondent volume of Cu-rich water treated per day for each condition studied.

**Table 4.4.** Consent levels of Brazilian regulatory authorities for industrial waste discharge and synthetic mine water composition, before and after biosulfidogenic treatment.

**Chapter 5**

**Table 5.1.** Initial and final redox potential (mV) in the inoculated and non-inoculated flasks.

**Table 5.2.** Acidophilic prokaryotes used to inoculate the bioleaching reactor at different days throughout the experiment.

**Table 5.3.** Amounts of transition metals calculated to have accumulated within the aSRBR and comparison of corresponding maximum actual concentrations when operated as a leaching bioreactor.

**Table 5.4.** Amounts of residual nickel, cobalt and zinc in the porous beads/precipitates mixture and amount of undigested residues (mean values of duplicate samples).

**Table 5.5.** Acidophilic microorganisms used in the experiments at different temperatures.

**Table 5.6.** Initial amounts of metals (mg $L^{-1}$) at the different pulp densities used, and maximum concentrations of metals leached in the experiment.

**Table 5.7.** Viability tests of acidophiles in the experiments described in this Chapter. (-) no growth observed; (+) growth observed.

**Table 5.8.** Amount of metals precipitated in the bioreactor and percentage of that leached in both bioreactor and second phase (bio)leaching experiments.

**Chapter 6**

**Table 6.1.** Variations in feed liquor pH and HRT in the Mn (II) oxidation bioreactor.

**Table 6.2.** Average flow rates and HRTs (and standard deviation) of the MnOB in each phase of tests carried out with the column bioreactors.

**Table 6.3.** Concentrations of dissolved organic carbon (DOC; mg $L^{-1}$) in influent and effluent liquors from the sulfidogenic bioreactor (aSRBR) and the effluent liquors from the MnOB, as mean values and standard deviations (*n* = 5)

**Table 6.4.** Identity of cloned archaeal genes (16S rRNA gene) obtained from the biofilm-colonised pebbles collected from the stream in Snowdonia (*n* = 32).

**Table 6.5.** Identity of cloned bacterial genes (16S rRNA gene) obtained from the biofilm-colonised pebbles collected from the stream in Snowdonia (*n* = 40).

**Table 6.6.** Identity of cloned eukaryotic genes (18S rRNA gene) obtained from the biofilm-colonised pebbles collected from the stream in Snowdonia (*n* = 80).

**Table 6.7.** Temperature limits for MnI1 growth. Key: (-) no growth observed; (+) some growth observed; (++) extensive growth observed.

**Table 6.8.** pH limits for MnI1 growth. Key: (-) no growth observed; (+) growth observed; (++) extensive growth observed.

**Table 6.9.** Utilization of organic substrates by MnI1. Key: (-) no growth observed; (+) growth observed.

**Chapter 7**

**Table 7.1.** Combinations of methanol and glycerol in the influent liquor and their combined electron donor potentials. Influent liquor containing 100% methanol was not tested.

**Table 7.2.** Interference test of alcohols and growth medium compounds on determination of methanol in acidic samples.

**Table 7.3.** Combinations of ethanol and glycerol in the influent liquor and their respective combined electron donor potential.

**Table 7.4.** Duration of each phase of the ethanol experiment and its respective ethanol content and bioreactor pH values.

**Table 7.5.** Identity of cloned bacterial genes (16S rRNA gene) obtained from the sulfidogenic bioreactor (*n* =19).

**Chapter 8**

**Table 8.1.** Minimum inhibitory concentrations (MICs) of some metals and sodium chloride on the growth of the isolates AC1 and ITV. Numbers in parentheses are the highest concentrations at which growth of the isolates was observed. Concentrations are expressed in mM.

**Table 8.2.** Conditions tested in the experiment. The presence or absence of each component is indicated by plus or minus, respectively.

**Table 8.3.** Values of pH measured at the end of the four weeks of the experiment. The pH of all suspensions at the start of the experiment was 4.0.

**Table 8.4.** Comparison of total DOC concentrations and those of the combined small molecular weight organic compounds identified in the mesocosms. Samples were analysed 2 hours after the experiment had been set up.

**Table 8.5.** Mean concentrations (in mM) of small molecular weight organic compounds identified at the end of the experiment in duplicate AC1 biomass mesocosms. Values of the negative controls are from single mesocosms in each case.

**Table 8.6.** Mean concentrations (in mM) of small molecular weight organic compounds identified at the end of the experiment in duplicate ITV biomass mesocosms. Values of the negative controls are from single mesocosms in each case.

**Table 8.7.** Differences between slurries AC1a and AC1b.

## Abbreviations

| | |
|---|---|
| 16/18 S rRNA | Small subunit of ribosomal ribonucleic acid |
| AAS | Atomic absorption spectrophotometry |
| ABS | Autotrophic basal salts |
| ADH | Alcohol dehydrogenase |
| ADP | Adenosine diphosphate |
| ALD | Anoxic limestone drains |
| AMD | Acid mine drainage |
| AMP | Adenosine monophosphate |
| AO | Alcohol oxidase |
| APS | Adenosine-5'-phosphosulfate |
| ARD | Acid rock drainage |
| aSRB | Acidophilic sulfate-reducing bacteria |
| aSRBR | Acidophilic sulfate-reducing bacteria reactor |
| ATP | Adenosine triphosphate |
| BLASTN | Basic local alignment search tool for nucleotide similarity |
| bp | Base pair |
| BSA | Bovine serum albumen |
| ºC | Degrees Celsius |
| DGGE | Denaturing gradient gel electrophoresis |
| DMSO | Dimethylsulfoxide |
| DNA | Deoxyribonucleic acid |
| dNTP | Deoxyribonucleotide triphosphate |
| DOC | Dissolved organic carbon |
| Dsr | Dissimilatory sulfite reductase |
| EDTA | Ethylenediaminetetraacetic acid |
| EDAX | Energy dispersive analysis of X-rays |
| e.g. | *exempli gratia* (in example) |
| $E_H$ | Redox potential |
| EPS | Extracellular polymeric substances |
| Eq.(s) | Equation(s) |
| ER | Enzyme reagent |
| FAD | Flavin adenine dinucleotide |
| $FeS_o$ | Iron and sulfur overlay (solid medium) |
| Fig. | Figure |

| | |
|---|---|
| FDH | Formaldehyde dehydrogenase |
| *g* | Gravitational acceleration |
| h | Hour |
| HEPES | 4-(2-hydroxyethyl)-1-piperazineethanesulfonic acid |
| HPLC | High-performance liquid chromatography |
| IC | Ion Chromatography |
| i.e. | *id est* (that is) |
| $iFe_o$ | Inorganic iron overlay (solid medium) |
| kb | Kilobase |
| kg | Kilogram |
| $K_{sp}$ | Solubility product equilibrium constant |
| L | Litre |
| LED | Light emitting diodes |
| M | Molar |
| MAR-FISH | Microautoradiography - Fluorescence in situ hybridization |
| MnOB | Manganese (II)-oxidizing bioreactor |
| mV | Millivolt |
| MIC | Minimum inhibitory concentration |
| NAD | Nicotinamide adenine dinucleotide |
| NADH | Nicotinamide adenine dinucleotide hydrate |
| NCBI | National Center for Biotechnology Information |
| n.d. | Not determined |
| nt | Nucleotide |
| OFN | Oxygen-free nitrogen |
| PAL | Pressure acid leaching |
| PAPS | Adenosine 3'-phosphate-5'-phosphosulfate |
| PAR | 4-(2-pyridylazo) resorcinol |
| PCR | Polymerase chain reaction |
| PDCA | Pyridine-2,6-dicarboxylic acid |
| $pH_{PZC}$ | pH of point zero charge |
| pKa | Acid dissociation constant |
| PLS | Pregnant leaching solution |
| *p*mol | Picomole |
| ppm | Parts per million |
| p.s.i. | Pounds per square inch |
| RFLP | Restriction fragment length polymorphism |
| RISC | Reduced inorganic sulfur compounds |

| | |
|---|---|
| RNA | Ribonucleic acid |
| RO | Reverse osmosis |
| rpm | Revolutions per minute |
| SAG | Semi-autogenous grinding |
| SEM | Scanning electron microscopy |
| SDS | Sodium dodecyl sulfate |
| SIP | Stable isotopes probing |
| SMW | Sossego mine water |
| SMWOC | Small molecular weight organic compounds |
| sp./spp. | Species |
| SRR | Sulfate reduction rate |
| SX-EW | Solvent extraction/Electrowinning |
| TBE | Tris-borate-EDTA |
| TE | Trace elements |
| TOC | Total organic carbon |
| T-RF | Terminal restriction fragment |
| T-RFLP | Terminal restriction fragment length polymorphism |
| UK | United Kingdom |
| USA | United States of America |
| UV | Ultraviolet |
| v | Volume |
| w | Weight |
| X-gal | 5-bromo-4-chloro-3-indolyl-β-D-galactopyranoside |
| YE | Yeast extract |
| ZVI | Zero-valent iron |
| ZVS | Zero-valent sulfur |

# 1 Introduction

## 1.1 The sulfur cycle

Chemically, sulfur is one of the most interesting but also the most complex element; geochemically is one of the most abundant elements on the Earth's crust and biochemically it is most important (Steudel, 2000). The complexity of sulfur originates from its 9 valence states (ranging from -2 to +6) that can be transformed both chemically and biologically. In addition, the sulfur cycle is intimately related to carbon and nitrogen cycles. The most reduced states (-2 and -1) are found in metal and metalloids sulfides (e.g. chalcocite, $Cu_2S$ and pyrite, $FeS_2$), zero-valent sulfur (ZVS), which is widely distributed in the lithosphere, the +2 and +4 valencies that have only a transitory existence in the geochemical cycle and are usually reaction intermediates. Sulfate (+6) is the most oxidized form and it is the second most abundant anion in sea water (after chloride) and some rivers (after bicarbonate) (Middelburg, 2000). The equilibrium composition of aqueous sulfur species is shown in the Pourbaix diagram (Fig. 1.1), in which the thermodynamic favourable forms are shown as function of redox and pH values.

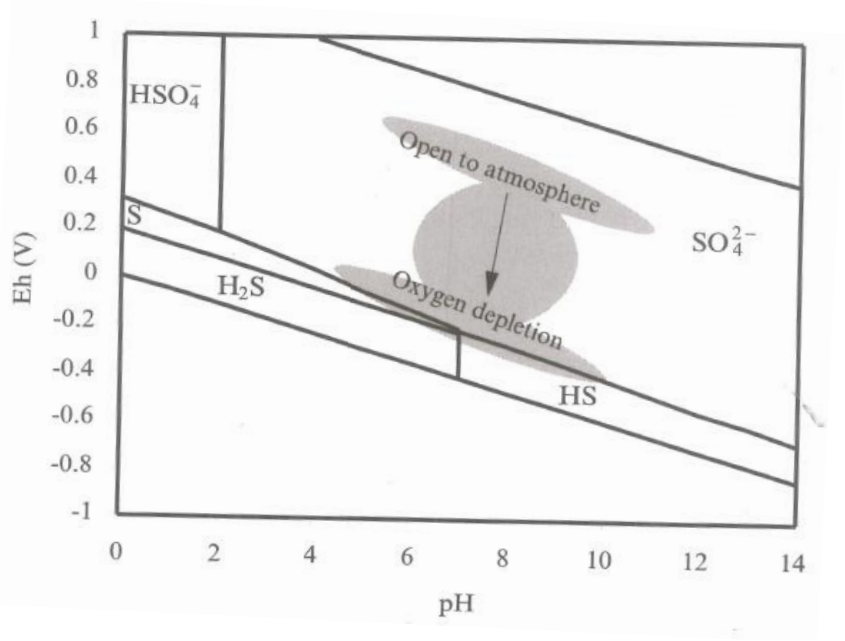


**Fig. 1.1.** Pourbaix diagram for aqueous sulfur cycle. The distribution of $E_H$-pH in natural systems is shaded (from Middelburg, 2000).

Sulfur is abundant in all organisms, as constituent part of many organic compounds such as amino acids, (poly-)peptides, enzyme cofactors, antibiotics, lipids or carbohydrates which can have either catalytical, structural or regulatory functions. Bio-transformation of sulfur compounds (Fig. 1.2) have been regarded as one of the major driving forces for many existing forms of life during the early planet conditions (Lens and Kuenen, 2001). In brief, sulfate-reducing bacteria use sulfate as a terminal electron acceptor and organic carbon compounds or hydrogen as electron donors, resulting in the generation of hydrogen sulfide ($H_2S$). This sulfide can be oxidized aerobically by chemolithotrophic sulfur-oxidizing bacteria, or anaerobically by phototrophic sulfur bacteria (to elemental sulfur, $S^0$). Other transformations, such as sulfur reduction and sulfur disproportionation are also catalysed by specific group of microorganisms (Muyzer and Stams, 2008).

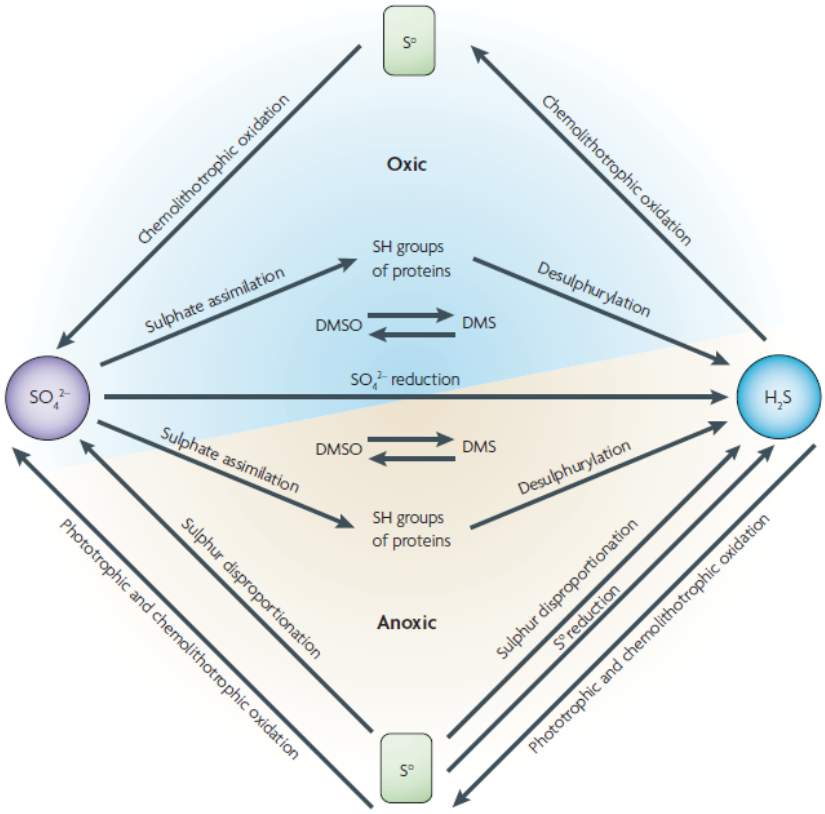


**Fig. 1.2.** The biological sulfur cycle (from Muyzer and Stams, 2008).

In natural environments, the most common inorganic sulfur compounds are sulfate, bisulfate, elemental sulfur, polythionates and thiosulfate (Table 1.1). Assimilatory reduction of sulfate is common in prokaryotes, fungi and plants, but the dissimilatory pathways are restricted to bacteria and archaea. In dissimilatory pathways, the turnover of sulfur compounds is high and the final product is released to the environment, whereas in assimilatory pathways the turnover is relatively low and the sulfur compounds are incorporated into organic compounds (Brüser et al., 2000).

**Table 1.1.** Inorganic sulfur compounds and its biological formation (Brüser et al., 2000).

| Compound | Chemical formula | Oxidation state | Formation |
|---|---|---|---|
| **Sulfide** | $H_2S/HS^-$ | -2 | Biological sulfate respiration; desulfuration of S-containing organic compounds; minerals in soils and rocks or sulfide enriched springs |
| **Polysulfides** | $^-S(S)_nS^-$ | -1 | Reductive elemental sulfur ring opening with sulfide; partial oxidation of sulfide |
| **Thiosulfate** | $S_2O_3^{2-}$ | -1 | Non-biological reaction of sulfite with sulfur and polythionates; oxidation of sulfidic minerals; taurine fermentation; oxidative sulfur metabolism |
| **Polythionates** | $^-O_3S(S)_nSO_3^-$ | 0 | Biological incomplete oxidation of thiosulfate |
| **Elemental S** | $S_n$ rings | 0 | Biological sulfide oxidation; non-biological oxidation of polysulfides; content of soils and rocks |
| **Bisulfate** | $HSO_4^-$ | +6 | Biological oxidation of sulfide (pH<1.9) |
| **Sulfate** | $SO_4^{2-}$ | +6 | Aerobic and anaerobic oxidation of sulfur compounds |

Inorganic sulfur compounds are also produced by abiotic processes, which can strongly influence the species composition in natural habitats. Abiotic processes and the biological sulfur cycles are interconnected.

## 1.2 Dissimilatory reduction of oxidized sulfur compounds

### *1.2.1 Sulfate reduction pathways*

In the microbial sulfur cycle, sulfate is converted to sulfide by sulfate-reducing bacteria (SRB) via dissimilatory sulfate reduction. Sulfate is used as a terminal electron acceptor in this process of bacterial respiration which occurs under strictly anaerobic conditions. Electron donors in this case are usually organic carbon compounds and hydrogen. From a chemical perspective though, sulfate is an unfavourable electron acceptor for microorganisms due to the very low redox potential of the sulfate-sulfite couple ($E^{0'}$ -516 mV) that precludes direct reduction by the intracellular electron mediators present in sulfate-reducers, such as ferredoxin ($E^{0'}$ -398 mV) or NADH ($E^{0'}$ -314 mV). To overcome this, sulfate is activated by an ATP sulfurylase, generating adenosine-5'-phosphosulfate (APS) and pyrophosphate, the latter is hydrolysed to 2-phosphate by the enzyme pyrophosphatase. The assimilatory process is far more widespread in nature (including the domain Eukarya) than dissimilatory sulfate reduction. In this process, APS is converted to adenosine 3'-phosphate-5'-phosphosulfate

(PAPS) by APS kinase, which also leads to sulfide, however, the product in this case is used in the synthesis of thiols, such as cysteine. The $E^{0'}$ of the couple APS-sulfite plus AMP is -60 mV, which allows the reduction of APS by the electron mediators. The AMP generated by the reduction of APS, is converted into 2 molecules of ADP by the ATP-dependent adenylate kinase, which means that the activation of sulfate requires 2 ATP molecules. Sulfite is then reduced to sulfide in the cytoplasm of the cells ($E^{0'}$ of the couple sulfite-sulfide is -116 mV). The pathway through this reduction reaction occurs is still not clear, though 2 models have been described: the *Rees* and trithionate pathways.

The *Rees* model was described by Rees (1973) and involves a six-electron reduction step of sulfite to sulfide by the enzyme dissimilatory sulfite reductase (Dsr). In this model, reactions upstream of sulfite reduction are reversible and those downstream are unidirectional and only $H_2S$ is produced (Fig. 1.3A). A criticism of this model is that several studies have also detected the production of sulfur intermediates. Kobayashi et al. (1969) proposed a model that included production of sulfur intermediates, such as trithionate and thiosulfate, referred to as the trithionate pathway. In this model, the enzyme Dsr produces trithionate via a 2-electron reduction step (Fig. 1.3B). Subsequently, the enzyme trithionate reductase catalyses the reduction of trithionate to thiosulfate in a 2-electron transfer reaction. Next, a third enzyme, thiosulfate reductase, catalyses the final step by reducing thiosulfate to sulfide. However, this model has also been questioned. Later studies suggested that trithionate and thiosulfate reduction is not coupled to proton translocation and that the main benefit of this step is the formation of sulfite which can be reduced by Dsr (Peck and Legall, 1982).

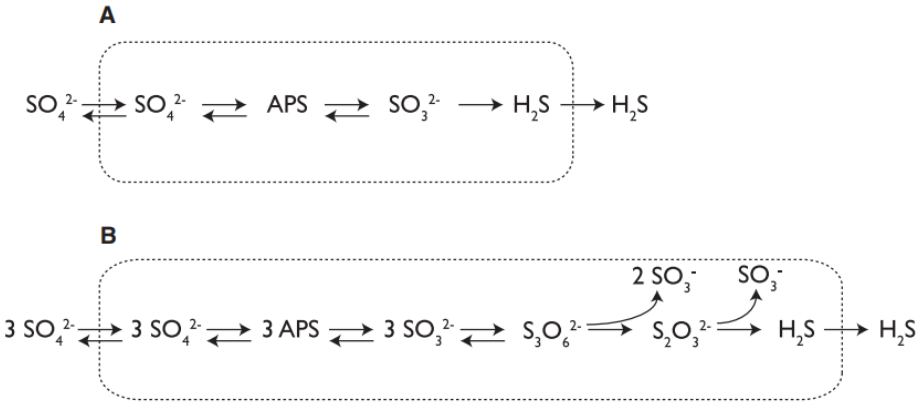


**Fig. 1.3.** Schematic representation of the (a) *Rees* pathway and (b) trithionate pathway (from Bradley et al., 2011).

More recently, studies on the protein structure of Dsr showed that the crystal structures of sulfite reductases consists of two subunits, DsrA and DsrB, with both containing an active site for binding sulfite prior to its reduction and each site is bound to an iron-sulfur cluster that mediate electron transfer (Oliveira et al., 2008). An additional iron-sulfur cluster assists the

electron transfer from an external electron donor, resulting in the net capacity of DsrAB complex to reduce sulfite to elemental sulfur. The crystal structure of Dsr contains a second protein (DsrC) associated with DsrAB complex. The DsrC contains a terminal cysteine (Cys104) and is thought to play an important role in the reduction of ZVS produced by DsrAB during sulfite reduction within the active sites (Oliveira et al., 2008). Bradley et al. (2011) suggested a revised network for sulfate reduction. This model incorporates aspects from both previously described pathways and suggests that sulfite is mainly reduced in a 2-step process which involve a ZVS intermediate by the complex interaction between DsrAB and DsrC (Fig. 1.4). Trithionate and thiosulfate are the likely products of side reactions between sulfite and partially reduced sulfur in the DsrAB complex. Once formed, these products can be either released into the extracellular environment or recycled within the cytoplasm, back into the thionate loop, for further sulfide production (Bradley et al., 2011).

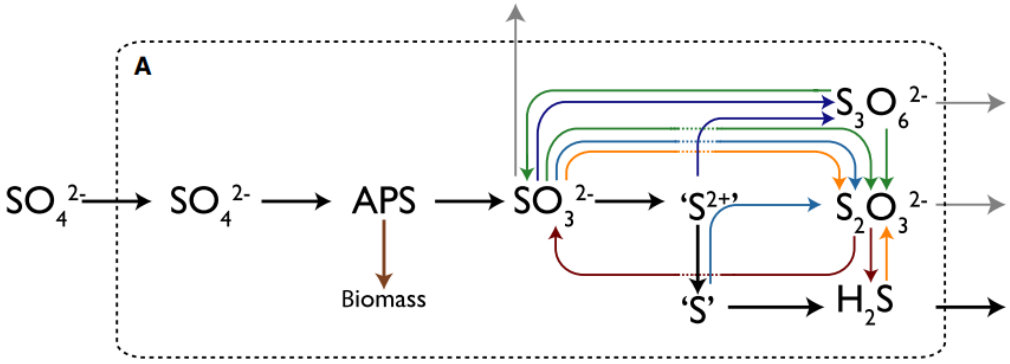


**Fig. 1.4.** Schematic representation of the revised model for sulfate reduction network proposed by Bradley et al. (2011).

### *1.2.2 Sulfate-reducing prokaryotes*

#### 1.2.2.1 Physiology

Sulfate-reducing prokaryotes are ubiquitous in anoxic environments where they use sulfate as terminal electron acceptor for the oxidation of many organic compounds and hydrogen, which results in the production of hydrogen sulfide, a process referred to as dissimilatory sulfate reduction or biosulfidogenesis. Even though they are named after their ability to use sulfate as electron acceptor, other sulfur intermediates (sulfite, thiosulfate and tetrathionate) as well as organic (e.g. fumarate, dimethylsulfoxide) and inorganic compounds (e.g. nitrate and nitrite for some marine SRB) have also been reported to be used as terminal electron acceptors for these prokaryotes (Jonkers et al., 1996; Dalsgaard and Bak, 1994; Muyzer and Stams, 2008). In a few cases, sulfate-reducers can also respire aerobically (Dilling

and Cypionka, 1990). In addition, Krekeler and Cypionka (1995) reported that *Desulfovibrio desulfuricans* strain CSN used oxygen preferentially (when present in small amounts) as electron acceptor rather than sulfur compounds. Some species of SRB are autotrophic and use $CO_2$ as carbon source and hydrogen as electron donor (Lens and Kuenen, 2001). In environments where concentrations of sulfate are low (e.g. freshwaters), sulfate-reducers can also have important roles in fermenting organic compounds, e.g. fermentation of pyruvate and formation of $CO_2$, acetate and hydrogen.

More than one hundred compounds have been reported to serve as electron donors for sulfate-reducers, including sugars (fructose, glucose, etc.), alcohols (ethanol, methanol, etc.), amino acids (serine, alanine, etc.), monocarboxylic acids (acetate, propionate, etc.), dicarboxylic acids (fumarate, succinate, etc.) and aromatic compounds (e.g. phenol) (Hussain et al., 2016). Sulfate-reducing prokaryotes have often been differentiated as (i) the complete oxidizers (which oxidize substrates exclusively to $CO_2$) and (ii) the incomplete oxidizers (which generate both acetate and $CO_2$ as end products). Bottcher et al. (2005) reported SRB growth by disproportionation of thiosulfate, sulfite and sulfur, producing sulfate and sulfide as end products. The use of long-chain alkanes and alkenes by SRB has also been reported (Cravo-Laureau et al., 2004). Polymeric organic compounds, such as cellulose, proteins and fats are not directly metabolised by sulfate-reducers and they rely on other microorganisms that are able to break down and ferment these substrates into small molecular weight compounds which SRB can metabolise as electron donors and carbon sources.

#### 1.2.2.2. Distribution and ecology

Sulfate-reducing prokaryotes are not only versatile in their metabolism, but also in the wide range of different habitats they can thrive. They can be found in both natural and engineered environments where sulfate is present, such as marine and freshwater sediments, deep-sea hydrothermal vents, hydrocarbon seeps, hypersaline microbial mats, mud volcanoes, oil field environments, human and animal intestines, industrial wastewaters treatment plants, rhizosphere of plants, aquifers, etc. In some of these ecosystems, sulfate-reducers need to cope with extremes conditions, including very high or very low temperatures and high pressure. In addition, they have also been detected in environments with extreme pH values, such as acid mine drainage sediments (~ pH 2) (Sen and Johnson, 1999) and soda lakes (~ pH 10) (Geets et al., 2006). Because they are ubiquitous, these prokaryotes play an important role in the overall biogeochemistry of the environment by actively influencing both the sulfur and carbon cycles.

1.2.2.3. Diversity of sulfate-reducing prokaryotes

Sulfate-reducing bacteria and archaea have been isolated from many different habitats. In order to survive in these environments, they have developed a complex physiology which greatly increased their diversity. Different techniques have been used to study the diversities and activities of sulfate-reducers. The most traditional technique used is cultivation, though this is probably a highly limited approach considering that less than 1% of bacteria in nature have been estimated to have been cultivated *in vitro*. In the last few decades, the use of marker genes was introduced and most of the information about diversity of microorganisms in general was obtained based on the gene that encodes 16S ribosomal RNA (rRNA). For sulfate-reducers, the 16S rRNA gene is widely used as well as functional genes which encode specific enzymes related to sulfate reduction, such as *dsr*AB (dissimilatory sulfite reductase) or *apr*BA (adenosine-5'-phosphosulfate reductase). Fingerprinting methods (e.g. cloning and DGGE) can be used on PCR-amplified gene fragments for determination of SRB diversity in many different habitats (Wagner et al., 2005).

To date, more than 60 genera and 220 species of dissimilatory sulfate-reducers have been described and the vast majority of these are species of bacteria. Comparative analysis of 16S rRNA gene sequences showed that they belong to 7 divisions (phyla). Five of them belong within the Bacteria domain: (i) *Deltaproteobacteria*, Gram-negative mesophilic SRB (e.g. *Desulfovibrio* spp.), (ii) Firmicutes, Gram-positive spore-forming SRB (e.g. *Desulfosporosinus* spp.), (iii) tree lineages of thermophilic SRB, Nitrospirae (*Thermodesulfovibrio* spp.), Thermodesulfobacteria (*Thermodesulfobacterium*, spp.) and Thermodesulfobiaceae (*Thermodesulfobium narugense),* and two within the Archaea domain: thermophilic archaeal sulfate-reducers *Archaeoglobus* (Euryarchaeota) and *Thermocladium* and *Caldivirga* (Crenarchaeota) (Sánchez-Andrea et al., 2014; Hussain et al., 2016).

Different techniques can be applied to obtain information about diversity in an environment. Quantitative real-time PCR (qPCR) is highly sensitive and has been used to quantify the number of sulfate-reducers, for example, in industrial wastewaters (Ben-Dov et al., 2007). Another technique used to quantify the number of sulfate-reducers is fluorescence *in situ* hybridization (FISH), which allows direct visualisation of uncultured microbes as well as their spatial distribution (Sanz and Köchling, 2007). This technique in combination with radioactively-labelled substrates (MAR-FISH) allows analysis of the activity of the populations (Ito et al., 2002). Stable isotopes probing (SIP) using $^{13}$C-acetate is another technique that has been applied to determine de composition of active SRB community constituents in sulfate-reducing sediment enrichments (Webster et al., 2006). Because all these techniques have their own advantages and limitations, an integrated approach, using classic and modern

methods, has been suggested to be the best alternative to obtain a comprehensive understanding of the diversity of sulfate-reducers in natural and engineered environments (Muyzer and Stams, 2008).

## 1.3 Mining activity and its waste products

From ancient times to the current day, mining has played a crucial role in human existence (Madigan,1981). The history of mining and evolution of civilization were brought up alongside each other with important eras in human history being associated with and identified by name of metals, such as the Stone Age (prior to 4000 B.C.), the Bronze Age (4000 to 1500 B.C), the Iron Age (1500 B.C to 1780 A.D), and more recently the Steel (1780 – 1945) and Nuclear (1945 to the present) Ages (Hartman and Mutmansky, 2002).

The increasing exploitation of high-grade oxide and sulfidic ores throughout human history has led to the depletion of such and therefore lower grade ores became the most suitable alternative for obtaining metals. One consequence of this is that the amount of waste material generated by metal mining is significantly greater.

Metal and coal mining give rise to solid and liquid waste products that are potentially hazardous to aquatic and terrestrial ecosystems. Solid wastes can be divided into two main groups: waste rocks and mine tailings. The former comprises dumps of waste rocks in various particles sizes that are less threatening to the environment. Mine tailings are crushed and ground and the target metal minerals are concentrated and separated from other gangue minerals (Johnson, 2014). This approach facilitates the recovery of economically valuable minerals as concentrates while non-targeted minerals sink to the bottom of the flotation tank and are disposed of as mineral tailings (Ñancucheo, 2011). The composition of the ore bodies will strongly influence the composition of the tailings, which can be highly variable; pyrite ($FeS_2$) is often the most common and most reactive mineral phase present in these wastes. After processing, mine tailings can still contain large amount of commercially valuable metals from sulfidic minerals which can be naturally leached (abiotic or microbial-driven leaching), contributing to the generation of metal-contaminated waters.

Aqueous wastes are generally either streams that drain abandoned (underground or open cast) mines, mine tailings and waste rocks or pit lakes, which are abandoned opencast voids flooded with groundwater due to termination of mine dewatering (Fig. 1.5). The chemical characteristics of different mine waters can vary considerably. Waters draining mines or mine spoils may be acidic, alkaline, saline, iron-rich and may contain a variety of other soluble metals depending on the geochemical nature of the ore body and even within the same mine, the water composition can differ.

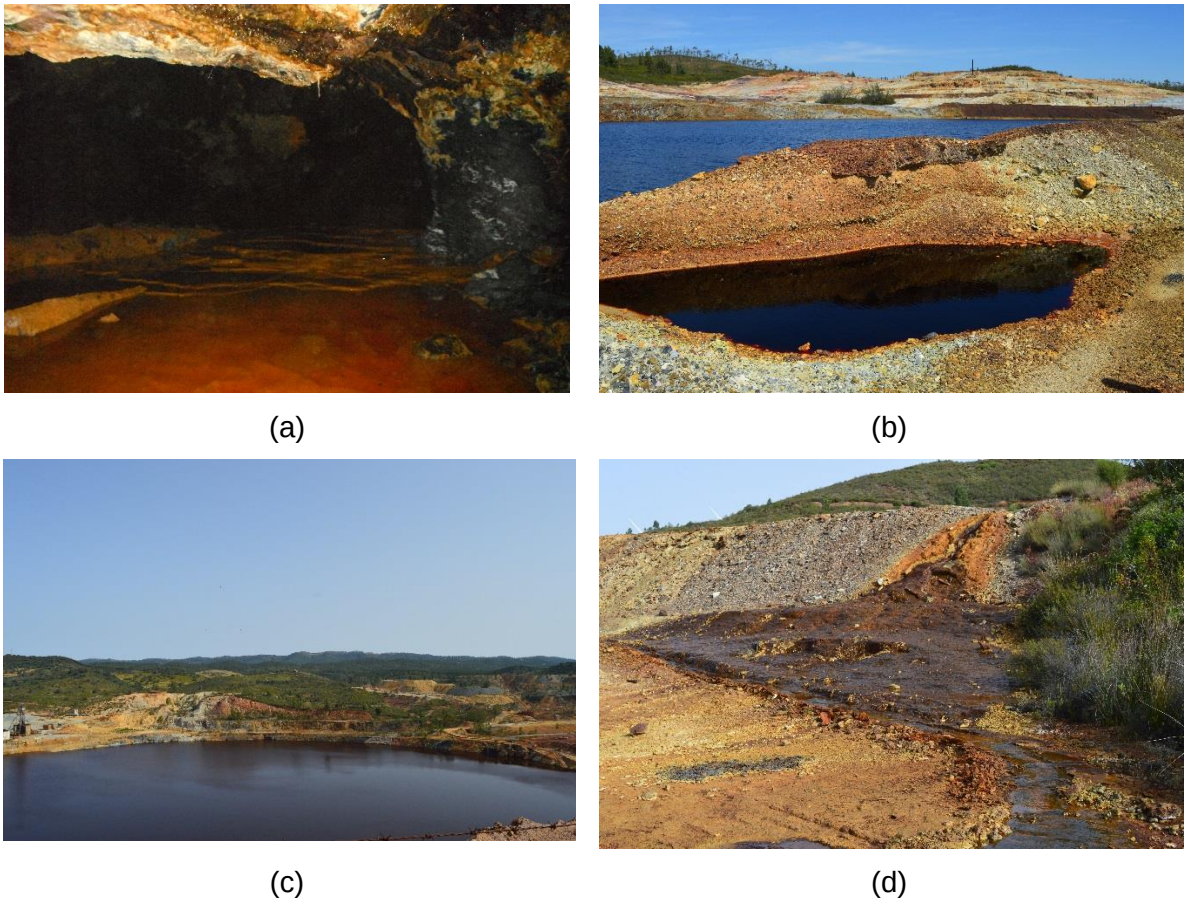

(a) (b)

(c) (d)

**Fig. 1.5.** Pit lakes and streams of acidic waters draining some abandoned mines and mine spoils. (a) AMD draining Cae Coch mine, an underground pyrite mine in North-west Wales, UK, (b) acidic lagoons draining São Domingos copper mine in South-east Portugal, (c) pit lake at San Telmo copper mine, Huelva, Spain, and (d) AMD draining Cantareras copper mine, South-west Spain.

### *1.3.1 Generation of acid mine drainage*

In general, sulfide minerals are chemically (and biologically) stable when both water and oxygen are absent. The rate of sulfide mineral oxidation is particularly slow in large rock fragments, however it can be considerably accelerated when small and fine mineral particles, which present greater surface areas, are exposed to both water and air. The oxidative dissolution of sulfide minerals can occur spontaneously with either molecular oxygen or ferric iron acting as electron acceptor, and the mechanisms involved in that process have been widely described in the literature (Johnson, 2014; Vera et al., 2013; Johnson and Hallberg, 2005; Banks et al., 1997; Gray, 1996; Nordstrom, 1982). Pyrite ($FeS_2$) is the most abundant sulfide mineral in the lithosphere and it can be associated with other metals/metalloids, such as copper, cobalt, nickel, zinc, lead, aluminium, cadmium, arsenic, etc. When oxidized, pyrite

releases ferrous iron, sulfate and protons (Eq. 1.1), which are the main components of acid mine drainage. Once the oxidative dissolution of pyrite is initiated, a cycle is established in which Fe (II) is oxidized (Eq. 1.2) and the Fe (III) generated is then reduced by pyrite, causing further production of sulfate and acidity (Eq. 1.3). The generation of Fe (III) at low pH is the key for promoting the ongoing oxidation of the mineral. Hydrolysis of ferrous iron can simultaneously occur with generation of ferric hydroxide and protons (Eq. 1.4).

$$FeS_2 + 3.5O_2 + H_2O \rightarrow Fe^{2+} + 2SO_4^{2-} + 2H^+ \quad (1.1)$$

$$Fe^{2+} + 0.25O_2 + H^+ \rightarrow Fe^{3+} + 0.5H_2O \quad (1.2)$$

$$FeS_2 + 14Fe^{3+} + 8H_2O \rightarrow 15Fe^{2+} + 2SO_4^{2-} + 16H^+ \quad (1.3)$$

$$Fe^{2+} + 3H_2O \rightarrow Fe(OH)_{3\,[s]} + 3H^+ \quad (1.4)$$

Environments in which these reactions are occurring to appreciable extents can become moderately to extremely acidic, and the sulfuric acid produced not only increases the rate of sulfide mineral dissolution (solubility of ferric iron is increased at low pH), but also allows many transition metals and aluminium to remain in solution (Johnson, 2014). The total acidity of mine waters is related to, at least, three different types of acidity:

(i) proton acidity: a measure of free hydronium $H_3O^+$ ions;

(ii) organic acidity: associated with dissolved organic compounds; and

(iii) mineral acidity: as a result of hydrolysis of soluble metal ions (Al, Fe, Mn).

In low pH liquors (< 3.5), the chemical re-oxidation of Fe (II) (Eq. 1.2) is negligible (Stumm and Morgan, 1981) and Fe (III) becomes the limiting factor of the process, therefore, for the reaction to continue, a catalyst is required. Acidophilic prokaryotes (iron-oxidizing bacteria and archaea) play a crucial role in the generation of acid mine drainage, since they can increase rates of Fe (II) oxidation at low pH by several orders of magnitude.

### *1.3.2 The microbiology of acidic mine wastes*

#### 1.3.2.1 Indigenous acidophilic prokaryotes

Microorganisms that are metabolically active in natural and man-made extreme acidic environments (pH < 3) are distributed in all domains of life, but mostly in the domains Bacteria and Archaea. Acidophilic bacteria and archaea have been characterised in terms of their physiologies, such as temperature ranges and optima (mesophiles, thermophiles and moderate thermophiles), pH ranges and optima (moderate acidophiles and extreme

acidophiles), carbon metabolism (autotrophs, heterotrophs and mixotrophs), energy acquisition (electron donors and acceptors), as well as their phylogeny by using DNA sequencing for metagenomics, metaproteomics, metabolomics, etc. analysis. Tables 1.2 and 1.3 list the physiological properties of some acidophilic bacteria and archaea.

**Table 1.2.** Physiological properties of some acidophilic bacteria (Dopson, 2016).

| Species | Electron donors | Electron acceptors | Carbon metabolism |
|---|---|---|---|
| **Low temperature adapted mesophiles (able to grow at 5ºC)** | | | |
| *Acidithiobacillus ferrivorans*$^T$ | $Fe^{2+}/S^0$/RISC | $O_2/Fe^{3+}$ | Autotroph |
| '*Ferrovum myxofaciens*'$^T$ | $Fe^{2+}$ | $O_2$ | Autotroph |
| **Mesophilic bacteria (optimum between 15 to 39ºC)** | | | |
| *Acidithiobacillus albertensis*$^T$ | $S^0$/RISC | $O_2$ | Autotroph |
| *Acidithiobacillus ferridurans*$^T$ | $Fe^{2+}/S^0$/RISC/$H_2$ | $O_2/Fe^{3+}$ | Autotroph |
| *Acidithiobacillus ferrooxidans*$^T$ | $Fe^{2+}/S^0$/RISC/$H_2$ | $O_2/Fe^{3+}$ | Autotroph |
| *Acidithiobacillus thiooxidans*$^T$ | $S^0$/RISC | $O_2$ | Autotroph |
| *Acidiferrobacter thiooxidans*$^T$ | $Fe^{2+}/S^0$/RISC | $O_2/Fe^{3+}$ | Autotroph |
| *Leptospirillum ferriphilum*$^T$ | $Fe^{2+}$ | $O_2$ | Autotroph |
| '*Leptospirillum ferrodiazotrphum*'$^T$ | $Fe^{2+}$ | $O_2$ | Autotroph |
| *Leptospirillum ferrooxidans*$^T$ | $Fe^{2+}$ | $O_2$ | Autotroph |
| *Acidiphilium acidophilum*$^T$ | $S^0$/RISC/C | $O_2/Fe^{3+}$ | Facultative autotroph |
| *Sulfobacillus benefaciens*$^T$ | $Fe^{2+}/S^0$/RISC/$H_2$/C | $O_2/Fe^{3+}$ | Facultative autotroph |
| *Alicyclobacillus aeris*$^T$ | $Fe^{2+}/S^0$/RISC/C | $O_2$ | Facultative autotroph |
| *Acidiphilium cryptum*$^T$ | C | $O_2/Fe^{3+}$ | Heterotroph |
| *Acidiphilium rubrum*$^T$ | RISC/C | $O_2/Fe^{3+}$ | Heterotroph |
| *Acidithrix ferrooxidans*$^T$ | $Fe^{2+}$/C | $O_2$ | Heterotroph |
| *Acidocella facilis*$^T$ | C | $O_2$ | Heterotroph |
| *Acidocella aromatica*$^T$ | C | $O_2/Fe^{3+}$ mineral | Heterotroph |
| *Alicyclobacillus disulfidooxidans*$^T$ | $Fe^{2+}/S^0$/RISC/C | $O_2$ | Heterotroph |
| *Alicyclobacillus ferrooxydans*$^T$ | $Fe^{2+}$/RISC/C | $O_2$ | Heterotroph |
| *Alicyclobacillus tolerans*$^T$ | $Fe^{2+}/S^0$/C | $O_2/Fe^{3+}$ | Heterotroph |
| *Ferrimicrobium acidiphilum*$^T$ | $Fe^{2+}$/C | $O_2/Fe^{3+}$ | Heterotroph |
| *Acidomonas methanolica*$^T$ | C | $O_2$ | Facultative methylotroph |

**Table 1.2.** continued

| **Moderately thermophilic and thermo-tolerant acidophiles (optimum between 40 and 59ºC)** | | | |
|---|---|---|---|
| *Acidithiobacillus caldus*$^{T}$ | $S^0$/RISC/$H_2$ | $O_2$ | Autotroph |
| '*Acidithiomicrobium*' P2 | $Fe^{2+}$/$S^0$ | $O_2$ | Autotroph |
| *Acidimicrobium ferrooxidans*$^{T}$ | $Fe^{2+}$/$H_2$/C | $O_2$/$Fe^{3+}$ | Facultative autotroph |
| *Aciditerrimonas ferrireducens*$^{T}$ | C/$H_2$ | $O_2$/$Fe^{3+}$ | Facultative autotroph |
| *Sulfobacillus acidophilus*$^{T}$ | $Fe^{2+}$/$S^0$/RISC/$H_2$/C | $O_2$/$Fe^{3+}$ | Facultative autotroph |
| *Sulfobacillus sibiricus*$^{T}$ | $Fe^{2+}$/$S^0$/RISC/C | $O_2$ | Facultative autotroph |
| *Sulfobacillus thermosulfidoxidans*$^{T}$ | $Fe^{2+}$/$S^0$/RISC/$H_2$/C | $O_2$/$Fe^{3+}$ | Facultative autotroph |
| *Sulfobacillus thermotolerans*$^{T}$ | $Fe^{2+}$/$S^0$/RISC/C | $O_2$ | Facultative autotroph |
| *Acidicaldus organivorans*$^{T}$ | $S^0$/C | $O_2$/$Fe^{3+}$ | Heterotroph |
| *Ferrithrix thermotolerans*$^{T}$ | $Fe^{2+}$/C | $O_2$/$Fe^{3+}$ | Heterotroph |
| **Thermophilic bacteria (temperature optimum 60ºC)** | | | |
| *Hydrogenobaculum acidophilum*$^{T}$ | $S^0$/RISC/$H_2$ | $O_2$ | Autotroph |
| *Methylacidiphilum infernorum*$^{T}$ | $CH_4$ | $O_2$ | Heterotroph |

**Table 1.3.** Physiological properties of archaeal isolates of the family *Sulfolobaceae* and order *Thermoplasmatales* (modified from Golyshina et al., 2016).

| **Species** | **Temperature growth range (optima); ºC** | **pH growth range (optima)** | **Metabolism** |
|---|---|---|---|
| **Family *Sulfolobaceae*** | | | |
| *Sulfolobus acidocaldarius* | 55-85 (75-80) | 1.5-6 (3) | Aerobic mixo/heterotroph, oxidation of $H_2$ and organic C |
| *Sulfolobus solfataricus* | 50-87 (85) | 2-5.5 (3-4.5) | Aerobic mixo/heterotroph, oxidation of $H_2$ and organic C |
| *Sulfolobus shibatae* | n.d-86 (81) | n.d. (3) | Aerobic mixo/heterotroph, oxidation of $S^0$, $H_2$ and organic C |
| *Sulfolobus metallicus* | 50-75 (65) | 1-4.5 (2-3) | Aerobic lithoautotroph, oxidation of $Fe^{2+}$, $S^0$ and sulfidic ores |
| *Sulfolobus tokodaii* | 70-85 (80) | 2-5 (2.5-3) | Aerobic chemolithotroph/ heterotroph, oxidation of $S^0$ and C |

**Table 1.3.** continued.

| | | | |
|---|---|---|---|
| '*Sulfolobus islandicus*' | 65-88 (78) | 2-5 (2.7) | Aerobic chemolithotroph/ heterotroph |
| '*Sulfolobus technogensis*' | 65-95 (85) | 1.7-6-5 (3.5) | Aerobic chemolithotroph/ heterotroph |
| *Metallosphaera sedula* | 50-80 (75) | 1-4.5 (2-3) | Aerobic facultative chemolithoautotroph, oxidation of $H_2$, $S^0$ and organic C |
| *Metallosphaera prunae* | 55-80 (75) | 1-4.5 (2-3) | Aerobic facultative chemolithoautotroph, oxidation of $H_2$, $S^0$ and organic C |
| '*Metallosphaera yellowstonensis*' | n.d. (65) | n.d. (3) | Aerobic facultative chemolithoautotroph, oxidation of sulfidic ores, $Fe^{2+}$and $S^0$ |
| *Metallosphaera hakonensis* | 50-80 (70) | 1-4 (3) | Aerobic facultative chemolithoautotroph, oxidation of metal sulfides, $S^0$, RISC and C |
| *Metallosphaera cuprina* | 55-75 (65) | 2.5-5.5 (3.5) | Aerobic facultative chemolithoautotroph, oxidation of sulfide ores, polythionates and C |
| *Sulfurococcus mirabilis* | 50-86 (70-75) | 1-5.8 (2-2.6) | Aerobic facultative chemolithoautotroph, oxidation of $Fe^{2+}$, $S^0$, sulfide minerals and C |
| *Sulfurococcus yellowstonii* | 40-80 (60) | 1-5.5 (2-2.6) | Aerobic facultative chemolithoautotroph, oxidation of $Fe^{2+}$, $S^0$, sulfide minerals and C |
| *Acidianus brierleyi* | 45-75 (70) | 1-6 (1.5-2) | Facultative anaerobe, chemolithoautotroph, oxidation of $H_2$, sulfidic ores, C; oxidation/reduction of $S^0$ |
| *Acidianus infernus* | 65-95 (85-90) | 1-5.5 (2) | Facultative anaerobe, chemolithoautotroph, oxidation of $H_2$, sulfidic ores, C; oxidation/reduction of $S^0$ |
| *Acidianus ambivalens* | n.d.-87 (80) | 1-3.5 (2.5) | Facultative anaerobe, obligate lithoautotroph; oxidation/reduction of $S^0$ |
| *Acidianus sulfidivorans* | 45-83 (74) | 0.35-3 (0.8-1.4) | Facultative anaerobe, obligate chemolithotroph, oxidation of sulfidic ores $Fe^{2+}$, $S^0$ |
| '*Acidianus manzaensis*' | 60-90 (80) | 1-5 (1.2-1.5) | Facultative anaerobe, chemolithoautotroph, oxidation of $H_2$, $S^0$ and C; reduction of $Fe^{3+}$ |
| *Sulfurisphaera azoricus* | 57-89 (80) | 1-5 (1.2-1.5) | Obligate anaerobe, chemolithoautotroph, oxidation of $S^0$ and $H_2$ |
| *Sulfurisphaera ohwakuensis* | n.d.-94 (84) | 1-5 (2) | Facultative anaerobe, mixo/heterotroph, oxidation of organic C and reduction of $S^0$ |
| *Thermoplasma acidophilum* | 45-63 (59) | 0.5-4 (1-2) | Facultative anaerobe, chemoheterotroph, reduction of $S^0$ |

**Table 1.3.** continued.

| | | | |
|---|---|---|---|
| *Thermoplasma volcanium* | 33-67 (60) | 1-4 (2) | Facultative anaerobe, chemoheterotroph, reduction of $S^0$ |
| *Picrophilus torridus* | 47-65 (60) | 0-3.5 (0.7) | Obligate aerobe, chemoheterotroph |
| *Picrophilus oshimae* | 47-65 (60) | 0-3.5 (0.7) | Obligate aerobe, chemoheterotroph |
| *Ferroplasma acidiphilum* | 15-45 (35) | 1.3-2.2 (1.7) | Facultative anaerobe, chemoheterotroph, oxidation of sulfidic ores and $Fe^{2+}$ |
| '*Ferroplasma acidarmanus*' | 23-46 (42) | 0-4 (1.4-1.6) | Facultative anaerobe, chemo-mixo/heterotroph, oxidation of sulfidic ores and $Fe^{2+}$ |
| *Acidiplasma cupricumulans* | 22-63 (54) | 0.4-1.8 (1.1) | Facultative anaerobe, chemo-mixotroph, oxidation of sulfidic ores and $Fe^{2+}$ |
| *Acidiplasma aeolicum* | 15-65 (43) | 0-4 (1.4-1.6) | Facultative anaerobe, chemo-mixo/heterotroph, oxidation of sulfidic ores and $Fe^{2+}$ |
| *Thermogymnomonas acidicola* | 38-68 (60) | 1.8-4 (3) | Aerobic chemoheterotroph |
| *Cuniculiplasma divulgatum*$^T$ | 10-48 (40) | 0.5-4 (1-1.2) | Facultative anaerobe, heterotroph |
| *Cuniculiplasma divulgatum* PM4 | 10-45 (37) | 0.5-4 (1-1.2) | Facultative anaerobe, heterotroph |

Prokaryotic and eukaryotic microorganisms are not visible to the naked eye, though prokaryotic and micro-algal communities can be very evident as larger gelatinous, filamentous macroscopic structures such as biofilms, "streamers," and "microbial stalactites" (Fig. 1.6) within which bacteria and archaea are immobilised in extracellular polymeric substances (EPS) (Johnson, 1998). The colour of acid streamer and stalactites growths varies from white/light pink to shades of brown and black, though in surface waters they may be green due to the presence of phototrophic acidophiles (Rowe et al., 2007).

**Fig. 1.6.** Acid streamer growths (dominated by '*Ferrovum'*-like bacteria) in an abandoned copper mine in Spain (left) and microbial stalactites in an abandoned pyrite mine (Cae Coch, Wales) (right).

Within many acidophilic communities, there are prokaryotes which are capable of solubilising minerals (accelerating mineral dissolution) and some which are not. Iron- and sulfur-oxidizing bacteria and archaea are known to participate actively in the oxidation of ferrous iron and/or elemental sulfur and/or reduced inorganic sulfur compounds (RISCs) from sulfidic minerals which generates sulfuric acid, therefore, facilitating the solubilization of base metals (e.g. zinc, nickel) and extraction of precious metals (e.g. gold) (Johnson and Hallberg, 2003). In the past 50 years or so, the number of microorganisms that have been described to be involved in sulfide mineral oxidation has greatly increased due, in part, to advances in molecular biology. The most common iron-oxidizing bacteria found in acidic waters and mine tailings are often *Leptospirillum* spp., *Acidithiobacillus* spp. and *Sulfobacillus* spp. and these same bacteria are considered to be the most important players in "biomining" operations for metal extraction (Schippers et al., 2014).

Rates of pyrite oxidation at low pH (< 3) are significantly higher when using ferric iron as an oxidant rather than oxygen. This is related to the solubility of ferric iron, which is pH dependent (Stumm and Morgan, 1981). Oxidation of Fe (II) in acidic abiotic systems is also pH dependent and occurs very slowly, even in oxygen-saturated solutions (Stumm and Morgan, 1981). Different sulfide minerals may display different susceptibility to oxidation. For example, pyrite ($FeS_2$) can be oxidized by ferric iron, which is generated by acidophilic iron-oxidizing prokaryotes (e.g. *Acidithiobacillus* spp., *Leptospirillum* spp., *Ferroplasma acidiphilum*, etc). Sulfide minerals that are acid-soluble, such as chalcocite ($Cu_2S$), can be oxidised by prokaryotes that generate sulfuric acid, (the sulfur-oxidizers, e.g. *At. thiooxidans* and *Sulfolobus* spp.). In contrast, the dissolution of some Fe (III)-containing minerals (e.g. limonitic laterites and jarosites) can be accelerated by mesophilic iron-reducing bacteria under strictly anaerobic conditions (e.g. some *Acidithiobacillus* species) and by heterotrophic

mesophilic bacteria under microaerophilic conditions, such as *Acidiphilium cryptum*, and by moderate thermophiles, such as *Sulfobacillus* spp..

Extremely acidic mine waters are generally oligotrophic environments, since the concentration of dissolved organic carbon is often relatively low (< 20 mg $L^{-1}$) (Johnson, 1998). Primary production in these environments is based on both chemolitho-autotrophy and phototrophy, though the most dominant metabolism would often depend whether the site receives light or not. Lithotrophy-based primary production can be found in subterranean chambers (e.g. caves and abandoned underground mines) in which, microorganisms (predominantly bacteria) use energy derived from ferrous iron and/or RISCs oxidation to fix $CO_2$ (Johnson, 2012a). During active growth or lysis of dead/dying cells, acidophilic chemolithotrophic bacteria can lose a great amount of the carbon they fix as exudates (mainly as small molecular weight organic compounds); organic carbon also arises from lysis from dead cells. Schnaitman and Lundgren (1965), identified pyruvic acid as one of the exudates leaked into the growth medium of *At. ferrooxidans* using labelled carbon ($^{14}CO_2$). Organic acids have also been identified as exudates in cultures of *At. thiooxidans* in concentrations that caused inhibition of the bacterium (Borichewski, 1967). It has been reported that chemolitho-autotrophic primary producers are able to sustain the growth of other acidophilic heterotrophs and mixotrophs (e.g. *Acidimicrobium ferrooxidans* and *Sulfobacillus* spp., respectively) which also catalyse the dissimilatory oxidation of ferrous iron and/or RISCs (Ñancucheo and Johnson, 2010). The acidophilic chemolithoautotrophic primary producers (which provide potentially inhibitory organic compounds, as a result of their intrinsic metabolism), and the chemolithohetero/mixotrophs (which metabolise these potentially toxic organic compounds) rely on this mutualistic relationship to thrive in the environment; the same concept has been applied in commercial bioprocessing operations in order to sustain sulfide mineral dissolution (Rawlings and Johnson, 2007).

There are also acidophilic microorganisms found in mine-impacted areas (mine waters and mine tailings) which do not directly catalyse the oxidative or reductive dissolution of minerals, though have other important roles to play. For instance, some heterotrophic prokaryotes, such as *Acidocella* (Kimura et al., 2006) and *Thermoplasma* (Segerer et al., 1988), have been shown to contribute indirectly to mineral dissolution by “detoxifying” the environment for iron- and sulfur-oxidizers. Other prokaryotes are not involved in mineral dissolution but can use the products generated from that process (e.g. sulfur and/or sulfate and acidity) and the organic compounds released by primary producers, which is the case for sulfate-reducing prokaryotes.

1.3.2.2 Biosulfidogenesis in low pH environments and laboratory cultures

Biological reduction of sulfate to sulfide has been reported to occur in acidic environments, such as wood dust-containing acidic waters (Tuttle et al., 1969), black streamers (Johnson et al.,1979), lakes and rivers sediments (Koschorreck, 2003; Gyure et al., 1990), and mine tailings (Praharaj and Fortin, 2004). Although, sulfate reduction has been demonstrated to occur in acidic environments, isolation and characterisation of acid-tolerant and acidophilic SRB has often proved to be elusive. Studies involving the use of neutral pH media to enrich sulfate-reducers from acidic environments have been reported. Gyure et al. (1990) enriched SRB from mine tailings at pH 3 in liquid media containing high concentration of lactate at pH 5.5. However, the same approach failed when using media containing acetate. That is because organic acids can be potentially toxic to acidophilic bacteria. Organic acid toxicity depends on their dissociation constants. For example, acetic acid (a by-product of SRB that incompletely oxidize organic substrates) has a $pK_a$ of 4.75, and in solutions with pH < 4.75 its undissociated form is dominant. This can permeate cell membranes into circum-neutral pH cytoplasm causing the acid to dissociate, releasing protons and causing the intracellular pH to decrease, which can severely affect metabolic activities. The choice of substrate to enrich for acidophilic SRB is therefore crucial. Lactate is frequently used to enrich and cultivate neutrophilic SRB, but since this predominantly exists as lactic acid at low pH it presents the same potential toxicity problem as acetic acid. Non-ionic substrates, such as methanol, glycerol, are more appropriate for enriching for and cultivating sulfate reducing bacteria at low pH (Hard et al., 1997; Sen and Johnson, 1999).

An alternative approach to develop systems that reduce sulfate at low pH has involved adapting neutrophilic SRB to acidic conditions. A series of laboratory experiments reported by Bijmans et al. (2008; 2009; 2010) described a gas-lifted bioreactor containing a neutrophilic microbial community, fed with either hydrogen or formate, for treatment of process and wastewaters. In these studies, the bioreactor pH was incrementally lowered (from ~7 to pH 6, 5, 4.5 and 4) while the activity of sulfate-reducers and biomass yield were monitored. Results showed that the activity of the SRB decreased with pH and the biomass yield at pH 4 was 100-fold lower than that at pH 6 and it was suggested that the energy needed for growth was directed to maintain pH homeostasis (Bijmans, 2008).

Sulfate reduction at low pH consumes more protons than when it is carried out at circum-neutral pH (Eqs. 1.5 and 1.6). This, can be used to help mitigate the pH of AMD. In addition, most of the sulfide produced is present as undissociated $H_2S$ (($pK_{a1}$ = 6.9 ($H_2S \rightarrow HS^- + H^+$); and $pK_{a2}$ = 12.4 ($HS^- \rightarrow S^{2-} + 2H^+$) which is poorly soluble in water and more readily removed from solution (e.g. by gassing) than soluble $HS^-$ which is extremely toxic to all

organisms. Also, low pH environments often contain high concentrations of chalcophilic transition metals which can be removed from solution by precipitating them as solid sulfides (Eq. 1.7).

$4\ C_3H_8O_3 + 7\ SO_4^{2-} + 1.5\ H^+ \rightarrow 3\ CO_2 + 9\ HCO_3^- + 3.5\ H_2S + 3.5\ HS^- + 7\ H_2O$ (pH 6.9; Eq. 1.5)

$4\ C_3H_8O_3 + 7\ SO_4^{2-} + 14\ H^+ \rightarrow 7\ H_2S + 12\ CO_2 + 16\ H_2O$ (pH 4; Eq. 1.6)

$H_2S + Me^{2+} \rightarrow MeS\downarrow + 2\ H^+$ (Eq. 1.7)

Early studies suggested that sulfate reduction in low pH only occurred due to higher pH microsites around the cells which generated a gradient of pH and oxygen (e.g. Alldredge and Cohen, 1987). However, a later study showed that sulfate reduction was detected in an acidic mine lake sediment at pH as low as 3 and by increasing the sediment pH, sulfate reduction was temporarily inhibited (Gyure et al., 1990). Low or undetectable sulfate reduction activity in acidic environments may be due to limitation of substrates and competition with other bacterial groups rather than pH, especially because not only the quantity but also the nature of the organic compounds is important for the occurrence of sulfate reduction (Koschorreck, 2008). In addition, reduction of Fe (III) by iron-reducing bacteria is thermodynamically more favourable than sulfate-reduction and, as noted, ferric iron is often very abundant in low pH environments. More recently, acidophilic or acid-tolerant SRB have been isolated from acid mine drainage sediments: '*Desulfobacillus acidavidus*' CL4 (Ñancucheo and Johnson, 2012a), *Peptococcaceae* CEB3 (Ñancucheo and Johnson, 2012a), *Desulfosporosinus acidiphilus* (Alazard et al., 2010) and *Desulfosporosinus acididurans* (Sen and Johnson, 1999).

In some sedimentary environments, SRB also play an important role by mediating the genesis of sulfide minerals (e.g. CuS) from the generation of $H_2S$ and its reaction with metal ions (Eq. 1.7) (Gadd, 2010). Labrenz et al. (2000) reported sphalerite (ZnS) particles formed within natural biofilms from a flooded tunnel within carbonate rocks that host the Piquette Pb-Zn deposit (Wisconsin, USA) dominated by SRB of the families *Desulfobacteriaceae* and *Desulfovibrionaceae*.

The concept of biomineralisation (i.e. collective processes by which organisms form minerals; Dove et al. 2003) using sulfate-reducing bacteria is a recognised approach for remediating metal-contaminated wastewaters is discussed (section 1.5.2.2).

1.3.2.3 Acidophilic eukaryotes indigenous to mine-impacted environments

Within mine water research, prokaryotic microorganisms have been given much more attention and, over the past decades, their diversity and metabolism have been extensively investigated by several research groups worldwide, and much less attention has been dedicated to eukaryotic microorganisms, such as fungi and algae. The latter, however, play important roles in mine-impacted areas either by acting as adsorption agents or by providing a suitable environment for the prokaryotes to thrive. As highlighted previously, prokaryotic microorganisms are involved in geochemical processes associated with mineral oxidation generating extremely acidic wastewaters, which may contain high concentration of potentially toxic metals. Algal and fungal species are, in general, often more sensitive to acidity and metals than bacteria and archaea species (though there are notable exceptions) which would explain the more limited number of species found in these environments when compared to bacteria species. Bortnikova et al. (2001) investigated the geochemical consequences of AMD discharge from a gold mine in South-west Siberia into a natural reservoir and its effects on the indigenous community. They found that both phytoplankton and zooplankton numbers decreased sharply in mesocosms which contained AMD.

Many transition metals are essential to metabolic processes across all three domains of the tree of life, but they can also be fatal to many organisms if exposed to high concentrations. In algae and fungi, metals can affect protein denaturation, by obstructing functional groups, modifying the active conformation of the molecule or compromising the integrity of cellular membrane (Gadd, 1993). The response of algae when exposed to heavy metals includes the production of reactive oxygen species (ROS) producing enzymes, such as catalase and peroxidase and, in cases where the concentration of metals is extremely high, ROS production can reach toxic concentrations causing damage to algal cells (Pinto, 2003). At low pH, cell membranes are more susceptible to influx of metals, which may cause severe damage to the cell and ultimately death. One way to prevent the entrance of metals into the algal cytoplasm involve their ability to form complexes outside the cells, acting as a barrier (Novis and Harding, 2007). Algal tolerance to metals is also thought to be due to internal detoxification and metal transformation, extracellular binding and precipitation, impermeability and exclusion (Reed and Gadd, 1990). In fungi, the mechanisms developed to resist high concentrations of metals may include: extracellular precipitation, complexation and crystallization, biosorption and sequestration and metal transformation (Gadd, 1993).

In natural and man-made acidic environments, algal mats have been reported to populate streams, riverbanks and channels that drain metal and coal mines (Fig. 1.7). Algal species, such as *Chara* sp., *Nitella* sp., *Mougeotia* sp., *Ulothrix* sp. and others have been

found naturally inhabiting AMD (Prasad, 2007; Orandi et al., 2007). Studies on the extremely acidic river in Spain, the Tinto River, showed that a total of 14 taxa were recognised as constituents of the eukaryotic group and the biofilms observed along the river were dominated by species of *Dunaliella* and *Cyanidium* (Aguilera et al., 2007). Amaral et al. (2002) reported that more than 60% of the total biomass was composed by a highly diverse algal community.

Most acidic mine waters contain relatively low concentrations of dissolved organic carbon (DOC), mainly because primary productivity is limited by low nutrient concentrations, high metal concentrations and high acidity (Hamsher et al., 2003). Algal primary production in AMD also depends on other limiting factors, such as light intensity (Gyure et al., 1987). Ferric hydroxide precipitates deposited onto the stream bed can severely impact light penetration, limiting photosynthesis which in turn can disrupt the ecosystem. Fungi occur in a wide pH range (pH 1 - 11) and have been detected in acidic environments, such as volcanic springs, industrial wastewaters and AMD (Gross and Robbins, 2000). Most of them are acid-tolerant (e.g. *Aspergillus* sp., *Penicillium* sp.) but acidophilic fungi have also been reported (e.g. *Acontium velatum*, *Geotrichum candidum*, *Scytalidium acidophilum*) (Das et al., 2009).

Algae and fungi can influence the remediation of acidic metal-rich wastewaters in several ways, though little is known about their direct contribution to the AMD treatment. One of the most important roles of algae on AMD is thought to be the production of organic compounds used by heterotrophic microorganisms, such as sulfate-reducing bacteria which produce alkalinity and hydrogen sulfide (Molwantwa et al., 2000). Das et al. (2009) listed several studies using algae for AMD remediation as carbon source for SRB, absorption and adsorption agents, alkalinity production by nitrate and inorganic carbon assimilation, etc..

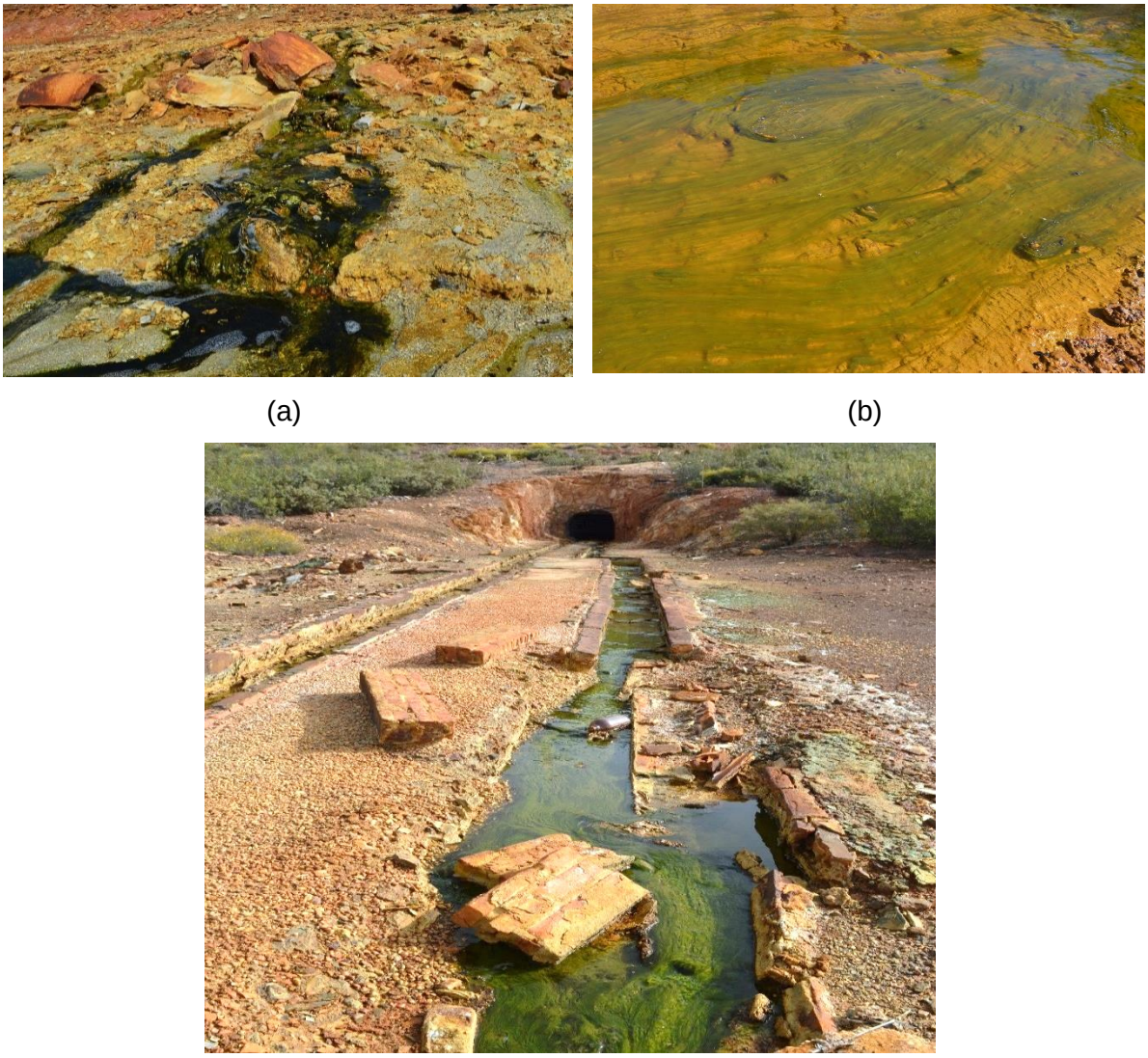

(a) (b)

(c)

**Fig. 1.7.** Surface algal growth on a microbial mat in a stream draining abandoned copper mines in the Iberian pyrite belt (a) San Telmo, Spain, (b) São Domingos, Portugal and (c) Cantareras, Spain.

Rowe et al. (2007) described the microbial community and geochemical dynamics in an acidic stream draining a copper mine in Spain. Evidence of micro-algae supporting SRB growth was based on field analysis by the increase of DOC concentrations in the section of the channel that received sunlight comparing to that within the adit, where no algal or bacterial streamer growth was observed. Laboratory analysis also confirmed the production of organic compounds by one of the indigenous algae which was used to support the growth of heterotrophs. The geochemical dynamics proposed by Rowe et al. (2007) is shown in Fig. 1.8. In brief, the surface layer of the acid streamer growth in the drain channel was dominated by photosynthetic acidophilic algae (CL1). The primary producers then release DOC, which is used as substrate for the heterotrophic bacteria in the underlayer (CL2 and CL3) while the

CL4 layer is populated by sulfate-reducing bacteria, that generates $H_2S$ and precipitates copper sulfide.

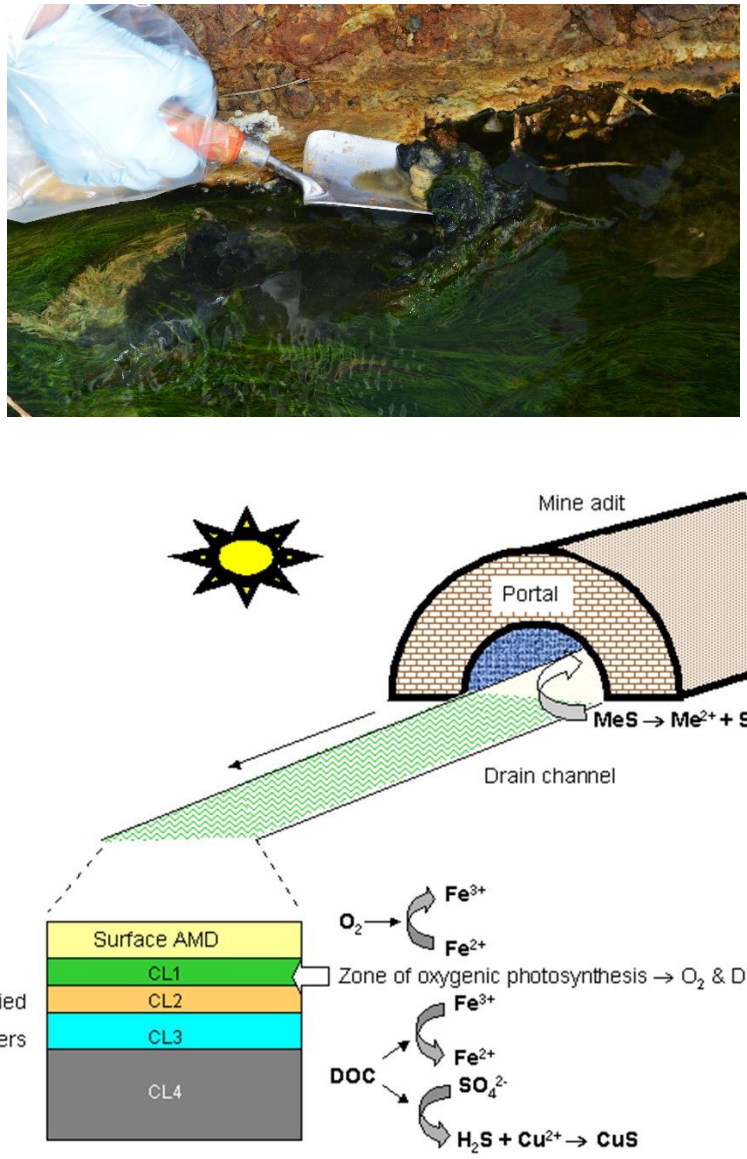


**Fig. 1.8.** Stratification of an acidic stream draining the abandoned Cantareras mine in Spain (top) and model of the biogeochemical cycling of iron and sulfur at the abandoned Cantareras mine proposed by Rowe et al. (2007) (bottom).

The use of harvested algal biomass to support bacterial sulfate reduction was also investigated by Russell et al. (2003). The green algae *Carteria* sp. and *Scenedesmus* sp., isolated from an artificial wetland filter at the Ranger uranium mine, Australia were used in the experimental work. Manganese (II) and $UO_2^{2+}$ were successfully removed from the mine water, but little sulfate. Results of the experiment showed that bacterial sulfate reduction was

supported solely by degradation of algal biomass and sulfate concentrations decreased. It has also shown that concentration of biomass directly impacted daily sulfate reduction rates. Boshoff et al. (2004) reported an upflow anaerobic bioreactor fed with dried *Spirulina* sp. as organic carbon source and results showed that sulfate reduction occurred, however only 31% of added biomass was found to be used by SRB, suggesting that the low efficiency was due to other microbial reactions competing with SRB for electron donors. The High Rate Algal Pond (HRAP) technique has been successfully applied in order to provide carbon from algal biomass for SRB-mediating AMD treatment (Molwantwa et al., 2000). Mixed algal cultures were grown under optimized conditions for maximum EPS production. Results showed that 57% of the sulfate present was removed by a mixed population of SRB within 14 days using harvested EPS fractions.

While these studies have shown that algal biomass does provide organic carbon for SRB growth; however, the efficiency of biomass utilization in commercial scale is still below expected level (Das et al., 2009).

### *1.3.3 Effects of acid mine drainage on animal, plant and microbial life*

The oxidation of sulfide minerals generates sulfuric acid which, in turn, promotes the solubilisation of a wide range of metals, including aluminium and transition metals. Once this acidic metal-rich waters flows into groundwater, rivers and streams, severe environmental problems can arise. Acid mine drainage is particularly toxic to aquatic life forms and it can destroy whole ecosystems (Singh, 1987).

Many of the components and pollutants in AMD are dangerous to human life, though to cause any effect on human health it is necessary to be exposed to the pollutants (Simate and Ndlovu, 2014). Metals, such as aluminium and cadmium and metalloids, such as arsenic, are extremely toxic and are thought not to have any biological function, whereas the transition metals copper, cobalt, zinc are relatively less toxic, but important in biochemical reactions acting for example as co-factors. Iron is the least toxic of them and by far the most important transition metal that has a function in living systems (e.g. iron-containing proteins for oxygen transport and electron transfer). However, exposure to high concentrations has serious implications on human and animal health due to their acute and chronic toxicity (Ndlovu et al., 2013). These metals are threatening to humans and animals because of their ability to persist in natural ecosystems for an extended period and to accumulate in different levels of the biological chain causing therefore acute and chronic diseases (Simate and Ndlovu, 2014). In biological systems, transition metals, such as mercury, lead, cadmium, etc. can act disrupting vital metabolic functions by: (i) accumulating in the organs, such as kidneys, brain, heart and

liver and (ii) inhibiting absorption of nutritional minerals. For example, exposure to high concentrations of mercury and chromium can cause damage to the nervous system whereas cadmium can cause lung and kidney damage, bone marrow cancer, renal disfunction, etc. (Singh, et al., 2011; Monachese et al., 2012). The extreme acidity of AMD can also have a destructive effect on biological systems, especially in aquatic ecosystems. Animal cells (as well as human cells), have a circum-neutral cytoplasmic pH (~ 7) at which all metabolic pathways and enzymatic reactions are active and, in cases where the external pH is lower (or higher), mechanisms to maintain the pH gradient are needed. For example, sulfuric acid in water can directly and indirectly affect the survival of freshwater fish by promoting formation of mucus in their gills, which preclude intake of oxygen potentially causing asphyxia and/or by releasing toxic metals, such as aluminium ($Al^{3+}$), which can accumulate in their organs, causing severe damage and ultimate death (Solomon, 2008).

Contamination of soil by transition metals can severely impact the growth of various plants. The presence of potentially toxic metals in plant tissue can cause oxidative stress leading to cellular damage and imbalance of ionic homeostasis (Yadav et al., 2010). For example, nickel can cause reduction of seed germination, protein and chlorophyll production whereas copper can inhibit photosynthesis and reproductive process (Gardeatorresdey et al., 2005; Akpor and Muchie, 2010). The effects of acidity on plants is mainly related to the availability of macro- and micro-nutrients in the soil which dictates the growth of different plants. Nitrogen, phosphorus and potassium become increasingly unavailable to plants and calcium and magnesium may be deficient or even absent in low pH soils. In addition, low pH can affect the microbial community in the soil which are responsible for improving soil tilth, aeration, root development and better nutrient uptake (Halcomb and Fare, 2002).

In aquatic ecosystems, organisms tend to accumulate metals directly from contaminated water and indirectly via the food chain (Khayatzadeh and Abbasi, 2010). Acute exposure of transition metals, such as zinc, lead, cadmium and copper can kill aquatic organisms immediately whereas chronic exposure can cause non-lethal effects, such as deformities, reduced reproduction, but also mortality (Lewis and Clark, 1997). The effect of pH on aquatic life can vary depending on its values, i.e. there is no definitive pH range within which all aquatic organisms are unharmed and outside which detrimental effects occur, though there is a gradual “weakening” in tolerance outside the “normal” range (pH 6.0 – 8.5) (Khayatzadeh and Abbasi, 2010). Values of pH within 6.5 and 9.0 are harmless to most fish, below 3.5 and above 11.0 are lethal to all fish, though some plants and invertebrates can survive. In freshwater lakes and streams with pH values between 5.0 and 6.0, a great change in ecology occurs in terms of diversity, less diversity of fish (e.g. salmon), algae, zooplankton and aquatic insects (Thoreau, 2002).

## 1.4 Prevention of acid mine drainage

As highlighted previously, the environmental effects caused by generation and migration of AMD are of a great concern. Environmental agencies all around the world have been implementing more strict laws regulating industrial effluent discharge levels and disposal. Besides, a considerable amount of research has been dedicated to the development of sustainable prevention and remediation processes of AMD.

Oxidation of sulfide minerals occurs naturally in the environment, though the exposure of these minerals to air, water and microorganisms, as a result of mining activities, can greatly accelerate the oxidative process. To prevent generation of AMD at source, sulfide minerals need to be protected from these main reactants. The traditional technique used is to remove water (by pumping) before its contact with sulfide minerals, which helps to minimise AMD formation, though it does not eliminate it (Simate and Ndlovu, 2014). Source control techniques developed in the last decades to prevent or minimise the formation of AMD include (Johnson and Hallberg, 2005; Zinck et al., 2010; Olds et al., 2012; Blowes et al., 2014, Johnson et al., 2008):

(i) control of water migration: water is diverted away from the waste materials;
(ii) flooding/sealing of underground mines: prevent water and air infiltration;
(iii) underwater storage: water acts as a diffusion barrier to oxygen, since this is much less reactive underwater, due to its very low solubility;
(iv) dry covers: isolation of sulfide-containing wastes, limiting the access to water and oxygen using synthetic materials (e.g. geosynthetic clay layers, plastics) or earthen materials (e.g. soil, organic materials, such as wood wastes);
(v) blending of mineral wastes: mixture of acid generating and acid consuming materials;
(vi) use of anionic surfactants: inhibit bacterial activity, preventing acid generation;
(vii) “bioshrouding”: biofilm formation due to microbial colonisation of sulfide minerals by iron-reducing bacteria, limiting access of iron-oxidizers to attach to and oxidize minerals.

Despite all different techniques developed over the years to minimise or eliminate formation of AMD, they have been proven costly, impractical and/or inefficient in a long-term (Kefeni et al., 2017). Therefore, studies have mostly been directed towards migration control of the resulting drainage.

## 1.5 Remediation of acid mine drainage

Remediation techniques have been extensively discussed in the literature (Skousen et al., 1998; Johnson and Hallberg, 2005; Egiebor and Oni, 2007; Ñancucheo et al., 2017; Kefeni et al., 2017). In brief, options for AMD treatment are typically divided in two categories: abiotic and biological systems. Within these categories, there are subgroups described as either active or passive processes (Fig. 1.9). The choice of options to treat AMD rely on several factors, including AMD chemistry, location, and environmental and economic factors. In general, active methods are usually more appropriate to be applied in mines that are still in operation, where fast remediation is required whereas passive methods have been developed towards abandoned mine sites which require a low cost, long lasting and environmentally-friendly option with no need of artificial energy (Simate and Ndlovu, 2014).

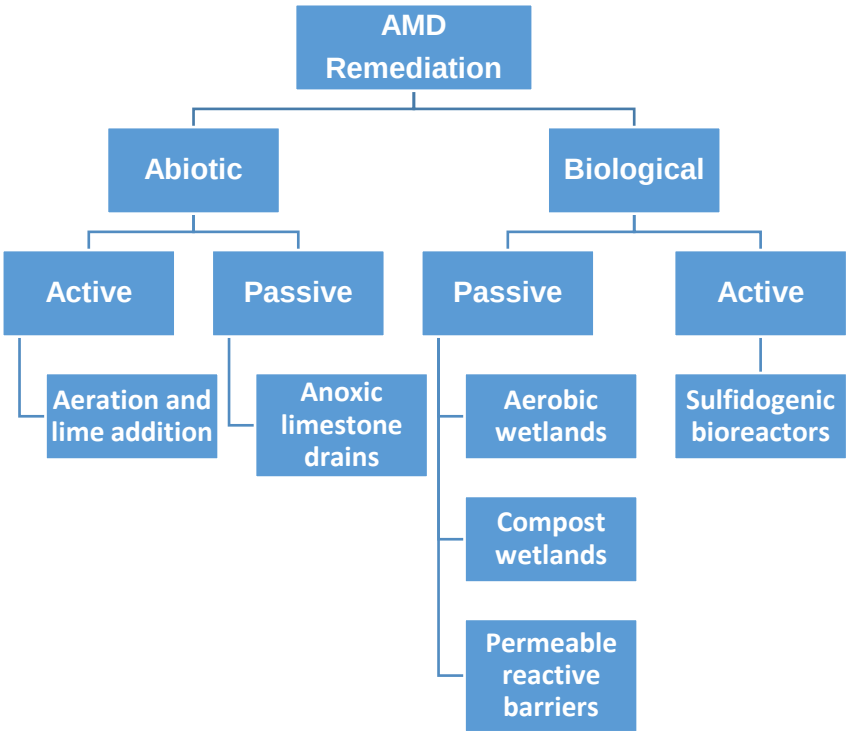


**Fig. 1.9.** Abiotic and biological strategies for remediating metal-contaminated mine waters.

### *1.5.1 Abiotic treatment*

The most widely used abiotic approach to mitigate the impact of acid mine drainage is to use alkaline chemicals to neutralise pH and remove metals, as carbonates and hydroxides, combined with aeration to promote oxidation of ferrous iron. Among the most popular alkaline industrial chemicals are: limestone ($CaCO_3$) and soda ash ($NaCO_3$), sodium and ammonium hydroxides and calcium oxide (CaO) (Watten et al., 2005). In brief, this active process

involves: (i) addition of alkaline chemicals to increase pH, (ii) active aeration, (iii) addition of a chemical flocculant agent to promote the rapid settling of metal hydroxide/carbonate flocs and (iv) dewatering of the sludge to reduce its bulk, which typically contains ~ 2-4% solids (Johnson and Hallberg, 2005). These chemicals are commercially produced and considerably expensive as well as infrastructure and operating costs. Besides, the final product is mixed-metal sludge that contains potentially valuable metals from the mine waters which are not recovered but are locked up in the sludge produced. These are usually categorised as hazardous wastes and require disposal in designated landfill sites. In the long term, metals (and As) can be remobilised from these sludge and released into the environment (Veloso et al., 2012).

An alternative (passive) approach for addition of alkalinity to remediate AMD is the use of anoxic limestone drains (ALD). Acid mine drainage percolates through trenches which contain a plastic liner surrounding a layer of limestone and a plastic liner covering the limestone bed, which are designed to exclude entrance of oxygen (Hedin et al., 1994). The aim of this system is to increase the pH of AMD by adding alkali and maintain iron as $Fe^{2+}$, which would avoid its oxidation and subsequent precipitation of ferric hydroxides on the limestone layer, causing it to be passivated (Johnson and Hallberg, 2005). The key for AMD neutralisation in these systems relies on limestone dissolution, which consequently increases the concentration of alkalinity within the drain. ALD systems often require low maintenance after constructed, though metal removal must occur downstream of the drains or as an integrated system especially in cases of aluminium and ferric iron-rich AMD (e.g. ALD and aerobic/compost wetlands). The major drawback of these systems is that after a long-term performance the drains can get clogged with particulate materials and hydroxide precipitates which may cause premature failure (Kleinmann et al., 1998).

In recent years, research studies regarding the use of naturally available resources for remediating AMD have increased. Natural materials, such as crushed seashell, lignite, bentonite and attapulgite have been studied and found to be effective in removing metals from contaminated waters. For example, crushed seashell, which is a hard material mainly formed by calcium carbonate, has been used as an absorption medium for trace metals. Masukume et al. (2014) studied the effectiveness of the crushed seashells absorption medium in batch and column systems and revealed that the use of this low-cost material has a great potential as an alternative for AMD treatment. Falayi and Ntuli (2014) reported the use of inactivated attapulgite (a magnesium aluminium phyllosilicate) as an adsorbent for the removal of trace metals from a drainage of a gold mine. Removal of metal ion in this study was remarkable with over 95% of copper, nickel and ferrous iron removed after a reaction time of 4h. Even though

these natural resources have a high metal adsorption capacity, their cost effectiveness and desorption techniques to recover metals must be considered (Kefeni et al., 2017).

Plant and animal-based wastes, such as dairy manure compost and spent coffee grounds have been investigated as bio-sorbents for AMD treatment. For example, biochar is a carbon-rich product generated from thermal decomposition of plant and animal biomass under limited supply of air. It is important for stable metal immobilisation due to formation of metal complexes and precipitates hindering re-mobilisation of toxic metals (Uchimiya et al., 2010).

### *1.5.2 Biological treatments*

#### 1.5.2.1 Passive systems

The passive systems most commonly used to remediate AMD are permeable reactive barriers (PRB) and constructed wetlands. The former is used to treat polluted groundwater and consist of a reactive material mix (organic solids and limestone) buried in a narrow trench that is sufficiently permeable that contaminated water is treated as it flows through the barriers. Kefeni et al. (2017) reported that the reactive materials may also include zero-valent iron (ZVI), and less often modified zeolites, limestone, activated carbon and organic substrates inoculated with SRB, and listed the existing biological PRB installed worldwide for the removal of different type contaminants from the groundwater, which included Shilbottle in North-east England, UK and Aznalcólla in the vicinity of Seville, Spain.

Constructed wetlands are divided into two groups: aerobic and anaerobic. In aerobic wetlands, the main reaction that occurs is ferrous iron oxidation and subsequent hydrolysis of ferric iron, which is a net acid generating reaction, therefore this treatment is usually applied to net alkaline mine waters. These systems are relatively shallow in order to maintain oxidizing conditions and macrophytes are planted to help regulating water flow and to filter and stabilise the accumulating ferric precipitates. In addition, some aquatic plants may accelerate $Fe^{2+}$ oxidation rates by transferring oxygen from aerial parts to their roots systems (Brix, 1997).

In contrast, with compost bioreactors (also referred to as anaerobic wetlands) the main reactions involved in AMD remediation are mediated by bacteria that degrade the compost into small molecular weight organic compounds which are then metabolised by sulfate-reducing bacteria, generating alkalinity and sulfide. The reductive reactions that occur within compost wetlands are driven by electron donors that derive from the organic matrix of the compost itself (e.g. cow, horse manure or mushroom compost) and the choice of organic materials used vary according to their effectiveness and local availability.

Constructed wetlands/compost reactors have the advantage of low running costs, though their construction can be expensive and large areas of suitable land are required. More significantly, compost-based systems are noted to have variable (and often non-predictable) performance and, as with active chemical treatment, metals in AMD are not recovered but are contained in the spent composts, which must be disposed of as hazardous waste materials.

#### 1.5.2.2 Active systems: sulfidogenic bioreactors

Given the issues associated with passive biological systems (e.g. the generation of new wastes that require further treatment or disposal), alternative methods have been considered. Among these are active biological systems, which generally involve the use of bioreactors to precipitate metals as oxy-hydroxide phases (mostly iron) (Hedrich and Johnson, 2012; Jones and Johnson, 2016) or as sulfides (copper, zinc etc.). These systems were designed not only for neutralizing AMD, but to recover potentially valuable metals and reduce the amount of waste that requires disposal (by recycling and reusing water and metals). In addition, the metals recovered from wastewaters can be used to off-set the cost of the treatment while dealing with the environmental problem.

Sulfate reduction can be beneficially applied to biotechnologies which harness the metabolic diversity and versatility of SRB in order to address and design bioremediation processes. Chemical or biogenic sulfide not only remove potentially toxic metals from wastewaters, but can also provide a selective metal precipitation. The metal removal is based on the reaction of $H_2S$ with some metal cations to form insoluble metal sulfide precipitates, usually metals with +2 oxidation states, such as Zn, Fe, Cu, Ni, and Cd (Lewis, 2010).

Tabak and Govind (2003) reported the use of polypropylene hollow fibre membrane bioreactor systems for remediating acid mine water from the Berkeley Pit (Montana, USA) using SRB obtained from an anaerobic digester sludge. One of the advantages of using membrane bioreactors is that it prevents washout of cells as occurs in bioreactors using free flowing or suspended cultures. Results showed that SRB were immobilised on the surface of the hollow fibre membranes and sulfate reduction rates were considered feasible for treating the acidic mine water. Based on the data obtained, a pilot-scale was designed using membrane modules operated in series in order to reduce the sulfate content more rapidly and effectively.

Macingova and Luptakova (2012) described the use of a selective sequential precipitation process for remediating AMD containing Fe, Cu, Al, Zn and Mn using both biological and chemical processes. Iron was completely removed by oxidizing $Fe^{2+}$ using hydrogen and subsequent precipitation with sodium hydroxide. Sulfate-reducing bacteria were

used to generate $H_2S$ that was directed to a contactor filled with AMD where metal sulfide precipitation occurred. After filtration of the precipitate, the pH of the filtrate was adjusted to a higher value and metal hydroxide precipitated. Metal hydroxide precipitates were removed by filtration, and the filtrate was returned to the contactor and the process repeated. Over 99% of the metals were removed using this approach.

Sulfate reduction has been widely applied for remediation of metals, metalloids and sulfate in laboratory scale, however there are only two commercial-scale applications based on microbial mediated sulfate reduction using bioreactor systems for the treatment of acidic metal-rich wastewaters: the BioSulfide®, developed by BioteQ, Canada and the integrated system SULFATEQ™ and THIOTEQ™ Metal by Paques, The Netherlands.

The BioSulfide® process involves the precipitation and selective recovery of metals using hydrogen sulfide generated by the reduction of zero-valent sulfur by sulfur-reducing bacteria (Eq. 1.8). By using sulfur rather than sulfate, no process water is required other than that contained in the reagents.

$$4S^0 + CH_3COOH + H_2O \rightarrow 4H_2S + 2\,CO_2 \qquad \text{(Eq. 1.8)}$$

A simplified flowsheet of the process is shown in Fig. 1.10. In brief, $H_2S$ generated in the sulfidogenic bioreactor is delivered to the contactor where copper is precipitated from the stockpile drainage as CuS. The final product contains approximately 40% Cu. The off-gas in the contactor is directed to the bioreactor where it is used to strip $H_2S$ from the bioreactor liquor to the gas phase. Nitrogen is recycled as a carrier gas. The sulfide concentrate is recovered in a clarifier and subsequently dewatered using a filter press. This product is then sent to smelters. The copper-free solution in the clarifier is reused in further copper leaching. In cases where more than one metal product is to be recovered, multiple contactor and clarifier units are used (Ashe et al., 2008).

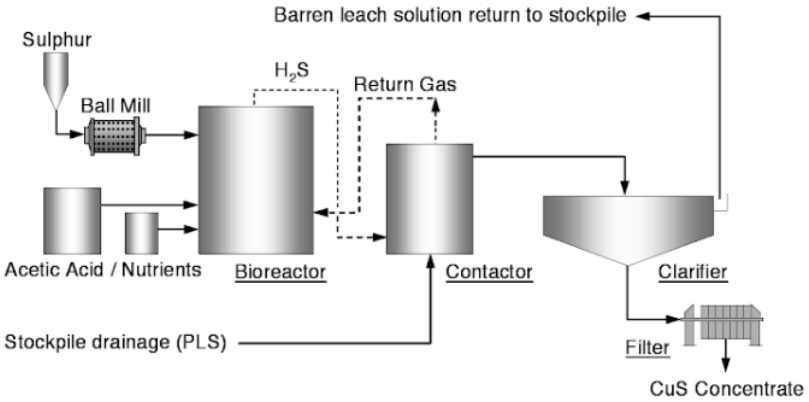


**Fig. 1.10.** Schematic representation of the BioSulfide® process (from Ashe et al., 2008).

The SULFATEQ™/THIOTEQ™ process operates at a zinc smelter in Budel (The Netherlands) and involves the treatment of a zinc sulfate-containing process water via sulfate reduction and oxidation of the excess $H_2S$ into ZVS (Fig. 1.11). Sulfide is generated in a sulfate-reducing gas lift reactor which uses a steam-reforming natural gas as electron donor. The gas is composed by 76% $H_2$, 20% $CO_2$, 3% $N_2$ and 1% CO. The $H_2S$ generated is directed to a contactor where zinc is precipitated as sulfide. Next, ZnS is collected and reused in the smelters. Using this technology (THIOTEQ™ Metal), 95% of the dry sludge generated is zinc sulfide. The excess of hydrogen sulfide, present as $HS^-$, is oxidized to $S^0$ under oxygen-controlled conditions by sulfide-oxidizing bacteria in the $S^0$-generating bioreactor (SULFATEQ™). Both ZnS and $S^0$ generated in this process can be reused.

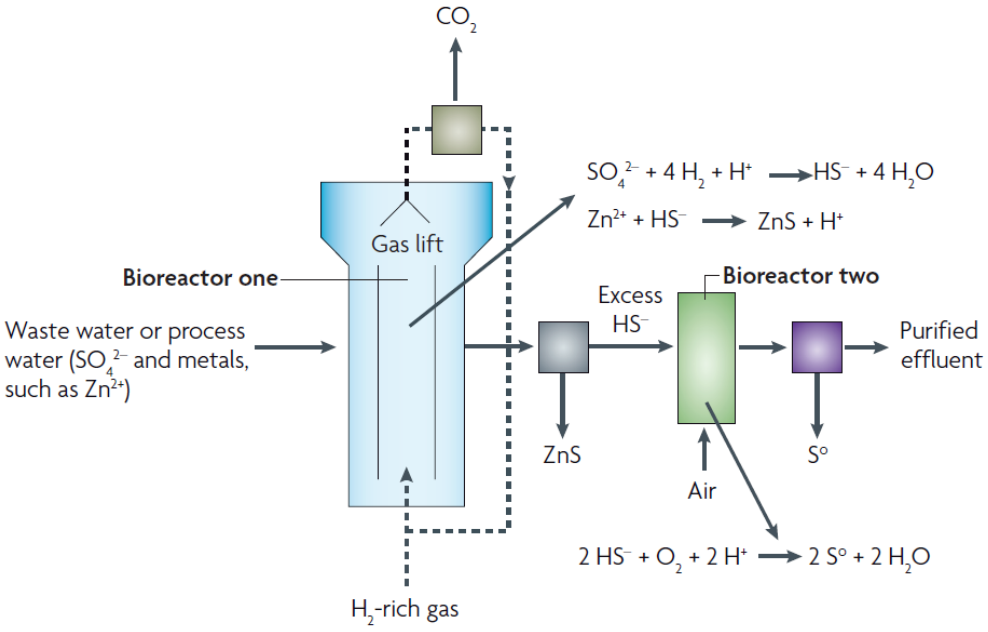


**Fig. 1.11.** Schematic representation of the SULFATEQ™/THIOTEQ™ processes (from Muyzer and Stams, 2008).

Both of the above processes, however, use bacteria that are acid-sensitive (even to moderate acidity) and some metals, and therefore these bacteria need to be isolated from the AMD itself. As a result, the engineering complexity of the reactor systems can cause financial implications for both their construction and operation. To circumvent this issue, the development of acidophilic sulfidogenic bioreactors using consortia of acidophilic/acid-tolerant sulfate-reducing and other acidophilic bacteria have been reported (Jameson et al., 2010; Ñancucheo and Johnson, 2012a, 2014; Hedrich and Johnson, 2014; Santos and Johnson, 2017). In this case, the contact between these bacteria and AMD is feasible, and a single bioreactor can be used to grow the bacteria and to precipitate target metals. Since the reaction

catalysed by these bacteria consumes protons, the bioreactors can be operated as continuous flow systems where pH is maintained by balancing the bacterial production of alkalinity by the inflow of acidic mine water. The system operates with minimal control and input of reagents, and has proven to be robust throughout continuous testing using laboratory modules and different water chemistries. This greatly reduces engineering complexity and operating costs, making the acidophilic sulfidogenic system a highly attractive alternative to existing technologies. Metals precipitated in the bioreactors can be recovered either as sulfide minerals, or remobilized (by sulfide-oxidizing acidophiles) to generate concentrated metal liquors, from which metals can be reclaimed in pure forms using, for example, solvent extraction and electrowinning (SX/EW).

In addition, biosulfidogenesis can be used as an integrated approach to treatment metal-rich mine water and, at the same time, selectively recover potentially valuable metals. The choice of the systems to be applied will depend mainly on the AMD composition. For example, Hedrich and Johnson (2014) described an integrated system designed to selectively remove the two major metals (zinc and iron) from an AMD at the Maurliden mine in Sweden (Fig. 1.12).

The first step was to remove soluble arsenic from the mine water upstream of the bioreactor modules using schwertmannite as an adsorbent agent avoiding the co-precipitation of this toxic metalloid in the following modules. The second step involved a bioreactor used to oxidize ferrous iron in the AMD to ferric, and to produce schwertmannite, a small portion of which (~ 11%) was used to remove As in the previous step. Soluble copper and cadmium were removed in the next stage by contacting with biogenic $H_2S$ in an off-line reactor vessel. The partly-processed mine water was then dosed with glycerol and fed into an acidophilic sulfidogenic bioreactor. By maintaining the pH of this unit at 4.0, co-precipitation of aluminium and manganese was avoided while most of the zinc was removed. The integrated system developed by Hedrich and Johnson (2014) did not include modular systems to remove aluminium and manganese from the Maurliden AMD. However, the use of either a second, higher pH sulfidogenic bioreactor (to remove Al as hydroxysulfate minerals) or by addition of sodium hydroxide would allow both metals to be selectively precipitated. As an alternative, manganese could also be removed using microbially catalysed oxidation of Mn (II) to Mn (IV) and precipitation of manganese oxides (section 1.5.3).

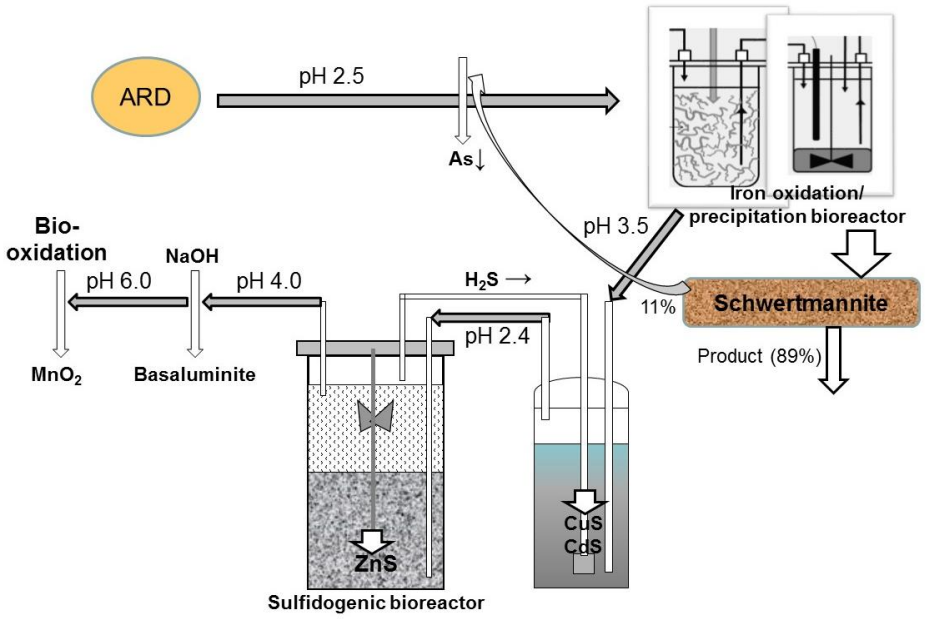


**Fig. 1.12.** Schematic representation of the integrated system designed to remediate AMD at the Maurliden mine, Sweden (modified from Hedrich and Johnson, 2014).

### *1.5.3 Remediation of manganese-rich wastewaters*

Manganese, like many other transition metals, can occur in elevated concentrations in coal and metal mine wastewaters. The removal of this metal from surface- and groundwater is desirable because as well as iron and aluminium, manganese hydrolysis also contributes to the total mineral acidity of mine waters. Soluble manganese can also be problematic in domestic water supplies, by obstructing water distribution networks (due to oxidation of soluble Mn (II) and precipitation of Mn (IV)), impairing a metallic taste to water and staining laundry (Hallberg and Johnson, 2005).

Manganese (II) oxidation occurs at circum-neutral pH and can be catalysed by heterotrophic microorganisms found in different habitats, such as the deep sea (forming manganese nodules), hydrothermal vent plumes, pipes conducting Mn-rich waters, stones submerged in streams and rivers, etc. Manganese (II)-oxidizing bacteria include *Roseobacter* sp. strain AzwK-3b, *Bacillus* sp. strain SG-1, *Leptothrix* sp., *Pseudomonas putida* GB-1 and *Aurantimonas manganoxydans* (all of which are *Proteobacteria*), and members of the *Firmicutes* and *Actinobacteria* phyla (Akob et al., 2014). Several fungal species belonging to the phyla *Ascomycota* and *Basidiomycota* have also been identified as Mn (II)-oxidizers (Miyata et al., 2004; Bohu et al., 2016). The most studied Mn (II)-oxidizing fungi are the white rot fungi (largely *Basidiomycota*), known for their abilities to degrade lignin and a broad range of aromatic pollutants. Manganese (II) oxidation by these organisms is primarily a result of

manganese peroxidase (MnP) activity (Gadd, 2010; Tebo et al., 2005). The Mn (II)-oxidizing *Ascomycota* belong to a number of different genera, such as *Pyrenochaeta, Alternaria, Phoma*, and *Acremonium*, though the mechanism of Mn (II) oxidation by *Ascomycete* fungi remains poorly understood (Miyata et al., 2004; Tebo et al., 2005; Hansel et al., 2012; Miyata et al., 2007).

With more stringent discharge limits, technologies for removing manganese from wastewaters have been developed. However, many of them are found to be impractical and/or expensive, such as (i) aerobic wetlands since biological Mn (II) oxidation does not occur rapidly in presence of ferrous iron, thus manganese is not removed efficiently, (ii) compost wetlands and acidophilic sulfidogenic bioreactors since the formation of MnS is favoured in alkaline sulfide-rich waters (pH > 8) due to its high solubility product ($K_{sp}$ of $3 \times 10^{-11}$ $M^2$).

A more effective approach to remove soluble manganese from wastewaters is based on the formation of Mn (IV) oxides (which have lower solubility product than Mn (II) sulfides) by oxidation of Mn (II) to Mn (IV) and precipitation of solid-phase Mn (IV) oxides. Thornton (1995) described an abiotic Mn-removal system using limestone-filled columns in order to increase the pH, resulting in oxidation of soluble Mn (II) and subsequent precipitation of Mn (IV) oxides. In terrestrial environments, birnessite ($(Na,Ca)_{0.5}(Mn^{4+},Mn^{3+})_2O_4 \cdot 1.5H_2O$), lithiophorite ($(Al,Li)MnO_2(OH)_2$) and hollandite ($Ba(Mn^{4+}_6Mn^{3+}_2)O_{16}$) are the most common Mn oxides (Bohu et al., 2015).

Alternative approaches for removing Mn (II) have been described, some of them relying on oxygenic photosynthesis to increase the pH to above which Mn oxidation can occur, such as the use of photosynthetic algal ponds (Phillips et al., 1995) or the use of cyanobacteria-immobilized columns (Bender et al., 1994). To allow algae to proliferate in such systems, sufficient solar radiation, warm temperatures and low turbidity are necessary to promote photosynthesis.

More recently, novel technologies have been described using fixed bed bioreactors containing ferromanganese nodules (Hallberg and Johnson, 2005) and Mn(IV)-coated pebbles from a freshwater stream (Mariner et al., 2008). In both studies, the manganese-oxidizing bioreactors were aerated, and the immobilised Mn-oxidizers efficiently catalysed the removal of soluble manganese, by oxidation of Mn (II) and subsequent precipitation of Mn (IV) within the bioreactors. Manganese-oxidizing bioreactors can take place in integrated systems as a final step of mine water treatments which were designed to selectively remove and recover other metals.

## 1.6 Acid mine drainage as a resource

Although acidic metal-rich wastewaters are considered a great environmental concern, they can provide valuable products. Therefore, novel remediation technologies have been designed to “extract” these products as a more cost-effective strategy. Many of the constituents of AMD are potentially valuable, though the costs of recovering them can exceed their final value. In laboratory studies, chemicals such as, ferric hydroxide, ferrite, barium sulfate, gypsum, rare earth elements, sulfur and sulfuric acid are the most common resources obtained from AMD remediation using different recovery methods (Kefeni et al., 2017). The recovery and reuse of these products is an alternative way of sustainable mining, reducing its environmental impact and the possible generation of a new income stream that can be used, at least in part, to off-set the treatment costs.

Recovery of valuable metals is the most obvious potential commercial benefit which can be obtained from AMD remediation, though other saleable products, such as sulfur and sulfuric acid, can also be reused. For example, sulfuric acid can be recovered by acid retardation and crystallization, which are currently the most promising technologies for this (Nleya et al., 2015). The removal of metals from wastewaters simultaneously remediates water, which can possibly be reused, depending on the original chemistry of the AMD and the technology used in the remediation process. Iron oxides recovered from AMD can be used as ferrite nanoparticles, pigments and additives to ceramic, manufacturing of construction materials (e.g. cement) and in preparation of catalysts, which help reducing sludge discharge and further pollution (Cheng et al., 2011; Flores et al., 2012)

Recently, rare earth elements were found in higher concentrations in AMD than in naturally occurring water bodies (Ayora et al., 2016). These elements are important raw materials used in the development of modern technology, such as magnets, light emitting diodes (LED) and rechargeable batteries. Studies focused on fuel cell technology for recovering metals from AMD is a research field on the rise. For example, oxidation and calcination of iron to form $Fe_3O_4$/carbon composite using fuel cell technology has been used as an effective catalyst in the electron-Fenton process (i.e. oxidation of organic pollutants by ferrous iron and hydrogen peroxide; Sun et al., 2015). Microbial fuel cells (MFCs) have also emerged as a promising and sustainable technology for converting organic waste into electricity through metabolic activity of microorganisms (Pant et al., 2010). Cheng et al. (2007) demonstrated the use of an AMD fuel cell which could generate electricity at power levels similar to conventional MFCs and remove dissolved iron from tested synthetic AMD solutions.

The extensive research in the last decades and the development of novel technologies for remediating acid mine drainage show how much impact these waters have on human and

animal life, water bodies, vegetation, soil, etc. and how important is the development of new remediation processes. The emerging technologies, from which the potential pollution of AMD is mitigated, and resources are recovered promise a cost-effective treatment of AMD and clean environment.

## 1.7 Scope of the current project

The present study set out to develop an integrated system in which acidic and moderately acidic metal-contaminated mine waters could be treated to mitigate its potential pollution by essentially removing and recovering metals. The project was structured as 6 main areas:

- The use of a low pH sulfidogenic bioreactor (aSRBR) to selectively precipitate and recover copper, and to concentrate and remove other chalcophilic metals from a synthetic moderately acidic mine water draining a copper mine in Brazil.
- Evaluation of performance of the aSRBR at different pH values and temperatures, and the effects of these two parameters on the indigenous microbial communities.
- Development of a biological Mn (II) oxidation system as final stage of the integrated bioremediation process.
- Assessment of solubilization of metal sulfide concentrates from the aSRBR using bioleaching experiments.
- Evaluation of the performance of the aSRBR by comparing alternative substrates to fuel biosulfidogenesis.
- Characterisation of two species of acidophilic micro-algae and their potential use as feedstock for sulfidogenic bioreactors.

# 2 Materials and Methods

*Note: this chapter describes experimental methods that were common to different research areas contained in this thesis. Specific experimental procedures and techniques are described in detail on its respective chapters.*

## 2.1 Microorganisms

The acidophilic sulfate-reducing bacteria *Desulfosporosinus* (*D.*) *acididurans (*strain M1$^T$; (Sen and Johnson, 1999; Sánchez-Andrea et al., 2015*)*, *Peptococcaceae* CEB3 (Ñancucheo and Johnson, 2012a) "*Desulfobacillus* (*Db*.) *acidavidus"* CL4 (Ñancucheo and Johnson, 2012a) and *Firmicute* C5 (D.B. Johnson, unpublished data) were sourced from the *Acidophile Culture Collection* maintained at Bangor University.

The consortium used in the acidophilic sulfate-reducing bacteria reactor (aSRBR) consisted of all the microorganisms listed above plus an enrichment culture of an anaerobic streamer mat from an acidic metal-rich stream draining an abandoned mine in the Iberian Pyrite Belt, Spain (Rowe et al., 2007).

## 2.2 Cultivation techniques

### *2.2.1 Sterilization*

Heat-sterilisation of glassware, heat-stable solid and liquid materials was carried out by autoclaving at 120ºC for 30 min. Any heat-liable or volatile solutions were filter-sterilised using 0.2 µm (pore size) nitro-cellulose filter membranes (Whatman, UK).

*2.2.2 Microbial growth media*

2.2.2.1 Basal salts and trace elements solution

Liquid and solid media were prepared for different purposes using the basal salts and trace elements formulations listed in Table 2.1 and Table 2.2. Reverse osmosis (RO)-grade water RiOs™ 8 (Millipore, UK) was used to prepare liquid and solid media unless otherwise stated.

**Table 2.1.** Composition of the 50x concentrate basal salt solution.

| Chemicals | Concentration (g $L^{-1}$) |
|---|---|
| $Na_2SO_4 \cdot 10H_2O$ | 7.5 |
| $(NH_4)_2SO_4$ | 22.5 |
| KCl | 2.5 |
| $MgSO_4 \cdot 7H_2O$ | 25 |
| $KH_2PO_4$ | 2.5 |
| $Ca(NO_3)_2 \cdot 4H_2O$ | 0.7 |

**Table 2.2.** Composition of the trace elements solution. This mixture is 1000x concentrate.

| Chemicals | Concentration (g $L^{-1}$) |
|---|---|
| $ZnSO_4 \cdot 7H_2O$ | 10 |
| $CuSO_4 \cdot 5H_2O$ | 1.0 |
| $MnSO_4 \cdot 4H_2O$ | 1.0 |
| $CoSO_4 \cdot 7H_2O$ | 1.0 |
| $Cr_2(SO_4)_3 \cdot 15H_2O$ | 0.5 |
| $H_3BO_3$ | 0.6 |
| $NaMoO_4 \cdot 2H_2O$ | 0.5 |
| $NiSO_4 \cdot 6H_2O$ | 1.0 |
| $Na_2SeO_4 \cdot 10H_2O$ | 1.0 |
| $Na_2WO_4 \cdot 2H_2O$ | 0.1 |
| $NaVO_3$ | 0.1 |

To prepare the trace elements solution, 800 mL of RO-grade water was adjusted to pH 2.0. Then all the listed salts were added, in the order given, each being allowed to dissolve before adding the next. After addition of sodium vanadate ($NaVO_3$) the solution was made up to 1000 mL adjusted at pH 2.0, and autoclaved.

Ferrous sulfate ($FeSO_4 \cdot 7H_2O$; 100 µM) was added to all solid and liquid media that did not contain yeast extract. Ferrous sulfate stock solution (1 M) was prepared in acidic water (pH 1.8 – 2.0) and filter-sterilized to avoid iron oxidation caused by autoclaving.

2.2.2.2 Liquid media

The liquid media used routinely to grow sulfate-reducing bacteria contained basal salts and trace elements solution (ABS/TE), 0.1 g $L^{-1}$ yeast extract (YE), 4.0 mM $MgSO_4 \cdot 7H_2O$, 4.0 mM $ZnSO_4 \cdot 7H_2O$, with pH adjusted to 3.5 - 4.0. Glycerol (2.5 mM) was added as the electron donor. Liquid media and feed liquor for aSRBR were prepared as described above, unless stated otherwise.

2.2.2.3 Overlay solid media

Liquid media, described in section 2.2.2.2 (referred to as solution A), and agarose 2% (referred to as solution B) were heat sterilised separately and combined after cooling to avoid acid-hydrolysis of the polysaccharide, agarose. After autoclaving, solution A was cooled to about 40ºC and ferrous sulfate was added in a final concentration of 100 µM. Solution B was added to solution A and mixed thoroughly.

The overlay technique comprises a doubled-layered plate in which the bottom layer is inoculated with an acidophilic heterotroph bacterium (*Acidocella aromatica* strain $PFBC^T$ or *Acidiphillium cryptum* strain SJH) and the upper layer without inoculum (Ñancucheo et al., 2016). The heterotrophic microorganisms use the compounds released by the ongoing hydrolysis of agarose at low pH, which inhibit the growth of acidophiles (Johnson, 1995; Kusel, 2003; Johnson and Hallberg, 2009). The inoculated mixture was then poured into Petri plates to form a thin underlayer. Once these had set, the non-inoculated mixture was poured on top of it to form the overlayer. The plates were allowed to set and stored for up to 2 months at 4ºC. Composition of the solid media and organisms used in overlay plates are described in Table 2.3.

**Table 2.3** Solid media composition and microorganisms used in the overlay plate technique.

| Solid media | Chemical composition | pH | Underlay organism |
|---|---|---|---|
| **$iFe_o$** | ABS/TE; 20 mM $FeSO_4$ | 2.5 | *Acidiphilium* SJH |
| **$FeS_o$** | ABS/TE; 2.5 mM $K_2S_4O_6$; 0.025% tryptone soy broth | 2.5 | *Acidiphilium* SJH |

*2.2.3 Incubation under anaerobic atmosphere*

Cultures and experiments which required anaerobic conditions were incubated in 2.5 L sealable jars (Oxoid Ltd., UK) containing Anaero*Gen*™ AN25 anaerobic atmosphere-generating sachets where the oxygen was removed as $CO_2$. Anaerobic conditions were monitored using anaerobic indicators (Oxoid Ltd., UK) during culture incubation.

## 2.3 Mine water composition

A synthetic mine water, based on the composition of an actual mine water draining a copper mine in Pará state, Brazil, was prepared. Its chemical composition is shown in Table 2.4. As with most mine waters that drain sulfide mines, the dominant anion present was sulfate and, in this case, the dominant cation was copper. The relatively high pH (5.0) of this stream had caused rapid hydrolysis of ferric iron, and the concentration of total soluble iron measured on site was ~ 2 µM. Iron was omitted from the synthetic mine water as it was considered to be of little significance.

**Table 2.4.** Chemical composition of the synthetic AMD used in experimental work.

| Analyte | Concentration (mM) |
|---|---|
| $Cu^{2+}$ | 7.50 |
| $Ca^{2+}$ | 7.00 |
| $Mg^{2+}$ | 4.00 |
| $Na^{+}$ | 2.10 |
| $K^{+}$ | 0.28 |
| $Ni^{2+}$ | 0.25 |
| $Mn^{2+}$ | 0.15 |
| $Co^{2+}$ | 0.04 |
| $Zn^{2+}$ | 0.02 |
| $SO_4^{2-}$ | 22.1 |
| $Cl^{-}$ | 0.04 |

## 2.4 Sulfidogenic bioreactor

The aSRBR used in experimental work was similar in design and operation to those described elsewhere (Ñancucheo and Johnson, 2012a; 2014; Hedrich and Johnson, 2014). A sulfidogenic upflow biofilm reactor populated with a mixed microbial community containing

several species of aSRB and non-sulfidogenic acidophilic bacteria (section 2.1) was used in the experimental work. The bioreactor had a working volume of 2.0 L and was coupled to a FerMac 310/60 unit (Electrolab., UK) which controlled pH, temperature and agitation. pH electrode was inserted into the bioreactor vessel extended only in the liquid phase above the biofilm bed (Fig. 2.1). The volume of the bead bed in the bioreactor was ~ 1.3 L, which corresponded to 266 g dry weight of Poraver beads (D. B. Johnson, unpublished data).

Proton consumption resulting from biosulfidogenesis was counter-balanced by the inflow of synthetic AMD, which was therefore necessarily of lower pH than that of the liquid inside the bioreactor. pH homeostasis was met by coupling the pH control box in the FerMac unit with a pump that controlled the influx of AMD. Oxygen-free nitrogen (OFN) was bubbled through the bioreactor at an average of 150 mL $min^{-1}$, both to promote anoxic conditions within the vessel and to act as a carrier for the excess $H_2S$ generated.

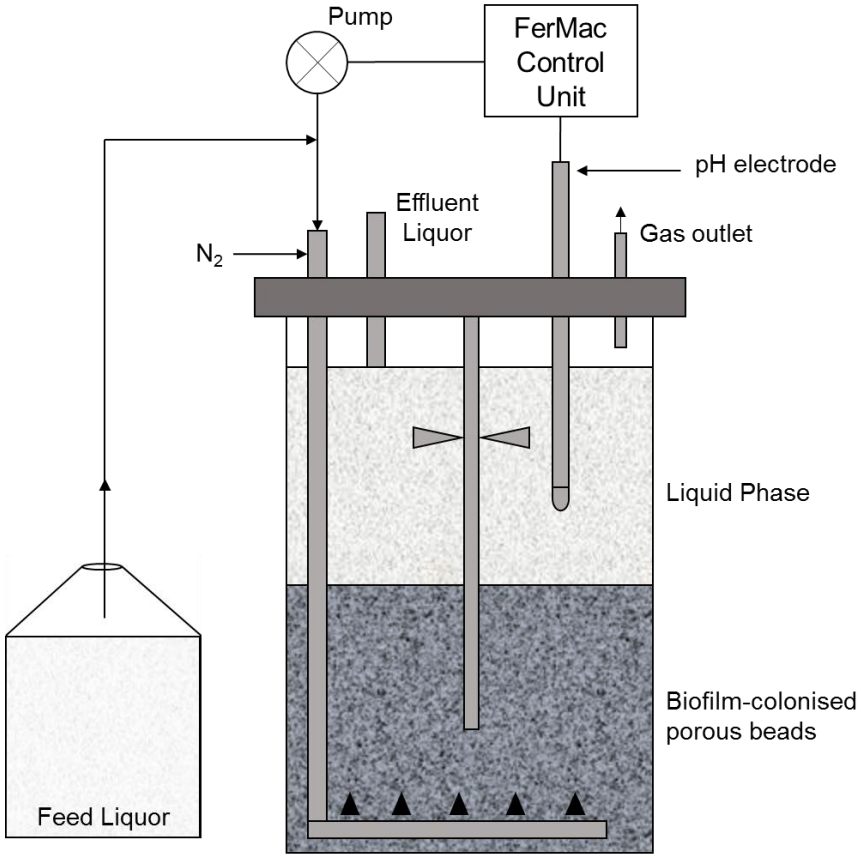


**Fig. 2.1.** Schematic representation of the low pH sulfidogenic bioreactor (aSRBR). The arrows indicate the direction of liquid/gas flow.

As indicated in Fig. 2.1, the feed liquor was delivered via an L-shaped stainless steel tube which had perforations on its lower length, causing it to percolate through the biofilm bed to the liquid phase. A drain tube placed above the liquid phase coupled to a second pump on the control unit ensured that the liquid volume within the bioreactor remained constant.

Only the liquid phase of the bioreactor was stirred gently (50 rpm) using a single impeller blade in order to not disturb the biofilm bed.

The aSRBR was set up at pH 4.0 and 30ºC supplied with a feed liquor (pH 2.5) containing ABS/TE, 0.1 g $L^{-1}$ yeast extract, 0.25 mM $FeSO_4 \cdot 7H_2O$ and 1.0 mM glycerol (as electron donor). The bioreactor was operated for 2 weeks to allow the system to pre-condition.

## 2.5 Analytical methods

### *2.5.1 Electrochemical analyses*

A pHase combination glass electrode (VWR, UK) calibrated between 1.0 and 7.0, coupled to an Accumet 50 pH meter was used to measure pH values. Redox potentials ($E_H$) were measured using a combined platinum-Ag/AgCl redox electrode (inLab®501, Mettler Toledo, USA) coupled to the meter mentioned above and calibrated against a standard (+440 +/- 5 mV; ZoBell's solution).

### *2.5.2 Colorimetric analyses*

Reagents and sample dilutions were prepared using ultrapure-grade water MiliQ® Synthesis A10 (Millipore, UK) unless otherwise stated.

#### 2.5.2.1 Determination of soluble copper concentrations

Soluble copper concentrations were determined using a colorimetric-based assay (Anwar et al., 2000). Reagents were prepared as follows: Tartrate buffer was prepared by mixing 14.11 g of potassium sodium tartrate with 100 mL RO-grade water and pH adjusted to 5.5 (0.5 M buffer final concentration). Bicinchoninic acid solution (0.2%, Sigma, USA) was diluted two-fold with tartrate buffer. Hydroxylamine solution (10% w/v) was prepared by dissolving 10 g analytical grade hydroxylamine·HCl (Sigma, UK) in 100 mL ultrapure-grade water. In order to determine total copper, 200 µL hydroxylamine solution was added to 50 µL sample. The mixture was allowed to react at room temperature for 10 min. Then, 650 µL tartrate buffer was added followed by 50 µL bicinchoninic acid solution. Absorbance was recorded at 562 nm against a reagent mix blank using a Cecil CE 1011 spectrophotometer (Cecil Instruments Ltd., UK). Calibration curve was constructed, ranging between 0.25 and 2.0 mM $Cu^{2+}$, by plotting the absorbance at 562 nm against copper concentrations.

2.5.2.2 Determination of soluble ferrous and ferric iron concentrations

Ferrous and ferric iron concentrations were determined using the Ferrozine assay (Stookey, 1970). Ferrozine reagent was prepared as follows: 50 mM HEPES buffer (11.915 g (4-(2-hydroxyethyl)-1-piperazineethanesulfonic acid) adjusted to pH 7.0 with KOH and 1.0 g ferrozine (3-(2-pyridyl)-5,6-di(4-phenylsulfonic acid)-1,2,4-triazine, disodium salt) was dissolved in 1 L RO-grade water. This solution was stored in the dark at room temperature. For the assay, 50 µL of sample (diluted with ultrapure-grade water pH 1.8, when necessary) containing ferrous iron was added to 950 µL of the ferrozine reagent and absorbance recorded at 562 nm against a blank (ferrozine reagent + 50 µL of RO-grade water). A calibration curve was constructed, ranging between 0.2 and 1.0 mM $Fe^{2+}$, by plotting the absorbance at 562 nm against ferrous iron concentrations.

To measure concentrations of total iron, an excess of L-ascorbic acid was added to the sample (or diluted sample) to reduce $Fe^{3+}$ to $Fe^{2+}$, and the solution analysed using the Ferrozine reagent. Ferric iron concentrations were determined from differences between total and ferrous iron concentrations.

2.5.2.3 Determination of soluble manganese concentrations

Soluble manganese concentrations were determined using a modified formaldoxime colorimetric method (Mariner et al., 2007). Reagents were prepared as follows: (i) FAD solution was prepared by mixing 10 g analytical grade hydroxylamine·HCl (Sigma), 5 mL formaldehyde solution 36% and 45 mL RO-grade water. (ii) $NH_4$-buffer was prepared with 7 g of ammonium chloride ($NH_4Cl$), 60 mL of ammonium hydroxide ($NH_4OH$ 35%) and 40 mL RO-grade water. (iii) 2.2 M hydroxylamine·HCl solution and (vi) 0.1 M EDTA adjusted to pH 8 with NaOH in RO-grade water. Samples were pre-filtered through 0.2 µm (pore size) filter membranes. For the assay, 0.3 mL FAD solution and 0.4 mL $NH_4$-buffer were added into 2 mL filtered sample (diluted in RO-grade water when necessary), mixed thoroughly and allowed to react for 3 min at room temperature. Then, 0.3 mL hydroxylamine·HCl solution and 0.4 mL EDTA were added into the mixture and allowed to react for 4 min. Absorbance was recorded at 420 nm against a reagent mix blank. Calibration curves were prepared, using known concentration of soluble manganese (generally between 0.25 and 1.0 µg Mn $mL^{-1}$).

## 2.6 Ion chromatography

Concentrations of acetic acid, sulfate, organic compounds and transition metals were determined using Dionex ion chromatography (Dionex, USA). Samples were pre-filtered through 0.2 µm nitro-cellulose filter membranes (Whatman, UK) and stored at -20ºC until analysed. Samples for transition metals analyses were acidified and kept at room temperature. Data obtained were analysed by Chromeleon software (version 6.4 SP2 Build 731; Dionex, USA). Reagents and sample dilutions were prepared using ultrapure-grade water (Millipore, UK).

### *2.6.1 Determination of anions*

Acetic acid and sulfate concentrations were determined using a Dionex IC25 ion chromatograph with an Ion Pac® AS-11 column, an ARSR ULTRA 4 mm suppressor and a DS11 conductivity detector. The pressure generated by a pump was maintained around 1,700 psi and 250 µL sample was injected into the system. Flow rate was set at 1.0 mL $min^{-1}$. The temperature of the column was kept at 30ºC and the suppressor current was set at 75 mA. The suppressor was used to minimize the background noise generated by temperature fluctuations in the detector. Standards solutions were prepared for each anion (0.1 – 1.0 mM for acetate and 0.5 – 5.0 mM for sulfate) and calibration curves were constructed using Chromeleon software.

### *2.6.2 Determination of organic compounds*

Glycerol concentrations and other small molecular weight organic compounds were determined using a Dionex ICS 3000 ion chromatograph equipped with a Carbo Pac™ Pa10 separation column, including a guard column (Pa10) and an ED 40 amperometric detector. The column pressure was maintained at around 1,700 p.s.i. kept at 30ºC during the analysis. Flow rate was set at 0.4 mL $min^{-1}$. Sodium hydroxide (0.5 M) was used as eluent and its pH was maintained between 10.0 and 13.0. Calibration curves were constructed using a range of 0.5 - 2.0 mM for glycerol and other organic compounds were identified according to their retention times.

*2.6.3 Determination of transition metals concentrations*

Concentrations of soluble transition metals ($Cu^{2+}$, $Ni^{2+}$, $Zn^{2+}$, $Co^{2+}$ and $Mn^{2+}$) were determined using Dionex 320 ion chromatograph fitted with an IonPAC® CS5A column, an AD25 absorbance detector and IP25 isocratic pump. Samples were acidified with concentrated nitric acid (~ 10 µL) and stored at room temperature. The analytical conditions were set as follows: flow rate 1.2 mL $min^{-1}$, column pressure around 1,600 psi and sample injection volume of 250 µL. The eluent contained 1.4 mM PDCA (pyridine-2,6-dicarboxylic acid), 13.2 mM KOH, 11.2 mM $K_2SO_4$ and 14.8 mM formic acid. PDCA complexed to the cationic metal forming an anionic compound that was retained for a specific duration within the column. Concentration of metals were determined by forming a derivative with the post-column reagent [4-(2-pyridylazo) resorcinol] and measuring changing in absorbance at 520 nm. The post-column reagent (PAR) was prepared by dissolving 0.12 g PAR in 1 L solution containing 1 M 2-dimethylaminoethanol, 500 mM ammonium hydroxide and 300 mM sodium bicarbonate at pH 10.4.

**2.7 Atomic Absorption Spectroscopy (AAS)**

Concentrations of soluble transition metals were also measured using a SpectrAA Duo atomic absorption spectrophotometer (Varian, UK). Samples were pre-filtered through 0.2 µm nitro-cellulose filter membranes (Whatman, UK) and a drop of concentrated nitric acid was added immediately after filtering in order to avoid metal precipitation. Samples were stored at room temperature. Dilutions were carried out in 1% nitric acid solution. Samples were combusted in air/acetylene for Fe, Cu, Ni, Zn, Co and Mn. Standard solutions were prepared for each element: Fe, Co, Cu and Zn (0.25 - 5.0 ppm), Ni and Mn (0.5 - 10.0 ppm). Reagents and sample dilutions were prepared using ultrapure-grade water (Millipore, UK).

**2.8 Dissolved Organic Carbon (DOC)**

Concentrations of total organic carbon (TOC; unfiltered samples) and dissolved organic carbon (DOC; samples pre-filtered through 0.2 µm nitro-cellulose membrane filter) were determined using a Protoc DOC analyser (Pollution and Process Monitoring Ltd., UK). Anhydrous potassium hydrogen phthalate (KHP) was used for constructing the calibration curve (1 - 10 mg DOC $L^{-1}$). Samples were diluted, when necessary, using ultrapure-grade water (Millipore, UK).

## 2.9 Biomolecular techniques

### *2.9.1 Preparation of DNA template*

#### 2.9.1.1 Lysates

Bacterial and fungal isolates lyses were prepared from single colonies or from harvested biomass from liquid cultures (by centrifugation at 16,000 *g* x 10 min) with 20 µL SDS buffer (0.25% sodium dodecyl sulfate in 0.5 M NaOH) and run through a lysis program (95ºC for 15 min) in a thermo-cycler. Ultrapure-grade water (80 µL) was added to the lysate, which was then stored at -20 ºC until use.

#### 2.9.1.2 DNA extraction kit

Liquid samples were routinely collected from the bioreactor and filtered through 0.2 µm nitro-cellulose filter membranes. The filtrate was discarded and the membrane containing trapped cells was used for DNA extraction, carried out using UltraClean™ PowerSoil Microbial DNA Isolation Kits (MoBio Laboratories, Inc. USA). DNA extracts were stored at -20 ºC.

### *2.9.2 Polymerase Chain Reaction (PCR)*

PCR amplification was carried out for bacterial and archaeal 16S rRNA genes, as well as for eukaryote 18S rRNA genes. Each reaction used a “PCR master mix” which was prepared by combining the reagents described in Table 2.5. One microliter of DNA extract was added to the PCR master mix. Concentrations of DNA in the template were not determined. Bacterial, archaeal and eukaryote primers are listed in Table 2.6. Thermal cycling was performed in a Techne® TC-312 (Midwest Scientific, USA) thermocycler and PCR programs used in the current study are shown in Table 2.7.

**Table 2.5.** Reagents used for PCR Master Mix.

| Reagents | Volume (µL) |
|---|---|
| Go*Taq* reaction buffer (5x) | 4.0 |
| dNTPs (2 mM)* | 2.0 |
| $MgCl_2$ (25 mM) | 2.0 |
| Forward primer (10 pmol $\mu L^{-1}$) | 0.4 |
| Reverse primer (10 pmol $\mu L^{-1}$) | 0.4 |
| DMSO (dimethyl sulfoxide) | 0.4 |
| Go*Taq* polymerase | 0.2 |
| Ultrapure-grade water | 9.6 |
| Total volume | 19.0 |

* 2 mM dATP, dCTP, dGTP and dTTP.

**Table 2.6.** Description of primer pairs used in this study. R = reverse, F = forward.

| Gene | Primer name | Sequence (5' – 3') | Reference |
|---|---|---|---|
| **Bacterial 16S rRNA** | 27F* | AGAGTTTGATC*M*TGGCTCAG | Lane, 1991 |
| | 1387R | GGGCGG*W*GTGTACAAGGC | Marchesi et al., 1998 |
| **Archaeal 16S rRNA** | Arch 20F | TCCGGTTGATCC*Y*GCCRG | Kay et al., 2013 |
| | Arch 915R | GTGCTCCCCCGCCAATTCCT | Kay et al., 2013 |
| **Eukaryote 18S rRNA** | Euk F | ACCTGGTTGATC*D*CTGCCAG | Mariner et al., 2008 |
| | Euk R | TGATCCTTC*Y*GCAGGTTCAC | Mariner et al., 2008 |

M = A/C, W = A/T, Y = C/T, R = A/G, D = A/G/T.
* 27F Cy5-labelled primer was used for T-RFLP purposes only.

**Table 2.7.** List of PCR programs and settings used in this study.

| Program | PCR settings |
|---|---|
| **Bacterial 16S rRNA gene** | 95ºC (5 min), 30 cycles at 95 ºC (30 s), 55 ºC (30 s) and 72 ºC (1.5 min), final extension at 72 ºC (10 min) |
| **Archaeal 16S rRNA gene** | 95ºC (5 min), 30 cycles at 95 ºC (30 s), 62 ºC (30 s) and 72 ºC (1 min), final extension at 72 ºC (10 min) |
| **Eukaryote 18S rRNA gene** | 95ºC (5 min), 35 cycles at 95 ºC (30 s), 45 ºC (30 s) and 72 ºC (1 min), final extension at 72 ºC (10 min) |

*2.9.3 Agarose gel electrophoresis*

PCR products were analysed by agarose gel electrophoresis. The concentration of agarose in the gel was 0.7% prepared with 0.5x TBE buffer (5.4 g tris-hydroxymethyl-

methylamine, 2.75 g boric acid and 2 mL of 0.5 M EDTA; pH adjusted to 8.0 with NaOH). Agarose was dissolved by heating in a microwave oven, and allowed to cool to around 50 ºC. The nucleic acid stain SafeView® (NBS Biologicals Ltd., UK) was added to the gel (5.0 µL in 30 mL gel) and then poured onto a gel mould and allowed to set. PCR products were mixed with Blue/Orange 6x DNA loading dye (Promega, USA) and loaded into a well in the agarose gel alongside 1Kb DNA ladder as molecular size reference (100 µg $\mu L^{-1}$, Promega, USA). The migration of the nucleic acid was produced by applying a constant voltage (90 mV) for 25 min using Bio-Rad PowerPac™ 300 power supply (Bio-Rad, USA). The gel was analysed under UV light using a Gel-Doc EQ and Quantity One software.

*2.9.4 Terminal Restriction Enzyme Fragment Length Polymorphism (T-RFLP) analyses*

Bacterial 16S rRNA genes were amplified by PCR (section 2.9.2) in three separate reactions using a forward fluorescent dye-labelled primer (27F) and a non-labelled reverse primer (1387R). The three PCR products combined were purified using SureClean® Plus (Bioline Reagents Ltd., UK) according to the manufacturer's instructions, and re-suspended in 20 µL autoclaved ultrapure-grade water prior to digestion with restriction enzymes.

The T-RFLP reaction mix was prepared as follows (10 µL final volume): 6.0 µL ultrapure-grade water, 1.0 µL restriction enzyme buffer, 1.0 µL bovine serum albumin (10 mg $mL^{-1}$), 1.0 µL restriction enzyme and 1.0 µL purified PCR product. The reaction tubes were incubated at 37ºC for 1 h. The enzymes used in this study (listed in Table 2.8) and the enzyme buffers were supplied by Promega, USA.

**Table 2.8.** List of restriction enzymes and their respective recognition sites. Arrows indicate where the enzymes cleave DNA.

| Restriction enzyme | Restriction site |
|---|---|
| **AluI** | 5'- AG▼CT -3'<br>3'- TC▲GA -5' |
| **CfoI** | 5'- GCG▼C -3'<br>3'- C▲GCG -5' |
| **HaeIII** | 5'- GG▼CC -3'<br>3'- GG▲CC -5' |

Genome Lab DNA size standard kit - 600 (Beckman Coulter, USA) was used to analyse DNA fragments up to 600 nucleotides in length. Twenty eight microliters DNA size standard (SLS 600) and 2 µL digest were added into each well of a 96-well conical bottom plate and a

drop of mineral oil was added on top. The corresponding row in a 96-well flat bottom plate was filled with Genome Lab separation buffer. Digests were analysed by capillary electrophoresis using a CEQ8000 Genetic Analysis System (Beckman Coulter, USA). The fragment length was identified by comparison to the database of acidophilic microorganisms held at Bangor University. Relative abundance of T-RFs were calculated on the basis of their peak areas.

### *2.9.5 Clone libraries*

Clone libraries, based on bacterial and archaeal 16S rRNA genes and eukaryote 18S rRNA genes were constructed to identify unknown T-RFs in the aSRBR as well as for screening environmental samples. Purified PCR products were obtained as described in previous sections.

#### 2.9.5.1 Ligation reaction

PCR product was added to a ligation mix containing 5 µL 2x ligase buffer, 1 µL pGEM®-T-easy cloning vector, 1 µL T4 ligase and 2 µL ultrapure-grade water (10 µL final volume). The mix was incubated for 2 h at room temperature. All reagents were supplied by Promega, USA.

#### 2.9.5.2 Transformation into *Escherichia coli*

Plasmids were transformed into *E. coli* strain DH5α according to the manufacturer's instructions (Promega, USA). To 200 µL competent cells, 5 µL ligated vector was added and placed on ice for 30 min before heat shocking at 42ºC for 50s. The mixture was cooled on ice for 2 min and 400 µL of LB medium was added to the mixture and incubated 37ºC for 1 h. LB medium was prepared by mixing 10 g tryptone, 5 g yeast extract, 10 g NaCl per litre of RO-grade water and pH adjusted to 7.0. Solid LB medium was also prepared by adding to the previous mixture 10 g agar nº1 (LAB M™, UK). Both media were heat-sterilised, allowed to cool down and 100 µL ampicillin was added (per 100 mL medium) from a stock solution containing 100 µg ampicillin $mL^{-1}$.

#### 2.9.5.3 Screening and purification of plasmids

Aliquots of transformed *E. coli* cultures (50 and 100 µL) were spread onto solid LB medium containing 20 µL X-Gal (50 mg $mL^{-1}$) and incubated it overnight at 37ºC. White

colonies were transferred into Eppendorf vessels containing 20 µL SDS buffer and cell lysis was carried out as described in section 2.9.1.1. PCR amplification was performed using SP6 (5' - ATTTAGGTGACACTATAG - 3') and T7 (5' - TAATACGACTCACTATAGGG -3') primers. PCR products were screened by RFLP analysis using MspI as restriction enzyme. All plasmid inserts that generated different fragment lengths were purified using StrataPrep Plasmid Miniprep kit (Agilent Technologies, USA) and sequenced (Macrogen Inc., Korea).

2.9.5.4 Sequencing analyses

Clone sequences and isolates were analysed using Chromas Lite version 2.1.1, aligned using BLASTN online software (National Centre of Biotechnology Information, NCBI) (Altschul et al., 1990) and compared with gene sequences deposited in the GenBank database.

*2.9.6 Phylogenetic analyses*

Phylogenetic analyses were applied to the 16S and 18S rRNA gene sequences obtained from the microorganisms isolated throughout this study. Analyses were performed using Clustal X version 2.0 (Larkin et al., 2007) for sequence alignments and imported to the tree drawing software NJplot version 2.3. Sequences were manually trimmed to the length of the shortest sequence in Clustal X for a complete alignment. Phylogenetic trees were built by performing bootstrapped (x1000) maximum likelihood, maximum parsimony and neighbour-joining analysis.

## 2.10 Microscopy

*2.10.1 Stereo-scan microscopy*

Colonies grown on solid media were observed and enumerated using a stereo-scan microscope (Leitz-Wild M32, Switzerland). The magnification used was between x50 and x400. Images of the colonies were captured with a GXCAM-5 (GT Vison Ltd.) digital camera attached to the microscope.

*2.10.2 Phase-contrast microscopy*

For enumerating individual cells and investigating microbial cell morphology, a Leitz Labolux phase-contrast microscope was used at x400 magnification. Phase-contrast images

were captured with a COOLPIX digital camera attached to an ECLIPSE E600 microscope (Nikon, Japan).

2.10.2.1 Cell counts

Microbial cells were dispersed and 10 µL of culture placed on a Thoma counting chamber and enumerated using a Leitz Labolux phase-contrast microscope. Equation 2.1 was used to calculate cell concentrations (cells $mL^{-1}$).

$$\text{Cell concentration} = \frac{\text{Total cell count}}{\text{Number of squares}} \times (2.5 \times 10^7) \quad \text{(Eq. 2.1)}$$

*2.10.3 Scanning Electron Microscopy (SEM) with Energy Dispersive Analysis of X-rays (EDAX)*

Scanning electron microscopy was used to obtain visual images of the beads from the biofilm bed of the aSRBR under high magnifications. Sample preparation and microscopy technique are described below.

2.10.3.1 Dehydration and fixation

Samples were fixed with glutaraldehyde 2% in Sorensen buffer 0.1 M at pH 7.4 for 4 h at room temperature. Then, washed three times for 10 - 30 min in phosphate buffer 4 - 8% sucrose. Dehydration was performed by passing the material through a series of ethanol solutions: (i) 30% ethanol for 30 min, (ii) 50% ethanol for 30 min, (iii) 70% ethanol for 30 min, (vi) 90% ethanol for 30 min and (v) 100% ethanol for 30 min, the latter was allowed to evaporate and the sample was kept sealed at room temperature until viewed.

2.10.3.2 Analysing samples with SEM/EDAX

The dehydrated sample was coated with a gold-palladium mix for 5 minutes immediately before viewed with Zeiss Supra 40VP scanning electron microscope (Carl Zeiss, Germany). To provide elemental identification and semi-quantitative composition information of the samples, energy dispersive analysis of X-rays (EDAX) were performed using an EDAX system (Ametek Inc., USA) attached to the SEM.

# Combined recovery of copper and mitigation of pollution of a metal-rich stream draining a copper mine in Brazil

3

## 3.1 Introduction

The generation, migration and environmental pollution caused by contaminated waters at sites of coal and metal mining are of global concern. Wastewaters from mines and mine spoils are potentially hazardous to the environment due to their intrinsic (though highly variable) characteristics, such as low pH (often < pH 3), elevated concentrations of dissolved metals and metalloids, and high osmotic potential associated with concentrations of sulfate salts (Nordstrom et al., 2015). A variety of transition metals may be present in acid mine drainage (AMD) though iron is frequently the most abundant of these, while some metalloids (notably arsenic) are of particular concern due to their acute toxicity.

Different approaches have been developed to remediate AMD (reviewed in Johnson and Hallberg, 2005). While some of these involve only chemical treatment others harness the abilities of microorganisms to promote biomineralisation of metals and metalloids present in AMD, either in constructed wetlands (e.g. Younger et al., 2002) or utilising iron-oxidizing and/or sulfate-reducing bioreactors (e.g. Hedrich and Johnson, 2014). Among the advantages of the latter is that they allow superior control of the remediation process, require far smaller footprints and potential recovery of metals at the end of the process (Johnson, 2014).

Biological sulfidogenesis can be used both to selectively precipitate chalcophilic transition metals present in AMD, as sulfide minerals, using hydrogen sulfide generated by sulfate-reducing bacteria in anaerobic bioreactors, and to increase mine water pH (biosulfidogenesis is a proton-consuming reaction below pH 7). Full-scale sulfidogenic bioreactors utilize neutrophilic species of sulfate-reducing bacteria (e.g. Boonstra et al., 1999), and therefore it is necessary to shield these from direct exposure to acidic mine waters. However, laboratory-scale low pH sulfidogenic bioreactors, operating between pH 2.2 and 4.5, have also been described (e.g. Ñancucheo and Johnson, 2012a; 2014). These utilize consortia of acidophilic and acid-tolerant sulfate-reducing bacteria (aSRB) that have been isolated from metal mine sites, which display far greater tolerance to both acidity and dissolved metals than neutrophilic species.

*3.1.1 Mine site: Sossego copper mine*

Brazil is the world's 15th largest producer of copper concentrates. The mining company Vale S.A. is responsible for the majority of the production, operating at Sossego and Salobo copper mines. The Sossego mine is the first Vale S.A. copper project and is located by a copper-gold ore discovered in early 1997. The operation of the mine and processing plant started in 2004 and its projected exhaustion date is 2025 (Vale S.A., 2017). The mine site is located in Carajás, state of Pará, Northern Brazil, and consists of two main copper ore bodies, Sossego and Sequeirinho (The Sossego complex, Fig. 3.1). The proved reserve is 245 million tonnes of copper ore with an average grade of 0.98% Cu and 0.28 grams of gold per tonne, which is produced as a co-product (Vale S.A., 2017). Vale has invested US$ 413 million to process 15 million tonnes of ore per year. In 2016, 93,000 tonnes of copper concentrate and 67,000 troy ounces of gold (equivalent 2.3 tonnes of gold) were produced in Sossego mine (Vale S.A., 2017). The copper ore is mined by an open-pit method, and run-of-mine ore processing involves standard primary crushing and conveying, subsequent semi-autogenous grinding (SAG), comminution in ball milling, froth flotation process, tailings disposal, concentrate thickening, filtration and load out (Vale S.A., 2017).

The Sossego complex has a processing facility to concentrate the ore on site. The concentrate is then trucked to a storage terminal in Parauapebas and ultimately transported via the Carajás railway to Ponta da Madeira maritime terminal in São Luís, in the state of Maranhão. Copper concentrates from Sossego are mainly sold under medium- and long-term contracts to copper smelters in Europe, India and Asia. The gold produced as a by-product of copper mining is sold to the Wheaton Precious Metals, which increases the total aggregated value of the operations. Vale has constructed a semi-industrial scale plant for copper processing, *Usina Hidrometalúrgica de Carajás* (UHC, acronym in Portuguese), that was designed to produce copper cathode using the hydrometallurgical technology process route. Sossego copper concentrate has been used to feed this plant, which is located at the mine in Carajás. Operations began in the third quarter of 2007, with an annual production capacity of 10,000 tonnes of copper.

Acid mine drainage generated from the mining activity flows continuously from an ore deposit along a channel in the soil that starts at an ore heap and terminates at a run-off area (Fig. 3.2). Currently, the drainage is treated with limestone along the course of the channel to increase the pH and precipitate heavy metals (Pereira et al., 2014; Ñancucheo et al., 2017).

(a)

(b)

(c)

(d)

**Fig. 3.1.** Aerial (a) and satellite (b) views of Sossego copper mine, Sossego copper complex: Sossego and Sequeirinho open-pits (c) and Sossego open-pit (d).

**Fig. 3.2.** Images of the moderately acidic stream draining the active copper mine in the state of Pará, Brazil, which has been remediated using limestone treatment. Images: Ivan Ñancucheo (personal communication).

Besides the issue regarding the moderately acidic mine drainage generation containing high concentrations of copper (7.5 mM) and other transition metals, the Sossego complex also contains a large tailing pond containing approximately 20 million cubic meters of water from the mineral extraction process as a mixture of water and pulverised rock containing low-grade copper (Fig. 3.3). The pond contains about 90 million tonnes of 0.07% copper-grade detritus, in which the residual copper is dissolved and the solid material is decanted at the bottom of the dam. If this amount of copper from the dam was recovered, Vale could earn, additionally, approximately US$ 1.4 billion, which is more than the company invested between 1997 and 2004 to make the mine operational, as well as reduce the environmental impact in the mine itself (Vasconcelos, 2012).

Research undertaken at the University of São Paulo in association with Vale S.A. has investigated an alternative strategy to recover copper from solid waste by exploiting the ability of some microorganisms to catalyse the oxidative dissolution of residual copper-containing minerals, i.e. conventional bioleaching technology (Vasconcelos, 2012). However, little attention has been given to the soluble copper present in the pond and the stream draining this copper mine.

This chapter describes the sequential selective recovery of copper and removal of other transition metals (apart from manganese) from a synthetic version of the moderately acidic mine water at the Sossego mine using a single low pH sulfate-reducing bioreactor.

**Fig. 3.3.** Tailings pond at the Sossego mine that receives the residues generated in the copper concentrate processing. Image: Vasconcelos, 2012.

## 3.2 Materials and methods

### *3.2.1 Composition of actual and synthetic mine water*

The composition of the Sossego mine water, including physico-chemical parameters (Table 3.1) and concentrations of metals and metalloids (Table 3.2), was provided from Vale Technological Institute, Pará, Brazil (ITV, acronym in Portuguese) and a synthetic version based on the actual mine water was reconstituted to carry out experimental work at Bangor University.

**Table 3.1.** Physico-chemical composition of mine water draining the Sossego copper mine.

| Parameter | Measurement |
|---|---|
| **Colour** | Clear blue/green |
| **Total alkalinity (mg $CaCO_3$ $L^{-1}$)** | 3.01 |
| **Water temperature (°C)** | 33.2 |
| **Conductivity (µS $cm^{-1}$)** | 2.99 |
| **$E_H$ (mV)** | 270 |
| **pH** | 5.0 |
| **GPS coordinates** | 6° 26' 25.625" S 50° 2' 03.068" W |

**Table 3.2.** Chemical composition of the actual Sossego mine water and its correspondent synthetic version. Concentrations are expressed in mM.

| Analyte | Actual SMW | Synthetic SMW |
|---|---|---|
| $Al^{3+}$ | 0.036 | 0 |
| $As_{total}$ | <0.01 | 0 |
| $Ca^{2+}$ | 7.03 | 7.00 |
| $Cd^{2+}$ | <0.001 | 0 |
| $Cl^{-}$ | 0.043 | 0.04 |
| $Co^{2+}$ | 0.040 | 0.04 |
| $Cr^{3+}$ | <0.01 | 0 |
| $Cu^{2+}$ | 7.50 | 7.50 |
| $F^{-}$ | 0.53 | 0 |
| $Fe^{2+}$ | <0.05 | 0 |
| $Fe^{3+}$ | 0.015 | 0 |
| $K^{+}$ | 0.282 | 0.28 |
| $Mg^{2+}$ | 4.01 | 4.00 |
| $Mn^{2+}$ | 0.154 | 0.15 |
| $N_{total}$ | 1.20 | 0 |
| $Na^{+}$ | 2.10 | 2.10 |
| $Ni^{2+}$ | 0.251 | 0.25 |
| $P_{total}$ | <0.01 | 0 |
| Pb | <0.01 | 0 |
| $Sulfide_{total}$ | <0.002 | 0 |
| $SO_4^{2-}$ | 15.68 | 20.6 |
| $Zn^{2+}$ | 0.016 | 0.02 |

The relatively high pH of the mine water causes rapid hydrolysis of ferric ion, and the concentration of total soluble ferric ion measured on site was very low (~ 2 µM). In view of this, ferric ion was omitted when preparing the synthetic mine water.

### *3.2.2 Phases of the experiment*

The experiment described in the current chapter comprises of three different phases which are described as follows, and summarised in Table 3.3.

***Phase 1*** is the phase in which the sulfidogenic bioreactor (aSRBR) was set up and allowed to condition prior to introduction of the synthetic mine water to the system. The feed

liquor used to prime the aSRBR (referred to as “standard SRB medium”) contained 2.5 mM glycerol (as electron donor), 0.1 g $L^{-1}$ yeast extract, 5.0 mM $K_2SO_4$, 100 µM $FeSO_4 \cdot 7H_2O$ plus basal salts and trace elements (ABS/TE; section 2.2.2.1) adjusted to pH 2.5. In order to confirm that the bioreactor was generating sulfide, a 500 mL off-line vessel containing 100 mL of a 25 mM $CuSO_4$ solution was used to monitor hydrogen sulfide production by measuring copper sulfide (CuS) mineralisation within this vessel (details about soluble copper determination are described in section 2.5.2.1). Once a relatively constant rate of $H_2S$ production was obtained, the second phase was initiated.

***Phase 2*** consisted essentially of removing copper from the synthetic mine water. In the protocol developed, copper was precipitated off-line using $H_2S$ generated in the aSRBR in excess of that required to precipitate metals in the bioreactor vessel itself (Fig. 3.4 - Phase 2). This caused the removal of > 99% of the copper (as CuS), but no other transition metal (Ni, Co, Zn, Mn) present, and the pH of the synthetic mine water to fall from 5.0 to 2.1. At this stage, a larger off-line vessel, containing 400 mL of the synthetic mine water, was used for biomineralization of CuS. Changes in concentrations of soluble copper in the off-line vessel were measured on a regular basis, together with flow rates into and out of the bioreactor, sulfate and glycerol consumption and acetic acid production. After each batch, the partly-processed mine water was filtered through folded paper filter (Whatman, UK) and the precipitate was allowed to dry at room temperature. In this phase, the initial pH of the feed liquor was 2.5, and this was gradually lowered to pH 2.2. Chemical composition of the feed liquor at this phase was the same used at Phase 1 (i.e. “standard SRB medium”).

***Phase 3*** involved the remediation of a more acidic (pH 2.1) synthetic mine water, based on the chemistry of the partly-processed mine water by precipitating, simultaneously, the remaining transition metals within the bioreactor vessel, and copper in the off-line vessel (Fig. 3.4 - Phase 3). In this case, an excess of $H_2S$ was required to sustain both systems, in order to obtain net consumption of hydronium ions and to operate the system as a continuous pH-controlled unit, and therefore the concentration of glycerol was increased to 5 mM. The off-line vessel at this stage contained 2 L of synthetic mine water.

**Table 3.3.** Phases of the experiment using the sulfidogenic bioreactor to remediate the synthetic mine water from Sossego copper mine.

| | Phases | Glycerol concentration (mM) | Feed liquor | Off-line vessel (volume and [Cu]) | Experiment duration |
|---|---|---|---|---|---|
| **1** | Priming phase | 2.5 | Standard SRB medium pH 2.5 | 0.1 L / 25 mM | 44 days |
| **2** | Off-line Cu precipitation | 2.5 | Standard SRB medium pH 2.5-2.2 | 0.4 L / 7.5 mM | 21 days |
| **3** | In-line and off-line metal precipitation | 5.0 | Partly-processed mine water pH 2.1 | 2 L / 7.5 mM | 63 days |

Throughout the experiment, temperature, pH and bioreactor volume were maintained constant at 30°C, 4.0 and 2 L, respectively, unless stated otherwise.

Flow rates were monitored regularly by measuring the volume of the outflow of the sulfidogenic bioreactor in a certain period of time (e.g. mL $h^{-1}$). Flow rates can be expressed as well in terms of hydraulic retention time (HRT) which is defined as the amount of time that a solution remains in a storage unit (in this case, a bioreactor) and was calculated by dividing the volume of the bioreactor (V) by the flow rate (F) i.e. V/F, and expressed in hours (h).

Sulfate reduction rates were calculated by the difference of the amount of sulfate in the inflow minus that in the outflow of the bioreactor (referred to as sulfate consumption). The amount of sulfate consumed was then multiplied by the flow rate of the bioreactor (L $day^{-1}$), and the final figure was divided by the working volume of the bioreactor (2 L). Sulfate reduction rates are expressed as g $SO_4^{2-}$ reduced $L^{-1}$ $day^{-1}$.

Rates of hydrogen sulfide production were calculated from rates of off-line copper precipitation, since the stoichiometry of $H_2S$ produced to CuS generated is 1:1. Concentrations of soluble copper were monitored regularly in the off-line vessel, and corresponding rates of $H_2S$ production expressed as mmoles $L^{-1}$ $day^{-1}$.

Concentrations of acetic acid were monitored throughout the experiment (section 2.6.1) and, in cases where the concentration of acetic acid was over 1.0 mM due to incomplete oxidation of glycerol, 10 mL of the acetotrophic acidophile *Acidocella aromatica*, strain $PFBC^T$, was added to the bioreactor. The bacterium was maintained in liquid medium contained ABS/TE solution and 5 mM fructose as sole carbon/energy sources adjusted to pH 3 with

sulfuric acid and filter-sterilized ferrous sulfate added (to 100 µM) to the cooled, heat-sterilized media. *Acidocella aromatica* had previously been shown to grow in syntrophic culture with *Desulfosporosinus acididurans*, converting acetic acid into hydrogen and carbon dioxide, and the hydrogen produced can be used as a supplementary electron donor by the sulfidogen (Kimura et al., 2006).

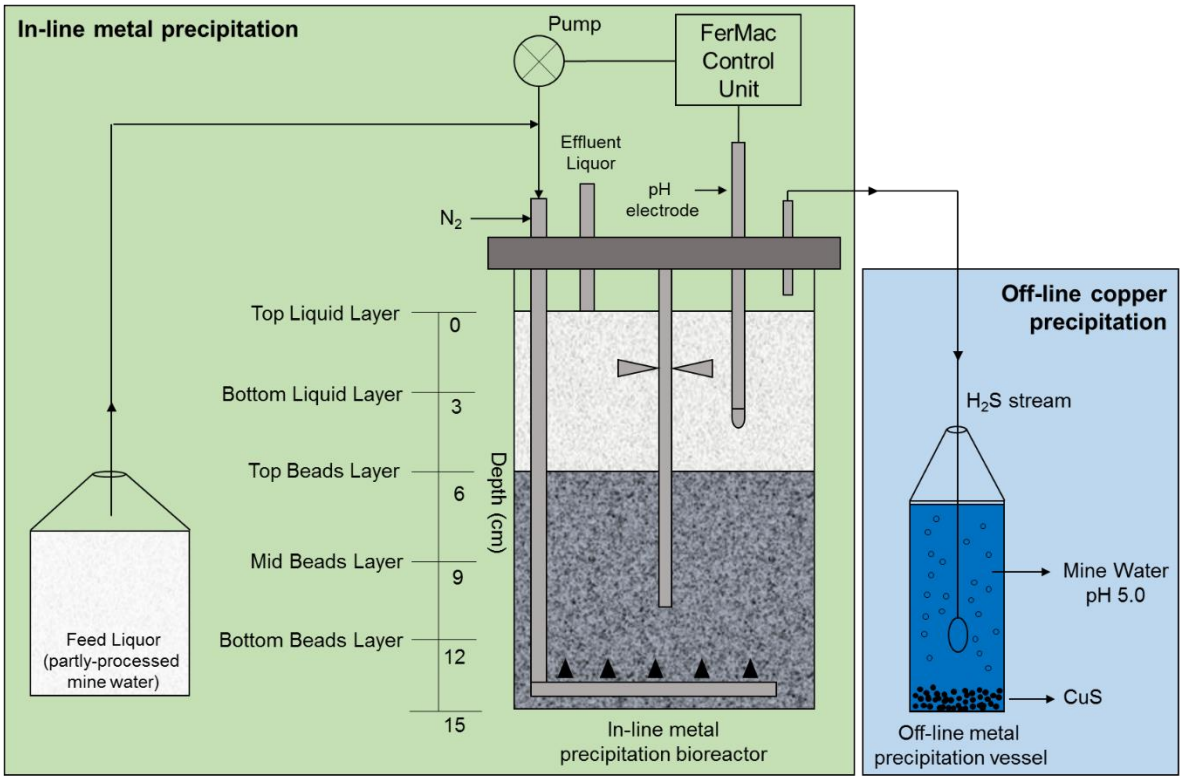


**Fig. 3.4.** Schematic representation of the low pH sulfidogenic bioreactor (aSRBR). The excess of hydrogen sulfide produced in the aSRBR was delivered to an off-line precipitation vessel, containing synthetic mine water in order to mediate selective removal of copper (Phase 2). After copper precipitation, the partly-processed water was used as feed liquor for the bioreactor (Phase 3).

## 3.3 Results

### *3.3.1 Priming phase: Phase 1*

The aSRBR biofilm bed was set up using a mixture of bacteria immobilised onto Poraver porous silica beads together with fresh (non-colonised) beads, and the 2 L total volume completed by adding sterile liquid medium (pH 4.0). Prior to operational phase (synthetic mine water treatment), the aSRBR was allowed to condition for a total period of 44 days, the first

10 days being to adapt to a higher pH (the pH of the bioreactor was 2.4 at the start of the experiment).

Fig. 3.5 shows the gradual increase of the bioreactor pH. Once it reached its set up value (4.0) the system started its continuous flow mode, and from this point flow rates and hydraulic retention times (HRTs) were monitored. Once the bioreactor had reached the pre-set pH and $H_2S$ started to be produced (day 12), a copper sulfate solution (25 mM) was added to an off-line vessel and production of copper sulfide was monitored. This step was required prior to using the synthetic mine water in order to confirm that the aSRBR was generating $H_2S$ in a constant rate and the system was working appropriately. The rate of copper precipitation was, on average, 16 mg $Cu^{2+}$ precipitated $L^{-1}$ $day^{-1}$ (corresponding to 8.6 mg $H_2S$ $L^{-1}$ $day^{-1}$).

Hydraulic retention times ranged between 19 and 200 h during the priming phase. Large HRT values were observed after 30 days of experiment due to short-term perturbations in the system when a reflux of copper sulfate from the gas trap into the reactor vessel occurred, mainly due to low nitrogen pressure, which caused the bioreactor to slow down considerably. On each occasion though, the bioreactor was able to subsequently recover.

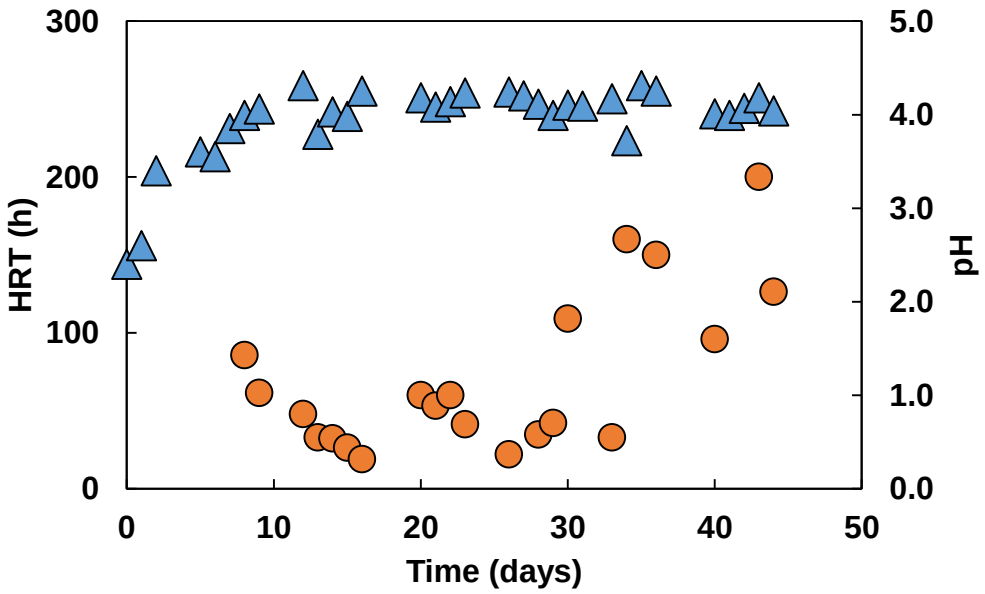


**Fig. 3.5.** Changes in pH (▲) values and HRT (●) in the priming phase of the aSRBR.

*3.3.2 Mine water treatment: Phases 2 and 3*

The aSRBRs at Bangor University are designed both to remediate and to recover metals from mine wastewaters and mine process waters that have pH values lower than 4.0. Dissimilatory sulfate reduction consumes protons at low pH, and the rate at which this occurs is used to control the flow of feed liquor into the bioreactor vessel (which is usually maintained

at pH 3.0 - 4.0). The pH of the synthetic Sossego mine water (SMW) used (5.0) would therefore appear to be too high to be processed using aSRBRs. To circumvent this problem, the aSRBR was set up to over-produce $H_2S$ (i.e. above that required to precipitate metals within the bioreactor vessel) (Eq. 3.1):

$$4\ C_3H_8O_3 + 7\ SO_4^{2-} + 14\ H^+ \rightarrow 7\ H_2S + 12\ CO_2 + 16\ H_2O \quad \text{(Eq. 3.1)}$$

This excess $H_2S$ was delivered in a continuous oxygen-free nitrogen (OFN) stream to a precipitation vessel containing synthetic mine water, where it reacted with soluble copper, forming insoluble copper sulfide (Fig. 3.6) and causing the pH of the synthetic mine water to decrease (Eq. 3.2):

$$Cu^{2+} + H_2S \rightarrow CuS + 2\ H^+ \quad \text{(Eq. 3.2)}$$

The copper-free mine water was then sufficiently acidic (pH 2.1) to be used as feed for the bioreactor.

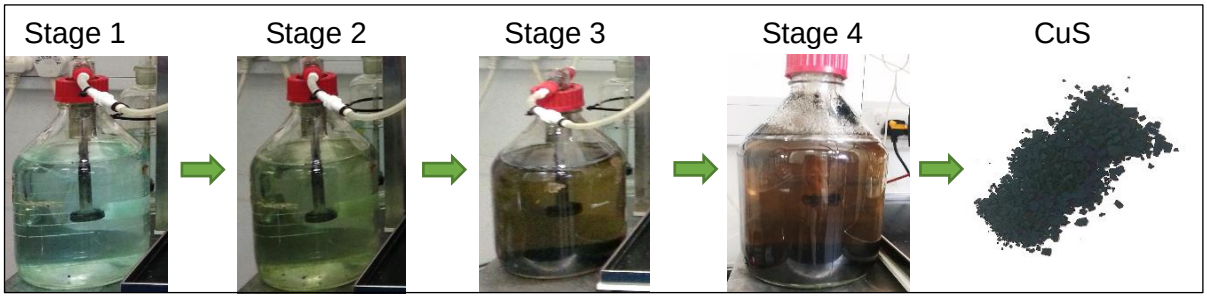


**Fig. 3.6.** Images of different stages of copper mineralisation in the off-line vessel. Stage 1: SMW at pH 5.0 (7.5 mM $Cu^{2+}$), Stage 2: SMW at pH 3.4 (7.0 mM $Cu^{2+}$), Stage 3: SMW at pH 2.5 (4.5 mM $Cu^{2+}$), Stage 4: SMW at pH 2.1 (0.7 mM $Cu^{2+}$) and lastly the dried CuS precipitate.

During Phase 2 (off-line copper mineralisation), the pH of the influent liquor ("standard aSRB medium") was lowered gradually from 2.5 to 2.2, generating a more acidic influent for the bioreactor. Table 3.4 shows changes in HRT and copper precipitation rate throughout this adaptation period. Typical rates of sulfate reduction at this point were approximately 0.2 g sulfate reduced $L^{-1}$ $day^{-1}$.

**Table 3.4.** Average rates of HRT and copper precipitation rates during the period where the pH of the influent liquor was gradually lowered from 2.5 to 2.2. Intervals shown in brackets represent minimum and maximum figures obtained in each pH experiment.

| Influent pH | HRT (h) | mg $Cu^{2+}$ precipitated $L^{-1}day^{-1}$ |
|---|---|---|
| **2.5** | 40.5 (25.5 – 63.2) | 57.1 (18.9 – 126.8) |
| **2.3** | 47.9 (17.6 – 85.7) | 51.7 (2.0 - 147.3) |
| **2.2** | 138 (92.3 – 218.2) | 85.6 (28.7 – 162.1) |

Hydraulic retention times increased each time the pH of the influent liquor was lowered (from 2.5 to 2.2) during Phase 2 of the aSRBR, as would be expected, due to corresponding increasing concentrations of both proton ($H_3O^+$) and bisulfate ($HSO_4^-$) acidity, but each time they subsequently decreased as the productivity of the bioreactor increased.

Once the feed liquor was changed (to Cu-free synthetic mine water amended with 5 mM glycerol; Phase 3), HRTs increased significantly and remained relatively high for about 10 days, before going into a steady decrease and eventually averaging ~ 37 h (Fig. 3.7). This increase can be ascribed to the presence of transition metals (Zn, Ni, Mn and Co) in the feed liquor that, at this stage, have direct contact with the microbial population within the bioreactor as well as a further drop in the pH of the feed liquor (to pH 2.1), which corresponded to that of the liquid in the off-line vessel containing synthetic mine water after > 99% biomineralisation of copper.

Off-line copper removal from the synthetic mine water was also monitored throughout both Phase 2 and Phase 3, as shown in Fig. 3.7. Rates of copper precipitation during Phase 2 ranged between 10 and 160 mg $Cu^{2+}$ precipitated $L^{-1}$ $day^{-1}$ (corresponding to 5.5 and 86 mg $H_2S$ $L^{-1}$ $day^{-1}$, respectively). During the first 20 days of Phase 3 (day 21 to day 44, Fig. 3.7) the precipitation rates did not change significantly from those observed in Phase 2, even though the amount of glycerol consumed at Phase 3 was about twice that consumed in Phase 2. These results could have been due to an initial inhibitory effect of using partly-processed mine water as feed liquor, which also caused a significant increase in the HRT. However, after becoming adapted to the partly-processed synthetic mine water (from day 57 onwards), HRTs decreased, the performance of the bioreactor increased and therefore the amount of copper precipitated increased and ranged between 170 and 610 mg $Cu^{2+}$ precipitated $L^{-1}$ $day^{-1}$, corresponding to 91 and 327 mg $H_2S$ $L^{-1}$ $day^{-1}$, respectively.

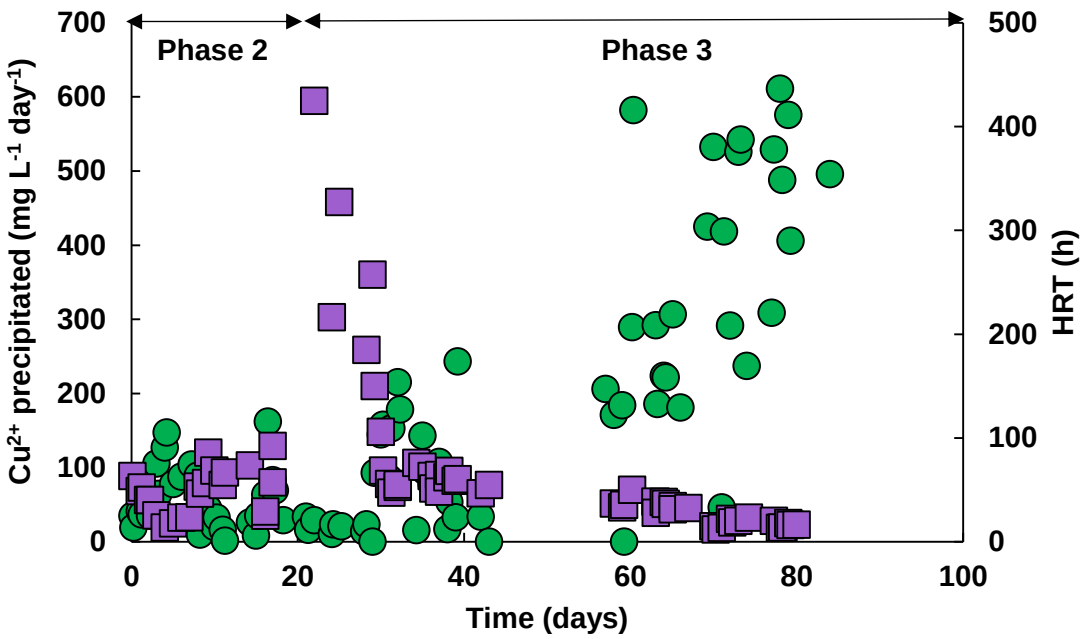


**Fig. 3.7.** Changes in HRTs (■) and copper precipitation rates (●) of the aSRBR during phases 2 and 3 of the experiment.

Rates of sulfate reduction (Fig. 3.8) on Phase 2 varied between 0.01 and 0.5 g sulfate reduced $L^{-1}$ $day^{-1}$ and on Phase 3 greater rates were observed, ranging between 0.2 and 1.35 g sulfate reduced $L^{-1}$ $day^{-1}$. Standard deviations of these data were large in Phase 3 reflecting, in part, the time taken for the system to reach equilibrium after changing the feed liquor composition.

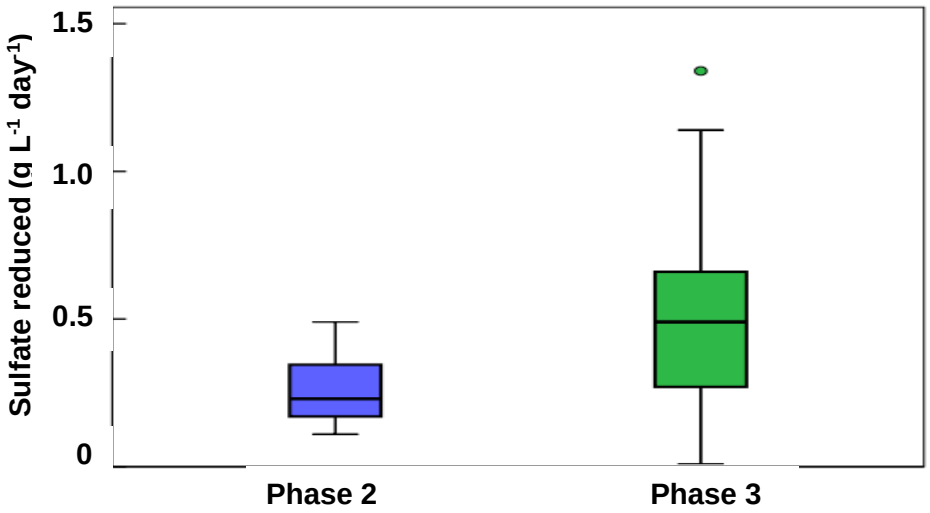


**Fig. 3.8.** Box plot representation of sulfate reduction rates in Phases 2 (blue) and Phase 3 (green). The single green circle represents an outlier, which did not fall into the inner fences of the box.

Concentrations of glycerol consumed and acetic acid produced are shown in Fig. 3.9. Since the pH of the aSRBR was set to 4.0 and the p$K_a$ of acetic acid is 4.75 (which infers that ~ 85% of the total acetic acid/acetate in the effluent was present as non-dissociated acetic acid and only 15% as anionic acetate), this organic material is referred to generically as “acetic acid”.

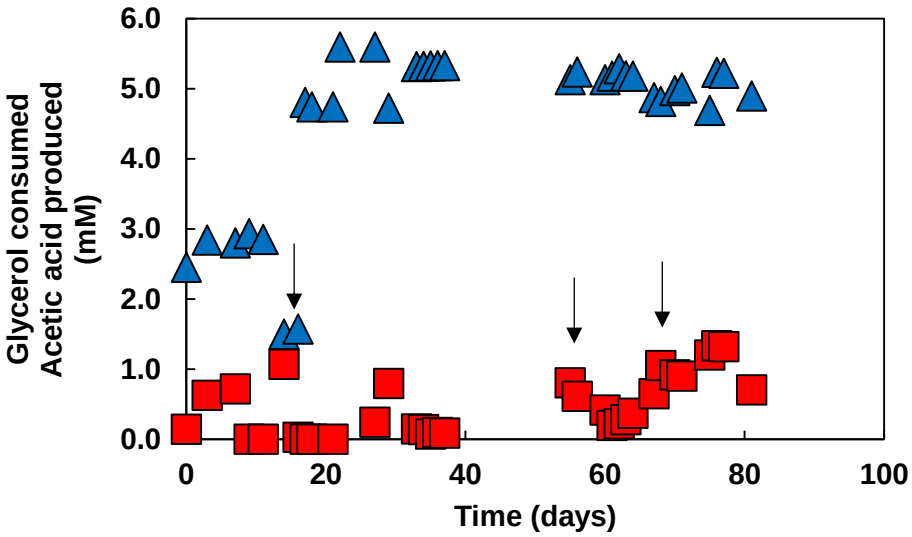


**Fig. 3.9.** Changes in concentrations of glycerol consumed (▲) and acetic acid produced (■) in the bioreactor in Phases 2 (day 1 to day 20) and 3 (day 21 to day 84). The downward-pointing arrows indicate times when an active culture of *Acidocella aromatica*$^T$ was added to the sulfidogenic bioreactor.

Most of the glycerol added to the bioreactor was oxidized completely to carbon dioxide (Eq. 3.1), though acetic acid was detected in low concentrations (< 1.3 mM), corresponding to an average of 8% of the glycerol that was oxidized throughout 80 days of experiment.

Peaks of acetic acid production (> 1.0 mM) were observed when the aSRB *Desulfosporosinus acididurans* was the most abundant microorganism in the reactor. This aSRB is known to be an “incomplete oxidizer” of glycerol, generating equimolar concentrations of acetic acid as a waste product (Kimura et al., 2006). High concentrations of acetic acid in biosulfidogenic systems imply that the efficiency of $H_2S$ production is far less than what would be desirable (the stoichiometry of glycerol oxidized to sulfate reduced is 4:3 (Eq. 3.3) in incomplete oxidation and 4:7 in complete oxidation (Eq.3.1)).

$$4\ C_3H_8O_3 + 3\ SO_4^{2-} + 6\ H^+ \rightarrow 4\ C_2H_4O_2 + 3\ H_2S + 4\ CO_2 + 8\ H_2O \quad \text{(Eq. 3.3)}.$$

In order to mitigate this problem 10 mL of the acidophilic heterotroph *Acidocella aromatica*$^{T}$ was added to the system on the days 14, 55 and 68 (Fig. 3.9). The addition of *Ac. aromatica* resulted in a rapid decrease of acetic acid concentrations in the bioreactor which was maintained at < 0.5 mM.

Phase 3 of the mine water treatment involved precipitating transition metals apart from copper, which had already been removed off-line, and manganese, present in the synthetic mine water, within the bioreactor vessel. Concentrations of cobalt, nickel, zinc and manganese present in the synthetic mine water are in excess of the requirements in the Brazilian regulation for industrial waste discharge (Industrial Effluent Discharge Act, 430/2011). The concept of precipitating and concentrating most of these metals within the bioreactor vessel presented as an opportunity for further recovery and recycling. Results are shown in Fig. 3.10.

Most transition metals were precipitated effectively within the aSRBR vessel. Zinc was the most readily removed of these metals, followed by nickel and cobalt, but very little of the manganese present was precipitated, as the pH of the bioreactor was too low for the mineralization of MnS or $Mn(OH)_2$, and reducing conditions precluded the oxidation of soluble Mn (II) to insoluble Mn (IV). Table 3.5 lists differences in the chemical composition of the synthetic mine water at different stages of its treatment.

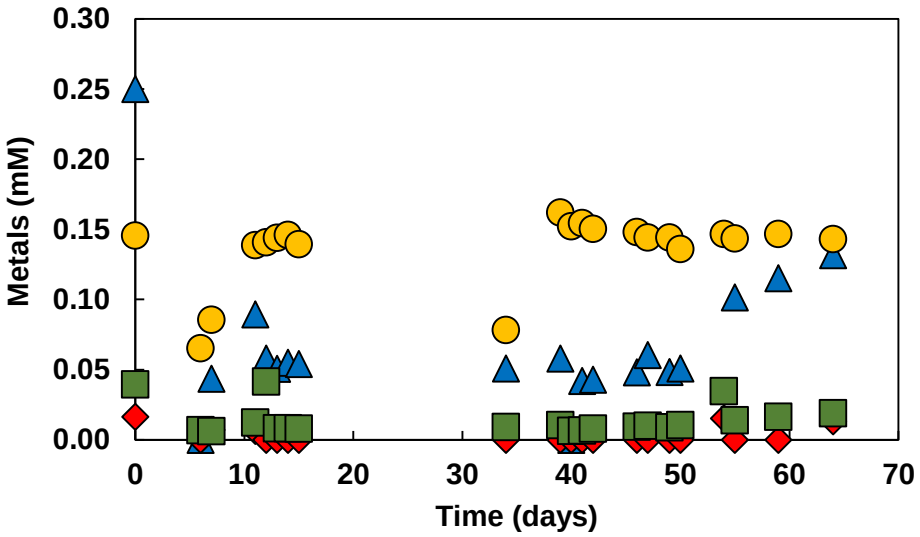


**Fig. 3.10.** Changes in concentrations of transition metals in the bioreactor effluent liquor throughout the time course of the experiment (Phase 3). Key: nickel (▲), zinc (♦), cobalt (■) and manganese (●).

Although the processed water was more acidic (pH 4) than the untreated mine water (pH 5), by precipitating copper, nickel, cobalt and zinc as sulfide phases the treatment protocol

removed 15.7 mmoles $L^{-1}$ of mineral acidity, which far exceeds the 0.1 mmole $L^{-1}$ of proton acidity measured by the pH decrease.

**Table 3.5.** Composition of the synthetic mine water at different stages of treatment (average concentrations, mM).

| | pH | $Cu^{2+}$ | $Ni^{2+}$ | $Mn^{2+}$ | $Zn^{2+}$ | $Co^{2+}$ | $SO_4^{2-}$ |
|---|---|---|---|---|---|---|---|
| **Untreated mine water** | 5.00 | 7.50 | 0.25 | 0.15 | 0.020 | 0.04 | 20.6 |
| **Phase 2 (CuS precipitation)** | 2.10 | < 0.01 | 0.25 | 0.15 | 0.020 | 0.04 | 19.9 |
| **Influent to bioreactor** | 2.10 | 0 | 0.25 | 0.15 | 0.020 | 0.04 | 22.1 |
| **Phase 3 (In-line metal precipitation)** | 4.00 | 0 | 0.04 | 0.14 | <0.01 | 0.01 | 14.5 |

The concentration of sulfate in the feed liquor differed from the untreated mine water due to the addition of basal salts to the feed liquor required to promote and sustain bacterial growth.

*3.3.3 Microbial community in the sulfidogenic bioreactor*

Bacterial 16S rRNA genes were routinely amplified from the bioreactor and analysed using the semi-quantitative terminal restriction enzyme fragment length polymorphism (T-RFLP) technique. All attempts to amplify archaeal 16S rRNA genes from DNA extracted from the bioreactor proved negative, and no eukaryotes (yeasts, etc.) were observed in microscopic observations and therefore the microbial community in the bioreactor was considered to be predominantly or exclusively bacterial. Microbial community analyses were performed only of planktonic cells.

Results from T-RFLP analyses showed a major shift when the composition of the feed liquor changed from “standard SRB medium” (used in Phase 1 and 2) to the partly-processed mine water used in Phase 3 (Fig. 3.11). When the bioreactor was being fed with “standard aSRB medium”, the dominant T-RF (219 nt) corresponded to *Clostridium* sp., isolate MCF105, followed by the moderately acidophilic SRB *Desulfosporosinus acididurans* (215 nt), the two accounting for ~ 90% of the microbial population in the bioreactor. Three other organisms were identified within the bacterial community: the sulfidogen *Peptococcaceae* CEB3 (137 nt), an *Actinobacterium* isolate AR3 (230 nt) and the facultative anaerobe *At. ferrooxidans* (253 nt).

The relative abundance of the planktonic bacterial community in the reactor changed once the partly-processed mine water was introduced to the system (Fig. 3.11). About 70% of

the microbial population was then composed of sulfate-reducers (137 nt and 215 nt) and the isolate MCF105 was no longer detected. *At. ferrooxidans* and the *Actinobacterium* AR3, on the other hand, were more abundant when using the partly-processed mine water as feed liquor.

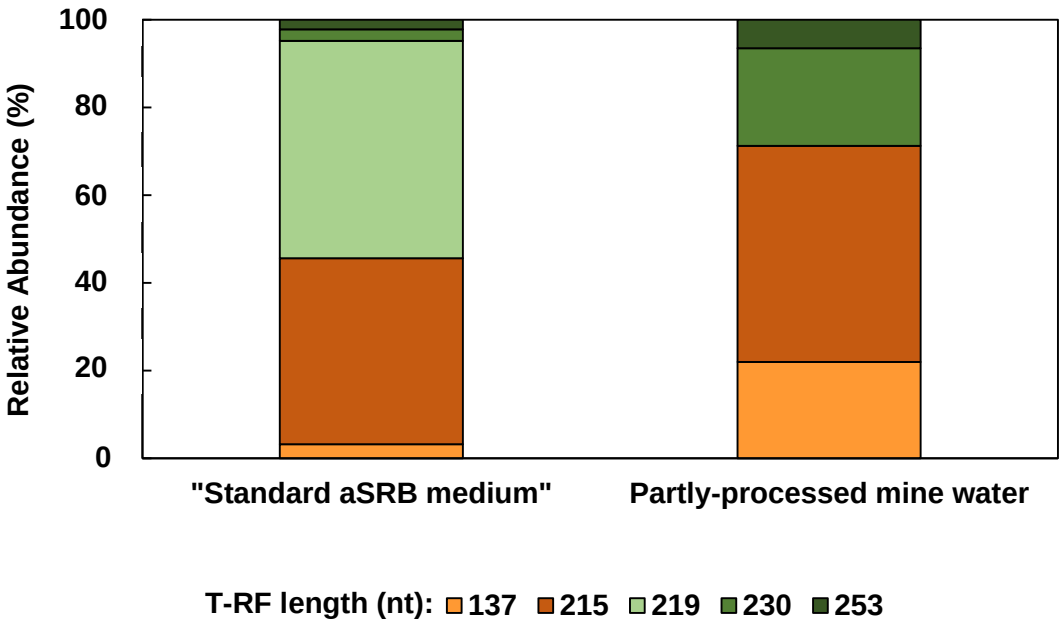


**Fig. 3.11.** Terminal restriction enzyme fragment length polymorphism (T-RFLP) profiles of bacterial 16S rRNA genes (digested with HaeIII) of planktonic samples taken from the sulfidogenic bioreactor with different feed liquor composition: “standard SRB medium” and partly-processed mine water. Shades of orange represent sulfate-reducing bacteria and shades of green represent non-sulfidogens. The digested fragments were identified as corresponding to: 137 nt, *Peptococcaceae* CEB3; 215 nt, *D. acididurans*; 219 nt, *Clostridium* sp. (isolate MCF105); 230 nt, *Actinobacterium* AR3 and 253 nt, *At. ferrooxidans*.

### 3.4 Discussion

The active biological mine water treatment described has several major advantages over alternative strategies that are currently being applied for treating mine waters: (i) controlled alkalinity production is possible, (ii) chalcophilic metals can be selectively precipitated as sulfides in defined locations, and (iii) sulfate concentrations are lowered. Amongst these, the most important is considered to be the potential for recovering commercially valuable metals.

Mine water generated as a waste product at the Sossego copper mine contains very elevated concentrations of copper and smaller concentrations of some other transition metals. The aims of this work were, therefore, to recover copper as potentially saleable product (CuS),

remove the other transition metals present in the synthetic mine water, ameliorate pH and lower the concentration of sulfate. Over 99% of the copper present was removed as CuS from the synthetic mine water using the off-line precipitation strategy where, due to the low pH generated, only copper sulfide was formed. Zinc was also efficiently removed (> 99%) within the bioreactor vessel, together with nickel (85%) and cobalt (75%) (all average values). Concentrations of nickel in the effluent liquor of the sulfidogenic bioreactor showed a progressive increase towards the end of the experiment (Fig. 3.10). Reasons for this are not yet understood, though further experiments were performed in order to enhance the removal of nickel, and are described in Chapter 4.

The water generated from the bioprocessing system described was moderately acidic and contained manganese as a residual transition metal. The fact that manganese was not removed from the synthetic mine water using biosulfidogenesis was expected. Elsewhere it has been shown that this metal can be removed in as a final stage by bacterially-mediated oxidation of Mn (II) and precipitation of Mn (IV) in a process that requires no additional electron donor (Mariner et al., 2008). This issue is addressed in Chapter 6 of this thesis.

As well as protons and sulfate, an electron donor is required for SRB to generate hydrogen sulfide. Glycerol was provided for this purpose, and concentrations added to synthetic mine water were increased in order to produce sufficient hydrogen sulfide for both off-line and in-line metal precipitation, and to increase the pH of the sulfidogenic bioreactor. Production of acetic acid was observed throughout the experiment due to incomplete oxidation of glycerol by the sulfate-reducing acidophile *D. acididurans*, and possibly by other members of the aSRBR consortium. Addition of *Ac. aromatica* mitigated this problem, seemingly by converting acetic acid to $CO_2$ and hydrogen, the latter being available, as a secondary electron donor for the sulfidogen (Kimura et al., 2006).

Changes in the planktonic microbial community of the bioreactor were observed when the partly-processed mine water was introduced to the system. The relative abundance of sulfate-reducing bacteria (*D. acididurans* and *Peptococcaceae* CEB3) increased significantly at this stage, while isolate MCF105, an acid-tolerant mesophile which grows only under strictly anaerobic conditions presumably by fermenting glycerol, was no longer detected by T-RFLP analysis. The latter may be related to the sensitivity of MCF105 to the presence of dissolved metals in the feed liquor (Falagán, 2015). Other non-sulfidogens were also detected: *At. ferrooxidans* and the *Actinobacterium* AR3. The former is a well-known iron-oxidizer/reducer which does not reduce sulfate to hydrogen sulfide, but may have been using dissolved oxygen present in the feed liquors, which were not de-oxygenated, to oxidize small amounts of $H_2S$ and possibly ferrous iron, and the latter is an obligate chemoorganotrophic isolate that grows aerobically or anaerobically on yeast extract (Santos and Johnson, 2017).

A major disadvantage of implementing bioreactor technologies for mine water treatment has traditionally been the costs involved in their construction and operation. The microbial community involved in the process can make these costs even greater because of the known sensitivity of most SRB to even moderate acidity. When neutrophilic sulfidogenic consortia are used, the microorganisms need to be shielded from acidic liquors, which requires them to be housed in reactors that are separated from acidic feed and processed liquors. In addition, much of the sulfide produced at neutral pH values is in the form of soluble $HS^-$, which needs to be removed in a liquid stream. In contrast, when, as in the current case, acidophilic consortia are used, these can be retained in a reactor that uses acidic mine waters directly as feedstocks (and to precipitate many transition metals in-line). Also, since the sulfide produced in almost exclusively in the form of gaseous $H_2S$, this can be readily removed in a gas stream and transferred to a separate contact vessel, as illustrated in the present experiments for off-line copper precipitation. The system described in this work utilize strains and species of acidophilic bacteria which allow the system to be designed and operated as modular units with minimum complexity and running costs. Sizes of bioreactors required in any situation would greatly depend on the chemistry (pH, metal content) and flow rates of the AMD.

Based on data from the laboratory-scale system, a hypothetical 10 $m^3$ sulfidogenic reactor could process simultaneously about 10 $m^3$ per day of AMD containing 476 mg $L^{-1}$ Cu and 15 $m^3$ litres per day of Cu-free AMD containing 14.7 mg $L^{-1}$ Ni, 2.36 mg $L^{-1}$ Co and 1.31 mg $L^{-1}$ Zn. The amounts and values (based on commodity prices quoted in December 2017, and assuming 100% recovery of all metals) of the metals recovered per $m^3$ AMD treated are shown in Table 3.6. By scaling up the sulfidogenic bioreactor described previously to a volume of 10 $m^3$ using the actual performance obtained in the laboratory-scale system, some additional considerations have to be taken into account. In theory, for an average flow rate of 15 $m^3$ $day^{-1}$ and 100% efficient coupling of 5 mM glycerol oxidation (to $CO_2$) to sulfate reduction, 393 moles $H_2S$ would be produced per day. The total amount of $H_2S$ required to precipitate both copper off-line and other metals in-line, assuming 100% metal removal from 15 $m^3$ of synthetic mine water, would be around 117.15 moles $H_2S$ $day^{-1}$ (4.65 moles $H_2S$ for in-line and 112.5 moles for off-line precipitation), i.e. 3.5 times less than the maximum amount that could be theoretically produced. However, the laboratory system displayed less efficient coupling of glycerol oxidation to sulfate reduction. The maximum rate of $H_2S$ production observed under the conditions described (evaluated by combining the amount used to precipitate copper off-line and other transition metals in-line) was 10.4 mmoles $day^{-1}$, and scaling up for a hypothetical 10 $m^3$ sulfidogenic bioreactor, this corresponds to 104 moles $H_2S$ $day^{-1}$. While this would be enough to precipitate metals within the bioreactor vessel, only 13

$m^3$ Cu-rich water could be treated per day in an off-line vessel using the excess $H_2S$ generated. To have a self-sufficient system, at least 15 $m^3$ of Cu-rich water should be processed per day (Phase 2 of the experiment) as this is the volume required to feed the aSRBR for a day.

Regarding the sulfate reduction reaction at low pH (Eq. 3.1) there are 3 components that could be limiting the process: (i) glycerol concentration, (ii) sulfate concentration and (iii) proton (hydronium ion) concentration. The concentration of sulfate in the feed liquor (22.1 mM) is far in excess of that required for oxidation of 4.6 mM glycerol (8.05 mM sulfate, assuming all of the glycerol is oxidized to $CO_2$ rather than partially oxidized to acetic acid). According to Eq. 3.1, complete oxidation of 4.6 mM glycerol coupled exclusively to sulfate reduction should generate 8.05 mM $H_2S$ and, theoretically at least, increasing the glycerol concentration in the feed liquor should generate more $H_2S$. However, the major factor limiting $H_2S$ production would then be the concentration of total acidity in the feed liquor. The feed liquor (Phase 3) was pH 2.1 and contained 7.95 mM free proton acidity, 8.84 mM $HSO_4^-$ (bisulfate) acidity, and about 0.62 mM metal acidity (combination of soluble cobalt, nickel and zinc, but excluding manganese). The total acidity of the feed liquor (partly processed synthetic mine water, as used in Phase 3) was therefore 17.41 mM. This would limit the amount of hydrogen sulfide production to a theoretical maximum of 8.71 mM, which is similar to that predicted from the amount of glycerol consumed, and would therefore restrict greater amounts of $H_2S$ production if glycerol concentrations were increased. There are several possible ways of circumventing this impasse. One way would be to lower the pH of the feed liquor further, which would increase the concentrations of both hydronium and bisulfate ions. Alternatively, the bioreactor could be operated at a higher pH value, so that some bicarbonate ($HCO_3^-$) and $HS^-$ would be generated as end products (rather than almost exclusively $CO_2$ and $H_2S$), which would reduce the amount of acidity required to fuel the equivalent amounts of sulfate reduction. This aspect is addressed in Chapter 4.

**Table 3.6.** Economics of the synthetic mine water treatment.

| | Cu | Ni | Co | Zn |
|---|---|---|---|---|
| **Metal concentration in the synthetic mine water (mM)** | 7.50 | 0.25 | 0.04 | 0.02 |
| **Metal concentration in the synthetic mine water (g $m^{-3}$)** | 476 | 14.7 | 2.36 | 1.31 |
| **Metal price (USD $kg^{-1}$)*** | 6.70 | 10.8 | 70.0 | 3.10 |
| **Amount recovered (USD $m^{-3}$ AMD)** | 3.20 | 0.16 | 0.17 | 0.005 |
| **Total amount recovered** | **USD 3.53 per $m^3$ AMD** | | | |

* Metal prices quoted in Dec 2017 (Source: InfoMine, http://www.infomine.com).

The amount of glycerol (electron donor) needed, considering the 10 $m^3$ sulfidogenic bioreactor, would be around 6.9 kg $day^{-1}$ (equivalent to 75 moles, considering 100% complete oxidation). The price of glycerol (quoted in June 2017) was USD 0.05 per mole (Oleoline Ltd., 2017) costing USD 3.75 per day as a consumable, compared to USD 52.95 worth of metals recovered per day using this approach. The large potential excess in value of the metal recovered is considered more than enough to offset the operating costs of using a low pH sulfidogenic bioreactor for processing Sossego mine water. Additionally, if the other transition metals were also 100% recovered (as addressed in Chapter 4 of this thesis), this approach would deliver not only financial but also environmental benefits.

For the development of a pilot-scale operation to bioremediate the actual mine water draining the Sossego copper mine in Brazil, the parameters evaluated in this thesis should be considered as a base line study.

# Effects of variations in chemical and operational parameters on the kinetics of an acidophilic sulfidogenic bioreactor and indigenous microbial communities

4

## 4.1 Introduction

Biosulfidogenesis, the microbial generation of hydrogen sulfide by reduction of more oxidized sulfur species, is a very useful technology for remediating acidic, metal-rich wastewaters, such as acid mine drainage. Many transition metals form highly insoluble sulfide phases when contacted with $H_2S$, and bacterial reduction of sulfate to sulfide is, in acidic liquors, a proton-consuming reaction. Commercial-scale sulfidogenic bioreactors use neutrophilic species of sulfate- (or sulfur-) reducing bacteria that need to be shielded from direct contact with acidic wastewaters, which is not the case with acidophilic and acid-tolerant species (aSRB). However, information about the kinetics and microbial communities in sulfidogenic bioreactors that operate at low pH is scarce. Rates of sulfate reduction and bacterial community profiles of aSRB reactors have been assessed previously in sulfate-reducing bioreactor operated at between pH 2.2 and 4.5, but the effect of temperature or other changes in the chemical composition of the influent liquor were not examined in the report of Ñancucheo and Johnson (2012a). This chapter describes the kinetics and microbial dynamics of a low pH, laboratory-scale sulfidogenic bioreactor, operated as a continuous flow system, at pH values between 4.0 and 5.0, temperatures between 30 and 45°C, concentrations of yeast extract in the feed liquor of between 0 and 0.1 g $L^{-1}$ and sodium chloride concentration in the feed liquor between 0 and 100 mM.

While changing an operating parameter caused minor perturbations in the performance of the bioreactor, these were usually transient, and the system performed consistently well throughout the entire test period, with pH 5.0 and 35°C being marginally the optimum operating conditions. Two species of aSRB mediated sulfide formation: *Desulfosporosinus acididurans*, preferentially at higher pH and lower temperatures, and *Peptococcaceae* CEB3, at lower pH and higher temperatures. The relative abundances of these two bacteria changed in response to operational (pH, temperature) and chemical (yeast extract and sodium chloride) changes. The results obtained highlighted the robustness and adaptability of the low pH microbial consortium used to generate sulfide, and to precipitate transition metals within the bioreactor vessel, at a range of pH values and temperatures. Previously, the performance of the aSRB

reactors was described when maintained at 30°C, while one objective of the current study was to examine how such modules might function at higher temperatures, since this approach, if proved efficient, could be widely applied in tropical areas, such as Amazonia.

## 4.2 Materials and methods

### *4.2.1 Sulfidogenic bioreactor*

A sulfidogenic upflow biofilm reactor, described in section 2.4, populated with a mixed microbial community containing several species of aSRB and non-sulfidogenic acidophilic bacteria was used in the experimental work described in this chapter. Proton consumption resulting from biosulfidogenesis was counter-balanced by the inflow of synthetic AMD, which was therefore necessarily of lower pH than that of the liquid inside the bioreactor. pH homeostasis was met by coupling the pH control box in the FerMac unit with a pump that controlled the influx of AMD. Oxygen-free nitrogen (OFN) was bubbled through the bioreactor, both to promote anoxic conditions within the vessel and to act as a carrier for the excess $H_2S$ generated.

The standard feed liquor of the aSRBR contained ABS/TE (section 2.2.2.1), 5 mM glycerol, pH 2.1 and the same metal concentrations (Table 4.1) of the partly processed (copper-free) mine water used in Phase 3 of the experiment (section 3.2.2). The concentration of yeast extract in the feed liquor was 0.1 g $L^{-1}$ unless stated otherwise.

**Table 4.1.** Chemical composition of the partly processed mine water used in experimental work.

| Analyte | Concentration (mM) |
|---|---|
| $Ca^{2+}$ | 7.00 |
| $Mg^{2+}$ | 4.00 |
| $Na^{+}$ | 2.10 |
| $K^{+}$ | 0.28 |
| $Ni^{2+}$ | 0.25 |
| $Mn^{2+}$ | 0.15 |
| $Co^{2+}$ | 0.04 |
| $Zn^{2+}$ | 0.02 |
| $SO_4^{2-}$ | 22.1 |
| $Cl^{-}$ | 0.04 |

Variations in the operating pH and temperature of the bioreactor, as well as concentrations of yeast extract and sodium chloride in the feed liquor, were performed in order to evaluate the effect of these parameters on the kinetics and microbial dynamics of the low pH sulfidogenic bioreactor.

#### 4.2.1.1 Performance of the aSRBR when maintained at different pH values and temperatures

The data described below came from operating the sulfidogenic bioreactor in continuous flow mode for a period of 462 days. For the first 229 days of the experiment, the bioreactor was maintained at 30°C. Initially (from day 0 – 51), the pH of bioreactor was held at pH 4.0, but this was increased, initially to pH 4.5 (at day 51) and then to pH 5.0 (at day 85) before being returned to pH 4.0 at day 136. The aSRB reactor continued to be maintained at pH 4.0 up to day 373, though the temperature was increased during this period (to 35°C at day 229, 40°C at day 292, and 45°C at day 344). The bioreactor pH was increased on day 373 to pH 5.0 and maintained at this value for the duration of the experiment, and the temperature was lowered in two stages (to 40°C at day 380, and 35°C at day 442).

For each combination of these parameters, flow rates (referred to in terms of HRTs) concentrations of soluble metals in the influent and effluent liquors, rates of sulfate reduction, glycerol consumption, acetic acid production and numbers and compositions of planktonic bacteria were monitored at regular intervals.

#### 4.2.1.2 Variations in yeast extract concentrations in the feed liquor

The effect of yeast extract (YE) on the performance of the aSRBR was evaluated by adding different concentrations (0, 0.05 and 0.1 g $L^{-1}$) of this complex organic material to the feed liquor. For this experiment, the bioreactor was operated at pH 4.0 and 30ºC using copper-free mine water (pH 2.1) amended with ABS/TE, 5 mM glycerol and different concentrations of yeast extract as feed liquor. Hydraulic retention times (expressed in hours), glycerol consumption, acetic acid production, cell numbers, concentrations of metals in the effluent liquor, sulfate reduction rates and the composition of planktonic bacterial communities within the bioreactor vessel were monitored over a period of 70 days.

#### 4.2.1.3 Variations in salt (NaCl) concentrations in the feed liquor

Preliminary tests using different concentrations of sodium chloride in the feed liquor of the sulfidogenic bioreactor were carried out for a period of 120 days in order to assess the

effect of salt on the indigenous population and performance of the sulfidogenic bioreactor. The bioreactor was operated at pH 4.0 and 35ºC and copper-free mine water (pH 2.1) amended with ABS/TE, 5 mM glycerol and 0.1 g $L^{-1}$ yeast extract was used as the feed liquor.

*4.2.2 Compositions of the community structure of immobilised bacteria in the aSRBR*

Bacterial communities in the aSRBR were routinely monitored using liquid samples taken from the bioreactor, which therefore only assessed the relative abundances of planktonic cells. Collecting samples from the biofilm bed was avoided during experimental runs in order not to disturb the fixed bead bed, which could have affected the performance of the bioreactor and biased some results.

At the end of the pH and temperature experiment (section 4.2.1.1), samples from the biofilm bed were collected at three different depths (6, 9 and 13 cm) measured from the top of the liquid phase in the bioreactor vessel. A sterile 1.5 cm diameter core sample was used to collect samples of the colonised Poraver porous glass beads from the bottom to top layers by dispensing the samples in different sterile universal bottles. A representative sampling scheme is shown in Fig. 4.1. Simultaneously, pH was measured in each layer of the biofilm bed as well as in the liquid phase. For comparison, two samples from the liquid phase (0 and 3 cm depth) were also collected for pH measurements and one for microbial community analysis.

Bacterial populations were assessed using semi-quantitative T-RFLP analysis (section 2.9.4) in one sample of the liquid phase (bottom liquid layer; Fig. 4.1) and all three colonised beads samples (top, mid, bottom layers).

A mixed bead sample (from all layers) was withdrawn from the biofilm bed of the sulfidogenic bioreactor, and visualised using scanning electronic microscopy (SEM) and analysed by the energy dispersive analysis of X-rays (EDAX) to provide elemental identification and semi-quantitative composition of the samples. Sample preparation and microscopy settings are described in section 2.10.3.

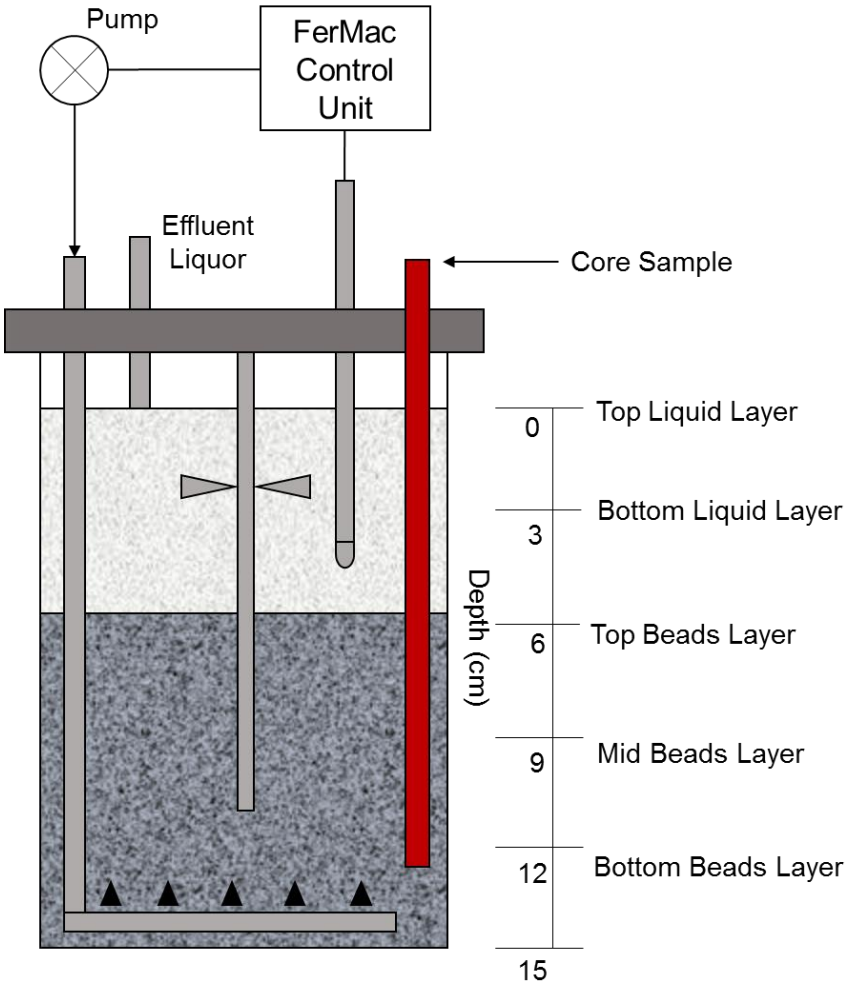


**Fig. 4.1.** Schematic representation of the biofilm bed sampling. Liquid samples were withdrawn using sterile glass pipettes in two different depths (0 and 3 cm) and samples of the biofilm bed were withdrawn at 6, 9 and 12 cm using a sterile core sampler. The total depth of the working volume of the bioreactor (biofilm bed plus surface liquor) was 15 cm.

## 4.3 Results

### *4.3.1 Performance of the aSRBR as impacted by variations in pH and temperature*

Time-related changes in hydraulic retention times (HRTs) of the aSRBR during experiments in which the pH or temperature were varied are shown in Fig. 4.2. Flow rates (and HRTs) were related directly to the rates of sulfate reduction, since the pH and chemical composition of the synthetic AMD remained constant during these experiments.

Changing the influent liquor from “standard SRB medium” to the partly processed mine water (section 3.2.2; Phase 3) resulted in a dramatic increase in HRT (from 50 to 220 h) though this subsequently declined, stabilizing at ~37 h by day 38. As shown in Fig. 4.2, changing an

operational parameter (pH or temperature) usually caused the HRT to increase, though this was always a transient feature, and HRTs subsequently declined until the next operational change.

The effect of operating the bioreactor at different pH values and temperatures on rates of sulfate reduction in the aSRBR is shown in Fig. 4.3. While standard deviations were large in each case (reflecting, in part, the time taken for the system to reach equilibrium after a parameter was changed) some general trends were apparent. Mean rates of sulfate reduction increased with increasing pH between pH 4.0 and 5.0 when the bioreactor was maintained at 30°C, while the opposite trend was apparent at 35 and 40°C (no measurements were recorded at pH 4.5 at these temperatures). Fig. 4.3 also shows that the mean rate of sulfate reduction increased between 30 and 35°C, but decreased (marginally) at higher temperatures. The maximum rate of sulfate reduction (1.432 ± 0.518 g $L^{-1}$ $day^{-1}$) was observed when the aSRB reactor was maintained at 35°C and pH 4.0. Sulfate concentrations in the liquors draining the bioreactor ranged between 6.5 and 20 mM (624 and 1,920 mg $L^{-1}$ of sulfate).

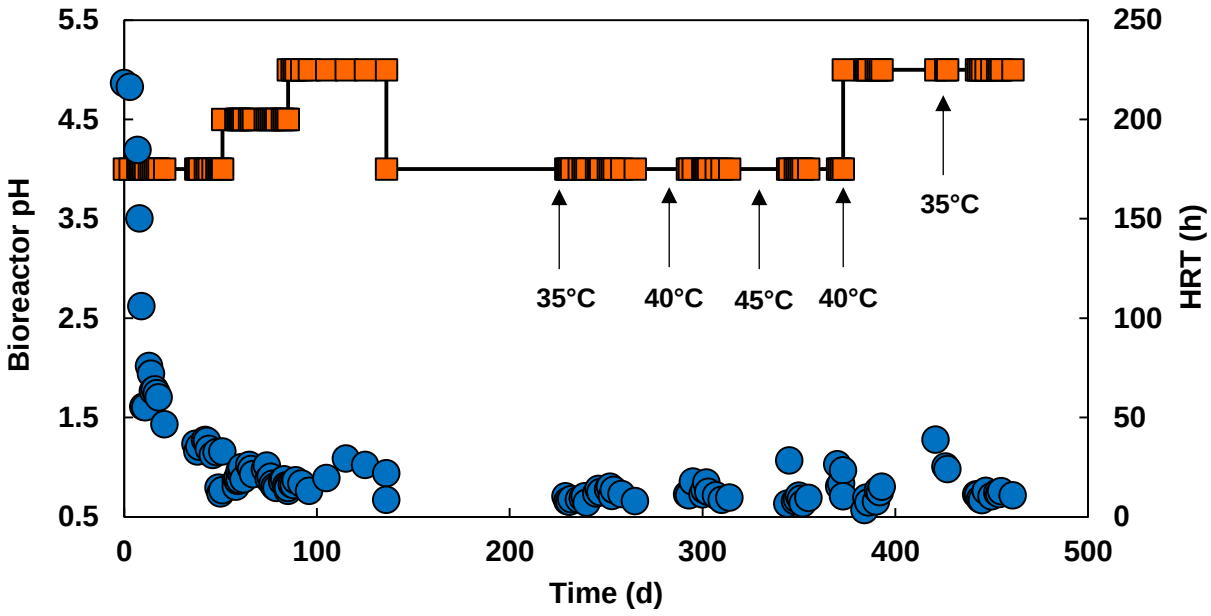


**Fig. 4.2.** Changes in HRTs (●) and pH values (■) in the aSRBR. The bioreactor was maintained at 30°C for the first 229 days of the experiment, and the upward-pointing arrows indicate when it was subsequently changed.

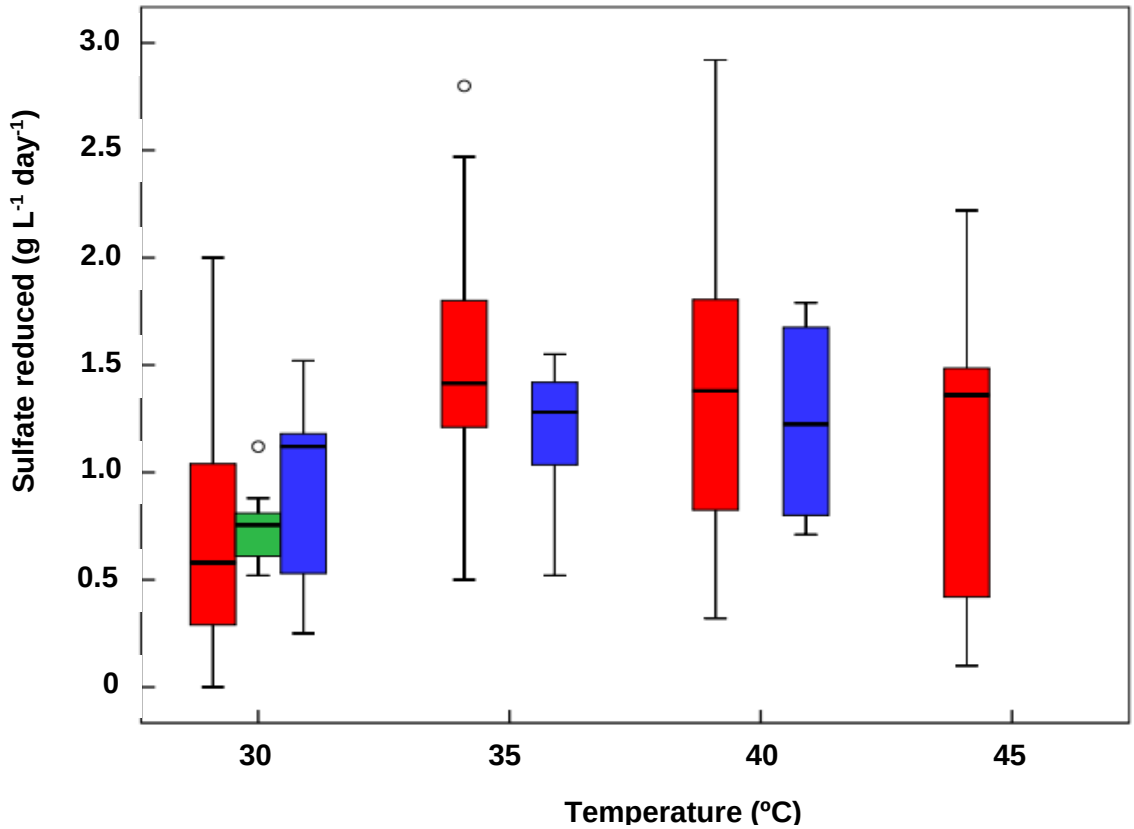


**Fig. 4.3.** Box plot representation of variations in rates of sulfate reduction with changing operational (pH and temperature) parameters. Key: pH 4.0 (red), pH 4.5 (green), pH 5.0 (blue). The open circles represent outlier data points which did not fall into the inner fences of the box.

Fig. 4.4 shows differential removal of transition metals from the copper-free synthetic AMD within the bioreactor vessel, as effected by pH and temperature. Zinc was the most readily removed of these metals, followed by nickel and cobalt, but very little of the manganese present in the influent liquors was precipitated as the pH of the bioreactor was too low for the mineralization of MnS or $Mn(OH)_2$.

Concentrations of glycerol consumed and acetic acid produced during the time course of the experiment are shown in Fig. 4.5. While overall most of the glycerol added to the influent synthetic mine water was metabolised, but changing the pH or temperature of the bioreactor often resulted in transient decrease in glycerol consumption. Acetic acid, which is produced by aSRB that oxidize glycerol incompletely (and possibly by the *Actinobacterium* AR3 when fermenting glycerol) was also detected regularly in bioreactor effluent. Addition of the acetoclastic acidophile, *Acidocella aromatica*$^T$ (Jones et al., 2013), to the bioreactor at day 70 caused the concentration of acetic acid to decline to 0.5 mM (by day 94). Subsequently, although concentrations of acetic acid were variable and often also peaked after either the

operating pH or temperature of the bioreactor was changed, they tended to stabilize at ~ 0.5 mM.

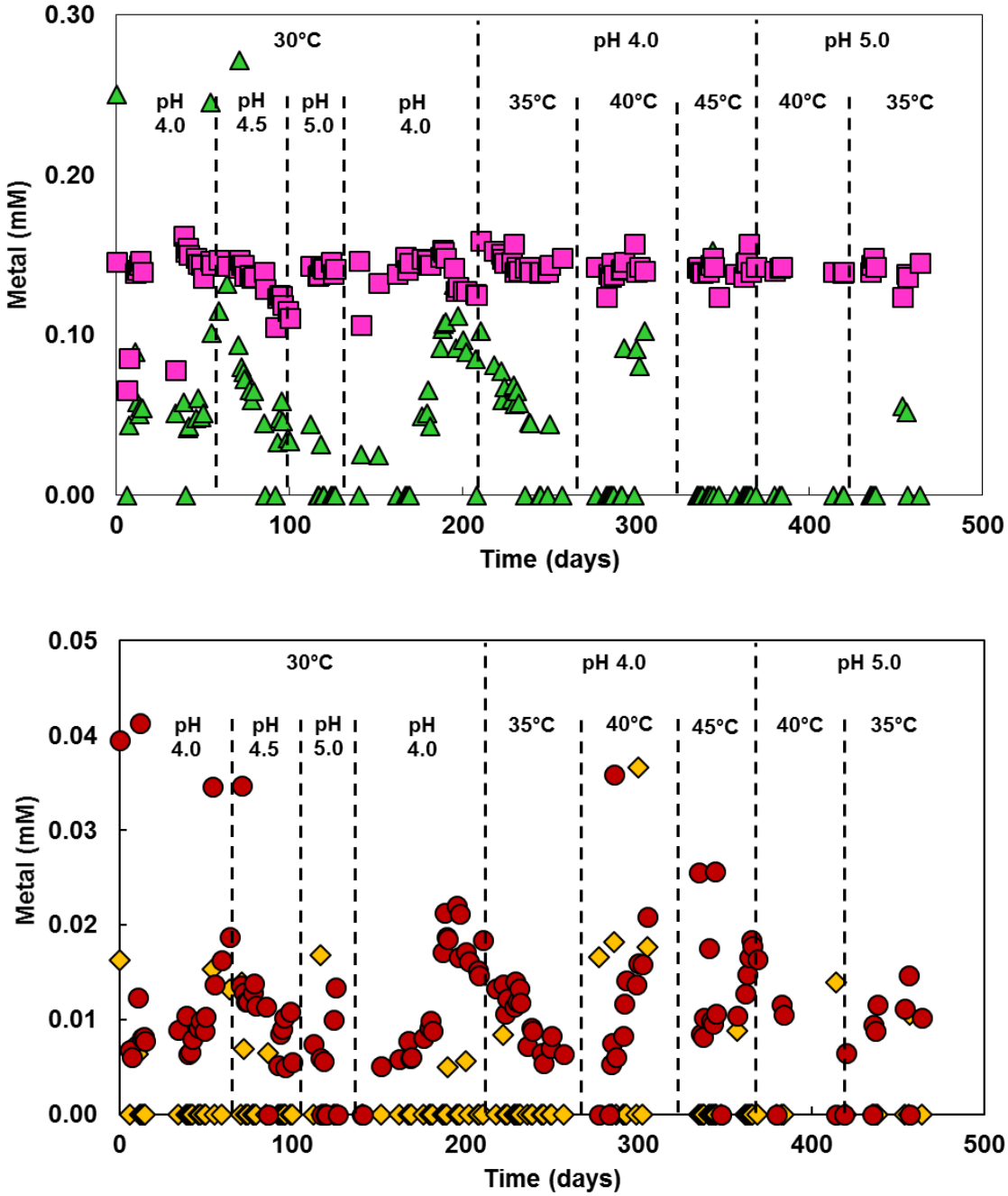


**Fig. 4.4.** Changes in concentrations of transition metals, Ni (▲), Mn (■), Zn (♦) and Co (●) in the bioreactor effluent liquor.

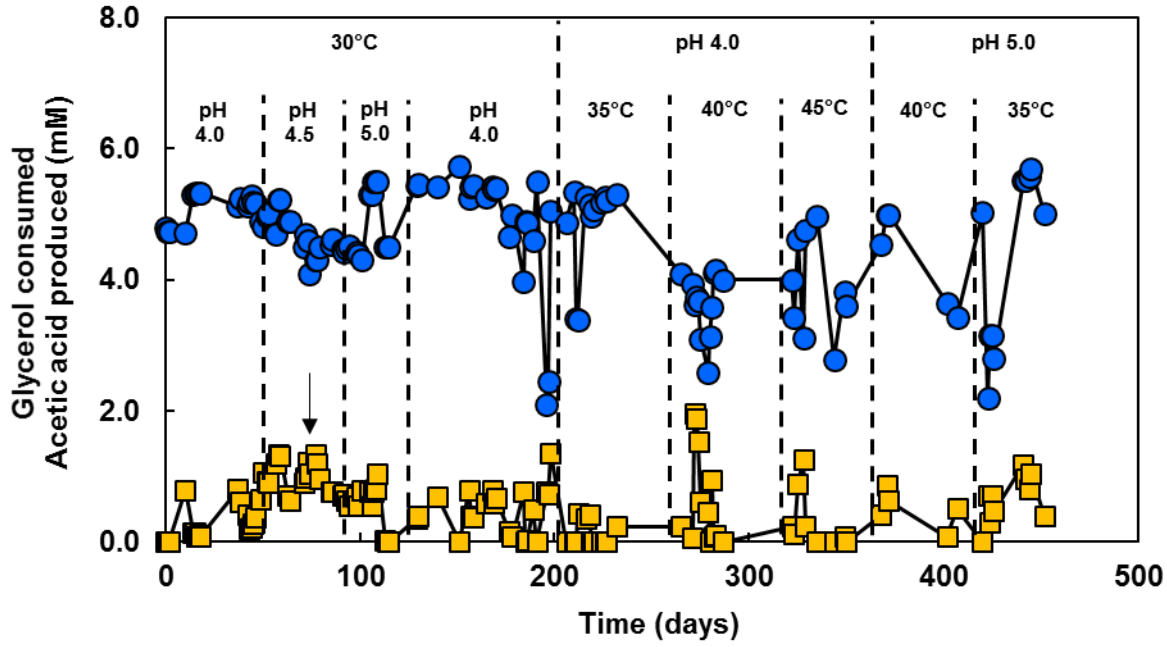


**Fig. 4.5.** Changes in concentrations of glycerol consumed (●) and acetic acid produced (■) in the sulfidogenic bioreactor. The downward-pointing arrow indicates the time when an active culture of *Acidocella aromatica*$^{T}$ was added to the sulfidogenic bioreactor.

Bacterial 16S rRNA genes were routinely amplified from the bioreactor liquors, but regular attempts to amplify archaeal genes all produced negative results. Results from semi-quantitative T-RFLP analysis of these genes (Fig. 4.6) showed that the microbial community within the bioreactor was dominated by four species of bacteria, two of which were known sulfidogens (*Desulfosporosinus acididurans* and *Peptococcaceae* CEB3) while the other two (*Acidithiobacillus ferrooxidans* and *Actinobacterium* AR3) do not catalyse the dissimilatory reduction of sulfate.

While T-RFs corresponding to all four bacteria were detected on each sampling occasion, their relative abundances varied greatly. T-RFLP analysis indicated that, when operated at 30°C and pH 4.0, the liquid phase was dominated by non-sulfidogenic bacteria, though *D. acididurans* and *Peptococcaceae* CEB3 were far more abundant and dominant under all other conditions, sometimes accounting for 90% of the summated T-RF peak areas. In general, *Peptococcaceae* CEB3 tended to become more relatively abundant at temperatures above 30°C, while *D. acididurans* was the most abundant bacterium detected in bioreactor liquors when operated at pH 4.5 and 30°C. However, at pH 5.0 and higher temperatures *D. acididurans* and *Peptococcaceae* CEB3 were fairly evenly relatively abundant (Fig. 4.6). Despite being added to the bioreactor at day 70, no T-RF corresponding to *Ac. aromatica* was detected in any bioreactor liquor sample.

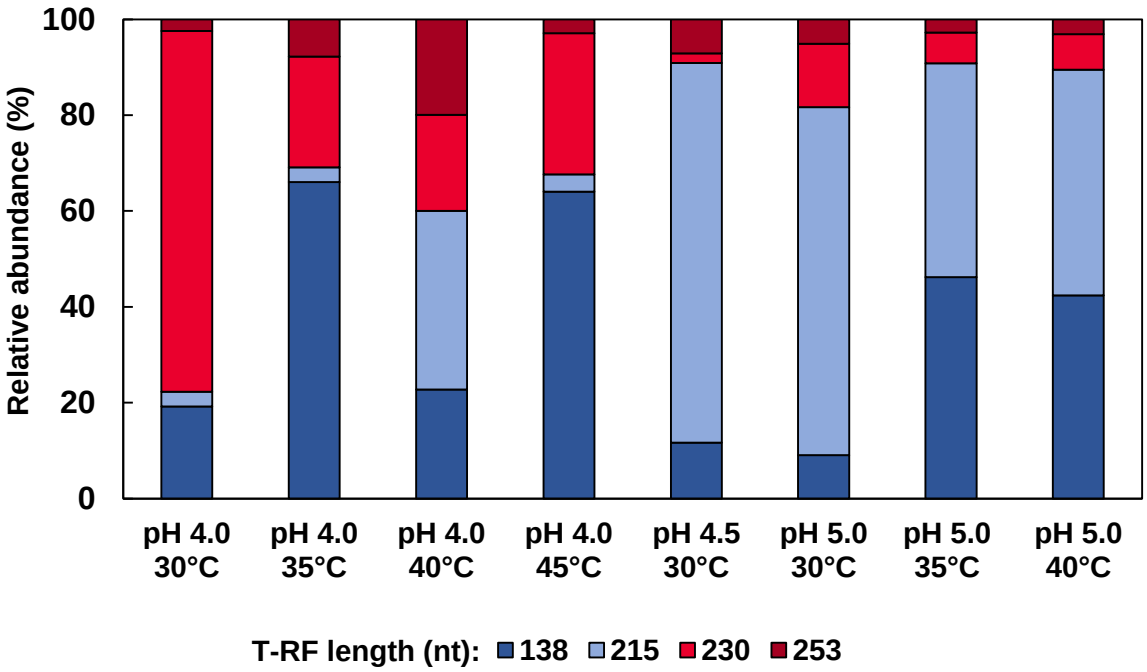


**Fig. 4.6.** Terminal restriction enzyme fragment length polymorphism (T-RFLP) analysis (HaeIII digests of amplified 16S rRNA genes) of planktonic bacterial communities in the aSRB reactor operated at different temperatures and pH values. Shades of blue represent sulfate-reducing bacteria and shades of red represent non-sulfidogens. 138 nt: *Peptococcaceae* CEB3; 215 nt: *D. acididurans*; 230 nt: *Actinobacterium* AR3 and 253 nt: *At. ferrooxidans*.

*4.3.2 Performance of the aSRBR as impacted by variations in yeast extract concentrations*

Yeast extract has been used as a component of the feed liquor for low pH sulfidogenic bioreactors at Bangor University for a number of years. This is a complex mixture of (mostly) organic materials that facilitates microbial growth by providing nutrients and growth factors to promote biomass growth, but can also act of a potential secondary electron donor. The low pH acidophilic sulfidogenic bioreactors are usually fed with feed liquor containing 0.1 g $L^{-1}$ yeast extract. This experiment evaluated the performance of the bioreactor by monitoring several parameters while varying the concentration of yeast extract (0, 0.05 and 0.1 g $L^{-1}$) in the feed liquor.

Figure 4.7 shows changes in HRTs and planktonic cell numbers throughout this experiment. Hydraulic retention times increased on each occasion that the concentration of yeast extract changed, but each time they subsequently decreased as the productivity of the bioreactor increased. When using 0.1 g $L^{-1}$ YE, a HRT peak was observed on day 10, suggesting that the bioreactor performance decreased significantly at that time, though the reason for this downturn in performance was not known, and no external perturbations (such

as reflux of copper sulfate from the attached off-line vessel into the bioreactor) had occurred. The number of planktonic cells remained fairly constant during the first phase of this experiment (0.1 g $L^{-1}$ YE), at around 3.5 x $10^7$ cells $mL^{-1}$. When there was no yeast extract present in the influent liquor, HRTs ranged from 11 to 22 h and a sharp decrease in planktonic cell numbers, which fell to 0.4 x $10^7$ cells $mL^{-1}$, was observed. However, after 15 days with zero yeast extract feed liquor (day 35) cell numbers increased slightly, possibly due to bacterial adaptation (e.g. by synthesising growth factors previously provided in yeast extract). When yeast extract was re-introduced to the feed liquor at an intermediate concentration (0.05 g $L^{-1}$), HRTs remained relatively high for about 10 days, before going into a steady decrease averaging 8.5 h (Fig. 4.7). Planktonic cell numbers increased slightly compared to the zero YE feed, though they were about 50% of those when using twice as much yeast extract.

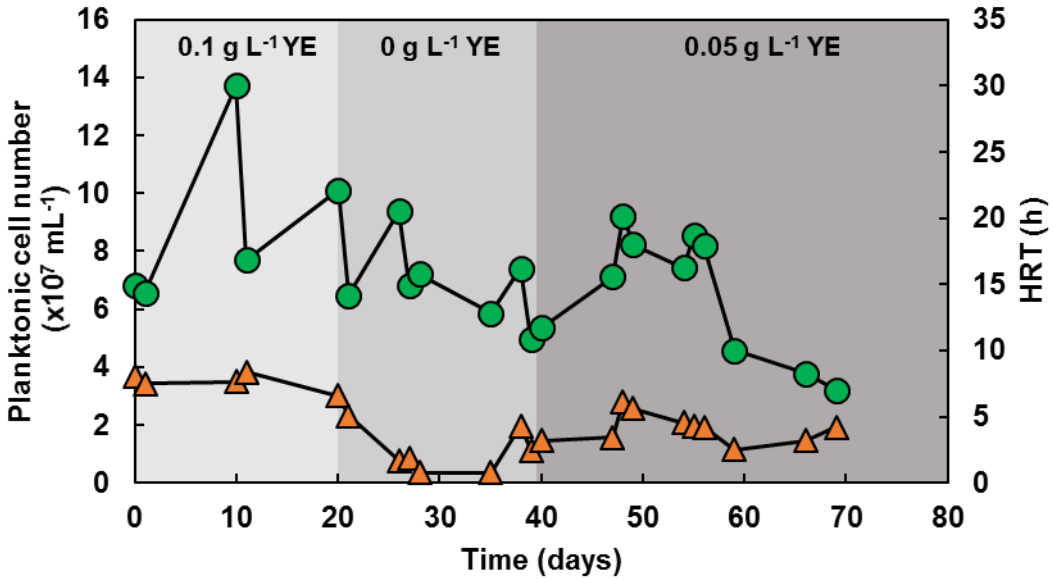


**Fig. 4.7.** Changes in planktonic cell numbers (▲) and HRTs (●) in the aSRBR with different concentrations of yeast extract (0, 0.1 and 0.05 g $L^{-1}$) added to the feed liquor.

Metal concentrations in the effluent liquor of the aSRBR was monitored throughout this experiment; results are shown in Fig. 4.8. Most transition metals were precipitated effectively within the aSRBR vessel when using 0.1 g $L^{-1}$ YE in the feed liquor. Over 99% zinc was removed, ~ 90% of both nickel and cobalt, but very little of the manganese present was precipitated (~ 7%) for reasons explained previously. Similar results were observed in a previous experiment (section 3.3.2), demonstrating the reproducibility of the system developed.

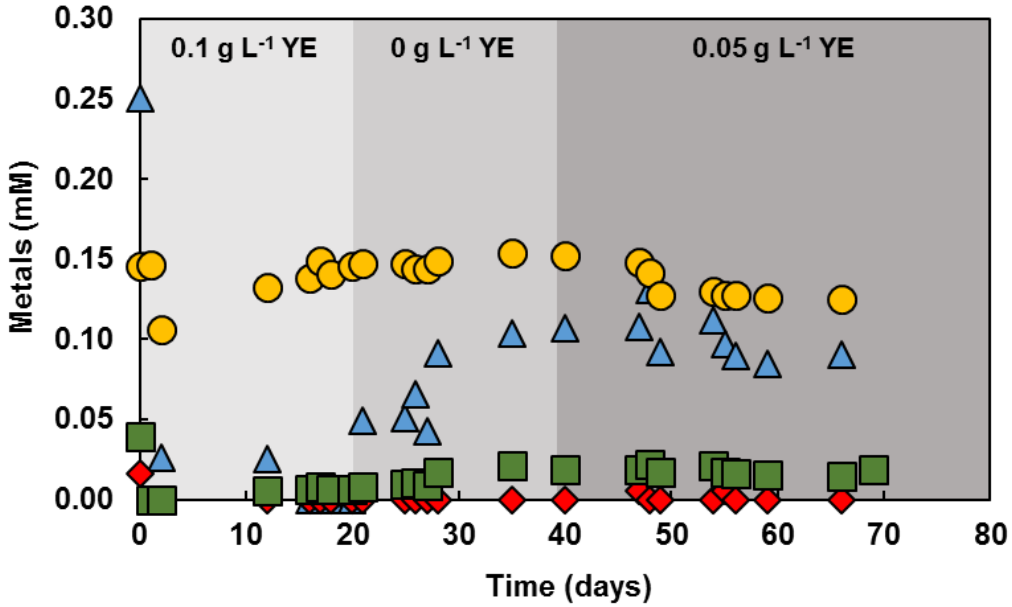


**Fig. 4.8**. Changes in concentrations of transition metals in the bioreactor effluent liquor using different concentrations of yeast extract (0, 0.05 and 0.1 g $L^{-1}$ YE) in the feed liquor. Key: nickel (▲), zinc (♦), cobalt (■) and manganese (●).

Major changes in the extents to which transition metals were removed were observed when the concentration of yeast extract in the feed liquor was altered. On average, only 73% of nickel and 70% of cobalt were precipitated when no yeast extract was present in the feed liquor. Surprisingly, these figures were even lower when using 0.05 g $L^{-1}$ YE in the feed liquor, with only 60 and 54% of nickel and cobalt, respectively, being removed. However, no significant change was observed for zinc, where > 99% was removed from the influent liquor irrespective of yeast extract concentration.

Concentrations of glycerol consumed and acetic acid produced in this experiment are shown in Fig. 4.9. Most of the glycerol added to the bioreactor was oxidized completely to carbon dioxide, though acetic acid was detected throughout in low concentrations (< 1.3 mM). There was no significant differences in acetic acid production throughout this experiment, though glycerol consumption decreased slightly from day 55 when using 0.05 g $L^{-1}$ YE. While most of the glycerol was consumed and little acetic acid was produced, which suggests that rates of $H_2S$ production and therefore of metal sulfide precipitation should have been fairly consistent, this does not equate with data reported in Fig. 4.8.

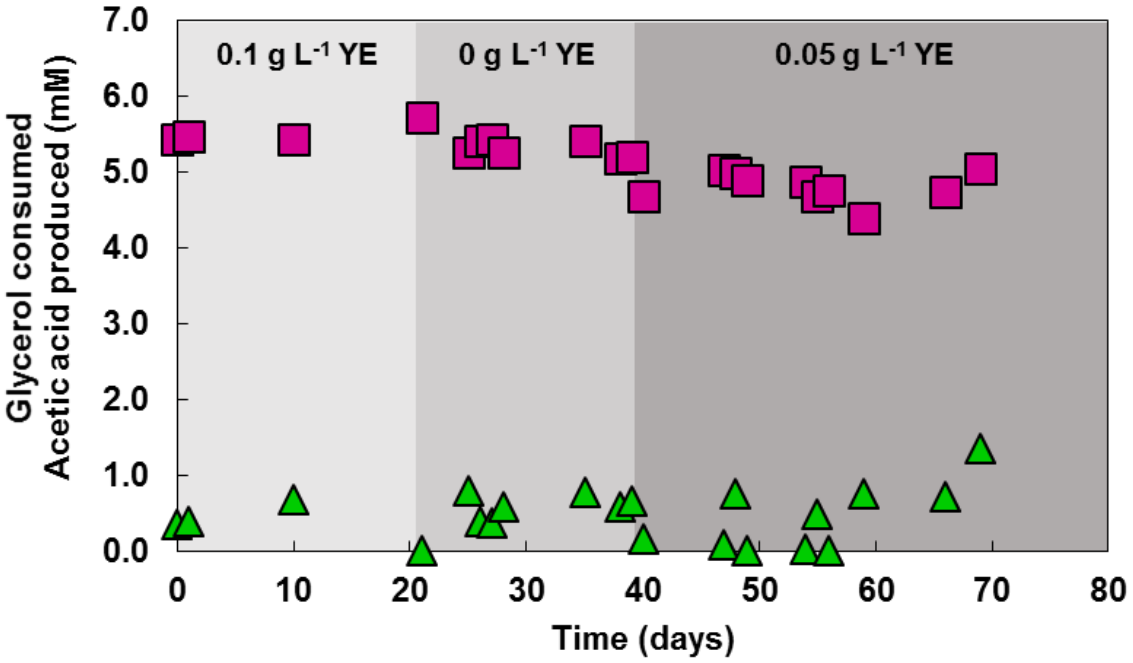


**Fig. 4.9.** Changes in concentrations of glycerol consumed (■) and acetic acid produced (▲) in the bioreactor using different concentrations of yeast extract (0, 0.05 and 0.1 g $L^{-1}$ YE) in the feed liquor.

Variations in rates of sulfate reduction during this experiment are shown in Fig. 4.10. Average sulfate reduction rates obtained in the first phase of this experiment (using 0.1 g $L^{-1}$ YE) was around 1.3 g $SO_4^{2-}$ reduced $L^{-1}$ $day^{-1}$. A rapid sharp decrease was observed when YE was eliminated from the feed liquor, which was followed by a gradual increase with rates of sulfate reduction ranging between 0.8 and 1.2 g $SO_4^{2-}$ reduced $L^{-1}$ $day^{-1}$. In the last phase of this experiment (aSRBR fed with 0.5 g $L^{-1}$ YE) variations were much more pronounced ranging between 0.3 and 1.2 g $SO_4^{2-}$ reduced $L^{-1}$ $day^{-1}$, with rates showing a progressive increase towards the end of the experiment.

Bacterial 16S rRNA genes were routinely amplified from liquid samples taken from the bioreactor and analysed using T-RFLP. Results (Fig. 4.11) showed relatively minor changes in the planktonic bacterial community when the concentration of YE in the feed liquor was changed. In the first phase of this experiment, the aSRBR was fed with 0.1 g $L^{-1}$ YE and sulfate-reducers accounted for ~ 92% of the population of which 72% correspond to the moderately acidophilic *D. acididurans*. When the concentration of YE was changed (to 0 and then to 0.05 g $L^{-1}$) the sulfate-reducing bacteria accounted, in both cases, for ~ 75% of the planktonic population within the bioreactor (138 nt: *Peptococcaceae* CEB3 and 215 nt: *D. acididurans*). The other T-RFs identified corresponded to the heterotroph *Actinobacterium* AR3 (230 nt) and the chemolithotrophic facultative anaerobe *At. ferrooxidans* (253 nt).

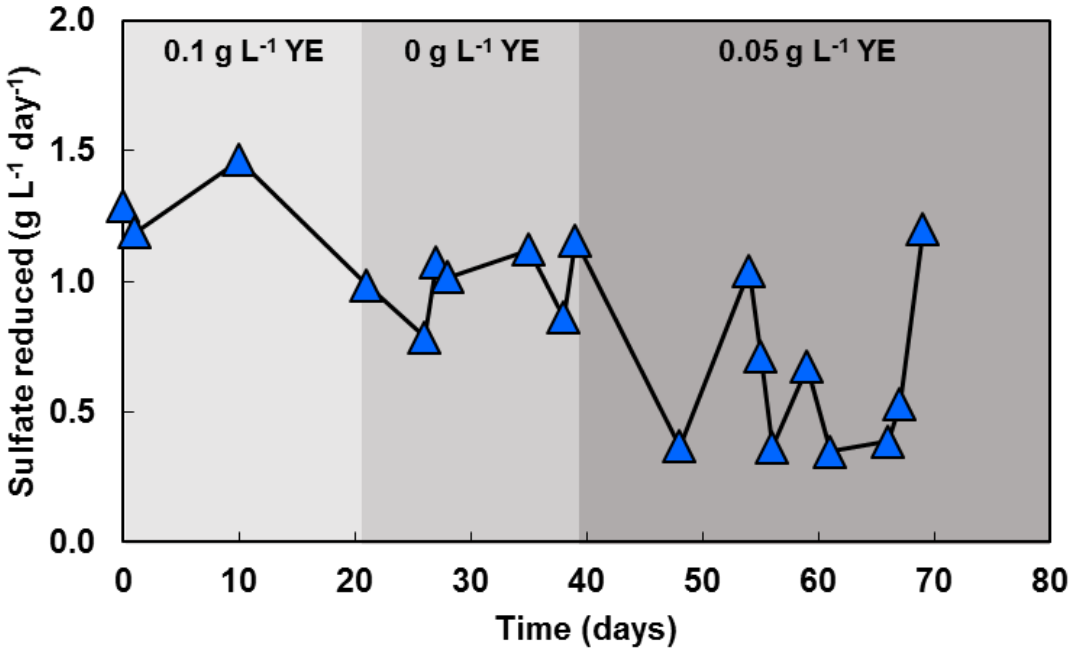


**Fig. 4.10.** Changes in rates of sulfate reduction in the bioreactor using different concentrations of yeast extract (0, 0.05 and 0.1 g $L^{-1}$ YE) in the feed liquor.

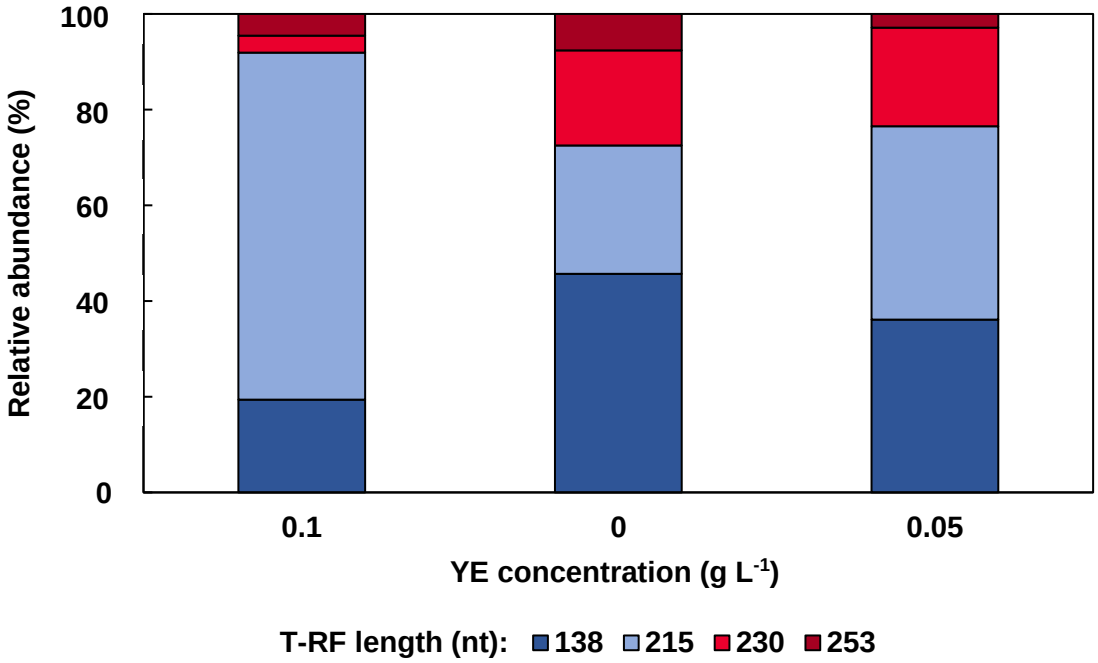


**Fig. 4.11.** Terminal restriction enzyme fragment length polymorphism (T-RFLP) analysis (HaeIII digests of amplified 16S rRNA genes) of planktonic bacterial communities in the aSRB reactor operated with different concentrations of yeast extract in the feed liquor. Shades of blue represent sulfate-reducing bacteria and shades of red represent non-sulfidogens 138 nt: *Peptococcaceae* CEB3; 215 nt: *D. acididurans*; 230 nt: *Actinobacterium* AR3 and 253 nt: *At. ferrooxidans*.

*4.3.3 Performance of the aSRBR as impacted by variations in salt (NaCl) concentrations*

The performance of the sulfidogenic bioreactor was tested using different concentrations of sodium chloride (50 and 100 mM) added to the influent liquor. These concentrations were selected from the limited data available on salt tolerance of one of the indigenous sulfidogenic bacteria (Sánchez-Andrea et al. (2015) reported that *D. acididurans* could tolerate up to ~ 250 mM NaCl).

Prior to adding salt to the feed liquor, the HRT of the aSRBR (fed with copper-free synthetic AMD, pH 2.1) was 11 $\pm$ 1.5 h. When 100 mM NaCl was added to the feed liquor, this increased within a very short time to ~ 120 h, though subsequently decreased to ~ 60 h (Fig. 4.12). However, after operating the aSRBR for about 13 days with 100 mM NaCl feed liquor, flow into and out of the bioreactor came to a halt due to the fact that net alkalinity production ceased. The pH of the bioreactor surface liquid layer remained at 4.0, though the lack of inflow of the more acidic feed liquor implied that net alkalinity production had been arrested. This period of inactivity continued for 2 weeks, at which time glycerol was injected directly into the reactor (10 mL of 1 M glycerol, corresponding to ~ 5 mM in the aSRBR) and the concentration of NaCl in the feed liquor was lowered to 50 mM. This resulted in flow into and out of the aSRBR restarting. The HRT during this period varied between 16 and 47 h (Fig. 4.12). In the final phase of this experiment, no salt was added to the feed liquor. The aSRBR continued to perform with no interruption, with HRTs varying between 18 and 32 h over the 40 days of duration of this phase of the experiment.

Cell numbers in the liquid phase of the bioreactor during this experiment are also shown in Fig. 4.12. An average of 6.0 x $10^7$ cells $mL^{-1}$ were found during the first 13 days of using feed liquor amended with 100 mM NaCl (day 13 to day 26), but these declined greatly (average of ~ 1.5 x $10^7$ cells $mL^{-1}$) during the period that the aSRBR was inactive (days 27 to 46). Relative little variation in cell numbers were recorded with 50 mM NaCl, however these figures were still considerably lower (~ 2.5 x $10^7$ cells $mL^{-1}$) than those obtained before salt-amended influent liquor was used (6.5 x $10^7$ cells $mL^{-1}$) and at the following stage (also with addition of NaCl) where cell numbers were as high as 7.0 x $10^7$ cells $mL^{-1}$. Samples were not collected between days 85 and 114; however no significant variations of HRTs and cell numbers were observed from day 115 to the end of this experiment at day 120.

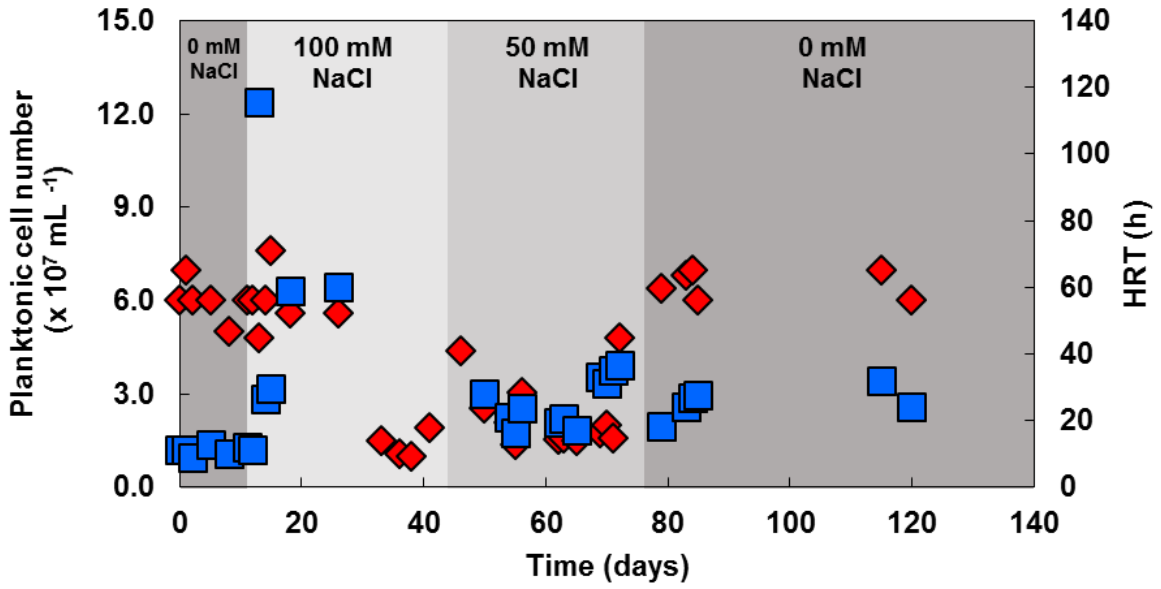


**Fig. 4.12.** Changes in planktonic cell numbers (♦) and HRTs (■) in the aSRBR using different concentrations of NaCl (0, 50 and 100 mM) added to the feed liquor. Gaps within data points (day 27 to day 46) represent no generation of effluent liquor and from day 85 to day 114 represent no sample collection.

Planktonic cell numbers had increased to ~ 4.0 x $10^7$ $mL^{-1}$ at the first time of sampling using the 50 mM NaCl feed liquor, though this was probably due to the effect of adding glycerol to the aSRBR just prior to changing the composition of the feed. These subsequently decreased and remained at ~ 1.5 x $10^7$ $mL^{-1}$ until the end of this phase of the experiment, when they increased again to ~ 6.5 x $10^7$ $mL^{-1}$.

Production of net alkalinity by the aSRBR during the first 13 days in which influent liquor containing 100 mM NaCl (day 13 to day 26) probably reflects the time taken to replace (at least in part) the salt-free liquor within the bioreactor. Up to the time (day 26) that flow into and out of the bioreactor came to a halt, 4.76 L of 100 mM NaCl influent liquor had entered the 2 L (working volume) bioreactor. The implication is that at day 26 the salt concentration had reached a critical concentration, at least in the biofilm bed where (as described in section 4.3.4) the SRB were most relatively abundant.

Concentrations of glycerol consumed and acetic acid produced in this experiment are shown in Fig. 4.13. Glycerol was readily consumed throughout the experiment independent on the concentration of sodium chloride in the feed liquor. Very small concentrations (< 0.05 mM) of acetic acid were detected in the effluent liquors while adding 100 mM NaCl to the feed liquor, suggesting that glycerol was mostly being completely oxidized to $CO_2$. During the period where the aSRBR was inactive (day 27 to day 46), liquid samples were not withdrawn from the bioreactor, therefore no analyses were carried out during this period. Acetic acid

production increased significantly intermittently when the bioreactor was been fed with 50 mM NaCl (Fig. 4.13) reaching concentrations as high as 2 mM, but decreased and remained stable at < 0.5 mM when salt-free feed liquor was reinstated.

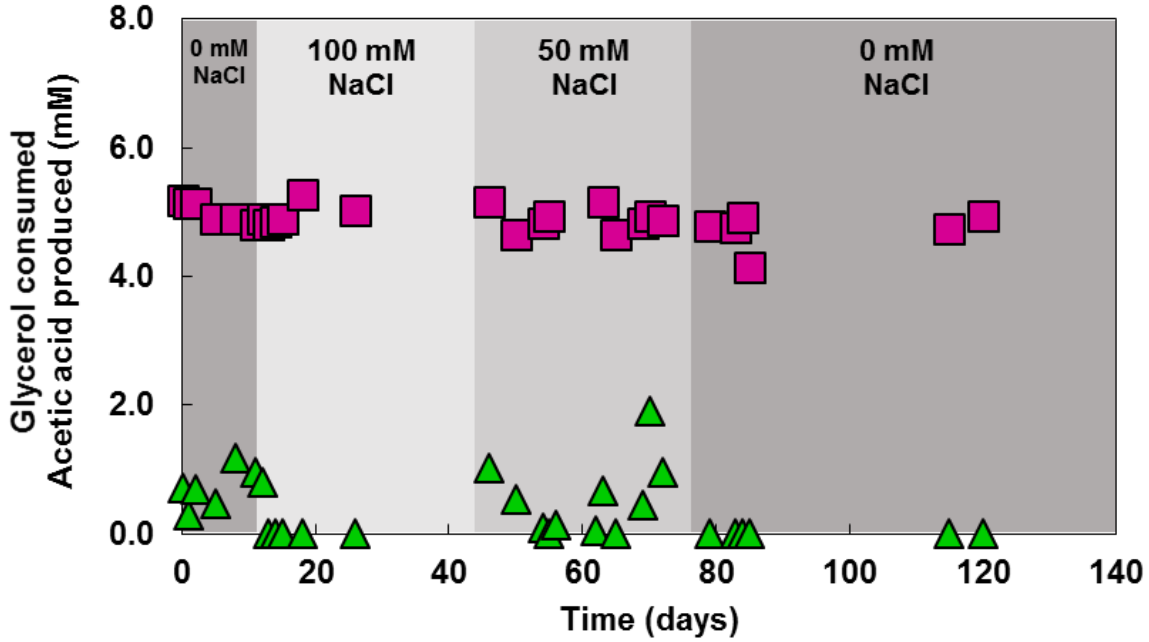


**Fig. 4.13.** Changes in concentrations of glycerol consumed (■) and acetic acid produced (▲) in the aSRBR using different concentrations of NaCl (0, 50 and 100 mM) added to the feed liquor. Samples were not collected on intervals from day 27 to day 46 and from day 85 to day 114.

Rates of sulfate reduction were monitored throughout this experiment, and results are shown in Fig. 4.14. During the first 13 days of feeding the aSRBR with 100 mM NaCl, relatively low rates of sulfate reduction were observed (~ 0.2 g $SO_4^{2-}$ reduced $L^{-1}$ $day^{-1}$), followed by the inactive period (day 27 to day 46) where sulfate reduction appeared to have stopped. By re-activating the aSRBR (by glycerol injection) and decreasing the concentration of NaCl in the feed liquor to 50 mM, sulfate reduction was restarted and rates monitored (Fig. 4.14). Major variations in rates of sulfate reduction were observed at the beginning of this phase of the experiment (day 46 to day 79). Significant increase in sulfate reduction rates were observed when the feed liquor of the aSRBR was again modified to eliminate NaCl, averaging 0.6 $\pm$ 0.11 g $SO_4^{2-}$ reduced $L^{-1}$ $day^{-1}$, though these were far less than those recorded before salt-amended liquors were first used (Fig. 4.14).

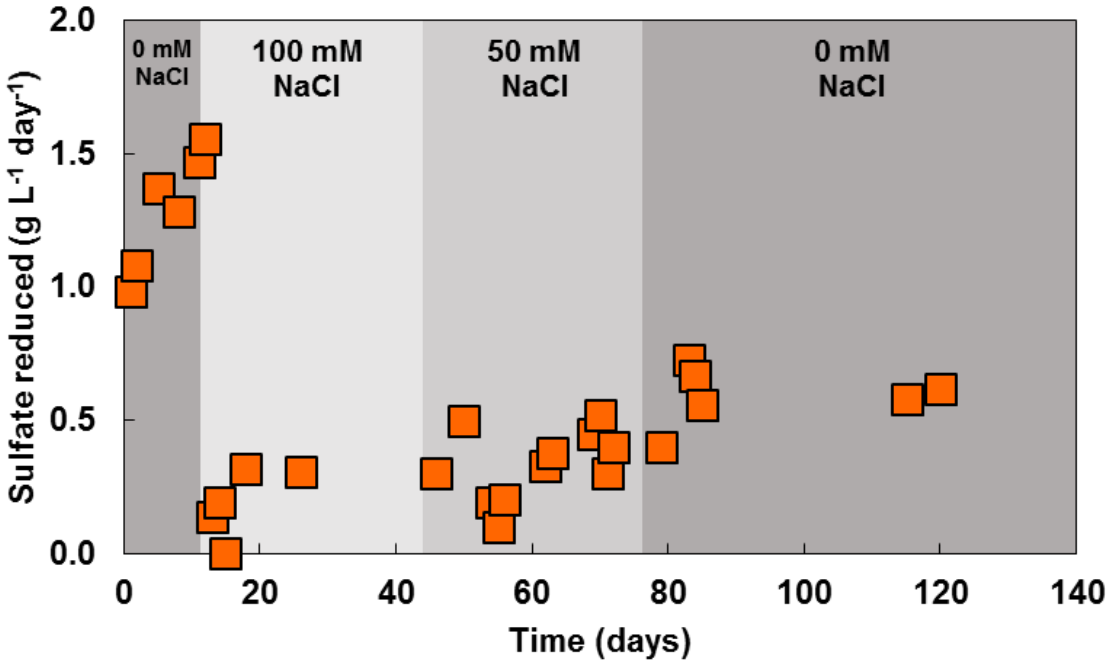


**Fig. 4.14.** Changes in rates of sulfate reduction in the bioreactor using different concentrations of NaCl (0, 50 and 100 mM) in the feed liquor. Samples were not collected on intervals from day 27 to day 46 and from day 85 to day 114.

Metal concentrations in the effluent liquor of the aSRBR were monitored throughout the experiment and are shown in Fig. 4.15. Zinc, which had been the most effectively precipitated metal hitherto, was only ~ 50% removed from the 100 mM NaCl feed liquor, though this increased to ~ 90% in the second stage of the experiment before falling again to ~ 70% when salt-free feed liquor was again used (all average values). Nickel was effectively (> 99%) removed at the initial stage of the experiment (100 mM NaCl in the feed liquor), but the extent to which this metals was precipitated within the aSRBR during the next stage (with 50 mM NaCl feed liquor) was variable, and around 95% nickel was precipitated when salt-free feed was again used. Cobalt was removed to relatively similar extents (73 - 80%) throughout the experiment. Manganese concentrations in the effluent liquors were occasionally greater than those present in influent liquors during this experiment, presumably due to re-solubilisation of some of the small amounts of manganese precipitates that had accumulated within the aSRBR in previous experiments. The average percentages (and standard deviations) of transition metal removal in this experiment are summarised in Table 4.2.

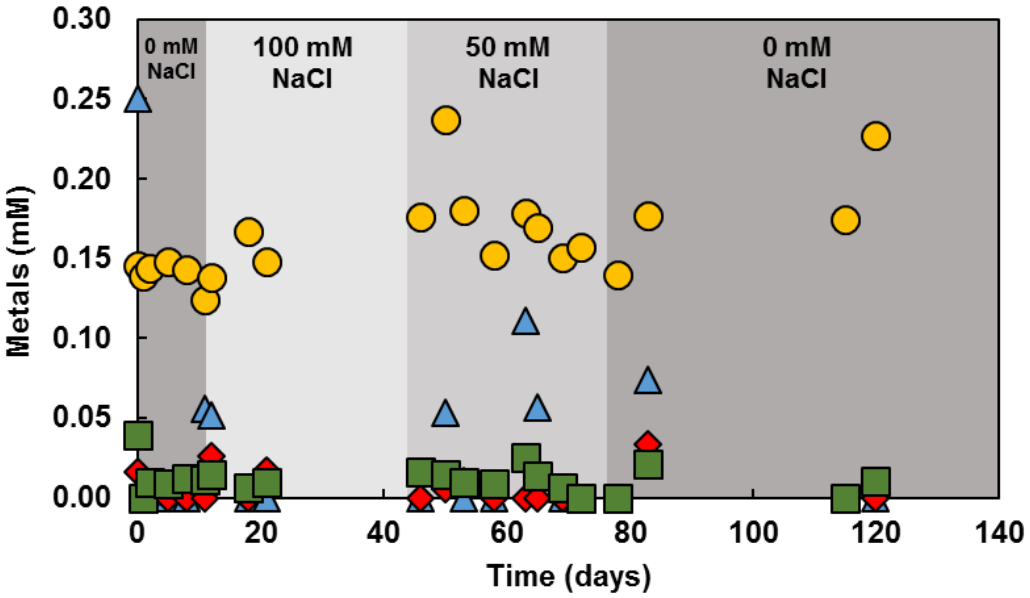


**Fig. 4.15.** Changes in concentrations of transition metals in bioreactor effluent liquors using different concentrations of NaCl (0, 50 and 100 mM) in the feed liquor. Samples were not collected on intervals from day 27 to day 46 and from day 85 to day 114. Key: nickel (▲), zinc (♦), cobalt (■) and manganese (●).

**Table 4.2.** Average percentage (and standard deviation) of metal removal (Ni, Zn, Co) using different concentrations of sodium chloride in the feed liquor.

| NaCl concentration (mM) | Metal removal (%) | | |
|---|---|---|---|
| | Ni | Zn | Co |
| **100** | 99 ± 0.5 | 50 ± 15.7 | 80 ± 8.8 |
| **50** | 82 ± 2.1 | 90 ± 6.4 | 74 ± 4.0 |
| **0** | 95 ± 5.0 | 70 ± 20.5 | 73 ± 6.8 |

The compositions of the planktonic bacterial communities in the aSRBR at different stages in this experiment, as determined by T-RFLP analysis, are shown in Fig. 4.16. As in previous experiments, all attempts to amplify archaeal genes proved negative. The results indicated that the microbial community within the bioreactor was dominated by the four species of bacteria identified previously (*Peptococcaceae* CEB3; *Desulfosporosinus acididurans*; *Actinobacterium* AR3 and *Acidithiobacillus ferrooxidans*), together with two new T-RF peaks (148 nt and 226 nt) which did not correspond to any bacterium logged within the *Bangor Acidophile* database. Attempts to isolate these bacteria on overlay plates (section 2.2.2.3) containing 10 and 50 mM NaCl (pH 4.0) were unsuccessful.

Fig. 4.16 shows that major changes occurred in the relative abundances of bacteria in the planktonic community when NaCl was added to the feed liquor and concentrations varied. Most notably, the sulfidogen, *Peptococcaceae* CEB3 appeared to be very negatively impacted by saline influent liquors. It was not detected at the end of the phase where the influent contained 50 mM NaCl though changing to a salt-free liquor resulted in its reappearance. *D. acididurans* appeared to be less negatively impacted, accounting for about 75% of the planktonic population in the aSRBR at the end of the experimental phase using 100 mM NaCl in the feed liquor, though decreasing to about 7% relative abundance with 50 mM NaCl before increasing again to 52% when salt was eliminated. The heterotrophic putative fermenting strain AR3 was detected at all four stages, though was more abundant at the end of the 50 mM NaCl phase, while the chemolithotroph *At. ferrooxidans* was found only in very small relative abundance throughout this experiment.

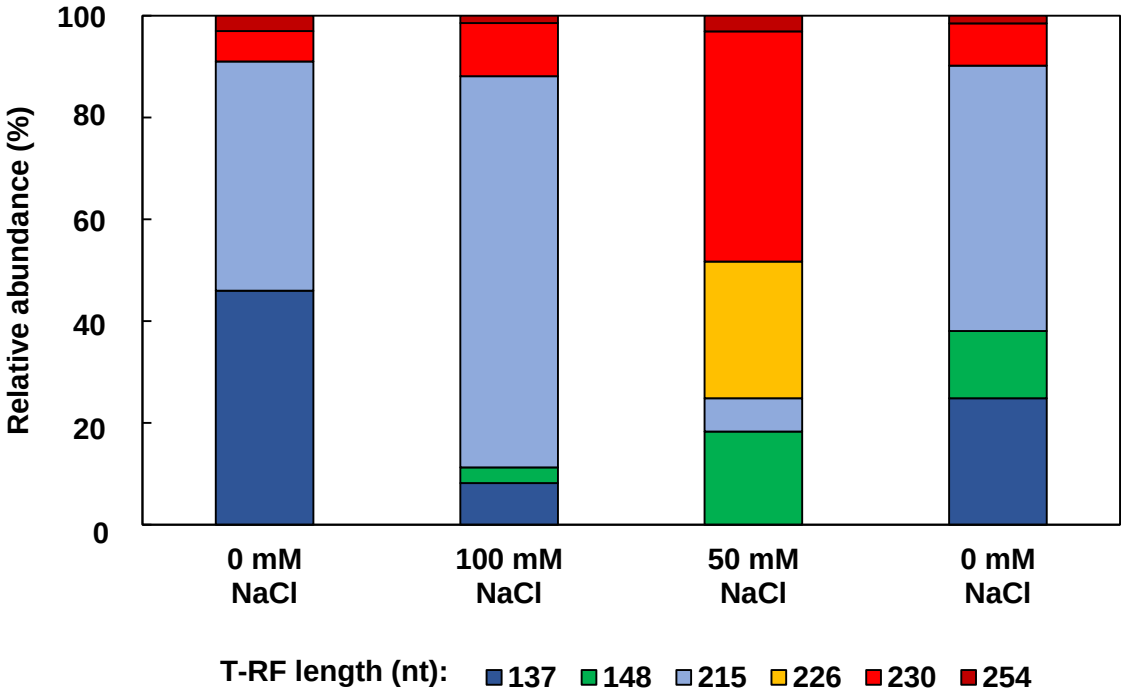


**Fig. 4.16.** Terminal restriction enzyme fragment length polymorphism (T-RFLP) analysis (HaeIII digests of amplified 16S rRNA genes) of planktonic bacterial communities in the aSRB reactor operated using different concentrations of NaCl in the feed liquor. Shades of blue represent sulfate-reducing bacteria and shades of red represent non-sulfidogens 137 nt: *Peptococcaceae* CEB3; 215 nt: *D. acididurans*; 230 nt: *Actinobacterium* AR3 and 254 nt: *At. ferrooxidans*; 148 and 226 nt: unknown.

*4.3.4. pH values and bacterial communities within the aSRBR biofilm bed*

Measurements of pH were carried out using a pH electrode coupled to a FerMac 310/60 unit positioned in the upper liquid layer of the aSRBR. Similarly, T-RFLP analyses were carried out routinely using DNA extracted from planktonic cells in the liquid layer above the top of the layer of colonized Poraver beads, in order to avoid perturbations in the system during the experiments. However, at the end of the experiment described in section 4.3.1, colonised beads were collected from three different depths in the bioreactor (top, mid and bottom layer), pH was measured in each layer and T-RFs of the microbial community were compared to results obtained from liquid phase. At this stage, the sulfidogenic bioreactor, was being operated at pH 5.0 and 35ºC. The T-RFLP profiles obtained and pH values recorded are shown in Fig. 4.17.

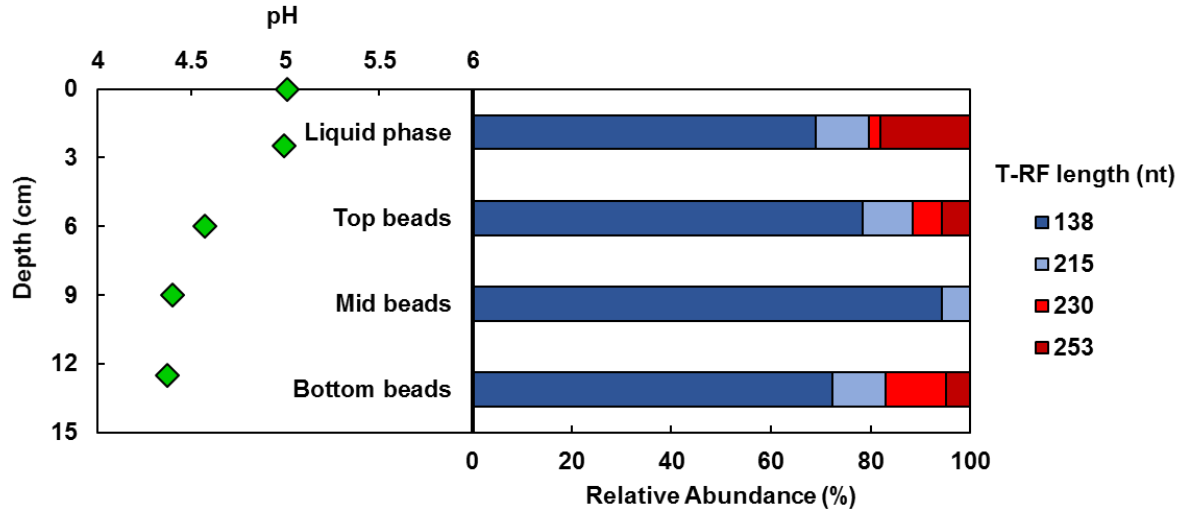


**Fig. 4.17.** Depth-related variations in pH (left) and T-RFLP profiles of the bacterial community (HaeIII digests of amplified 16S rRNA genes) of planktonic cells (liquid phase) and colonised beads (top, mid, bottom layers) (right) within the aSRB reactor, at pH 5.0 and 35ºC. 138 nt: *Peptococcaceae* CEB3; 215 nt: *D. acididurans*; 230 nt: *Actinobacterium* AR3 and 253 nt: *At. ferrooxidans.*

When the “pH of the bioreactor” is referred to in experiments described in this chapter, this refers exclusively to that of the liquid phase above the biofilm bed, measured by the pH electrode placed at this point within the aSRBR (section 2.4). However, as shown in Fig. 4.17, while there were no detectable differences in pH values at different depths in this layer (as would be expected, as it was continuously gently stirred), pH values declined with depth within the biofilm bed, reaching a lowest recorded value of 4.3. This equates to a concentration of hydronium ions in the bottom layer of the biofilm bed some five-times greater than those in the

overlying liquid phase (pH 5.0 = 0.01 mmol $L^{-1}$ $H_3O^+$ and pH 4.3 = 0.05 mmol $L^{-1}$ $H_3O^+$). This can be accounted for by the fact that the feed liquor used at this stage had a pH of 2.1 (corresponding to 7.95 mmol $L^{-1}$ $H_3O^+$), and it would be anticipated that neutralisation of this acidity would occur gradually during upward percolation of the influent liquor.

The aSRBR consortium contained species of acidophilic and acid-tolerant SRB and non-sulfidogens, and the bacterial communities would be anticipated to be affected by the pH gradients present within the bioreactor vessel. T-RFLP analysis showed that the relative abundance of bacteria in each layer of the biofilm bed was slightly different. The sulfidogen *Peptococcaceae* CEB3 was the most abundant microorganism in all layers, accounting for > 90% of the population in some cases. *D. acididurans* (also an aSRB) was present in all layers but was much less abundant (accounting for 5-10% of the summated T-RFs), and its relative abundance did not fluctuate significantly between layers. The non-sulfidogens *At. ferrooxidans* and *Actinobacterium* AR3 were detected in every layer except the mid layer of the biofilm bed (Fig. 4.17).

### *4.3.5 Scanning electronic microscopy and elemental composition analysis of the aSRBR biofilm bed*

Samples from each biofilm bed layer (top, mid and bottom) were aseptically mixed and analysed by SEM/EDAX in order to observe bacterial community immobilised on glass beads (Fig. 4.18) and also to detect metal precipitates, since Ni, Zn and Co were anticipated to have precipitated as sulfides within the sulfidogenic bioreactor. Fig. 4.18 A-C shows the irregular porosity of the glass beads, which provides greater surface area for microbial immobilisation. In Fig. 4.18 D-F, numerous rod-shaped bacteria can be seen, as well as thin filaments which may correspond to the *Actinobacterium* AR3 which was detected in T-RFLP analysis in the top and bottom bead layers. Amorphous particles were found in several images. Elemental identification and semi-quantitative composition analyses were performed on these, and results are presented in Fig. 4.19.

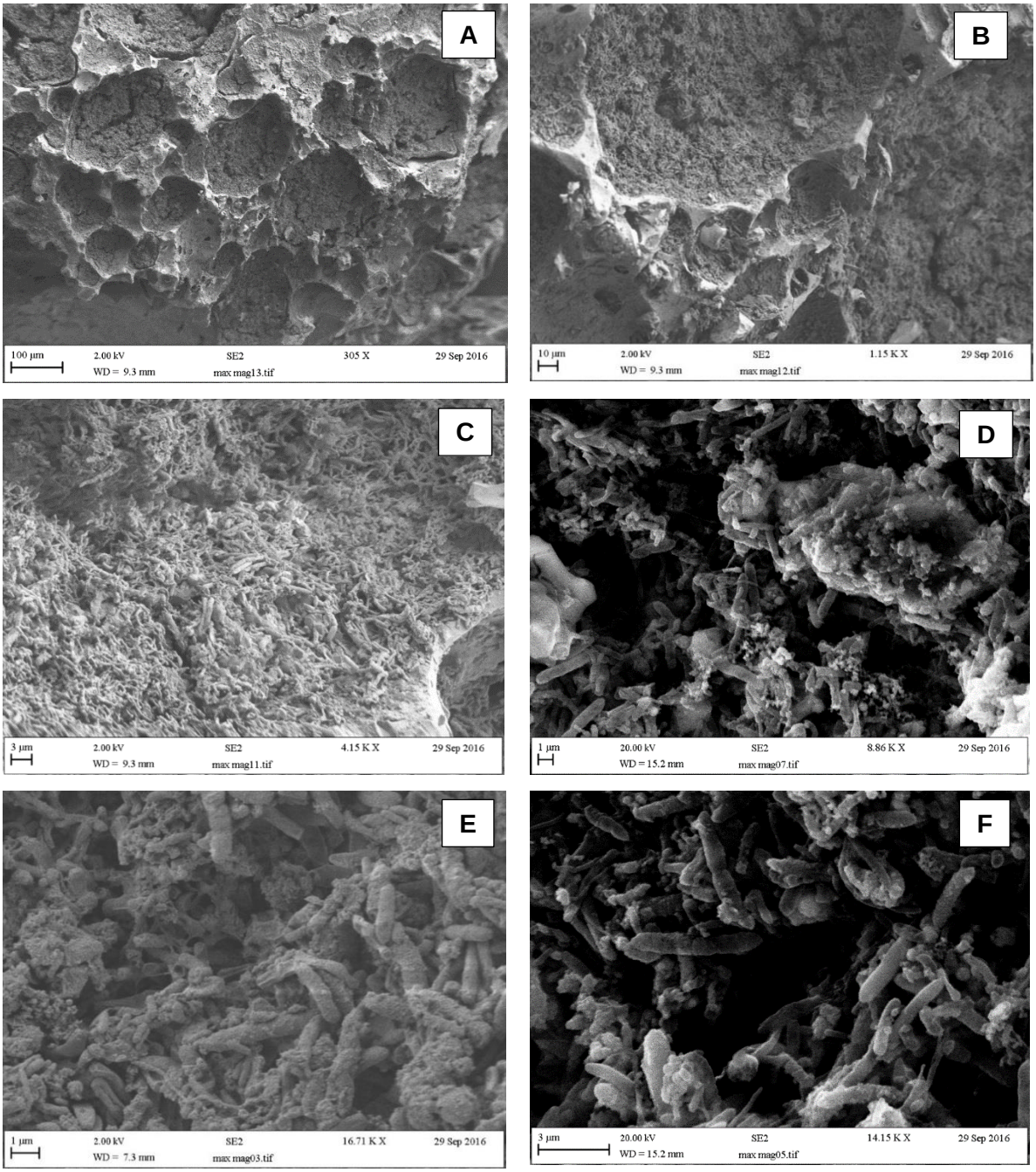


**Fig. 4.18.** Scanning electron micrographs of colonised Poraver beads combined from different depths within the biofilm bed in the aSRBR.

EDAX spectra (Fig. 4.18 B) of selected areas of the micrographs showed relatively high contents of transition metals (nickel, zinc, cobalt and iron) as well as sulfur, suggesting that those metals were, as anticipated, precipitated as sulfides onto the glass beads. High contents of silicon and oxygen were also observed in the EDAX spectra, which represent the structural material of the glass beads ($SiO_2$). Carbon was also identified as main element, possibly from microorganisms.

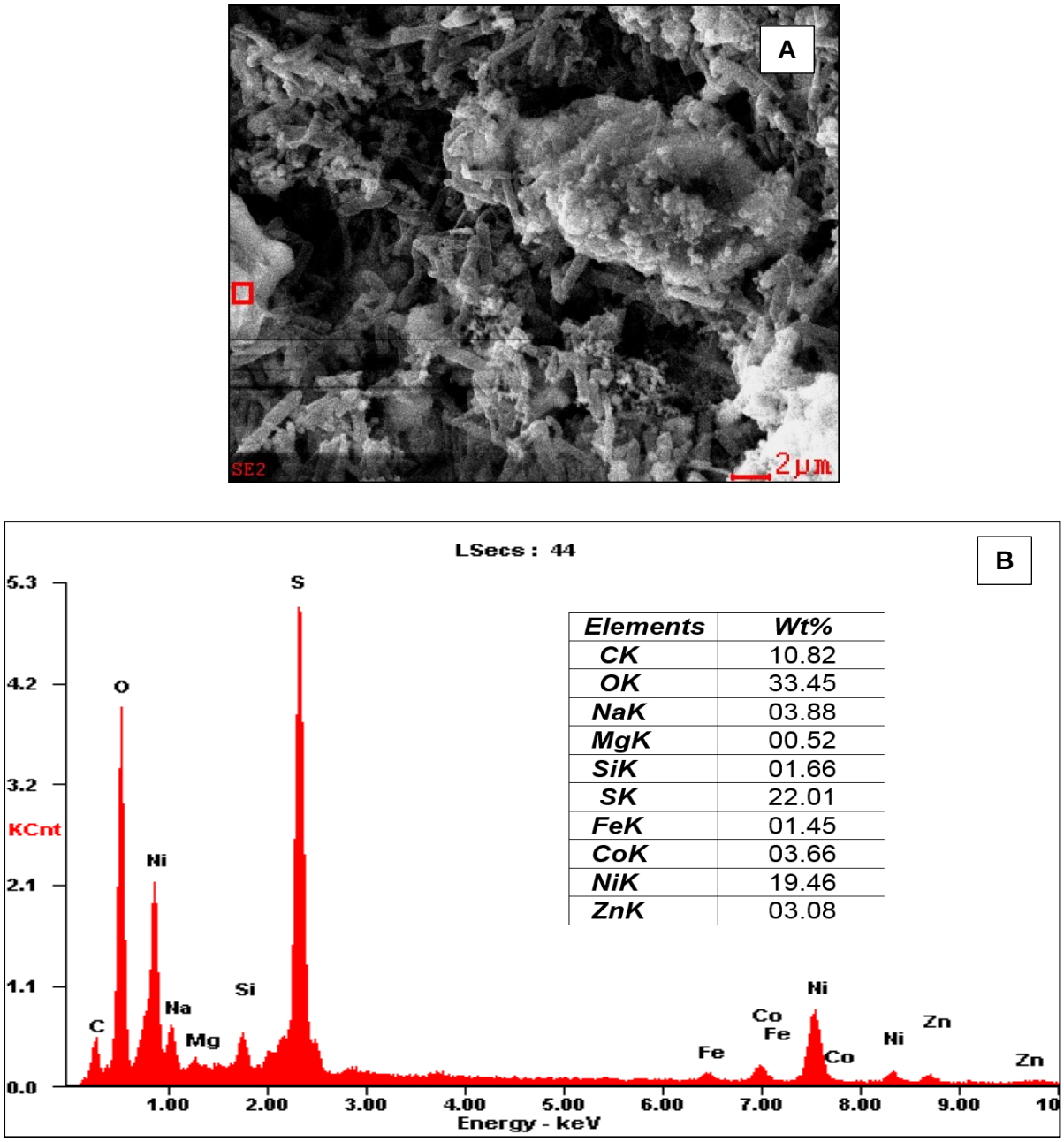


| Elements | Wt% |
|---|---|
| CK | 10.82 |
| OK | 33.45 |
| NaK | 03.88 |
| MgK | 00.52 |
| SiK | 01.66 |
| SK | 22.01 |
| FeK | 01.45 |
| CoK | 03.66 |
| NiK | 19.46 |
| ZnK | 03.08 |

**Fig. 4.19.** Micro-analysis of biofilm-colonised glass beads by electron dispersive analysis of X-ray. (A) SEM image displaying selected area (red square) and (B) EDAX spectra of the selected area plus elemental semi-quantitative analysis.

## 4.4 Discussion

Relatively little is known about the kinetics of and microbial communities in sulfidogenic bioreactors that operate at low pH. Although previous research has assessed rates of sulfate reduction and bacterial community profiles of aSRB reactors operated at between pH 2.2 and 4.5, few data were presented for pH values above 4.5, and the effect of temperature was not examined. Ñancucheo and Johnson (2012a) operated an aSRB reactor at pH 2.2 (and 30°C) in order to selectively precipitate copper (as CuS) within the reactor vessel, using synthetic mine water containing ferrous iron and zinc in addition to copper, and noted that *Peptococcaceae* CEB3 was the dominant planktonic bacterium under such conditions. A second aSRB reactor, used to selectively precipitate zinc (as ZnS) was operated at pH 4.0 and 30°C, and the dominant planktonic sulfidogenic bacterium present in this case was found to be *D. acididurans*, though *Peptococcaceae* CEB3 became increasingly abundant as the aluminium concentration in the feed liquor was progressively increased. Rates of sulfate reduction were not reported in that study, but in a later communication (Ñancucheo and Johnson, 2014) it was noted that these were depressed when the aSRB reactor was operated at lower pH values; rates of between about 0.12 g $SO_4^{2-}$ reduced $L^{-1}$ $day^{-1}$ (at pH 2.8) and 2.0 g $SO_4^{2-}$ reduced $L^{-1}$ $day^{-1}$ (at pH 4.5) were recorded.

The sulfidogenic bioreactor used in the present study used an inoculum of bacteria, immobilized on porous glass beads, from the bioreactor used by Ñancucheo and Johnson (2012a), which had, in turn, been inoculated with pure cultures of some aSRB maintained in the *Acidophile Culture Collection* maintained at Bangor University, and an environmental sample from an abandoned copper mine (Cantareras) in Spain. Switching from the liquor used to prime the bioreactor (standard SRB medium at pH 2.5) to copper-free synthetic AMD (pH 2.1) caused the HRT to increase rapidly, though this was not unexpected since the total acidity (combined proton acidity and bisulfate acidity) was far less in the former (5.2 mM) than in the latter (16.8 mM) with the consequence that more sulfate needed to be reduced (per unit volume of influent liquor) with synthetic AMD to maintain the bioreactor at its set pH value.

Although there were large variations in rates of sulfate reduction measured at each temperature and pH regime tested, some general conclusions may be drawn. One is that the bioreactor operated effectively over a wide temperature range (30 - 45°C) and that increasing pH from 4.0 to 5.0 marginally increased the performance of the bioreactor at 30°C, though not at 35° or 40°C. Rates of sulfate reduction measured were similar to those reported by Ñancucheo and Johnson (2014) when they operated an aSRB reactor at pH values around 4.5.

One of the main objectives of this work was to precipitate transition metals (other than copper, which was removed (as CuS) from the synthetic AMD in an off-line vessel using $H_2S$ generated within the bioreactor) within the aSRB reactor vessel itself, as part of the mine water remediation protocol. The solubility products ($K_{sp}$) of the sulfide phases of the four transition metals in the influent liquor (Co, Mn, Ni and Zn) are very different (ranging from $3 \times 10^{-25}$ $M^2$ for ZnS to $3 \times 10^{-11}$ $M^2$ for MnS; Monhemius, 1977), and this was reflected in the extents to which the metals were removed from the copper-free synthetic AMD. While zinc was very effectively removed at all operational pH values, manganese essentially remained in solution throughout. Nickel was only removed effectively at pH 5.0 and precipitation of cobalt was also optimized (though incomplete) at an operating pH of 5.0. Maximum metal precipitation was observed at pH 5.0 and 35ºC where over 99% of all the transition metals (other than manganese) present in the copper-free synthetic AMD were precipitated in the bioreactor vessel. Higher pH values were not used in the current tests, but may prove superior for precipitating CoS, though in mine waters containing significant concentrations of aluminium (as is often the case) this would promote the formation and accumulation of gelatinous oxy-hydroxysulfates of this metal, which could cause operating difficulties in a continuous flow bioreactor (Falagán et al., 2017).

In the experiment where bioreactor pH values and temperatures were varied, analyses of the microbial community within the aSRB reactor provided evidence that helped explain why changes in performance of this module tended to be transient, while overall the module was both robust and adaptable. The aSRB reactor housed a microbial community, rather than a pure culture. Changing either pH or temperature caused shifts in the relative abundance of the bacteria present in liquid samples taken from the surface of the reactor. Only two confirmed sulfidogens, *D. acididurans* and *Peptococcaceae* CEB3, were detected (as in previous studies of similar systems) though other aSRB (*Desulfobacillus acidavidus,* CL4 and *Firmicute* C5) had also been included in the original inoculum. *Desulfosporosinus acididurans* is a moderately acidophilic (pH optimum 5.5; range 3.8 - 7.0) mesophilic (temperature optimum 30°C; range 15 - 40°C) SRB, known to incompletely oxidize glycerol, producing stoichiometric concentrations of acetic acid (Sánchez-Andrea et al., 2015). Although not yet fully characterized, *Peptococcaceae* CEB3 appears to be a more thermo-tolerant and acidophilic SRB that can oxidize glycerol to $CO_2$ (D.B. Johnson et al., unpublished data). These observations help explain the fluctuations in the relative abundances of these two sulfidogens, as indicated by T-RFLP analysis, at the different pH and temperatures used.

The experiment where yeast extract concentrations were varied found that hydraulic retention times increased each time the concentration of yeast extract changed, but the sulfidogenic bioreactor was able to recover each time. The number of cells varied significantly from each condition tested, indicating that yeast extract was mostly used as carbon source for biomass growth rather than as an electron donor. Sáez-Navarrete et al. (2009) studied the influence of yeast extract concentration on biomass growth and sulfate reduction rates of the neutrophilic bacterium *Desulfobacterium autotrophicumin* in batch cultures at 38ºC using hydrogen as electron donor. They found that there was a direct relationship between concentrations of yeast extract, biomass growth and sulfate reduction rates, in which larger concentrations of yeast extract resulted in faster rates of sulfate reduction. Rates varied between 0.02 g $SO_4^{2-}$ reduced $L^{-1}$ $day^{-1}$ (with 0 and 0.5 g $L^{-1}$ YE) and 0.3 g $SO_4^{2-}$ reduced $L^{-1}$ $day^{-1}$ (with 2 g $L^{-1}$ YE).

Regarding metal removal and sulfate reduction rates in the present study, there was no significant difference in average of rates of sulfate reduction within the three conditions tested (0, 0.05 and 0.1 g $L^{-1}$ YE in the feed liquor), however metals were not being effectively precipitated within the bioreactor vessel with 0 and 0.05 g $L^{-1}$ YE, and only 60% nickel was removed in some cases. Analysis of the microbial population showed a minor shift in the relative abundance of aSRB in the bioreactor in which sulfate-reducing bacteria accounted for over 90% of the population with 0.1 g $L^{-1}$ YE and around 75% with 0 and 0.05 g $L^{-1}$ YE in the feed liquor. Concentrations of YE greater than 0.1 g $L^{-1}$ were not tested since this would be one of the more costly consumables used in a full-scale operation that harnessed this technology and operating the aSRBR effectively with a minimum input of YE was considered to be an important objective.

The addition of sodium chloride to the feed liquor supplied to the bioreactor resulted in a downturn of the performance of the aSRBR, both in sulfate reduction rates and metal removal efficiency. Zinc, which had been the most effectively precipitated metal in all experiments, was not in this case (e.g., only 50% zinc was removed when using 100 mM NaCl in the feed liquor). Nickel and cobalt also showed a relative low percentage of removal (56% for nickel and 38% for cobalt, in some cases). One reason for this behaviour would be the lower rates of sulfate reduction observed when NaCl was added to the feed liquor, though there was still sufficient $H_2S$ produced to predict > 99% precipitation of zinc. A second explanation here is the fact that chloride anions can act as ligands, forming zinc complexes that may be positively or negatively charged, or uncharged ($Zn^{2+} + Cl_n^- \rightarrow Zn(Cl)_n^{2-n}$, where $n$ = 1, 2, 3 or 4; Skou et al., 1977). Complexed zinc would be less readily precipitated as a sulfide than the non-complexed divalent metal. Manganese concentrations in the effluent liquors were

sometimes found to be higher than those in the influent liquor during this experiment, and this could have due to the re-solubilisation of small amounts of manganese precipitates that had accumulated within the bioreactor. Again, chloride may have been responsible for this. Gammons and Seward (1996) studied the stability of Mn (II) chloride complexes in different temperatures and they found that at low temperatures (~ 25ºC) these complexes are weak, but become stronger and more important at higher temperatures. Rates of sulfate reduction in this experiment were 5 to 10 times lower than those recorded before salt-containing liquors were first used, and even when NaCl was removed from the feed liquor (in the last phase of this experiment), the aSRBR did not return to its previous rates of sulfate reduction during the period monitored. Bacterial population analysis showed that the sulfidogen *Peptococcaceae* CEB3 was highly sensitive to NaCl and its relative abundance decreased significantly when using NaCl in the feed liquor, whereas *D. acididurans* was the most abundant bacteria within the bioreactor when this was being fed with 100 mM NaCl. Two unknown T-RFs (148 and 226 nt) were identified in this experiment. The reason for the appearance of T-RF peaks in the profiles that had not been observed in previous experiments is not known, though probably relates directly to the addition of salt in the feed liquor, as they either disappeared (the 226 nt T-RF) or became less relatively abundant (the 148 nt T-RF) when salt-free influent liquor was once again used. The consortium selected for this bioreactor contains an undefined enrichment culture from an acidic metal-rich stream draining an abandoned mine in Spain. Suppression of the sulfidogens (particularly *Peptococcaceae* CEB3) when NaCl-containing liquors would have allowed more salt-tolerant bacteria that were usually out-competed by the former, to emerge. Further studies are necessary in order to isolate, identify and characterise these unknown bacteria and ultimately to understand their role in the microbial community.

Production of acetic acid is an undesirable feature of the aSRBR, as it means that utilization of the electron donor (glycerol) is only partial, and (aerobic) downstream processing would probably be needed to remove this organic chemical before the remediated mine water could be released. Elsewhere it was demonstrated that *Ac. aromatica* can establish a syntrophic association with *D. acididurans*, in which the acetic acid generated by the latter is metabolized to $H_2$ and $CO_2$ by the former. The hydrogen produced in this acetoclastic reaction can be used as a secondary electron donor for the sulfidogens, making the net process far more efficient (Kimura et al., 2006). It is interesting to note that concentrations of acetic acid declined markedly follow addition of *Ac. aromatica* to the bioreactor. Although this heterotrophic acidophile was not detected in T-RFLP profiles of the surface liquid layer, the fact that concentrations of acetic acid always declined following sharp increases when operational parameters were changed suggests that *Ac. aromatica* was present throughout,

either in the biofilm community, and/or as a relatively minor member of the planktonic community. The consistent presence of the two other (non-sulfidogenic) bacteria in the bioreactor, albeit mostly as relatively minor members, is harder to explain. *Actinobacterium* AR3 (which is identical to isolate IR1 reported by Ñancucheo and Johnson, 2012a) has been isolated and partially characterized. This bacterium is micro-aerophile, which can also grow (though more slowly) under anoxic conditions. In the absence of an electron donor other than sulfate in the feed liquor, it was assumed that it grew either by fermenting glycerol or by scavenging small amounts of dissolved oxygen present in the feed liquor (which was sterilized but not de-aerated). *Acidithiobacillus ferrooxidans* is a facultative anaerobe, and can use ferric iron as electron acceptor in place of oxygen. However, no ferrous or ferric iron salts were included in the feed liquors, and therefore any iron present would be that present in yeast extract, and that this would exist solely as ferrous in the pH and redox conditions in the bioreactor. The presence of this ubiquitous AMD bacterium was therefore probably due to it coupling the oxidation of hydrogen sulfide generated by the aSRB to the reduction of trace amounts of oxygen present in the feed liquor. Measurements of dissolved oxygen in feed liquors used for sulfidogenic bioreactors at Bangor University showed that these were ~ 3.5 mg $L^{-1}$ in pre-autoclaved and 1.61 mg $L^{-1}$ in post autoclaved liquors, at pH 3.6 (the solubility of oxygen in water is strongly temperature-dependent; data provided by Roseanne Holanda and Barry M. Grail, Bangor University). These figures correspond to 109 and 50 µM oxygen, respectively, and since the stoichiometry of sulfide oxidized (to sulfate) to molecular oxygen reduced is 1:2 ($H_2S + 2\ O_2 \rightarrow 2\ H^+ + SO_4^{2-}$), this implies that a maximum of 25 µmoles $L^{-1}$ of $H_2S$ produced in the aSRBR would have been oxidized in this way. While this is obviously a detrimental aspect, de-oxygenating liquors fed into pilot- and full-scale sulfidogenic bioreactors would not be pragmatic, and the amount a $H_2S$ sacrificed to remove dissolved oxygen is relatively minor.

Analysis on the biofilm bed revealed depth-related changes in pH in the colonised bead layer, and also variations in the compositions of the bacterial communities that were attached to the Poraver beads. The pH gradient generated within the bioreactor vessel was due to low pH feed liquor percolating upward through the biofilm bed of the bioreactor within which proton-consuming sulfidogenesis ($4\ C_3H_8O_3 + 7\ SO_4^{2-} + 14\ H^+ \rightarrow 7\ H_2S + 12\ CO_2 + 16\ H_2O$) was occurring. The operating pH of the aSRBR was routinely set at 5.0, but this referred to the mixed layer of liquid above the biofilm bed. The total acidity of the feed liquor at pH 2.1 was 16.8 mM (7.95 mM proton/hydronium ion acidity and 8.84 mM bisulfate acidity). The pH of the interstitial liquid in the bead bed at about 3 cm above the base of the bioreactor vessel (the lowest sampling point) was 4.3, which corresponds to a total acidity of 0.14 mM (0.05 mM

proton/hydronium ion acidity and 0.087 mM bisulfate acidity). The means that 16.66 mM (99%) of total acidity had been neutralised by the time that the influent liquor had just percolated ~ 3 cm upwards through the biofilm bed. Assuming this was coupled to the complete oxidation of glycerol, this would have consumed 4.76 mM (95%) of the glycerol present in the influent liquor. The implication here is that most of the sulfidogenic activity in the aSRBR takes place within a relatively shallow depth of the biofilm layer. This has implications for the future development of these reactors. The sulfate-reducing acidophile *Peptococcaceae* CEB3 was by far the most abundant bacterium detected in the biofilm bed, in general accounting for 80 to over 90% of the population. SEM/EDAX analysis showed well colonised glass beads containing different cell morphologies as well as amorphous particles which contain mostly transition metals (Zn, Ni, Co) and sulfur, suggesting that these metals were precipitated, as predicted, from the copper-free synthetic mine water onto the glass beads as metal sulfides (NiS, CoS and ZnS).

This long-term experiment demonstrated that the microbial community in the aSRB reactor is, in most cases, both robust and adaptable. Changing temperature or pH (with the ranges tested) had only short-term impact on its performance, and bacteria that are more suitable to the new conditions rapidly emerged in greater abundance. This could have major advantage in some situations, where average ambient temperatures are relatively high (~30°C) but occasionally exceed 40°C, as there would be no requirement to have temperature control (heating or cooling) to maintain the integrity of the aSRBR. On the other hand, changes in chemical composition of the feed liquor (yeast extract and NaCl, within the ranges tested) should be thought of carefully, ideally in order to obtain the most out of the microorganisms without causing long-term or even irreversible impact to the system.

In section 3.4, a hypothetical scenario was described in which the sulfidogenic bioreactor was theoretically scaled up to a volume of 10 $m^3$ using laboratory-scale performance data, and some considerations were discussed. The issues highlighted included: (i) aSRBR did not efficiently removed nickel and cobalt (85 and 75%, respectively) from the partly-processed AMD and (ii) overall the system was not considered efficient since only 13 $m^3$ of Cu-rich water would be processed per day and at least 15 $m^3$ (volume required to feed the aSRBR for a day) should be processed per day to be a self-sufficient system. In the current chapter, both of these concerns were addressed. Firstly, by testing different combinations of pH and temperature, the maximum percentage of metal removal was obtained at pH 5.0 and 35ºC where > 99% of all the transition metals (other than manganese) present in the copper-free synthetic AMD were precipitated within the bioreactor vessel. The second issue was associated with $H_2S$ production rates, which varied significantly in each condition studied.

Table 4.3 summarises maximum rates of $H_2S$ production obtained throughout the experiment, equivalent rates for a 10 $m^3$ aSRBR and the volume of Cu-rich water treated per day.

**Table 4.3.** Maximum rates of $H_2S$ production for the laboratory-scale system, equivalent rates for a 10 $m^3$ aSRBR and the correspondent volume of Cu-rich water treated per day for each condition studied.

| Parameters | | $H_2S$ production (mmoles $L^{-1}$ $day^{-1}$) | $H_2S$ equivalent for a 10 $m^3$ aSRBR (moles $day^{-1}$) | Available for Cu off-line precipitation (moles $day^{-1}$) | Volume of Cu-rich water treated ($m^3$ $day^{-1}$) |
|---|---|---|---|---|---|
| **pH 4.0** | **30ºC** | 10.4 | 104 | 99 | 13 |
| | **35ºC** | 28.5 | 285 | 280 | 37 |
| | **40ºC** | 13.8 | 138 | 133 | 18 |
| | **45ºC** | 21.9 | 219 | 214 | 29 |
| **pH 4.5** | **30ºC** | 16.1 | 161 | 156 | 21 |
| **pH 5.0** | **30ºC** | 22.7 | 227 | 222 | 30 |
| | **35ºC** | 20.3 | 203 | 198 | 26 |
| | **40ºC** | 29.7 | 297 | 292 | 39 |

Among the operating conditions considered in Table 4.3, the only one that would not generate enough Cu-free AMD, on a daily basis, to act as feed liquor for the aSRBR, is pH 4.0 and 30ºC (described in Chapter 3). Increasing either temperature or pH of the bioreactor the volume of Cu-free AMD generated is, in most cases, 1.5 - 2.5 times more than enough to sustain the system. When considering both objectives (efficient in-line removal of transition metals and production of excess $H_2S$ for off-line removal of copper), the optimum condition to have a self-sufficient system in which over 99% of copper, nickel, zinc and cobalt are removed would be when the aSRBR is operated at pH 5.0 and 35ºC. It is noteworthy that, while the results obtained in this series of experiments underpin the physico-chemical and economic validity of the application of active biological treatment for this particular synthetic mine water, its use in other contexts would have to be considered on a case-by-case basis. However, the environmental benefits of this approach are remarkable. Table 4.4 compares physico-chemical requirements in the Brazilian regulation for industrial waste discharge (Industrial Effluent Discharge Act, 2011) to results obtained before and after remediation of the synthetic mine water via biosulfidogenesis.

**Table 4.4.** Consent levels of Brazilian regulatory authorities for industrial waste discharge and synthetic mine water composition, before and after biosulfidogenic treatment.

| | Discharge Consent Levels (Act nº430/2011) | Before treatment | After treatment |
|---|---|---|---|
| **Physico-chemical parameters** | | | |
| **pH** | 5.0 – 9.0 | 5.0 | 5.0 |
| **Temperature** | < 40°C | 33°C | 35°C |
| **Metal concentration (mg $L^{-1}$)** | | | |
| **Total Cu** | 0.5 | 476 | <0.1 |
| **Total Co** | 1.0 | 2.4 | <0.1 |
| **Total Zn** | 1.0 | 1.3 | <0.1 |
| **Total Ni** | 1.0 | 15 | <0.1 |
| **Soluble Mn** | 1.0 | 8.2 | 7.7 - 8.2 |

The use of biosulfidogenesis for remediating this synthetic mine water, the composition of which was based on an actual mine water draining a copper mine in Northern Brazil, was highly successful in generating a processed water that fell within the legal discharge levels, with the single exception of manganese. The fact that manganese was not removed from solution using the approach used in the present study was not unexpected. This metal can be removed in a final polishing stage by biological-mediated oxidation of Mn (II) and precipitation of Mn (IV) using aerobic systems like the one described by Mariner et al. (2008). A similar system was developed, as part of this thesis, to remove manganese of the synthetic AMD, and is addressed in Chapter 6.

# Solubilisation of metal sulfide concentrates generated from an acidophilic sulfidogenic bioreactor used to remediate acidic mine water

5

## 5.1 Introduction

Metal sulfide precipitation has been studied extensively due to its importance in hydrometallurgical treatment of ores and effluents. The use of biogenic hydrogen sulfide for precipitating metals from effluents, such as acid mine drainage, is a well-known and very promising technology. Even though hydroxide precipitation is widely used in industry for metal removal, sulfide metal precipitation displays some more attractive advantages, including the lower solubility of metal sulfide precipitates, potential for selectively metal recovery, better settling properties and potential for reuse of sulfide precipitates by smelting (Lewis, 2010). However, the corrosiveness and toxicity of the main component ($H_2S$) and its generation in excess are the major concerns amongst industries. In addition, in cases where co-precipitation of metals occurs, downstream processes need to be applied in order to selectively separate these metals and to generate pure metal-containing products.

A general traditional flowsheet of metal recovery from sulfidic ores involves mineral processing, smelting and refining processes. In the last few decades, more environmentally-friendly technologies, such as bioleaching, followed by metal recovery by solvent extraction and electrowinning (SX/EW), have been commercially used as an alternative to conventional smelting.

Several studies have shown efficient metal removal from wastewaters, such as mine waters and industrial effluents, using a variety of different systems based on biologically-generated $H_2S$. However, little is known in terms of actual metal recovery from mixed metal sulfide precipitates generated from these systems using hydrometallurgical processing. Moskalyk and Alfantazi (2002) summarised different nickel operating practices. Among these was the Murrin Murrin nickel laterite process which used sulfide precipitation to separate valuable metals (Ni, Co, Cu and Zn) from Mn, Mg and Ca impurities, which in turn are re-leached, using pressure acid leaching (PAL) technology, followed by solvent extraction to separate the nickel and cobalt fractions and, lastly, hydrogen reduction to produce metallic powder (Lewis, 2010). Essentially, pressure acid leaching uses series of autoclaves containing sulfuric acid which are operated under high temperatures (> 250ºC) and high pressures, resulting in an extremely high energy consumption technology. The use of

microorganisms which catalyse the oxidation of sulfide concentrates in aerobic systems operated in mild temperatures (25 - 45ºC) could be used ultimately as a more environmentally-friendly alternative. This chapter focused on the development of a bioleaching system in which metal sulfide concentrates (ZnS, CoS, NiS), generated from a sulfidogenic bioreactor remediation system, were solubilised into a concentrated metal-containing leachate.

## 5.2 Preliminary tests for recovering metals from sulfide precipitates

### *5.2.1 Materials and methods*

A sulfidogenic bioreactor (aSRBR) was used to remediate a synthetic mine water based on the chemical composition of an actual mine water which contained the following concentrations of transition metals: 7.5 mM Cu, 0.25 mM Ni, 0.02 mM Zn, 0.04 mM Co and 0.15 mM Mn (Chapter 2). Copper was removed and recovered, as CuS, from the synthetic mine water using the excess of $H_2S$ produced in the aSRBR which was delivered to an off-line precipitation vessel. However, since the concentrations of all other transition metals were considered to be too low for off-line metal removal, these were allowed to accumulate within the bioreactor vessel during in-line treatment of the copper-free synthetic mine water.

A sample of the porous beads (~ 5 g wet weight) containing bacterial biomass and metal sulfides (MS) was removed from the aSRBR, dried at ~ 40ºC and suspended in 16 mL of acidified (pH 2.0) ABS (section 2.2.2.1). A liquid sample (25 mL) was also removed from the aSRBR and stored at room temperature until used. An experiment was set up in which 12 mL of this liquid sample plus half (8 mL) of the porous beads/ABS suspension, 49.0 mL of a ABS/TE solution adjusted to pH 1.8 with sulfuric acid, 0.7 mL of 1 M $FeSO_4$ (10 mM final concentration) and 0.5 mL of an active culture of *Leptospirillum* (*L.*) *ferriphilum* strain MT63 (Okibe et al., 2003) was placed into a 250 mL conical flask. The final volume was 70 mL and the initial pH was 1.8. A non-inoculated control was set up in parallel. The flasks were incubated at 40ºC, and shaken at 50 rpm. Samples were withdrawn at regular intervals and analysed for pH, concentrations of transition metals (section 2.6.3) and redox potential ($E_H$). The pH values were adjusted using 100 µL of 25% (v/v) sterile $H_2SO_4$ when these increased above pH 3.0. Sterile RO-grade water was added to the flasks in order to compensate loss due to evaporation.

*5.2.2 Results*

The bioremediation of a synthetic mine water using biosulfidogenesis accumulated metal sulfide precipitates (mainly NiS, CoS, ZnS) within the bioreactor vessel over a 2 year period. A preliminary bioleaching experiment was carried out in order to assess the feasibility of recovering metals that were precipitated within the biofilm bed of the aSRBR. The pH values of inoculated and non-inoculated flasks throughout the experiment are shown in Fig. 5.1. Both inoculated and non-inoculated flasks displayed the same general trend of pH fluctuations during the 21 days of the experiment, though slightly lower pH values were found in the non-inoculated flask. On day 7, the pH values in both flasks were above 3.0 (pH 3.5 for the inoculated flask) which was adjusted with addition of sterile sulfuric acid. From day 12, pH values remained fairly constant (pH ~ 2.4) until the end of the experiment and no further addition of acid was required. Initial and final redox potentials are shown in Table 5.1. Increased redox potentials were recorded in both flasks with the inoculated flask displaying a more positive $E_H$ value (~ +885 mV) at the end of the experiment than the non-inoculated flask (+829 mV).

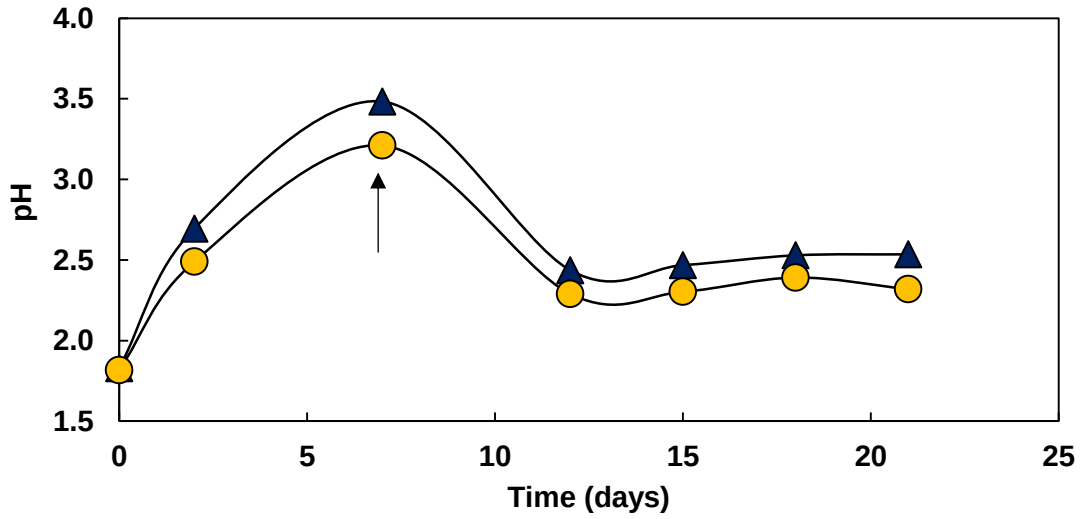


**Fig. 5.1.** Changes in pH values during the preliminary metal dissolution experiment carried out with porous beads and liquid samples taken from the aSRBR reactor: (▲) the inoculated and (●) the non-inoculated flask. The arrow indicates where pH values were adjusted by adding 100 µL of sterile $H_2SO_4$.

**Table 5.1.** Initial and final redox potential (mV) in the inoculated and non-inoculated flasks.

| Flasks | Initial $E_H$ | Final $E_H$ |
|---|---|---|
| **Inoculated** | +719 | +885 |
| **Non-inoculated** | +649 | +829 |

Concentrations of transition metals leached during the experiment are shown in Fig. 5.2. A progressive increase of metal concentrations in the pregnant leaching solutions (PLS) was observed in both inoculated and non-inoculated flasks. However, only minor differences in metal solubilisation was observed between the two treatments. For example, on day 21, nickel concentration in the leachate was 9.8 mM in the inoculated flask and 9.0 mM in the non-inoculated flask. Concentrations of other metals were very similar in both flasks (~ 7.0 mM Zn and ~ 1.2 mM Co). Although mostly manganese was not precipitated within the aSRBR vessel, occasionally this was not the case (Chapter 4) and this was reflected by the fact that small amounts of manganese were both leached from the beads in this experiment (Fig. 5.2 B).

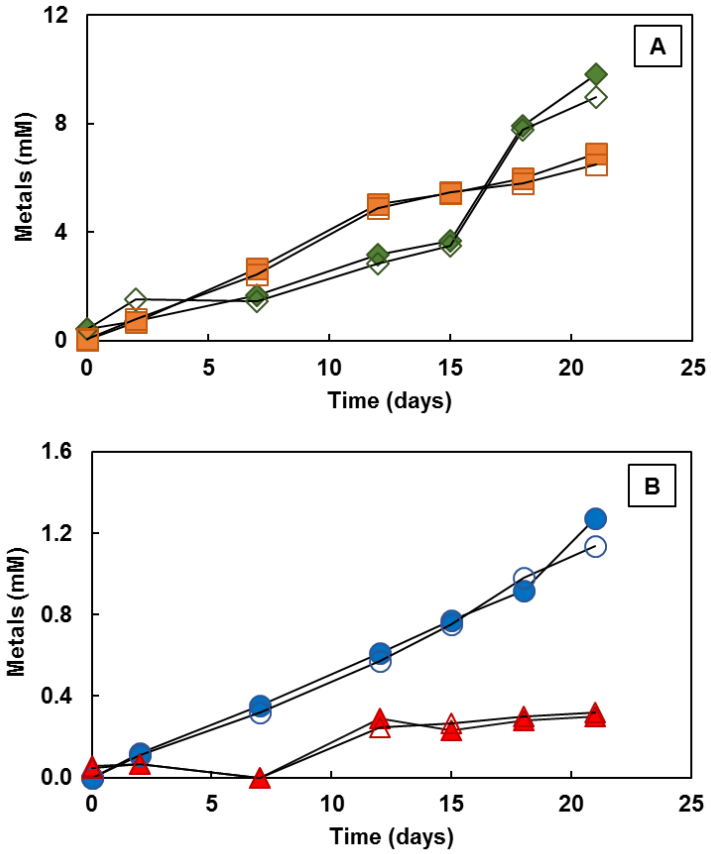


**Fig. 5.2.** Metals leached during the preliminary metal dissolution experiment carried out with porous beads and liquid samples taken from the aSRBR reactor: (A), Ni (♦) and Zn (■); (B), Co (●) and Mn (▲). Data from the inoculated flask are represented by filled symbols and those from the non-inoculated flask by open symbols.

## 5.3 Conversion of the aSRB reactor to a bioleaching reactor to extract metals from accumulated sulfides

### *5.3.1 Material and methods*

In order to facilitate the oxidative dissolution of the metal sulfides that had accumulated within the aSRBR vessel, conditions were changed from anaerobic to aerobic and the pH was lowered from 5.0 to 1.8 by the addition of 2 M sulfuric acid. The gas supply was changed from oxygen-free nitrogen to filtered atmospheric air and, since the impeller was located only in the upper liquid phase of the bioreactor (section 2.4), the air flow rate was increased in order to disturb the biofilm bed ensuring a more homogeneous mixture of the precipitates and the liquid phase (Fig. 5.3). Ferrous sulfate was added to the bioreactor to a final concentration of 10 mM. The reactor (now referred to as “bioleaching reactor”) was operated at 35ºC for a period of 55 days.

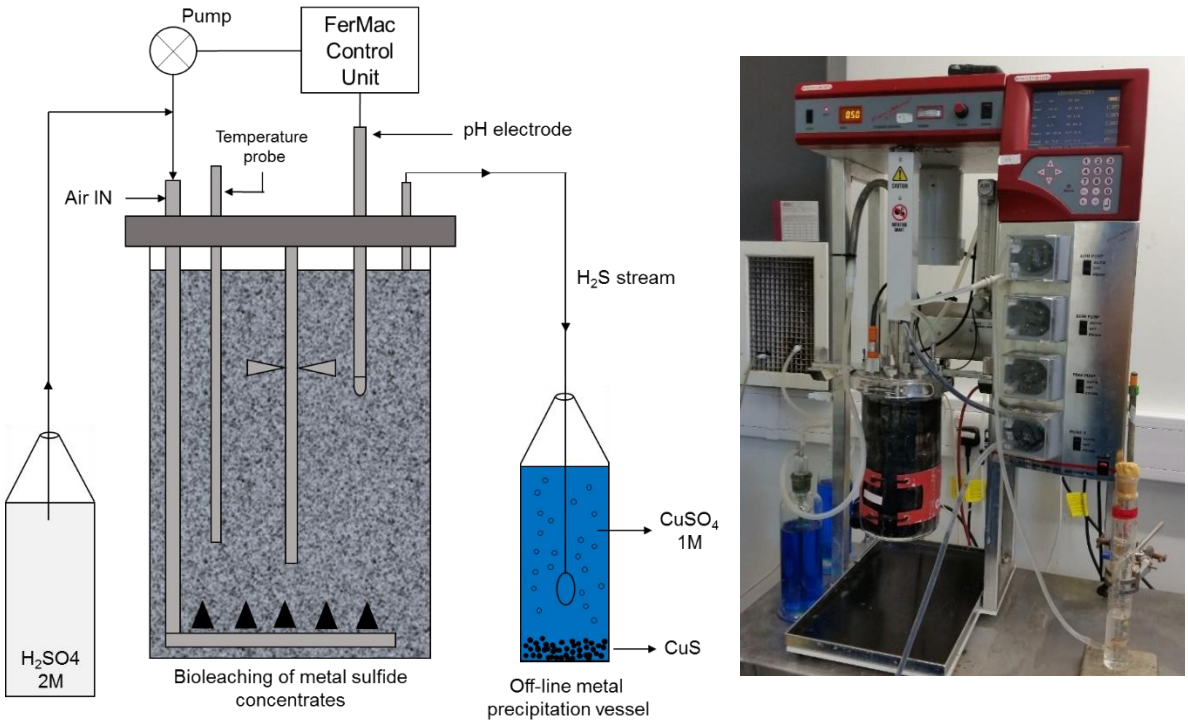


**Fig. 5.3.** Schematic representation of the bioleaching reactor (left) and image of the actual system (right).

The amount of hydrogen sulfide produced by the reactor during the oxidative phase was calculated from measuring changes in concentrations of soluble copper (section 2.5.2.1) in an attached off-line vessel containing 500 mL of 1 M $CuSO_4$ (Fig. 5.3).

The bioleaching reactor was first operated without any additional mineral-oxidizing microorganisms, as *At. ferrooxidans* was known to be present within the microbial consortium when the system was operated as a sulfidogenic bioreactor (Chapter 4). Later in the experiment, active cultures of other iron- and sulfur-oxidizing acidophiles, including several species of bacteria and one archaeon, were introduced to the system at different times, as shown in Table 5.2.

**Table 5.2.** Acidophilic prokaryotes used to inoculate the bioleaching reactor at different days of experiment.

| Day of experiment | Microorganisms | Characteristics (Johnson et al., 2017) |
|---|---|---|
| **Day 2** | *L. ferriphilum* strain MT63 | Thermo-tolerant; autotrophic $Fe^{2+}$ oxidizer |
| **Day 34** | *At. ferrooxidans*$^T$ | Mesophile; autotrophic $Fe^{2+}$, $S^0$, $H_2$ oxidizer |
| | *At. ferridurans*$^T$ | Mesophile; autotrophic $Fe^{2+}$, $S^0$, $H_2$ oxidizer |
| | *L. ferriphilum* strain MT63 | Thermo-tolerant; autotrophic $Fe^{2+}$ oxidizer |
| **Day 43** | *Acidithiobacillus* (*At.*) *caldus*$^T$ | Moderate thermophile; autotrophic $S^0$, $H_2$ oxidizer |
| | *Sulfobacillus* (*Sb.*) *thermosulfidooxidans*$^T$ | Moderate thermophile; mixotrophic $Fe^{2+}$, $S^0$, $H_2$ oxidizer |
| | *Ferroplasma* (*Fp.*) *acidiphilum* strain BRGM4 | Thermo-tolerant archaeon; heterotrophic $Fe^{2+}$ oxidizer |

Samples from the bioleaching reactor were removed and analysed for pH and redox potentials ($E_H$). Other samples were filtered through 0.2 µm nitro-cellulose membrane filters (Whatman, UK) and concentrations of copper (section 2.5.2.1), ferrous and total iron (section 2.5.2.2), sulfate and glycerol (section 2.5) determined. Concentrations of other transition metals were determined using both ion chromatography (section 2.6.3) and atomic absorption spectroscopy (AAS) (section 2.7).

*5.3.2 Results*

Hydrogen sulfide was immediately released (confirmed by the formation of CuS in the off-line vessel) when the bioreactor pH was lowered from 5.0 to 1.8 and continued to be produced over the following 3 days. The concentration of soluble copper in the off-line vessel fell from 1.0 M to 0.89 M, which is equivalent to 55 mmoles of CuS precipitated (and of $H_2S$ generated). A continued input of acid was also required to maintain the bioreactor at this pH value (Fig. 5.4). The production of $H_2S$ halted after 3 days, and the bioreactor pH was lowered further, to 1.5, on day 7, which resulted in a second phase of $H_2S$ generation.

Sixty-eight mL of 2 M sulfuric acid (136 mmoles) was required to drop to, and maintain the pH at, 1.8. At this pH value, the amount of sulfate present as sulfate ions ($SO_4^{2-}$) was 58.5 mmoles and as bisulfate ions ($HSO_4^-$) was 77.5 mmoles (since the $pK_a$ of the bisulfate/sulfate couple is 1.92). The equivalent to hydronium ions was 117 mmoles $H_3O^+$ for the former and 77.5 mmoles for the latter, therefore the total proton acidity added to the bioreactor (as sulfuric acid) at pH 1.8 was 194.5 mmoles $H_3O^+$. The difference in hydronium ion ($H_3O^+$) concentrations at pH 5.0 and 1.8 is ~ 16 mM, or 32 mmoles in the 2 L bioreactor. The total amount of copper sulfide produced in the off-line vessel was 55 mmoles CuS, which means that 55 mmoles of $H_2S$ was generated in the bioreactor. The stoichiometry of $H_3O^+$ consumed to $H_2S$ produced is 2:1, therefore 110 mmoles $H_3O^+$ were required for that amount of $H_2S$ produced at pH 1.8, assuming that it was generated entirely by acid hydrolysis of metal sulfides within the leaching bioreactor (Eq. 5.1). The total amount of acid required for the reactions aforementioned was 142 mmoles $H_3O^+$, and therefore the total amount of acid added to the bioreactor at this stage was enough to sustain these, and also suggests that other proton-consuming reactions may have occurred during acidification of the leaching bioreactor.

$$MeS + 2\ H_3O^+ \rightarrow Me^{2+} + H_2S + 2\ H_2O \qquad \text{(Eq. 5.1)}$$

Subsequently, to drop to and maintain the pH at 1.5, 42 mL of 2 M sulfuric acid (84 mmoles) was required. The difference in hydronium ion concentration at pH 1.8 (~ 16 mM) and 1.5 (~ 32 mM) is equivalent to 32 mmoles $H_3O^+$ (in the 2 L working volume bioreactor). At pH 1.5, bisulfate accounts for 72.5% of the total sulfate present (i.e. 60.9 mmoles of the added sulfuric acid) and sulfate accounts for the remaining (23.1 mmoles) fraction. The equivalent amounts of hydronium ions added in this case were 60.9 mmoles (as $H_3O^+$ + $HSO_4^-$) and 46.2 mmoles (as 2 $H_3O^+$ + $SO_4^{2-}$), totalling 107.1 mmoles $H_3O^+$, of which 32 mmoles $H_3O^+$ can be accounted for by the pH difference. In this case, the copper

concentration in the off-line vessel (which initially contained 480 mL of an 890 mM copper sulfate solution) declined by 420 mM, (equivalent to 201.6 mmoles CuS/$H_2S$), which would require 403.2 mmoles of $H_3O^+$ to be consumed if all of the $H_2S$ was generated by acid dissolution of metal sulfides inside the bioreactor, which is about four-fold greater than the 107.1 mmoles $H_3O^+$ calculated (above) to have been added as sulfuric acid.

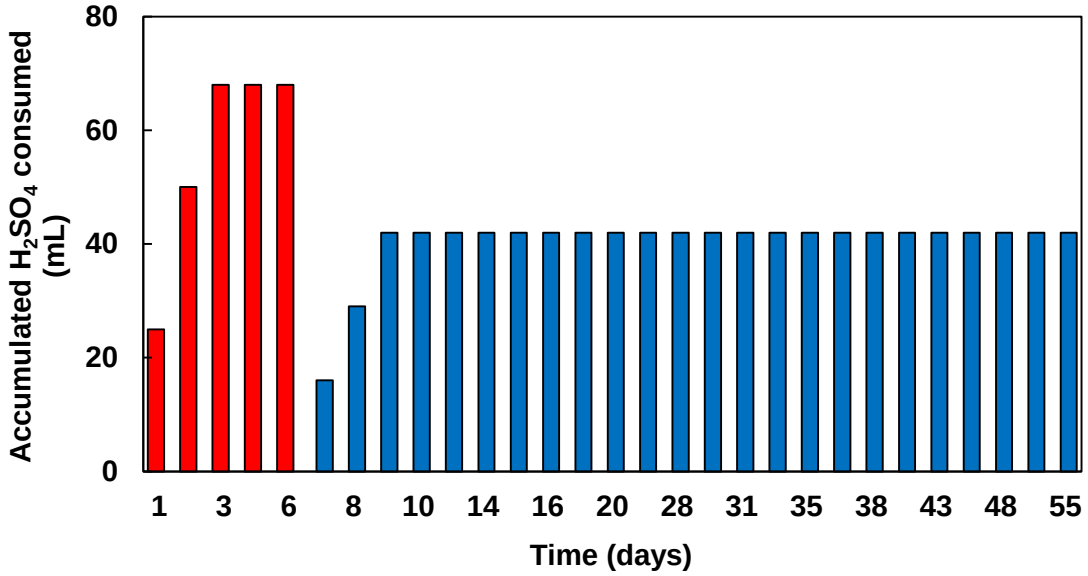


**Fig. 5.4.** Volume of accumulated sulfuric acid consumed in the bioleaching reactor to drop to and maintain at pH 1.8 (red bars) and pH 1.5 (blue bars).

Variations in redox potentials and concentrations of iron species in the bioreactor during the experiment are shown in Fig. 5.5. Redox potentials started to increase immediately after the aSRBR was converted to a bioleaching reactor, and was about +570 mV at pH 1.8, which was much more positive than when it was operated as a higher pH (5.0) anoxic module (average $E_H$ of ~ +250 mV). A progressive increase in redox potential was found, reaching ~ +650 mV by day 8, when the bioreactor pH was lowered to 1.5. Redox potential values in this phase (pH 1.5) did not show major changes and remained at ~ +660 mV until the end of the experiment. Figure 5.5 also shows that $Fe^{2+}$ was the dominant iron species throughout the time course of the experiment. From day 7 to day 35, the concentration of ferrous iron was fairly constant (~ 23 mM), whereas ferric iron concentration increased over this time period reaching up to 18 mM. Concentrations of total soluble iron increased relatively rapidly during the first 7 days, followed by a more moderate increase which continued until the end of the experiment, reaching a maximum of 56 mM total iron, of which 33 mM was $Fe^{2+}$ and 23 mM was $Fe^{3+}$.

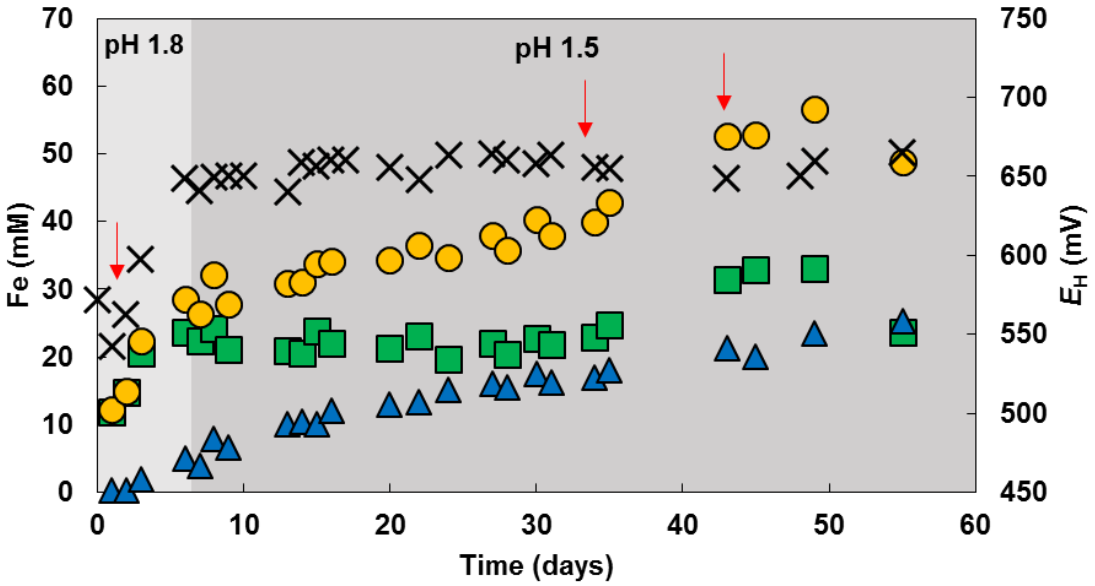


**Fig. 5.5.** Changes in iron concentrations and redox potential in the bioleaching reactor. Key: $Fe^{2+}$ (■), $Fe^{3+}$ (▲), total Fe (●) and $E_H$ (**X**). The red arrows indicate the points at which additional microorganisms were added to the bioreactor.

As mentioned previously, concentrations of ferrous iron increased over time and relatively little ferric iron was detected initially (~ 0.4 mM). This observation is closely related to the low redox potential values observed during this period (Fig. 5.5), and as soon as ferric iron was detected at higher concentrations in the bioreactor (~ 5.0 mM by day 6) redox potential values also increased. Overall, concentrations of soluble iron increased during the time that the module was operated as a bioleaching reactor. One reason for this was that iron (and sulfate) was present in the liquors used to inoculate the bioreactor at days 2, 34 and 43.

Concentrations of sulfate in the bioleaching reactor are shown in Fig. 5.6. Sulfate concentrations increased mostly due to the addition of sulfuric acid, reaching up to 130 mM by day 7 when the bioreactor was operated at pH 1.8. Sulfate concentrations increased further when the pH of the bioreactor was lowered to 1.5. There were fluctuations in sulfate concentrations during periods when there was no addition of sulfuric acid (e.g. day 34: 250 mM and day 36: 155 mM); however, an average of 203 mM sulfate was measured during the last 20 days of this experiment.

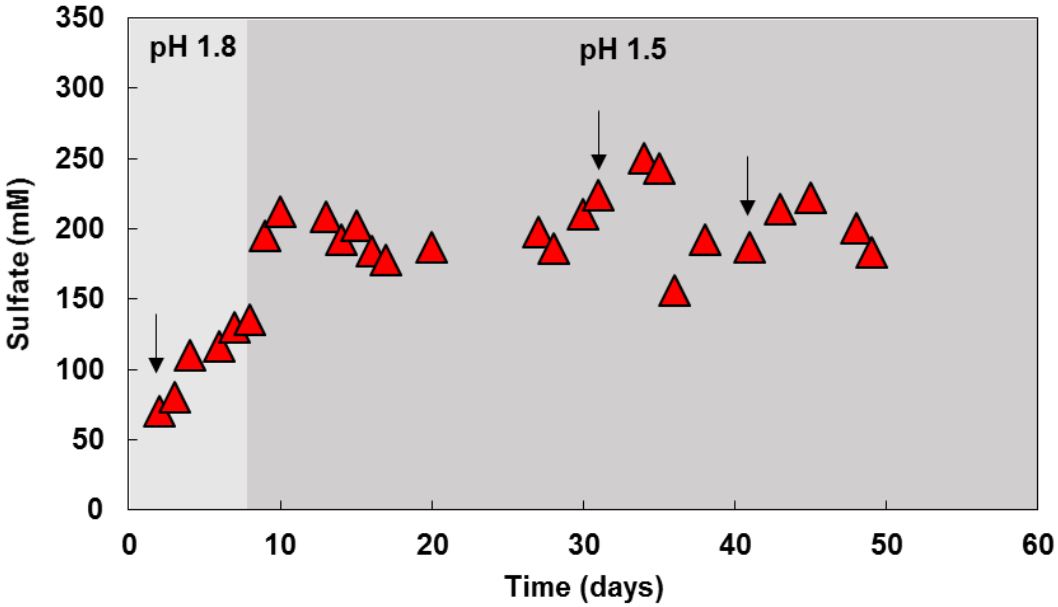


**Fig. 5.6.** Changes in sulfate concentrations in the bioleaching reactor at pH 1.5 and pH 1.8. Arrows indicate the points at which additional microorganisms were added to the bioreactor.

Concentrations of transition metals leached from sulfide precipitates increased with time and are shown in Fig. 5.7. These reached 8.7 mM Ni, 7.0 mM Zn, 1.3 mM Co and ~ 4.0 mM Cu after 7 days of leaching at pH 1.8. Following lowering the pH of the bioreactor to 1.5, sharp increases in the concentrations of Co, Ni and Cu were observed. Zinc, in particular, displayed a continuous trend until the end of the experiment regardless of pH change. Following day 34, when a mixture of additional microorganisms was introduced to the bioreactor (Table 5.2), there were notable increases in concentrations of all soluble transition metals (Fig. 5.7). The same occurred following day 42 when further additional microorganisms were added. After day 45, metal dissolution appeared to have reached a plateau in all cases.

The amounts of nickel, cobalt and zinc that had accumulated within the bioreactor vessel were calculated from the total volume (2,025 L) and concentrations of partly-processed synthetic mine water that was pumped through it during the time (2 years) that it was operated as an aSRBR, assuming that 100% of these three metals had been removed at all times (Table 5.3). From this, the theoretical maximum concentration of each of the three metals, i.e. assuming that 100% of precipitated metals were re-solubilised during the oxidative phase, was evaluated and compared with the actual concentrations obtained (Table 5.3).

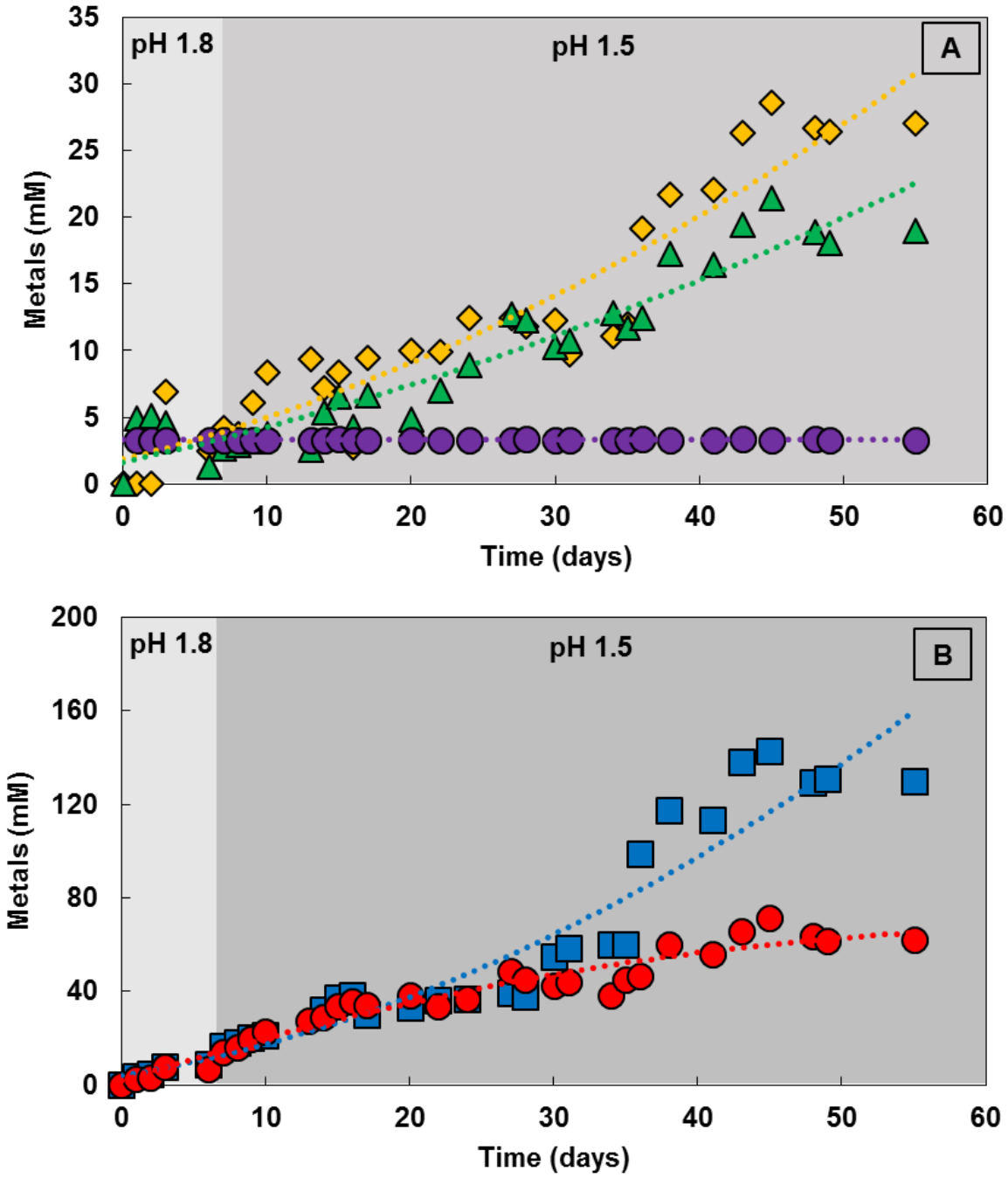


**Fig. 5.7.** Changes in concentration of metals in the leaching liquor of the bioreactor at pH 1.8 and pH 1.5: (A) Co (▲), Mn (●), Cu (♦); (B) Ni (■) and Zn (●).

**Table 5.3.** Amounts of transition metals calculated to have accumulated within the aSRBR and comparison of corresponding maximum actual concentrations when operated as a bioleaching reactor.

| Metals | Amounts of metals accumulated | | Concentration of metals leached (mM) | |
|---|---|---|---|---|
| | g | mmoles | Maximum theoretical | Actual |
| **Ni** | 14.9 | 253 | 126.5 | 131 |
| **Co** | 3.6 | 60.9 | 30.45 | 19.1 |
| **Zn** | 1.3 | 20.3 | 10.15 | 62.4 |

Comparison of the amounts of $H_2S$ generated during each phase (pH 1.8 and pH 1.5) at which the leaching bioreactor was operated and the amounts of transition metals (Ni, Co, Zn, Cu and Mn) solubilised show that acid dissolution of the latter (assuming they were present as metal sulfides; Eq. 5.1) could account for all of the former. For example, when the leaching bioreactor was maintained at pH 1.8, 55 mmoles of $H_2S$ were generated and the total increase in soluble transition metals was 30.6 mM (corresponding to an increase in 61.2 mmoles of these metals, and therefore of 61.2 mmoles of $H_2S$ generated, assuming they were present as sulfides). Corresponding figures for when the leaching bioreactor was operated at pH 1.5 are 202 mmoles $H_2S$ produced and an increase of 210 mM (420 mmoles) total soluble transition metals.

### 5.4 Second phase bioleaching of the porous beads/precipitates mixture

Data shown in Table. 5.3 clearly indicate that dissolution of the transition metals that were considered to have accumulated as sulfides within the aSRBR vessel was far from complete in the experiment described above. To try to improve upon this, the contents of the bioreactor vessel were removed. These were separated into the porous beads and the liquid phase that contained a precipitate which sedimented rapidly below a colloidal liquid phase. The upper liquid phase was poured off and the sediment combined with the beads, which were dried at 40ºC and then mixed together to prepare a porous beads/precipitate mixture. The metal concentrations in this mixture were determined by *aqua regia* digestion, and the mixture was also subjected to a second phase of bioleaching.

.

*5.4.1* Aqua regia *digestion of the* porous beads/precipitate mixture

*Aqua regia* is a yellow-orange fuming solution which contains a mixture of concentrated nitric acid and hydrochloric acid (ratio 1:3). The digestion protocol was carried out in triplicate and used replicate 1 g sample of porous beads/precipitate mixture, each digested with 5 mL of *aqua regia*. These were boiled to dryness using a heating block placed in a fume cupboard. Once dry, 1 mL of HCl was added and again boiled to dryness. The residues were re-dissolved in 20 mL $HNO_3$ 1% and filtered through 0.2 µm nitrocellulose membrane filters (Millipore, UK). Undissolved materials (mainly the more recalcitrant silicaceous fractions of the beads) were allowed to dry and their weights were subtracted from the total amounts of material initially used. Metal concentrations were determined using AAS (section 2.7).

The amounts of residual nickel, cobalt and zinc in the porous beads/precipitates mixture are shown in Table 5.4. The Table also shows the equivalent dry weights of these metals and those of the undigested silicaceous residues.

**Table 5.4.** Amounts of residual nickel, cobalt and zinc in the porous beads/precipitates mixture and amount of undigested residues (mean values of duplicate samples).

| Metal | Amount of metals (mg $g^{-1}$ of beads mix) | Amount of metal sulfides (mg $g^{-1}$) | Undigested residues (mg $g^{-1}$) |
|---|---|---|---|
| **Ni** | 17.5 | 26.4 | 510 |
| **Co** | 5.5 | 8.5 | |
| **Zn** | 7.0 | 10.4 | |

*5.4.2. Effect of temperature and pulp density on bioleaching of the porous beads/precipitates mixture*

5.4.2.1 Materials and methods

Shake flasks experiments were set up to evaluate the effects of temperature and pulp density on bioleaching of the residual metal sulfides in the porous bead bed, in order to further improve metal dissolution. Bioleaching experiments were carried out in duplicate at 30ºC and 45ºC using 5%, 10% and 20% (w/v) of dried porous beads/precipitates mixture in ABS/TE solution (section 2.2.2.1) at pH 1.5, with 10 mM (final concentration) ferrous sulfate added. Flasks were inoculated with mixed populations of known mesophilic and moderately thermophilic/thermo-tolerant iron- and/or sulfur-oxidizing bacteria (Table 5.5), and incubated,

shaken, at either 30ºC or 45ºC. The final volume of all flasks was 100 mL, and evaporation was compensated for by addition of sterile RO-grade water.

Samples were taken at regular intervals and analysed for pH and redox potential. Concentrations of transition metals and sulfate were determined as described previously.

**Table 5.5.** Acidophilic microorganisms used in the experiments at different temperatures.

| Temperature | Microorganisms |
|---|---|
| **30ºC** | *At. ferridurans*$^T$ |
| | *L. ferrooxidans*$^T$ |
| | *At. caldus*$^T$ |
| **45ºC** | *L. ferriphilum* strain MT63 |
| | *Sb. thermosulfidooxidans*$^T$ |
| | *At. caldus*$^T$ |

5.4.2.2 Results

Changes in pH values throughout the experiment are shown in Fig. 5.8. The pH values in the experiment carried out at 30ºC (Fig. 5.8 A) were fairly constant with 20% pulp density. On the other hand, the pH of the inoculated 10% pulp density cultures experiment increased especially after day 20, reaching pH 1.61 by day 30. The pH values of both 5 and 20% also increased from day 10 to day 20, however the final pH values were the same of that in the beginning of the experiment. At 45ºC, a similar trend was observed for all 3 pulp densities studied (Fig. 5.8 B). In the first 5 days of experiment, pH values decreased reaching pH 1.49 in the 20% pulp density, and subsequently increased by day 10. In the 10 and 20% pulp densities, pH values kept increasing progressively until day 20, decreasing again by the end of the experiment (day 30). No pH adjustment was necessary during the experiment.

Changes in redox potentials are shown in Fig. 5.9. Values for the 20% pulp density at 30ºC test did not show major changes, and ranged between +657 and +662 mV (Fig. 5.9 A). An increase in redox potential values was observed in the first 10 days of experiment for both 5 and 10% pulp density, however the 5% test reached a plateau after day 10 which continued until the end of the experiment. In contrast, the 10% test showed a sharp increase from day 20 reaching $E_H$ values of +700 mV by day 30. For the experiment at 45ºC, the redox potential values decreased in all conditions tested in the first 3 days. For example, in the 20% pulp density, the redox values decreased from ~ +656 mV to +620 mV. Subsequently, an increase was observed in all tests, however the final $E_H$ of the 10 and 20% pulp density (+636 and

+641 mV, respectively) were still lower than the initial values. In contrast, the final $E_H$ in the 5% pulp density was slightly higher than that at the start of the experiment (Fig. 5.9 B).

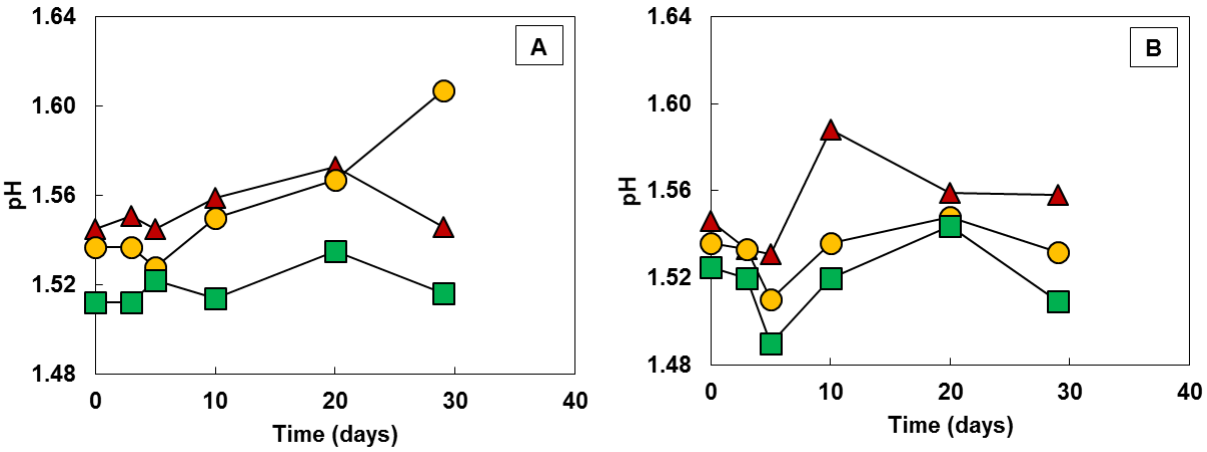


**Fig. 5.8.** Changes in pH in the bioleaching experiment at (A) 30ºC and (B) 45ºC. Key: 5% (▲), 10% (●) and 20% (■).The experiment was carried out in duplicate and differences in ranges between replicates are occluded by the symbols.

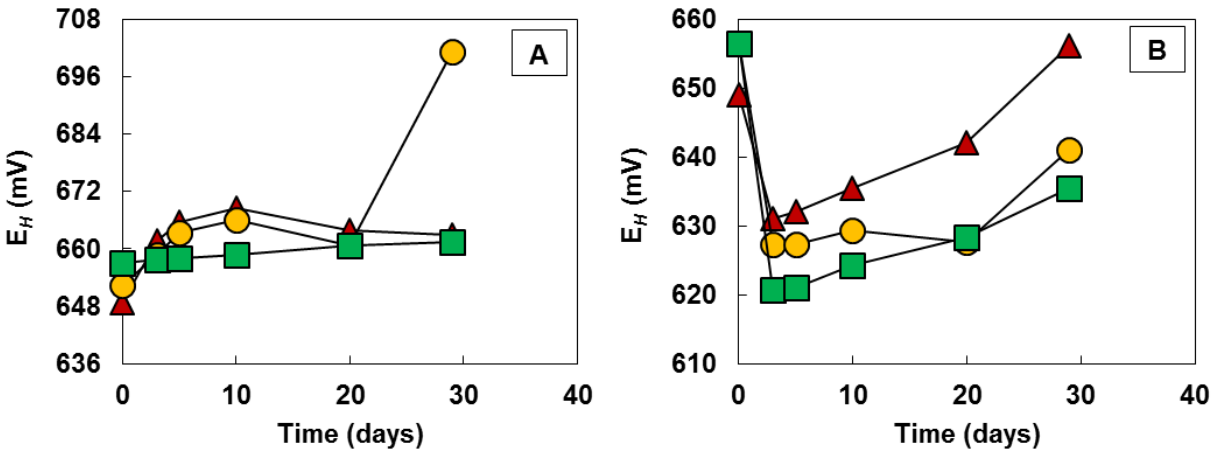


**Fig. 5.9.** Changes in redox potential in the bioleaching experiment at (A) 30ºC and (B) 45ºC. Key: 5% (▲), 10% (●) and 20% (■). The experiment was carried out in duplicate and differences in ranges between replicates are occluded by the symbols.

Sulfate concentrations in the leachate did not show any major change throughout the experiment in any of the conditions tested (Fig. 5.10). The different pulp densities used in this experiment showed a directly proportional relation to the concentration of sulfate, in which the higher the pulp density, the higher the sulfate concentration in the PLS. Regardless of temperature, the concentration of sulfate was fairly similar for each pulp density, except the

20% pulp density flasks, which had more sulfate at 30ºC (max. ~ 200 mM) than at 45ºC (max. ~ 170 mM).

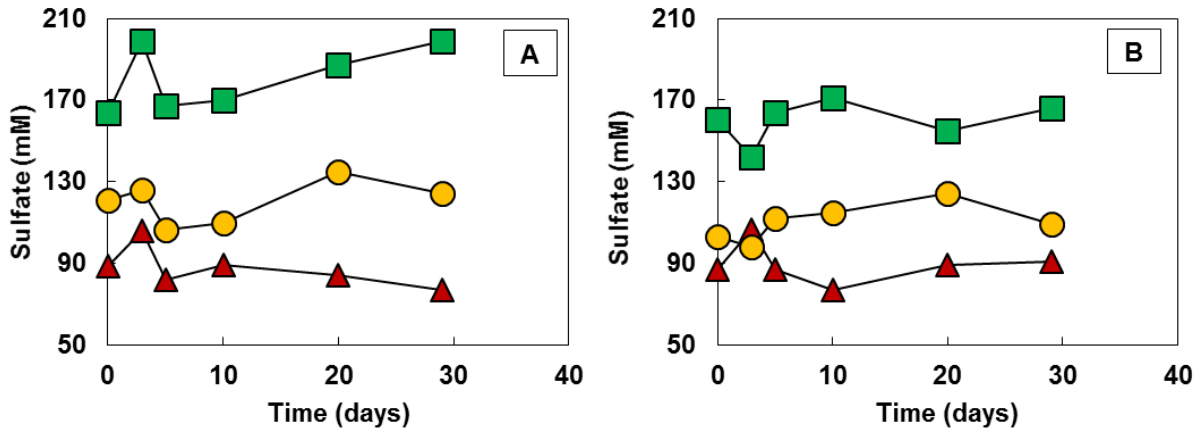


**Fig. 5.10.** Changes in sulfate concentrations in the bioleaching experiment at (A) 30ºC and (B) 45ºC. Key: 5% (▲), 10% (●) and 20% (■). The experiment was carried out in duplicate and differences in ranges between replicates are occluded by the symbols.

Manganese was not detected in the leachates, suggesting that all the solid Mn phase that had accumulated in the aSRBR reactor had been solubilised in the previous experiment (section 5.3). Concentrations of the other transition metals (Ni, Zn, Co, Cu and total Fe) are shown in Fig. 5.11.

In general, concentrations of metals in the leachates were directly proportional to the amount of porous beads/precipitates mixture in each flask (i.e. pulp density) and the effect of temperature did not show a major difference on metal recovery. In the case of nickel, a moderate increase was observed in the 5 and 10% pulp density flasks during the first days of experiment, followed by a stationary period between day 5 and day 12 at both temperatures; a subsequent increase in Ni concentration was observed by day 30, reaching ~ 24 and 31 mM at 30ºC and 45ºC, respectively. The 20% pulp density flasks showed a more pronounced increase during the time course of the experiment, reaching final concentrations of 52 mM at 30ºC and 61 mM at 45ºC. Maximum concentration of zinc recovered was obtained in the 20% pulp density at 30ºC reaching ~ 26 mM by day 30. The zinc concentration in the PLS was proportional to the pulp density, e.g., 5 and 10% pulp density tests, recovered ~ 5 mM and ~ 10 mM, respectively, both at 30ºC and 45ºC. Cobalt concentrations varied considerably throughout the experiment within the conditions tested. The final cobalt concentrations in the leachates in the 20% pulp density flasks were ~ 16 mM at 30ºC and 12 mM at 45ºC. Lower concentrations were found in the 10% (~ 6.5 mM) and 5% (~ 4.5 mM) pulp density flasks at both temperatures tested. As the pH and redox potential values of the 10% pulp density test

undertaken at 30ºC showed a great increase towards the end of the experiment (Fig. 5.8 and Fig. 5.9, respectively), this condition was evaluated for 40 more days in order to check whether that would show higher percentage of metal recovery due to the changes observed in pH and $E_H$. However, no further changes in metal concentrations were observed in this extended period except for total iron, which decreased considerably by day 70. Final pH and $E_H$ values (day 70) were 1.51 and +807 mV, respectively.

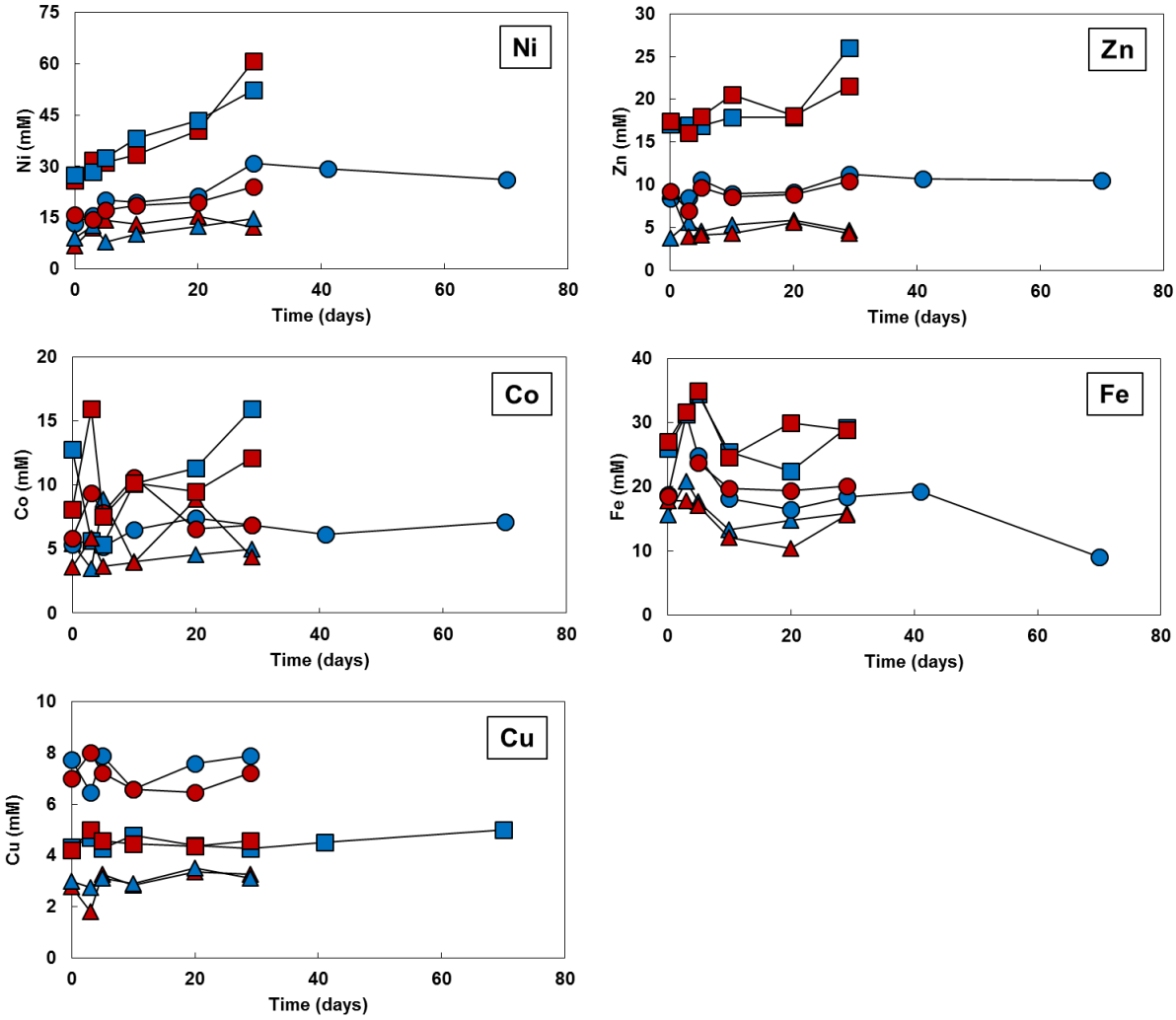


**Fig. 5.11.** Changes in metals concentration in the leaching liquor at 30ºC (▲, ●, ■) and 45ºC (▲, ●, ■). Key: 5% (▲,▲), 10% (●,●) and 20% (■, ■).

Table 5.6 shows the initial concentration of metals in each pulp density tested, based on the amount of metals in the porous beads/precipitates mix (Table 5.4), and the maximum concentration of metals leached in the experiment.

**Table 5.6.** Initial amounts of metals (mg $L^{-1}$) at the different pulp densities used, and maximum concentrations of metals leached in the experiment.

| Metals | Initial concentration | | | 30ºC | | | 45ºC | | |
|---|---|---|---|---|---|---|---|---|---|
| | 5% | 10% | 20% | 5% | 10% | 20% | 5% | 10% | 20% |
| Ni | 875 | 1,750 | 3,500 | 720 | 1,540 | 3,600 | 860 | 1,410 | 3,100 |
| Zn | 350 | 700 | 1,400 | 310 | 690 | 1,700 | 280 | 680 | 1,400 |
| Co | 275 | 550 | 1,100 | 290 | 420 | 940 | 260 | 410 | 710 |

Figure 5.12 shows that the extraction of the residual nickel, cobalt and zinc was often > 80% in this bioleaching experiment, and occasionally exceeded 100%, which was probably due to the heterogeneity of the porous beads/precipitate mixture. The minimum percentage of nickel, zinc and cobalt leached were 83%, 80% and 65%, respectively and the maximum percentage of these metals leached were over 99% in some cases.

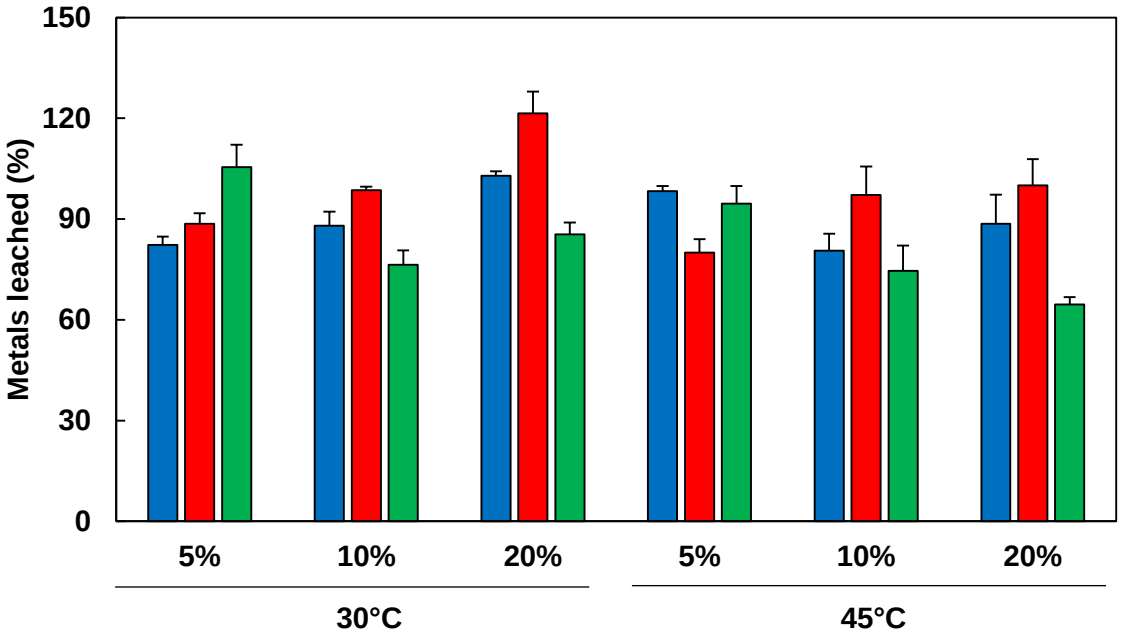


**Fig. 5.12.** Metal recovery from shake flasks experiment at different temperatures and pulp density. Nickel (blue), zinc (red), cobalt (green). The bars depict mean values and the error bars the range between replicate samples (*n* = 2).

## 5.5 Tests for the presence of viable microorganisms in the bioleaching reactor and the second phase bioleaching experiment

The iron- and sulfur-oxidizing acidophile *At. ferrooxidans* was detected consistently in the aSRBR (section 4.3) and, as described, other species of mineral-oxidizing prokaryotes were added to the leaching bioreactor and as inocula in the second phase bioleaching experiments (section 5.4). Empirical tests were carried out to find whether viable iron- and sulfur-oxidizing bacteria could be recovered at different times after they had been added.

### *5.5.1 Materials and methods*

Liquid samples from the bioleaching reactor (section 5.3) were withdrawn at regular intervals, streak-inoculated onto $iFe_o$ and $FeS_o$ overlay plates (section 2.2.2.3) and incubated aerobically at 30ºC in order to look for the presence of viable iron- and sulfur-oxidizing acidophiles. In the second phase bioleaching experiment, liquid samples were removed after 5 - 30 days of incubation and streak-inoculated onto $iFe_o$ and $FeS_o$ overlay plates, which were incubated at either 30ºC or 45ºC for 7 days.

A filtered (through Whatman nº 1 filter paper) sample of the colloidal liquid from the bioleaching reactor was also inoculated with iron- and sulfur-oxidizing acidophiles (Table 5.5). Liquid samples were removed after 5 - 30 days of incubation and streak-inoculated onto $iFe_o$ and $FeS_o$ overlay plates incubated at either 30ºC or 45ºC for 7 days.

### *5.5.2 Results*

The low-pH bioleaching of accumulated sulfides generated a dark black leachate liquor (Fig. 5.13 A). In the second phase bioleaching experiment, the liquid media in the shake flasks also darkened with time while the porous beads become increasing white in colour (Fig. 5.13 B). Plating liquid samples onto solid media was an easy and effective way to check whether the cells from an inoculum were viable or not, since only the viable ones would be able to grow. However, while the viability tests proved positive for the inoculating liquors, on no occasion were viable acidophiles recovered from either the bioleaching reactor or shake flasks from the second bioleaching experiment (Table 5.7 and Fig. 5.13 C).

**Table 5.7.** Viability tests of acidophiles in the experiments described in this Chapter. (-) no growth observed; (+) growth observed.

| | First phase bioleaching | Second phase bioleaching | | | | | | Bioreactor leachate | |
|---|---|---|---|---|---|---|---|---|---|
| Day | (bioreactor) | 30ºC | | | 45ºC | | | 30ºC | 45ºC |
| | | 5% | 10% | 20% | 5% | 10% | 20% | | |
| **0** | + | + | + | + | + | + | + | + | + |
| **5** | - | - | - | - | - | - | - | - | - |
| **10** | n.t. | - | - | - | - | - | - | - | - |
| **20** | n.t. | - | - | - | - | - | - | - | - |
| **30** | - | - | - | - | - | - | - | - | - |
| **55** | - | n.t. | n.t. | n.t. | n.t. | n.t. | n.t. | n.t. | n.t. |

n.t. - not tested.

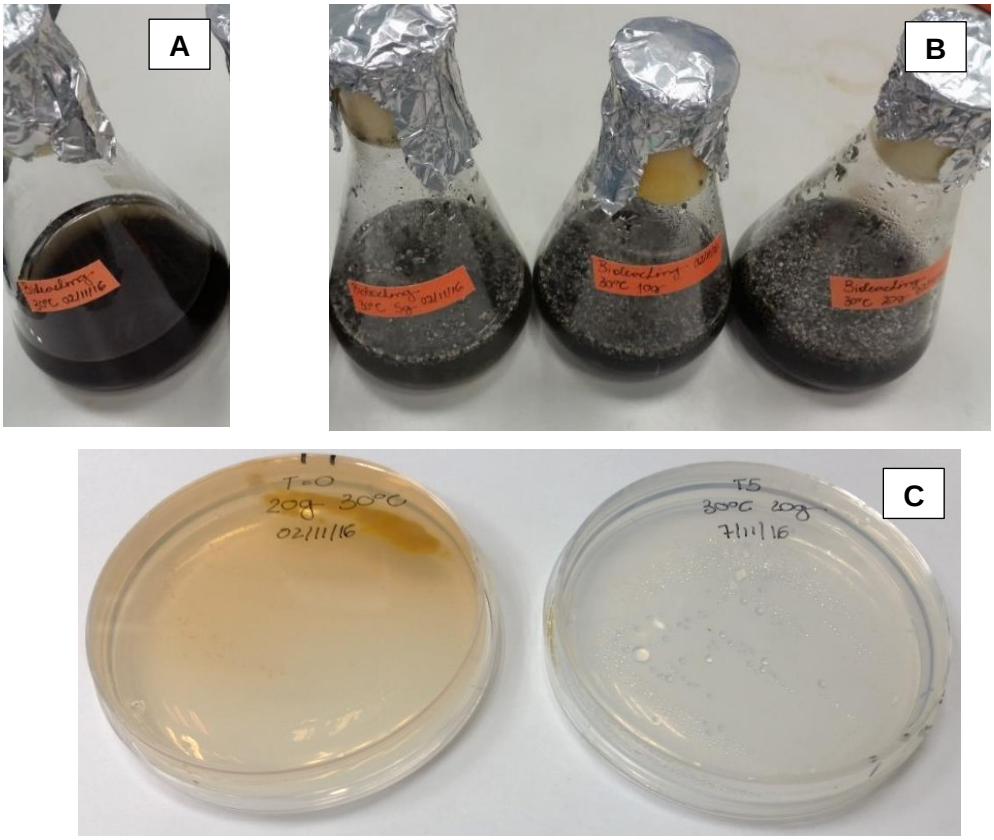


**Fig. 5.13.** Images from the second phase bioleaching shake flask experiment set up at 30ºC. (A) bioreactor filtered leachate; (B) porous beads/precipitates mixture in liquid media at pH 1.5; (C) $FeS_o$ overlay plates inoculated with samples from a shake flask on day 0 (left) and day 5 (right) of the experiment. Similar results were obtained with shake flasks incubated at 45ºC. Plates were incubated for 7 days at their respective temperatures.

## 5.6 Discussion

Although a considerable amount of research has been devoted to remediate metal-rich wastewaters using biologically-generated hydrogen sulfide, rather less attention has been paid to recover metal sulfides produced using this process. The focus of this chapter was therefore to describe a novel approach for recovering metals generated in a sulfidogenic bioreactor.

Metal sulfides (mainly CoS, NiS and ZnS) accumulated in the bioreactor over a 2 years period. A preliminary test comparing (bio)leaching of inoculated and non-inoculated precipitates in shake flasks did not show great difference between them, though it did show that metal dissolution occurred to some extent, as indicated by increases in pH and redox potentials (acid-mediated metal sulfide dissolution is a proton consuming reaction; Eq. 5.1) as well as soluble metal concentrations. It is noteworthy that the control flask in this experiment was not sterile, since the material used was originally from a sulfidogenic bioreactor which contained a consortium of sulfate-reducing bacteria and other acidophiles. The increase in redox potentials found in this experiment was presumed to be due to the generation of ferric iron by iron-oxidizing acidophiles. In the non-inoculated flask this would have been mediated by *At. ferrooxidans* which was found in the aSRBR on most occasions that the microbial population was examined (section 4.3). Tests for the presence of viable bacteria were not carried out with this experiment, though the fact that redox potentials increased significantly (to > +800 mV) during the experiment strongly indicates that iron-oxidizing acidophiles were present and active. The porous beads/precipitate mixture was acid-washed prior to the start of this experiment, and this may have caused some metal sulfide dissolution.

The bioleaching experiment carried out in the bioreactor showed that $H_2S$ was released immediately (confirmed by the formation of CuS in the off-line vessel) when the pH was lowered to 1.8; further $H_2S$ production occurred when the pH was further lowered to 1.5. Redox potential values increased by an average of ~ +250 mV (when operated as a sulfidogenic bioreactor) to over +540 mV at the initial stage when this was operated as bioleaching reactor, reaching up to +650 mV as time progressed. However, once it reached this value no further significant increases were observed, even though other changes occurred, such as decrease in pH and addition of iron-oxidizing acidophiles to the system. The standard redox potential ($E^0$) for the $Fe^{3+}/Fe^{2+}$ couple is generally quoted as +770 mV. However, this value only applies to situations where both ferric and ferrous iron are soluble and non-complexed (Johnson et al., 2012). In most natural and man-made extremely acidic

environments (acid mine drainage and leachates) ferric iron is complexed by hydroxyl and sulfate anions, and consequently the $E_H$ is significantly less depending on pH values, for example +657 mV at pH 2.25 and + 685 mV at pH 0.5 (Johnson et al., 2017). The current experiment showed a maximum $E_H$ of +660 mV (at pH 1.5), suggesting therefore that the system displayed net reducing conditions (i.e. ratio $Fe^{3+}/Fe^{2+} < 1$). The results obtained for iron speciation determined colorimetrically confirmed that ferrous iron was the dominant species present. While concentrations of both total iron and ferric iron increased with time, this did not affect redox potential values, as there were parallel increases in ferrous iron concentrations. The concentrations of both total and ferrous iron in the bioleaching reactor at the start of the experiment was 10 mM, and total iron concentration reached up to ~ 55 mM towards the end of the experiment. This increase in soluble iron in the leachate may have been due in part to the corrosion of the iron-containing components of the bioreactor (forming, for example FeS in less acidic microsites) during the time it was operated as an aSRB reactor and subsequent acid dissolution of these materials; no iron was added to the feed liquor used when the bioreactor was operated as a sulfidogenic unit. Sulfate concentrations in the bioleaching reactor increased from ~ 22 mM at the start of the experiment to ~ 130 mM when maintained at pH 1.8 and to ~ 200 mM at pH 1.5. This increase was mostly due to addition of sulfuric acid used to adjust the bioreactor pH. Large increases in sulfate concentrations were found following addition of microbial inocula due to the presence of sulfate in the latter.

Concentrations of metals in the leachate corresponded to the theoretical leaching of 150% Zn, ~ 26% Ni and ~ 16% Co (figures based on the amounts of these metals pumped into the bioreactor when it was operated as an aSRBR). Copper was also detected in relatively high concentration in the leachate, even though the sulfidogenic bioreactor had been fed with synthetic Cu-free mine water at all times. This was due to the occasional reflux of copper sulfate from the gas trap into the reactor vessel (described in section 3.3.1), causing some copper to be precipitated as CuS within the bioreactor vessel. The final concentration of zinc in the leachate (~ 62 mM) was considerably higher than the maximum theoretical concentration (~ 40 mM) which was thought due to the fact that a portion of the biofilm bed (beads plus biomass) used to set up the aSRBR came from the 'mother' sulfidogenic bioreactor which had been routinely fed with $ZnSO_4$–containing influent liquor, resulting in precipitation of ZnS.

The effect of temperature and pulp density in dissolution of the residual metal sulfides (i.e. that remaining after (bio)leaching within the bioreactor vessel) was assessed in shake flasks at two temperatures (30º and 45ºC) and three pulp densities (5%, 10% and 20%). pH values did not show major variations throughout the experiment in all conditions tested,

except in the 10% pulp density/30ºC flasks where they increased towards the end of the experiment. Redox potentials varied with incubation temperature. In the first few days of the experiment at 30ºC, an increase in $E_H$ was observed, whereas at 45ºC the $E_H$ initially decreased and increased again after 10 days. The maximum $E_H$ observed (+655 mV) again indicated that ferrous iron oxidation was again relatively ineffective. The reason for the decrease in $E_H$ at 45ºC was not understood. Concentrations of soluble metals did not show any temperature-related differences, though varying pulp densities did have an effect. Using 5 and 10% pulp density, zinc concentrations did not increase from day 1. The same was the case for copper in all shake flasks, and also for Ni at 5% pulp density. However, at 20% pulp density (and 10%, in some cases) there were continuous increases in metal extraction until the end of the experiment. In most cases, the concentrations of metals in the leachate were generally proportional to the pulp densities; for example, the 5%, 10% and 20% pulp densities tests recovered ~ 2 mM, ~ 4 mM and ~ 8 mM of copper, respectively, during the experiment. Even though cobalt concentrations fluctuated greatly throughout the experiment, similar general trends to those observed with Zn and Cu were also found with this metal, especially towards the end of the experiment.

There were major differences between this and the previous experiments designed to remobilise metals from the accumulated metal sulfides. One was that the material that was (bio)leached had already been subjected to leaching within the bioreactor vessel (section 5.3). Secondly, the actual concentrations of metals in the porous beads/precipitates mixture were determined (by digesting with *aqua regia*) prior to the start of the experiment, rather than inferred. This allowed accurate determinations of total metals solubilised. In the best case scenario (20% pulp density at 30ºC) over 99% Ni, 97% Zn and 85% Co were solubilised.

Initial calculations of the efficiency of metals that were extracted from the accumulated sulfides in the bioreactor were based on the volume of synthetic mine water that had been pumped into the aSRBR, assuming 100% precipitation of Zn, Ni and Co. This, as noted, greatly underestimated the amount of Zn present, due to ZnS being present in the Poraver bead bed originally added to the aSRBR. More accurate measurements were made using mass balance calculations. The volume of the bead bed in the bioreactor was ~ 1.3 L, which corresponded to 266 g dry weight of Poraver beads. Considering firstly zinc: the maximum concentration in the (bio)leaching reactor vessel was 62.4 mM (Table 5.3), which is equivalent to 8.16 g of soluble zinc in the 2 L (working volume) reactor vessel. Ten grams (dry weight) of the residual beads/precipitates contained 70 mg zinc (*aqua regia* digests), so by proportion the total amount of residual zinc precipitates was 1.86 g, making a total of 10.02 g of zinc present in the bioreactor at the start of the (bio)leaching experiments (i.e. far in

excess of the 1.3 g calculated to have been removed from the inflowing synthetic mine water; Table 5.3). Of this, 81% was (bio)leached in the bioreactor, and a further 17.6% in the subsequent shake flask experiment, totalling ~99% dissolution of ZnS (Table 5.8).

**Table 5.8.** Amount of metals precipitated in the bioreactor and percentage of that leached in both bioreactor and second phase (bio)leaching experiments.

| Metal | Amount of metals accumulated (g) | | Percentage of metals (bio)leached (%) | | |
|---|---|---|---|---|---|
| | From AMD treatment | Total (mass balance analysis) | Bioreactor | Second phase (bio)leaching | Total |
| **Ni** | 14.9 | 20.1 | 77 | 21 | 98 |
| **Co** | 3.6 | 3.7 | 61 | 31 | 92 |
| **Zn** | 1.3 | 10.02 | 81 | 18 | 99 |

Calculating similarly for nickel, the maximum concentration in the bioreactor was 131 mM (equivalent to 15.4 g Ni), while 10 g of the residue contained 175 mg of this metal (equivalent to 4.65 g remaining in solid form in the bioreactor, and therefore a total weight of 20.05 g Ni at the start of the experiment). This is higher than the 14.9 g of nickel calculated from its concentration in the feed liquor (Table 5.3) and can be accounted for by dissolution of Ni-Cr components of the bioreactor (as observed elsewhere; D. B. Johnson et al., unpublished data). A total of 98% of the accumulated Ni was re-solubilised (77% in the bioreactor and a further 21% in the shake flasks). In the case of cobalt, the maximum concentration in the bioreactor (19.1 mM) corresponded to 2.25 g Co. The solid residue (10 g) contained 55 mg Co, corresponding to 1.46 g, and a total weight of 3.71 g of this metal present at the start of the experiment. Interestingly, this is very close to the 3.6 g calculated from Co in the feed liquor and is due to the fact that, unlike Zn and Ni, there were no perceived additional extraneous sources of this metal. The amount of cobalt re-solubilised was 92% in total: 61% during (bio)leaching in the bioreactor and a further 31% in the shake flasks.

The actual contribution of microbial activity to the dissolution of the accumulated metal sulfides appears to have been minimal, except for in the first experiment where very positive (> +800 mV) redox potentials were obtained. Tests carried out in the bioreactor experiment and the second shake flask experiment for the presence of viable bacteria all proved negative, apart from plates that were inoculated immediately after the acidophiles had been added. One reason for the very limited mortality of introduced acidophiles could be the

presence of soluble transition metals which accumulated to elevated concentrations during leaching. *Leptospirillum ferriphilum* strain MT61 (which is phylogenetically identical to the strain that was used, MT63) can tolerate up to 500 mM Zn and ~ 80 mM Ni (Galleguillos Perez, 2011; cobalt tolerance data were not recorded), while strains of *Acidithiobacillus ferriphilus*, an iron/sulfur-oxidizing acidophile that is closely related to both *At. ferrooxidans* and *At. ferridurans*, grow in the presence of 400 - 700 mM Zn, 100 - 300 mM Ni and 200 - 400 mM Co (Falagán and Johnson, 2016). In most cases therefore the maximum concentrations of these metals that were leached in the bioreactor (62 mM Zn, 131 mM Ni and 19 mM Co) were below the toxicity thresholds for these metals, though it is possible that combinations of the three may be more toxic to mineral-leaching bacteria then when the metals are present individually. A more likely cause is thought to be $H_2S$ toxicity. Concentrations of hydrogen sulfides, even as low as 1 - 5 mM, are known to be toxic to many microorganisms (O'Flahert and Colleran, 2000). Acidification of the beads/precipitates mixture would have caused a rapid, though short-term, evolution of $H_2S$ which probably killed most or all of the bioleaching bacteria. It is worth noting in this context that the only experiment where iron-oxidizing bacteria appeared to be active was the preliminary experiment where the beads/precipitate were acid-washed well before being inoculated (though the non-inoculated flasks in this experiment also appeared to be microbially-active).

Based on the results from these experiments, a modified approach would seem to be required to remobilise metals from sulfides that accumulate within a sulfidogenic bioreactor. Indirect bioleaching, where the microbial regeneration of ferric iron is carried out in a separate vessel to mineral leaching (Carranza et al., 1993), might prove to be superior to bioleaching *in situ*, and a two-stage system, where abiotic acid leaching is followed by bioleaching would seem to be appropriate. Sequential indirect (bio)leaching has been used to successfully extract copper from a saline calcareous sulfide ore (Pakostová et al., 2015).

This study sought to identify a suitable approach for extracting metals from sulfide precipitates that accumulate within a sulfidogenic bioreactor used for remediating acid mine drainage. Although many of the results were encouraging, further investigations are required to optimise the process, and in particular to facilitate active bioleaching of these sulfides. The end product would be a concentrated lixiviant, from which metals could be recovered using techniques such as solvent extraction/electrowinning (SX/EW) and ion exchange (Prasad et al., 2007, El-Nadi, 2016, Sole et al., 2018).

# Biological Mn (II) oxidation and precipitation of Mn (IV) as part of an integrated bioremediation process for mitigating a moderately acidic metal-rich stream

6

## 6.1 Introduction

Manganese (Mn) is the second most abundant transition metal in the lithosphere, occurring at between 0.002 and 10% (w/w) in terrestrial ecosystems. It is an important component in a wide spectrum of geochemical processes (Gammons and Seward, 1996) and one of the metals frequently present in groundwater and in streams draining coal and metal mines. In biological processes, Mn (II) is an important micronutrient used as cofactors for a large variety of enzymes.

Manganese (II) is thermodynamically the most stable oxidation state of this metal in the absence of oxygen and at low pH (Fig. 6.1), whereas in the presence of oxygen, Mn (III) and Mn (IV), which occur primarily as insoluble Mn oxy-hydroxides, are favoured. Manganese (III) is unstable and disproportionate in aqueous media to Mn (II) + Mn (IV), being stable only when complexed by some organic ligands (Tebo et al., 2004).

Manganese oxides (including oxides, hydroxides and hydroxy-oxides) are highly reactive mineral phases that play an important role in biogeochemical cycles. Manganese (II) and Mn (IV) phases are known to be some of the strongest oxidants found naturally in the environment since the Mn (III)/Mn (II) and Mn (IV)/Mn (II) couples have particularly high redox potentials and they participate in a wide range of redox reactions with organic and inorganic chemical species and compounds (Tebo et al., 2004).

In terrestrial environments, birnessite, lithiophorite and hollandite are the most common Mn oxides (Bohu et al., 2015). These are thought to be primarily of biological origin since abiotic Mn (II) oxidation is slow in most natural environments and only occurs spontaneously in aerated high pH (> 8.0) situations. Manganese-oxidizing microorganisms are ubiquitous and diverse, and included both prokaryotic and eukaryotic species (Tebo et al., 2005). Biological manganese oxidation of Mn (II) to Mn (III/IV) occurs at circum-neutral pH (6.0 - 8.5) and the reaction rate is increased by several orders of magnitude relative to abiotic reactions.

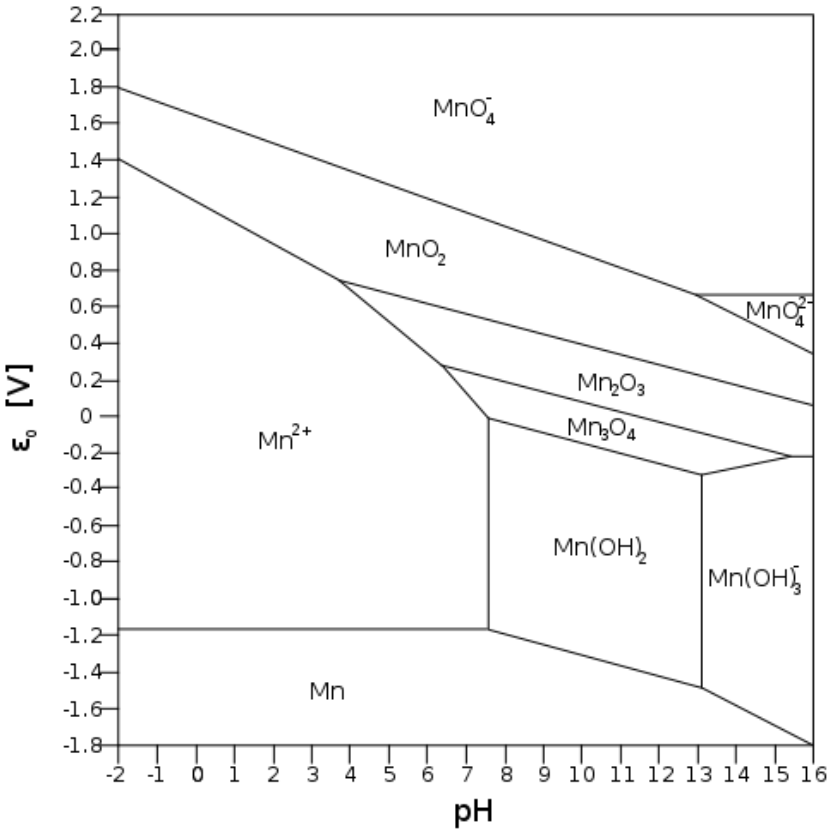


**Fig. 6.1.** Pourbaix diagram for manganese (Tekerlekopoulou et al., 2013).

Two potential mechanisms of Mn (II) oxidation by bacteria have been described (Nealson, 2006). Direct Mn (II) oxidation can be mediated by: (i) Mn-binding components, such as proteins, glycocalyxes and cell wall components, or (ii) Mn-oxidizing enzymes, which are manly linked to multi-copper oxidases (MCO). On the other hand, indirect oxidation of Mn (II) can occur if microorganisms: (i) modify the pH or redox potential of the local environment to allow spontaneous oxidation to occur, or (ii) release a chemical oxidant of Mn, such as reactive oxygen species (ROS), or (iii) produce Mn (II) chelators (Akob et al., 2014; Bohu et al., 2015; Nealson 2006).

Soluble manganese (Mn (II)) can be problematic in surface and ground waters, and in domestic water supplies, and research into ways of removing manganese from metal-contaminated wastewaters has increased in recent years. Even though manganese is not generally considered acutely toxic, it does have some undesirable effects, such as impairment of water distribution networks, tainting of potable water and the staining of laundry.

This chapter describes the construction and operation of a biological Mn (II) oxidation system as part of an integrated system for bioremediating a moderately acidic metal-rich mine water from a copper mine in north Brazil. It also details the indigenous microbial population of natural Mn (IV)-biofilm-colonised pebbles used in the remediation process.

## 6.2 Materials and methods

### *6.2.1 Mn (IV) biofilm-colonised pebbles*

Small pebbles covered with thin black coatings were collected from a catchment stream located in the Snowdonia National Park, North Wales, UK (GPS coordinates: 53° 11' 51.5112" N, 4° 7' 39.7596" W; Fig. 6.2). The irregular spherical-shaped pebbles (diameter ranging from 1.5 to 5.0 cm) were collected in the water stream, which contained 0.03 mM soluble Mn and had a pH of 6.5. The material was kept in plastic bottles at 4ºC until use. A study performed by Mariner et al. (2008) had previously shown that the coatings covering this pebbles contained Mn (IV) by positive reaction with hydrogen peroxide.

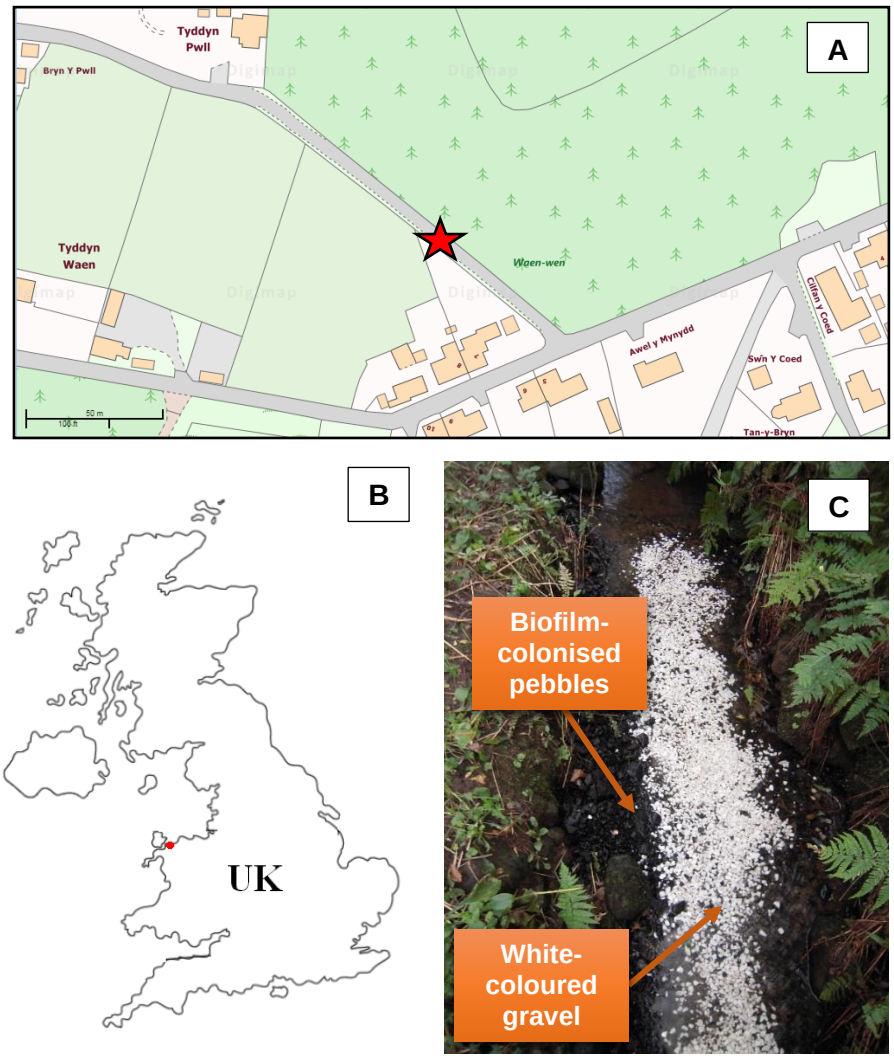


**Fig. 6.2.** Sampling site location at Snowdonia National Park, UK. (A) Location at Waen Wen (Source: Digimap; www.edina.ac.uk/digimap); (B) Location within the UK and (C) Catchment stream. Red stars represent sampling point. Images A and B: Mariner, 2008.

*6.2.2 Manganese oxidation and precipitation: batch tests*

Preliminary tests were performed using the biofilm-colonised pebbles in order to assess their effectiveness in processing the waste material from a biosulfidogenic reactor system designed both to recover copper and remove other transition metals (Ni, Zn and Co) which, as described in Chapter 4, afterwards contained only manganese as a residual transition metal. Two glass reservoirs were set up with an air stone placed at the bottom of both, through which non-sterile atmospheric air was bubbled in order to promote homogeneous aeration of the system. One reservoir was packed with inert gravel, to act as a control, and the other with Mn (IV) biofilm-colonised pebbles. Both reservoirs were filled with 300 mL of aSRBR effluent liquor (referred to now as Mn-rich processed mine water) at pH 5.0. The experiment was carried out at 30ºC. Initial and final pH values were measured, and total soluble manganese was determined in regular intervals using a colorimetric assay (section 2.5.2.3).

*6.2.3 Commissioning and operation of the Mn (II) oxidizing bioreactor (MnOB)*

An upflow fixed bed bioreactor for removing manganese from wastewaters was set up using an environmental sample of Mn (IV)-biofilm-colonised pebbles. Pebbles were packed into a 32.0 by 6.8 cm Perspex column to a depth of 24.5 cm (Fig. 6.3). Non-sterile atmospheric air was bubbled using an air stone placed at the bottom of the reactor in order to promote homogeneous aeration throughout the column. The influent liquor was pumped into the column through an L-shaped Perspex tube and sampling devices were placed in the bioreactor, as shown in Fig. 6.3. The column was filled (to 28 cm depth) with Mn-rich processed mine water. The system was maintained in continuous flow mode by pumping the influent liquor upwards through the column and the effluent being collected into a waste bottle.

6.2.3.1 Variations in operational and set up conditions

Four different experimental phases were tested in order to determine conditions for optimum removal of manganese. Phases C1, C2 and C3 were based on a 1-column system (Fig. 6.3 - A) in which variations in feed liquor pH and hydraulic retention time were evaluated, while C4 was based on an in-line 2-column system (Fig. 6.3 - B). Both columns were designed and operated similarly. Table 6.1 shows variations in parameters studied in each phase.

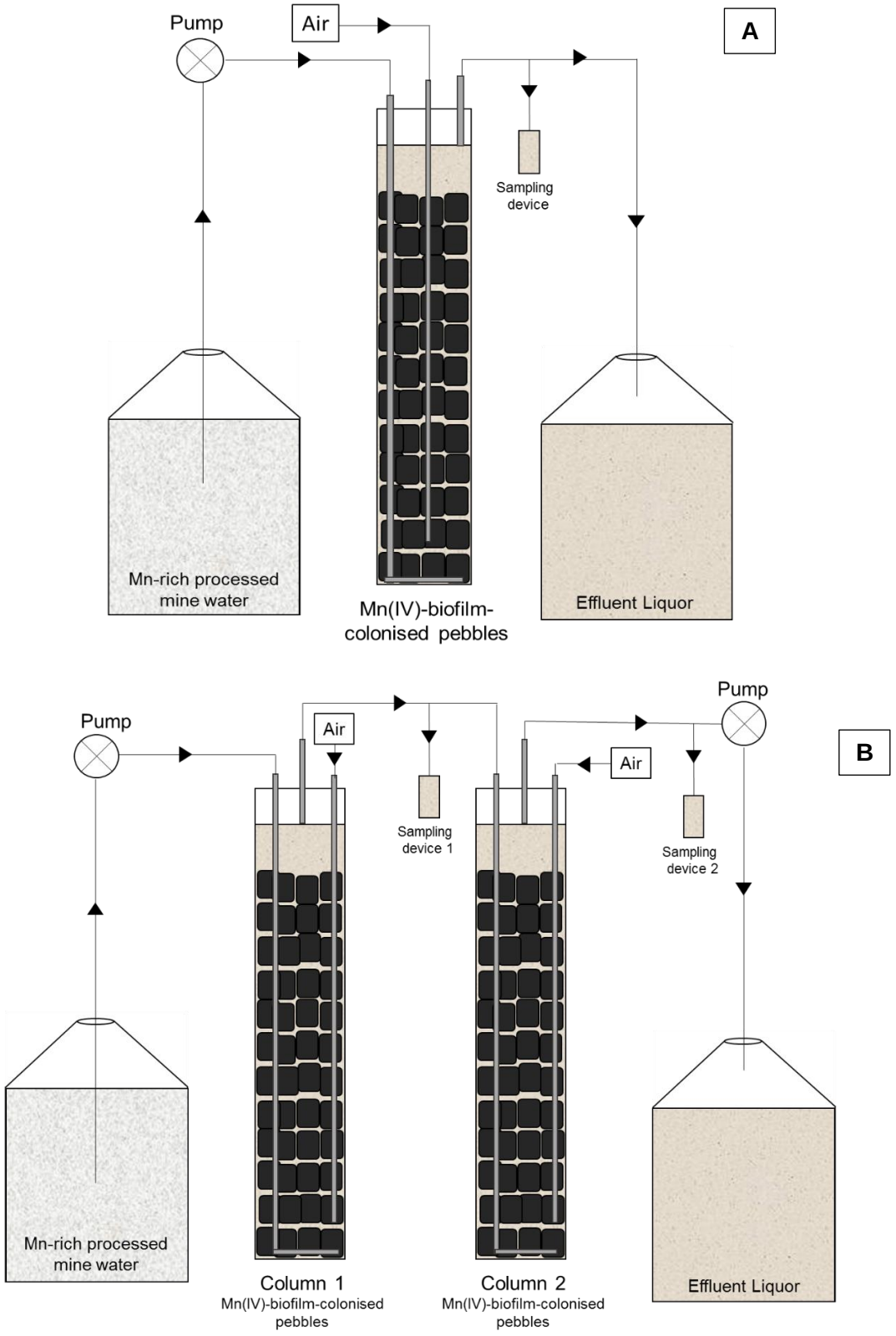


**Fig. 6.3.** Schematic representation of the Mn (II) oxidation bioreactor (MnOB). (A) 1-column system and (B) in-line 2-column system. Effluent liquor from column 1 was pumped upwards through column 2 and collected into an effluent bottle. Sampling devices were added to the top of each column and analysis were carried out on both sampling points.

**Table 6.1.** Variations in feed liquor pH and HRT in the Mn (II) oxidation bioreactor.

| Phases | Feed liquor pH | HRT (h) |
|---|---|---|
| **C1** | 5.0 | 12 |
| **C2** | 6.5 | 12 |
| **C3** | 6.5 | 24 |
| **C4** | 6.5 | 48 |

Flow rates (expressed as HRTs), cell numbers and pH were monitored throughout the experiment as described previously. Total soluble manganese was determined using a colorimetric assay and dissolved organic carbon (DOC) was measured using a Protoc Analyser (Pollution and Process Monitoring UK).

*6.2.4 Microbial populations in the Mn (IV) biofilm-colonised pebbles*

In order to assess the composition of the indigenous microbial populations present on the surface of the black pebbles taken from the stream in Snowdonia, biofilm samples were scraped off using a sterile spatula, DNA extracted, and bacterial and archaeal 16S rRNA genes and eukaryote 18S rRNA genes were amplified (section 2.9). Clone libraries were constructed from these (section 2.9.5) together with T-RFLP analysis (section 2.9.4). Theoretical T-RFs of the clones were obtained by measuring the length of the bacterial 16S or eukaryote 18S rRNA genes fragment cleaved by the restriction enzyme HaeIII.

Later, white-coloured gravel samples (diameter ranging from 0.5 to 3.0 cm) were placed in the stream and collected in regular intervals (week 0, week 2 and week 5). Biofilm samples were scraped off from these, DNA extracted, and 16S and 18S rRNA genes amplified and analysed (by T-RFLP) as described previously.

*6.2.5 Isolation and cultivation of Mn (II)-oxidizing microorganisms*

Biofilm samples were placed aseptically, using a sterile wire loop, into liquid and onto solid medium containing ABS/TE (section 2.2.2.1), amended with 0.5 mM $MnSO_4$ and 0.1 g $L^{-1}$ yeast extract. The final pH of the medium was 6.5 and, in the case of the solid medium, sterile agarose solution was added to a final concentration of 0.5% (w/v). Liquid and solid media cultures were incubated at 30ºC. Stock cultures of the isolates were maintained by serial transfer onto solid media.

*6.2.6 Identification and characterisation of a Mn (II)-oxidizing fungal isolate*

One Mn (II)-oxidizing fungus (coded MnI1) was isolated from an ABS/TE plate amended with 0.5 mM $MnSO_4$, and a single colony sub-cultured onto solid media at regular intervals. Tests were performed in order to assess its pH and temperature optima, growth on different substrates, and rates of Mn (II) oxidation. The 18S rRNA gene of the isolate was amplified, sequenced and compared with those in the GenBank database (section 2.9). Phylogenetic tree construction was carried out as described in section 2.9.6.

6.2.6.1 Effects of pH and temperature on the growth of isolate MnI1

Isolate MnI1 was cultured in 100 mL shake flasks on an orbital shaker at 50 rpm. To determine pH limits for growth, the temperature of incubation was maintained at 30ºC and initial pH was set at values between 4.0 and 8.0. Portions of fungal hyphae were transferred from the plate using a sterile wire loop into flasks and macroscopic growths were monitored for a period of 10 days. To determine the temperature limits for growth, the initial pH of the culture was set at 6.5 and temperatures ranged from 15 to 45ºC. Growth was semi-quantitatively measured by visual inspection of the cultures.

6.2.6.2 Mn (II) oxidation tests

The ability of isolate MnI1 to oxidize Mn (II) to Mn (IV) was tested by inoculating liquid media, amended with 0.1 g $L^{-1}$ yeast extract, containing 0.5 mM $MnSO_4$. Parallel non-inoculated controls were also set up. This experiment was carried out in duplicate. Oxidation of manganese was assessed in regular intervals by monitoring changes in culture pH and measuring changes in concentrations of soluble Mn (section 2.5.2.3).

6.2.6.3 Growth on different organic substrates

Tests for growth of isolate MnI1 on different organic substrates was carried out by sub-culturing the fungus in pH 6.5 ABS/TE liquid media containing 0.5 mM $MnSO_4$, amended with various organic compounds (Table 6.9). Different concentrations of substrates were used to approximately equalize their carbon-equivalents (5 mM for $C_6$ substrates, 10 mM for $C_3$ substrates, etc.).

Replicate universal bottle cultures containing 5 mL of test medium were inoculated, and incubated in an orbital shaker at 30ºC. Growth was determined by observing macroscopic

growth after 10 days and comparing with those obtained in both negative controls (no organic substrate added) and positive controls containing 0.1 g $L^{-1}$ of yeast extract.

## 6.3 Results

A sulfidogenic bioreactor system was initially used for remediating a moderately acidic mine water containing copper, which was effectively removed (as CuS) from the synthetic mine water in an off-line vessel using $H_2S$ generated by the aSRBR, and other transition metals (removed as NiS, ZnS, CoS), which were precipitated within the bioreactor vessel. Manganese, as expected, remained in solution throughout the process since it does not form a sulfide or oxy-hydroxide phase under the conditions tested. Elsewhere the removal of this metal using bioreactor systems with ferromanganese nodules has been described (Hallberg and Johnson, 2005) and by using colonised pebbles from water streams (Mariner et al., 2008).

### *6.3.1 Assessing the removal of soluble manganese using Mn (IV) biofilm-colonised pebbles*

The effluent liquor generated by the biosulfidogenic remediation process, described in Chapter 4, was used in batch tests in order to assess the removal of soluble manganese by the biofilm-colonised pebbles. Figure 6.4 shows changes in soluble manganese concentrations in the Mn-rich processed mine water over a period of 4 hours.

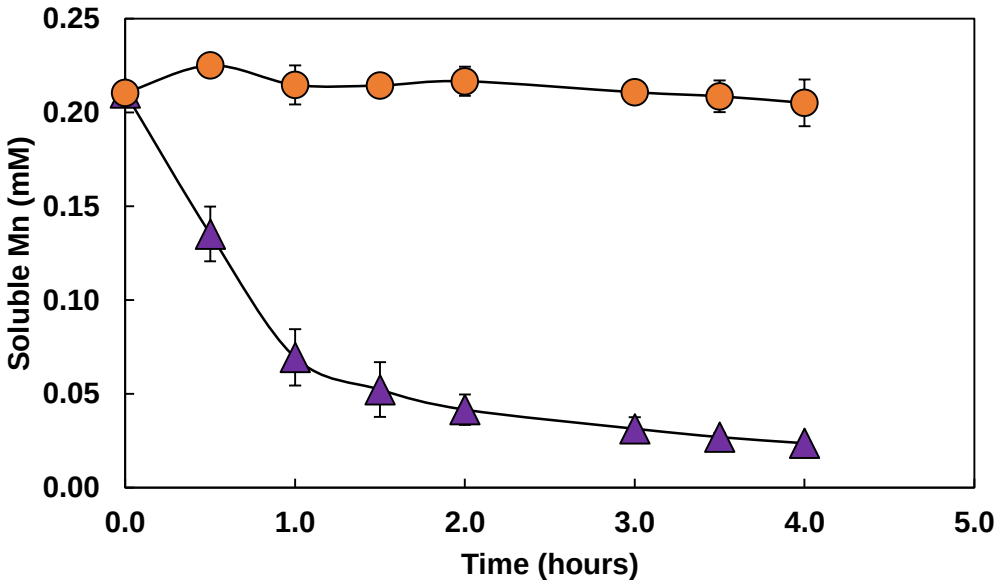


**Fig. 6.4.** Changes in soluble manganese concentrations in systems containing inert pebbles (●) and Mn (IV)-biofilm-colonised pebbles (▲). The symbols are mean values and the error bars represents standard deviation (*n* = 3).

Concentrations of soluble manganese remained fairly constant throughout the experiment when inert gravel was used. In contrast, the biofilm-colonised pebbles showed a rapid and sharp decrease in soluble manganese concentrations (Fig. 6.4). About 90% of Mn (II) was removed from the Mn-rich processed mine water within a period of 4 h. Corresponding changes in pH values are shown in Fig. 6.5. Initially, the pH of the Mn-rich processed mine water was 5.0 (pH value set for the aSRBR) and this increased to pH 5.5 with the inert gravel system, but was much higher (pH 6.8) with the biofilm-colonised pebbles.

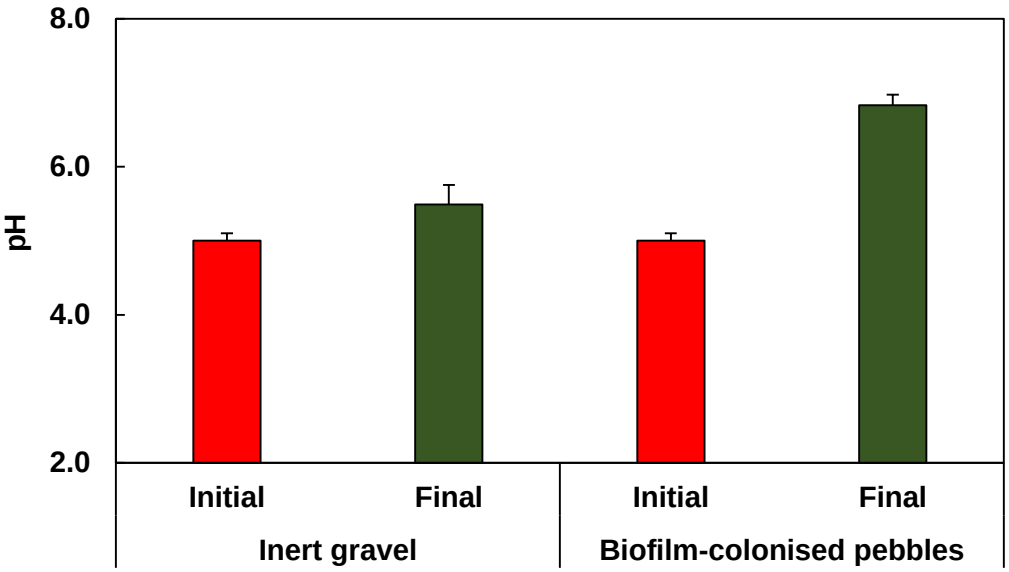


**Fig 6.5.** Average initial and final pH measured in the inert gravel and Mn (IV) biofilm-colonised pebbles systems.

*6.3.2 Commissioning and performance of the Mn (II) oxidation bioreactor (MnOB)*

Following the initial batch experiments, which showed that soluble Mn could be effectively removed by the Mn (IV) biofilm-colonised pebbles, a fixed bed bioreactor was designed and commissioned using these and additional colonised pebbles. The MnOB was operated in continuous flow in a working volume of 1.04 L for a period of 270 days at 30°C and the influent liquor used to circulate through the column contained 0.15 mM Mn (II). Changes in operational parameters, such as feed liquor pH and HRTs were tested in order to maximize removal of manganese. Images of the MnOB during its operation are shown in Fig. 6.6.

Removal of manganese from the Mn-rich processed mine water are shown in Fig. 6.7. In the first phase (C1), no pH adjustment was needed since the final pH of the effluent from the sulfidogenic bioreactor was 5.0. Within the first 30 days of operation, the percentage of

manganese removed decreased gradually from 80% to 10%, followed by a slight increase ranging between 20% and 55%. In order to enrich the indigenous Mn (II)-oxidizing microbial population on the pebbles and consequently increase manganese removal, a new column was set up using fresh biofilm-colonised pebbles and the pH of the feed liquor was adjusted to 6.5 with NaOH (the pH of the stream from which the pebbles were collected). For this phase (C2), a thin layer of pink-coloured inert gravel (average diameter: 1.0 cm) was added to the column between two layers of colonised pebbles in the MnOB (Fig. 6.6 - B) in order to obtain a visual impression of whether, and how fast, the inert gravel would become colonised by Mn-oxidizing biofilms and acquire the characteristic brown/black colouration of the already colonised pebbles.

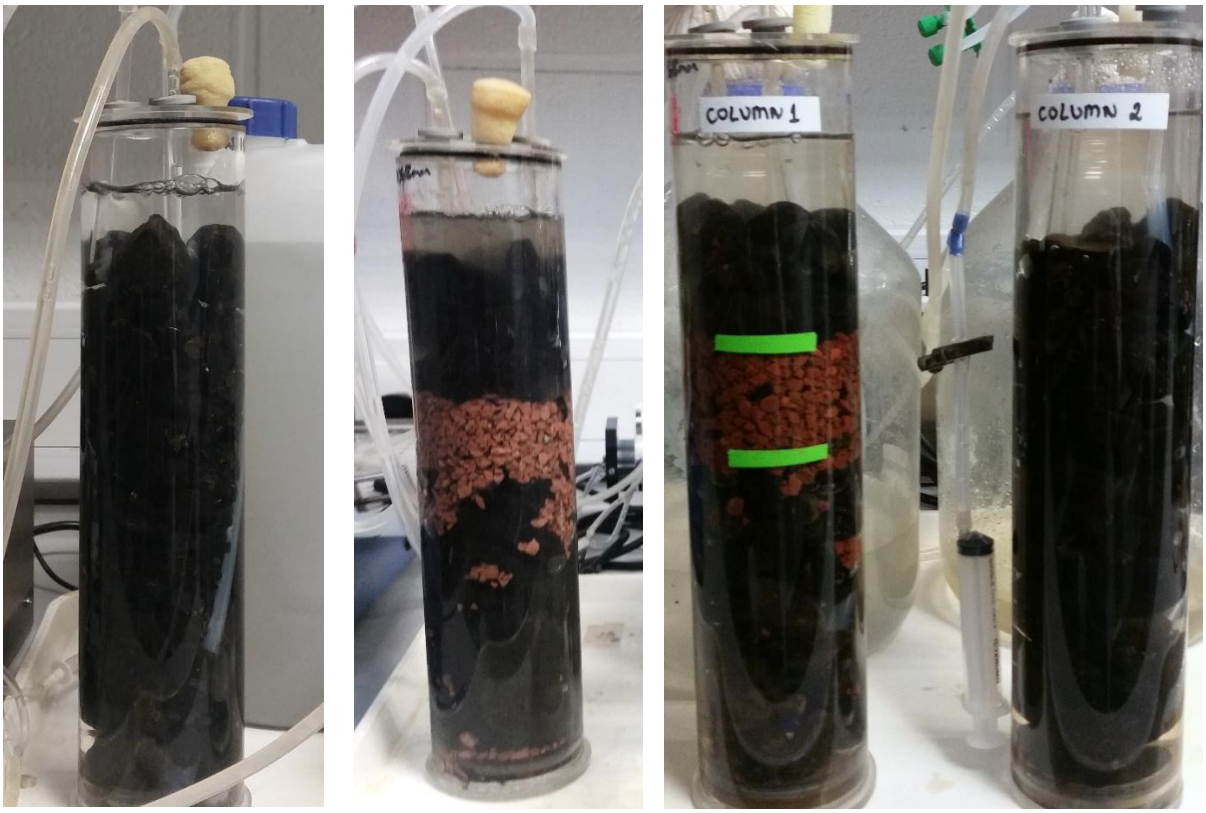


(a) (b) (c)

**Fig. 6.6.** Fixed bed bioreactor, packed with Mn (IV) biofilm-colonised pebbles. (a) 1-column system (C1: pH 5.0 and HRT 12h), (b) 1-column system (C2: pH 6.5 and HRT 12h and C3: pH 6.5 and HRT 24h), where a thin layer of inert gravel was added to the bioreactor to monitor manganese precipitation, and (c) 2-column system (C4: pH 6.5 and HRT 48h).

The trends observed for manganese removal in phase C2 were similar to those found in C1, and only ~ 35% soluble manganese was removed from the Mn-rich processed mine water. By increasing the pH of the feed liquor to pH 6.5 and doubling the HRT (from 12 h in

C2 to 24 h in C3) an increase in percentage of manganese removed was observed (Fig. 6.7), removing 30 - 60% of manganese from the Mn-rich processed mine water. However, regulation Nº 430/2011 set by the National Environmental Council (CONAMA, Brazil) has delineated a maximum contaminant level for industrial effluent discharge for manganese of 1.0 mg $L^{-1}$ which means that, for this particular case, at least 90% of the manganese present in the Mn-rich mine water would need to be removed prior to discharge. To attempt to overcome this problem, a second column was connected in-line to the system with the same specifications and operational parameters as the first one (Fig. 6.6 - C). The effluent liquor of the first column was then pumped into a second column where the remaining manganese was successfully removed (Fig. 6.7). Using this approach, over 90% of manganese was removed from the Mn-rich processed mine water.

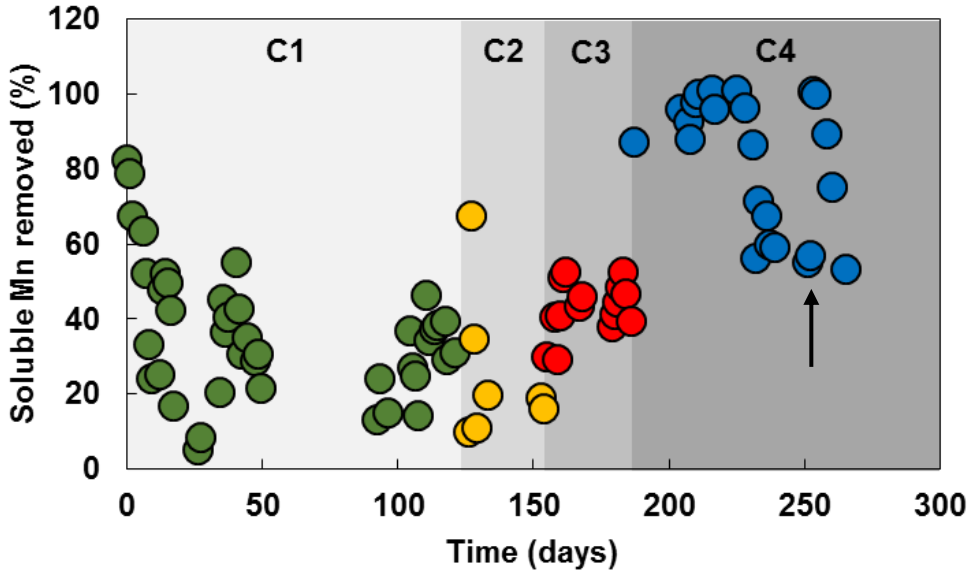


**Fig. 6.7.** Variations in the percentage of manganese removed during the time course of the experiment. Key: phase C1 (green): 1 column-system pH 5.0, HRT 12h; C2 (yellow): 1 column-system pH 6.5, HRT 12h; C3 (red) 1 column-system pH 6.5, HRT 24h and C4 (blue): 2 column-system pH 6.5, HRT 48h. The arrow indicates where yeast extract (final concentration 0.1 g $L^{-1}$) was added to both columns.

During most of the time course of the experiment, Mn-rich processed mine water was only amended with regard to its pH; electron donors and/or carbon sources for the microorganisms within the columns came exclusively of what remained from the sulfidogenic bioreactor (mostly small amounts of glycerol, acetate and possibly yeast extract). In Fig. 6.7, it can be seen that after 45 days of phase C4 (day 231) a gradual decrease in manganese removal occurred, falling to ~ 50%. At day 254, yeast extract was added to both columns from

a 5.0 g $L^{-1}$ concentrated solution to a final concentration of 0.1 g $L^{-1}$, and this was followed by an immediate response in terms of increased manganese removal (to over 99%).

The pH of the feed and effluent liquors was monitored throughout the experiment in each phase tested (Fig. 6.8). The feed liquor pH varied between 4.5 and 5.5 in phase C1 and between 6.0 and 7.0 in phases C2 - C4. The reason for this fluctuation could be related to the presence of active microorganisms from the sulfidogenic bioreactor (aSRBR) in the feed liquor, which was not sterilised prior to use in the MnOB. The pH values of effluent liquors from the MnOB ranged between 4.0 and 5.5 throughout the entire experiment. Lower pH in the effluent liquor was expected as Mn (II) oxidation and hydrolysis reactions are proton-generating reaction at circum-neutral pH (Eq. 6.1 - Eq. 6.3).

$$Mn\ (II) \rightarrow Mn\ (III) + e^- \qquad \text{(Eq. 6.1)}$$

$$Mn\ (III) + 2\ H_2O \rightarrow MnO(OH) + 3\ H^+ \qquad \text{(Eq. 6.2)}$$

$$MnO(OH) \rightarrow MnO_2 + H^+ + e- \qquad \text{(Eq. 6.3)}$$

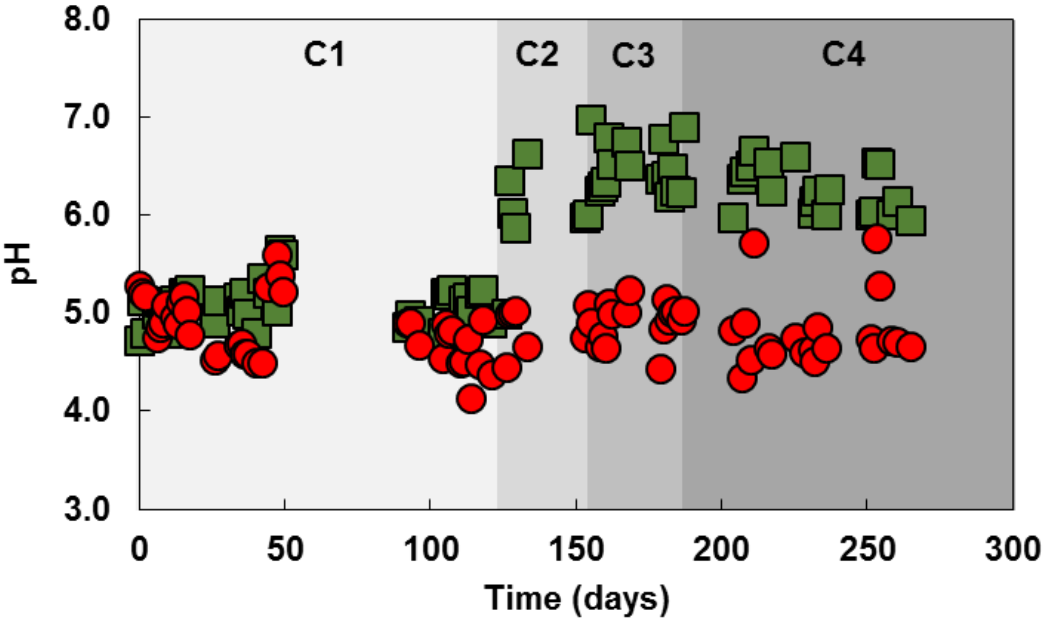


**Fig. 6.8.** Changes in pH in the feed liquor (■) and effluent liquor (●) of the MnOB. Phases C1-C3: 1-column-system; phase C4: in-line 2-column-system. The pH values of the effluent in phase C4 are those of liquors draining the second in-line column 2.

Flow rates and HRTs remained fairly constant during the various phases of this experiment (Table 6.2).

**Table 6.2.** Average flow rates and HRTs (and standard deviation) of the MnOB in each phase of tests carried out with the column bioreactors.

| Phases | Flow rate (mL $h^{-1}$) | HRT(h) |
|---|---|---|
| **C1** | 92.0 ± 9.7 | 11.3 ± 1.1 |
| **C2** | 92.0 ± 8.0 | 11.3 ± 1.3 |
| **C3** | 44.0 ± 2.0 | 23.6 ± 1.6 |
| **C4** | 23.0 ± 3.0 | 45.2 ± 3.5 |

Planktonic cell numbers in the feed and effluent liquor of the MnOB were monitored throughout the experiment (Fig. 6.9). Large numbers of cells were found in the feed liquors used, as anticipated from previous work (Chapter 4) since these were the effluent solutions generated by the sulfidogenic bioreactor. Numbers of planktonic cells in the waters draining the MnOB were, however, significantly lower than those entering the columns on some occasions (e.g. phases C1, C3 and C4-1; Fig. 6.9) though no great difference in cell numbers was observed in phases C2 and C4-2. Only prokaryotic cells were observed in planktonic phase of the MnOB.

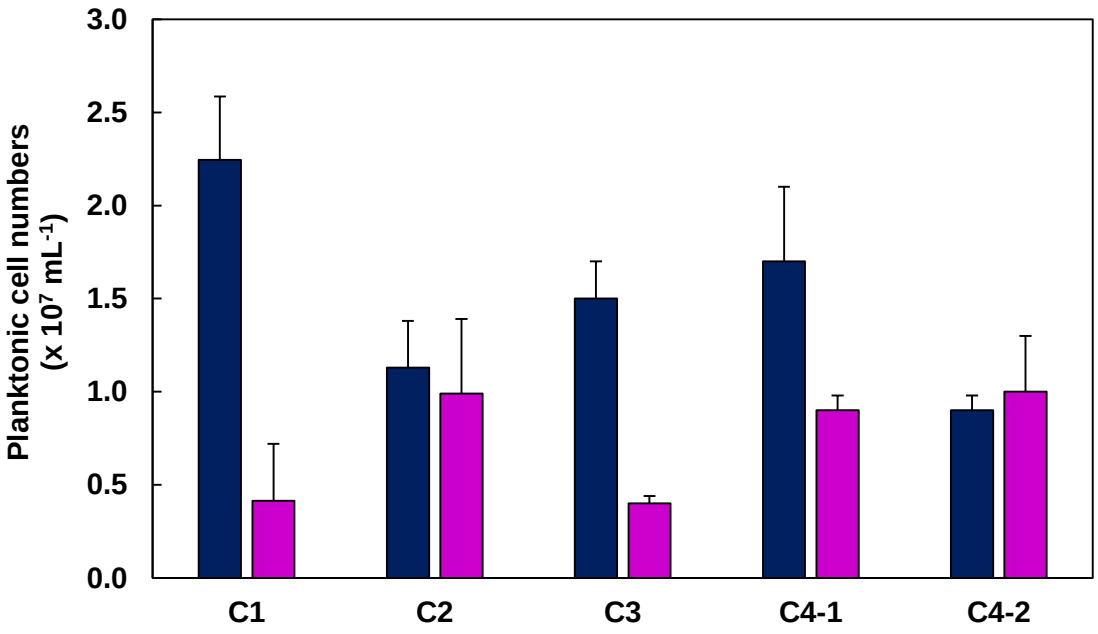


**Fig. 6.9.** Cell numbers in the feed liquor (blue) and effluent liquor (magenta) of the MnOB. Phases C1-C3: 1-column-system; C4-1 represents column 1 and C4-2 represents column 2 of the in-line 2-column-system. The bars depict mean values and the error bars standard deviations (*n* = 20).

In phase C4, two columns were used as an in-line system in order to improve manganese removal from the Mn-rich processed mine water. Interim (C4-1) and final (C4-2) concentrations of manganese in the effluent liquor were monitored, and results are shown in Fig. 6.10. During the first 45 days of phase C4, ~ 65% Mn was removed in the first stage of the process (C4-1), followed by ~28% in the second stage, totalling ~93% manganese removal (average values) using the 2-column system.

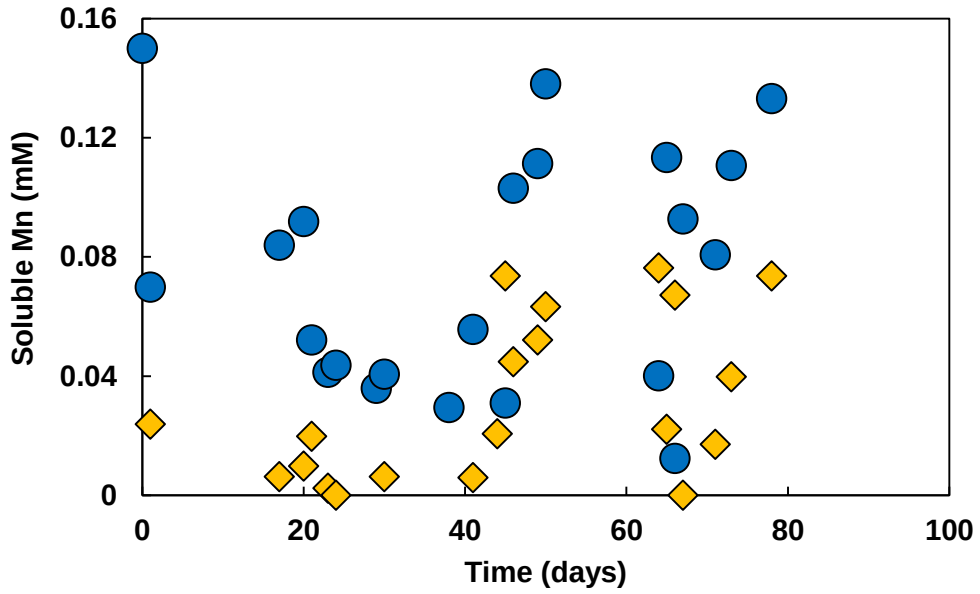


**Fig. 6.10.** Concentrations of manganese in effluent liquors from the two connected MnOB columns used in phase C4 of the experiment. Key: (●) water draining column 1; (♦) water draining column 2.

Concentrations of dissolved organic carbon (DOC) in influent and effluent liquors from the sulfidogenic bioreactor (aSRBR) and the effluent liquors from the MnOB were measured at the end of phase C3 of the experiment. Results are shown in Table 6.3.

**Table 6.3.** Concentrations of dissolved organic carbon (DOC; mg $L^{-1}$) in influent and effluent liquors from the sulfidogenic bioreactor (aSRBR) and the effluent liquors from the MnOB, as mean values and standard deviations ($n$ = 5)

| | aSRBR | MnOB |
|---|---|---|
| **Influent** | 233.5 ± 0.7 | 9.2 ± 0.5 |
| **Effluent** | 9.2 ± 0.5 | 2.4 ± 0.4 |

The data show that most (96%) of the DOC in the amended copper-free mine water (that added to the liquor as glycerol and yeast extract) was consumed in the anaerobic aSRBR and

that 74% of that remaining was metabolized in the aerobic MnOB, producing a final effluent liquor that contained < 3.0 mg $L^{-1}$ of DOC. For comparison, natural contents of DOC in rivers mainly dependent on environmental conditions and can vary from 1.0 mg $L^{-1}$ (e.g. mountainous Alpine environments) to 20 mg $L^{-1}$ (e.g. taiga rivers), and a world DOC average for rivers was established as 5.75 mg $L^{-1}$ (Meybeck, 1982). The values obtained in this current experiment were therefore below the world DOC average.

*6.3.3 Indigenous microbial population of the Mn (IV) biofilm-colonised pebbles*

The indigenous microbial community profile of the biofilm-colonised pebbles collected from the stream in Snowdonia was inferred from clone libraries which were constructed from sequence analysis of bacterial and archaeal 16S and eukaryote 18S rRNA genes. Figure 6.11 shows the relative abundance of microbial taxonomy (order level) of the clones obtained from the biofilm-colonised pebbles.

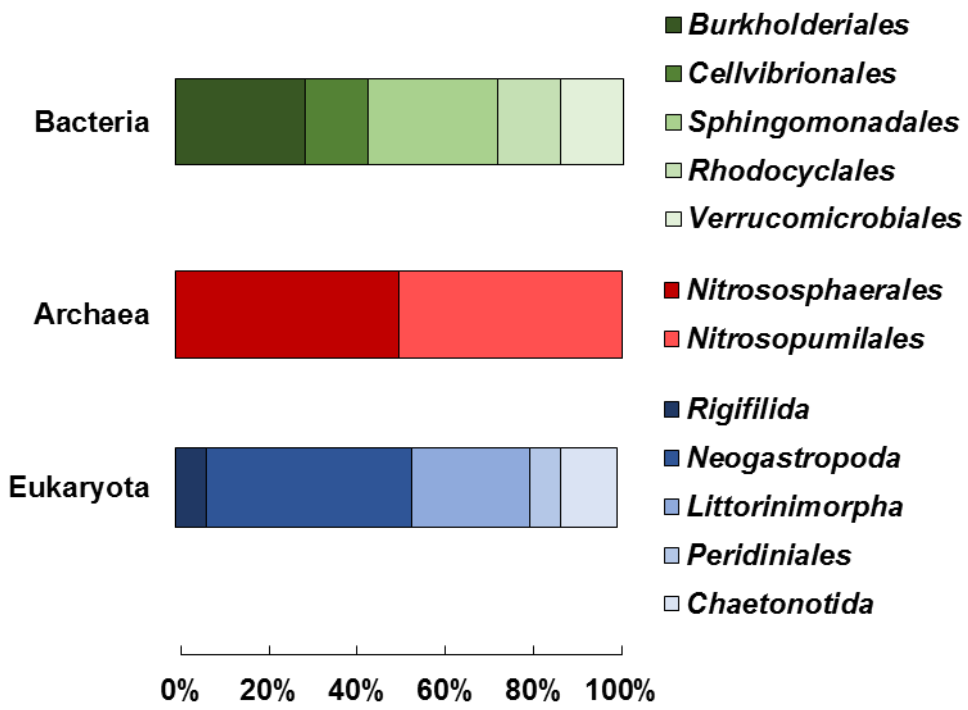


**Fig. 6.11.** Relative abundance of microbial taxonomy (order) of the clones obtained from the Mn (IV) biofilm-colonised pebbles collected from a stream in Snowdonia, UK, based on archaeal and bacterial 16S and eukaryote 18S rRNA genes.

Within the domain Bacteria, 16S rRNA genes sequences were dominated by *Burkholderiales* and most of these were related to *Leptothrix discophora* (96% identity), a well-characterised Mn (II)-oxidizer. Archaeal 16S rRNA genes sequences were affiliated with ammonia-oxidizers belonging to phylum *Thaumarchaeota*, dominated by the orders

*Nitrososphaerales* and *Nitrosopumilales*. Three of the five taxonomic groups (order level) of eukaryotic 18S rRNA genes sequences belonged to phylum *Mollusca*. No fungi were detected using this technique. Identity of cloned archaeal, bacterial and eukaryotic genes obtained from the biofilm-colonised pebbles collected from the stream in Snowdonia are presented in Table 6.4, Table 6.5 and Table 6.6, respectively. Uncultured clones found in the database were included in cases where clones were distantly related to other known species (identity < 96%).

**Table 6.4.** Identity of cloned archaeal genes (16S rRNA gene) obtained from the biofilm-colonised pebbles collected from the stream in Snowdonia (*n* = 32).

| Clone designation | Closest Relative | % identity (16S rRNA gene) | Reference |
|---|---|---|---|
| **MNPARCH1** (*n* = 2) | *Candidatus Nitrocosmicus oleophilus strain MY3* (CP012850.1) | 96 | Unpublished |
| **MNPARCH3** (*n* = 6) | Anaerobic methanogenic archaeon ET1-8 (AJ244284.1) | 94 | Chin et al., 1999 |
| **MNPARCH5** (*n* = 8) | *Nitrososphaera viennensis* strain EN76 (CP007536.1) | 93 | Stieglmeier et al., 2014 |
| | Uncultured archaeon clone Elev_16S_arch_651 16S ribosomal RNA gene (EF022795.1) | 98 | Lesaulnier et al., 2008 |
| **MNPARCH8** (*n* = 3) | *Candidatus Nitrosocosmicus exaquare* strain G61 (CP017922.1) | 98 | Sauder et al., 2017 |
| **MNPARCH13** (*n* = 7) | *Candidatus Nitrosopumilus adriaticus* strain NF5 (CP011070.1) | 95 | Bayer et al., 2016 |
| | Uncultured thaumarchaeote clone LM_8Mar11_CL_41 16S ribosomal RNA gene (KP866399.1) | 98 | Coci et al., 2015 |
| **MNPARCH17** (*n* = 1) | Anaerobic methanogenic archaeon ET1-10 (AJ244286.1) | 90 | Chin et al., 1999 |
| | Uncultured archaeon clone LCDARCH18 16S ribosomal RNA gene (EU247270.1) | 93 | Rastogi et al., 2009 |
| **MNPARCH32** (*n* = 5) | *Candidatus Nitrosoarchaeum koreensis* MY1 (HQ331116.1) | 96 | Jung et al., 2011 |
| | Uncultured archaeon 16S rRNA gene, clone N4-F10 (FN691645.1) | 98 | Auguet et al., 2011 |

Most of the bacterial clones (Table 6.5) belong to the phylum *Proteobacteria* except the clone MNPBAC19 which appears to belong to the phylum *Verrucomicrobia*, though the sequence identity match to its nearest known cultivated relative is very low (83%). The uncultured bacterial clone which closest matched clone MNPBAC19 (96% identity) was obtained from a hyporheic zone of a stream bed in California which contained iron (hydr)oxide precipitates (Duckworth et al., 2009). Another clone, MNPBAC16, showed high level of sequence similarity to *Leptothrix discophora* strain SP-6, a known Mn (II)-oxidizer.

**Table 6.5.** Identity of cloned bacterial genes (16S rRNA gene) obtained from the biofilm-colonised pebbles collected from the stream in Snowdonia (*n* = 40).

| Clone designation | Closest Relative | % identity (16S rRNA gene) | Theoretical T-RF (HaeIII) | Reference |
|---|---|---|---|---|
| **MNPBAC4** (*n* = 6) | *Burkholderia* sp. strain WSM4678 (MF949049.1) | 91 | 221/321/406 | Unpublished |
| | Uncultured bacterium clone FCPN480 16S ribosomal RNA gene (EF515927.1) | 99 | 221/321/406 | Cruz-Martınez et al., 2009 |
| **MNPBAC6** (*n* = 1) | *Dasania* sp. strain OUC005 (KY416514.1) | 91 | 39 | Unpublished |
| | Uncultured gamma proteobacterium clone MP-R100 16S ribosomal RNA gene (JN038769.1) | 96 | 39/401 | Unpublished |
| **MNPBAC9** (*n* = 8) | *Sphingopyxis rigui* strain HME8676 (KC157048.1) | 97 | 293/379 | Unpublished |
| **MNPBAC13** (*n* = 5) | *Novosphingobium tardaugens* strain ARI-1 (NR_028630.1) | 95 | 253/319/404 | Fujii et al., 2002 |
| **MNPBAC14** (*n* = 4) | *Rhodocyclus* sp. HOD 5 (AY691423.1) | 92 | 224/324/409 | Smith et al., 2005 |
| **MNPBAC16** (*n* = 11) | *Leptothrix discophora* strain SP-6 (L33974.1) | 96 | 223/231/406 | Siering and Ghiorse, 1996 |
| **MNPBAC19** (*n* = 5) | *Brevifollis gellanilyticus* strain DC2c-G4 (NR_113149.1) | 83 | 225/251 | Otsuka et al., 2013 |
| | Uncultured bacterium clone 3BH-4B 16S ribosomal RNA gene (EU937926.1) | 96 | 223/250/434 | Duckworth et al., 2009 |

Most of eukaryotic clones showed high level of similarity to known organisms which belong to the phylum *Mollusca*. Clone MnE80 was suggested to belong to *Apicomplexa* (though only 90% sequence similarity) which is a large phylum of parasitic alveolates.

**Table 6.6.** Identity of cloned eukaryotic genes (18S rRNA gene) obtained from the biofilm-colonised pebbles collected from the stream in Snowdonia (*n* = 80).

| Clone designation | Closest Relative | % identity (16S rRNA gene) | Theoretical T-RF (HaeIII) | Reference |
|---|---|---|---|---|
| **MnE1** (*n* = 6) | *Micronuclearia podoventralis* (AY268038.1) | 99 | 496 | Cavalier-Smith et al., 2008 |
| **MnE7** (*n* = 12) | *Gibbula magnus* (AY145375.1) | 98 | 281 | Passamaneck et al., 2004 |
| **MnE9** (*n* = 9) | *Chaetonotus aemilianus* voucher TK132 (JQ798556.1) | 96 | 180/276 | Kanneby et al., 2012 |
| **MnE26** (*n* = 16) | *Serpulorbis imbricatus* isolate LSGB21001 (HQ833992.1) | 98 | 282 | Zou et al., 2011 |
| **MnE27** (*n* = 17) | *Duplicaria dussumieri* isolate LSGB24501 (HQ834049.1) | 97 | 287 | Zou et al., 2011 |
| **MnE30** (*n* = 6) | *Chaetonotus neptuni* (AM231774.1) | 95 | 281 | Todaro et al., 2006 |
| | Uncultured eukaryote gene for 18S rRNA, clone: AD_S13clone24 (LC109078.1) | 95 | 282 | Unpublished |
| **MnE79** (*n* = 13) | *Nassarius festivus* isolate LSGB2340102 (HQ834036.1) | 98 | 281 | Zou et al., 2011 |
| **MnE80** (*n* = 1) | *Apicomplexa* sp. 1 KCW-2013 (KC890798.1) | 90 | 342 | Unpublished |
| | *Heterocapsaceae* environmental sample clone Elev_18S_1214 (EF024723.1) | 92 | 333 | Lesaulnier et al., 2008 |

T-RFLP analysis carried out on biofilm-colonised pebbles taken directly from the stream in Snowdonia (C0) and at the end of phases C1, C2 and C4 of the Mn (II)-oxidizing bioreactor experiment were based on bacterial 16S rRNA genes (Fig. 6.12) and eukaryote 18S rRNA genes (Fig. 6.13). Samples were not taken at the end of phase C3, and T-RFLP analysis was not carried out using amplified archaeal 16S rRNA genes.

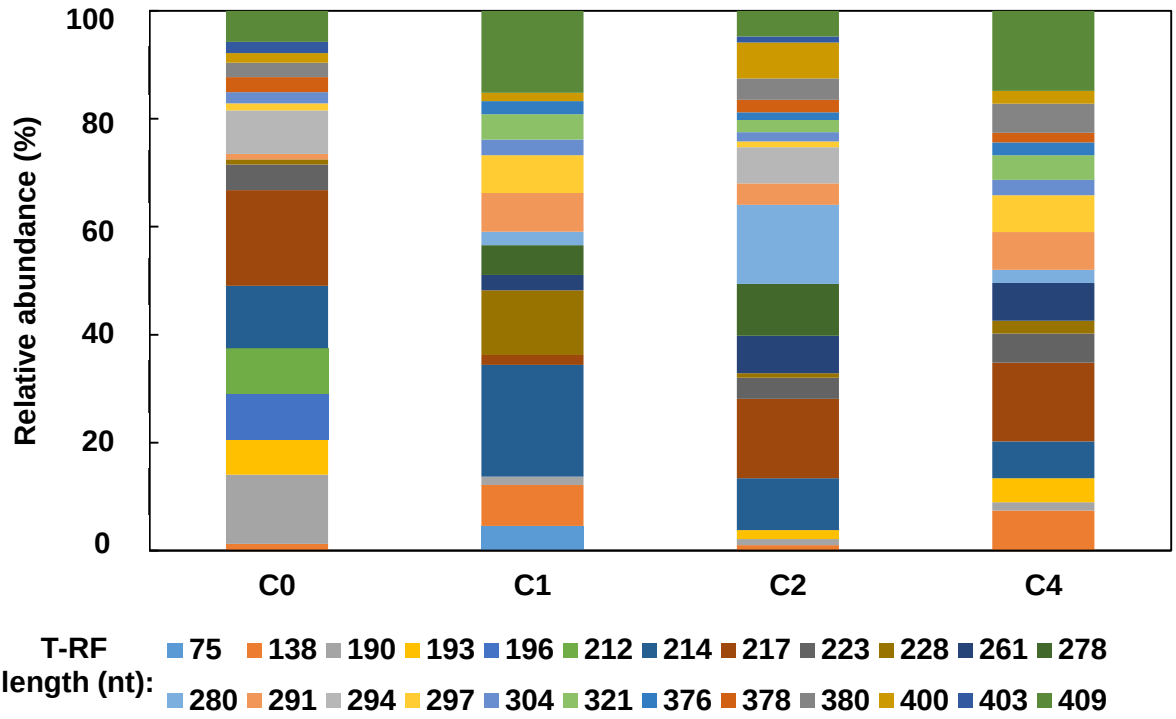


**Fig. 6.12.** Terminal restriction enzyme fragment length polymorphism (T-RFLP) analysis (HaeIII digests) of amplified 16S rRNA bacterial genes from the biofilm-colonised pebbles collected from the stream (C0) and at different phases (C1, C2 and C4) of operating the MnOB. The T-RFs are stacked upwards in each column in increasing fragment lengths.

T-RFLP analysis revealed a large number of T-RF peaks in all samples analysed. Figure 6.12 shows how T-RFLP bacterial profiles on the biofilm-colonised pebbles evolved within the MnOB. Many T-RFs of the same length were found in all samples. The 217 nt T-RF showed high relative abundance in most samples accounting overall for ~ 17% of the total bacterial population in phases C0, C2 and C4. The exception was phase C1, where a 214 nt T-RF was more dominant, accounting for 21% of the summated T-RFs. The 223 nt T-RF matched the theoretical T-RF of the clones which were closely related to *Leptothrix discophora*, overall its relative abundance in the bacterial community of the colonised pebbles was ~ 5%, however more than one organism shared the same T-RF length (Table 6.5), therefore it cannot be assumed that this T-RF corresponded only to the Mn (II)-oxidizing bacterium *L. discophora.* The theoretical T-RF length of the closest relative of clone MNPBAC6 listed in Table 6.5 was not detected in the T-RFLP analysis, possibly due to their low sequence similarity or low relative abundance in the sample. It is noteworthy mentioning that one organism can present more than one cleavage site for the same restriction enzyme, this fact was observed in several clones listed in Table 6.5 and therefore the relative abundance may be misrepresented.

Figure 6.13 shows how T-RFLP profiles of eukaryotes on the biofilm-colonised pebbles evolved within the MnOB. Major changes were observed in the eukaryotic populations in the experiment. The 280 nt T-RF was dominant in all phases of the MnOB, accounting for ~ 72% of the eukaryotic population in phase C4, however this same T-RF was shared with several organisms listed in Table 6.6.

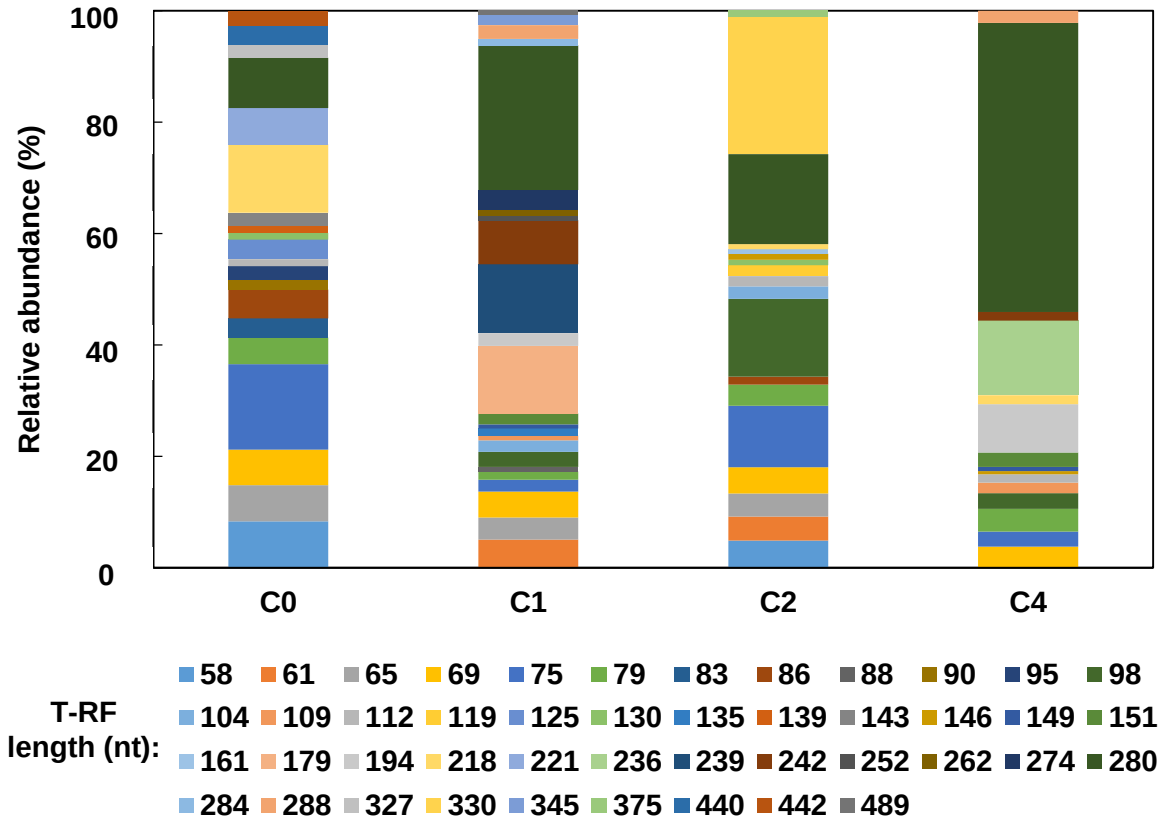


**Fig. 6.13.** Terminal restriction enzyme fragment length polymorphism (T-RFLP) analysis (HaeIII digests) of amplified 18S rRNA eukaryotic genes from the biofilm-colonised pebbles collected from the stream (C0) and at different phases (C1, C2 and C4) of operating the MnOB. The T-RFs are stacked upwards in each column in increasing fragment lengths.

Commercial white-coloured gravel samples were placed into the stream (Fig. 6.2 C) in order to monitor the evolution and relative abundance of the microorganisms with time (after 2 and 5 weeks). Figure 6.14 shows how these had darkened by week 2 and even more significantly by week 5. T-RFLP analysis of amplified bacterial 16S rRNA genes and eukaryote 18S rRNA genes, of DNA extracted from surface coatings of gravel samples, are shown in Fig. 6.15 and Fig. 6.16, respectively. Attempts to amplify bacterial and eukaryote genes from the fresh gravel samples in week 0 were unsuccessful.

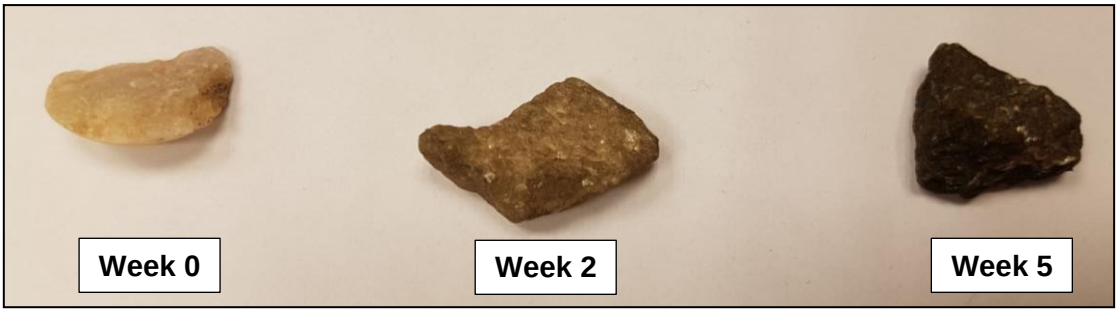


**Fig. 6.14.** Evolution of pigmentation of gravel samples at different times.

T-RFLP analysis based on bacterial 16S rRNA genes of the colonised gravel samples revealed a large number of T-RF peaks at both sampling occasions. The 217 nt T-RF was dominant at week 2, however it became less dominant by week 5. The opposite trend was noted with the 223 nt T-RF which was less dominant at week 2 and the most dominant T-RF peak by week 5, accounting for ~ 18% of the summated T-RFs.

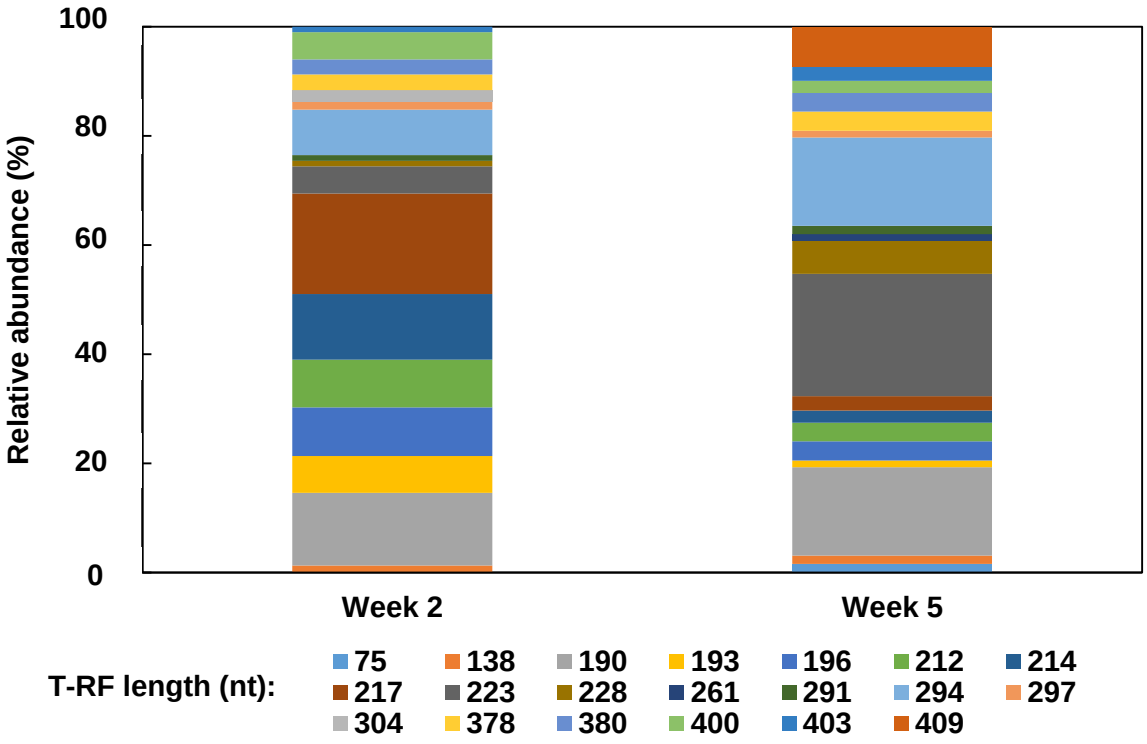


**Fig. 6.15.** Terminal restriction enzyme fragment length polymorphism (T-RFLP) analysis (HaeIII digests) of amplified 16S rRNA bacterial genes from the gravel samples collected in week 2 and week 5. The T-RFs are stacked upwards in each column in increasing fragment lengths.

T-RFLP eukaryote profiles on the gravel samples showed a relatively minor shift in the eukaryotic population between weeks 2 and 5. The 112 nt T-RF was more abundant at week 2, however it shifted to 139 T-RF by week 5. The 75 nt and 90 nt T-RFs became more relatively abundant with time.

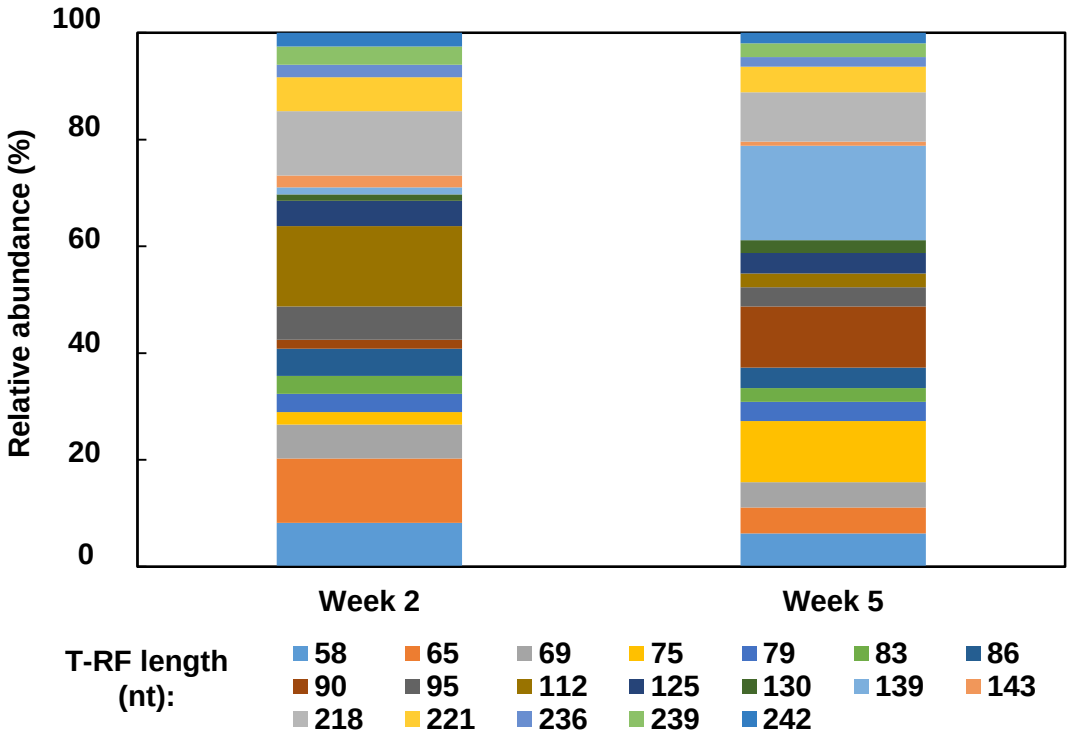


**Fig. 6.16.** Terminal restriction enzyme fragment length polymorphism (T-RFLP) analysis (HaeIII digests) of amplified 18S rRNA eukaryotic genes from the gravel samples collected on week 2 and week 5. The T-RFs are stacked upwards in each column in increasing fragment lengths.

*6.3.4 Characterisation of the Mn (II)-oxidizing fungal isolate MnI1*

6.3.4.1 Physiological and morphological characterisation of isolate MnI1

A brown/black-coloured fungal isolate, coded MnI1, was obtained on solid medium (ABS/TE amended with 0.1 g $L^{-1}$ yeast extract and 0.5 mM $MnSO_4$ at nominal pH 6.5) that had been inoculated with a biofilm from a pebble removed from the MnOB after 160 days of the experiment (during phase C3). The isolate grew on solid medium within a period of 5 days showing the characteristic brown/black colour of the mycelia (Fig. 6.17 A-B). The colonies had rhizoidal morphologies and filiform margins, with vegetative and aerial/reproductive mycelia, characteristic of filamentous fungus. Colonies of isolate MnI1 grown on Mn-free solid medium

had non-pigmented hyphae (Fig. 6.17 C), radiating from and overlying dark coloured colony centres (Fig. 6.17 D). Colonies adhered firmly to the solid medium and presented low emulsification in water. Figure 6.17 E shows MnI1 growing on solid medium in the presence and absence of soluble Mn. Even though the fungal mycelia on Mn-free plates were also dark coloured in the centre of the colonies, the difference between pigmentation of the colonies on Mn-containing and Mn-free plates is clearly noticeable, suggesting that brown/black-coloured insoluble Mn (IV) oxides were deposited onto fungal mycelium on plates containing soluble Mn. Micrographic images of the isolate growing on solid medium in presence and absence of Mn (II) are shown in Fig. 6.18. The isolate formed non-septate hyphae, and putative manganese oxides were found as particulate materials that were associated with the fungal hyphae (Fig. 6.18 A-B). Microscopic examination of the pigmented centres of these colonies did not reveal the presence of particulate materials, as found on Mn (II)-containing plates (Fig. 6.18 C-D).

Results of tests carried out to determine the temperature and pH ranges for growth on MnI1 are presented in Table 6.7 and Table 6.8, respectively. Isolate MnI1 was able to grow between 15 and 30ºC, but appeared (from visual inspection of cultures) to grow optimally at 25ºC. No growth was observed at 45ºC, and growth between 30ºC and 45ºC and below 15ºC were not tested. The isolate developed dark brown/black colour at all temperatures where growth was observed.

**Table 6.7.** Temperature limits for MnI1 growth. Key: (-) no growth observed; (+) some growth observed; (++) extensive growth observed.

| Temperature (ºC) | Growth | Mycelium colour |
|---|---|---|
| **15** | + | Brown/black |
| **25** | ++ | Brown/black |
| **30** | + | Brown/black |
| **45** | - | |

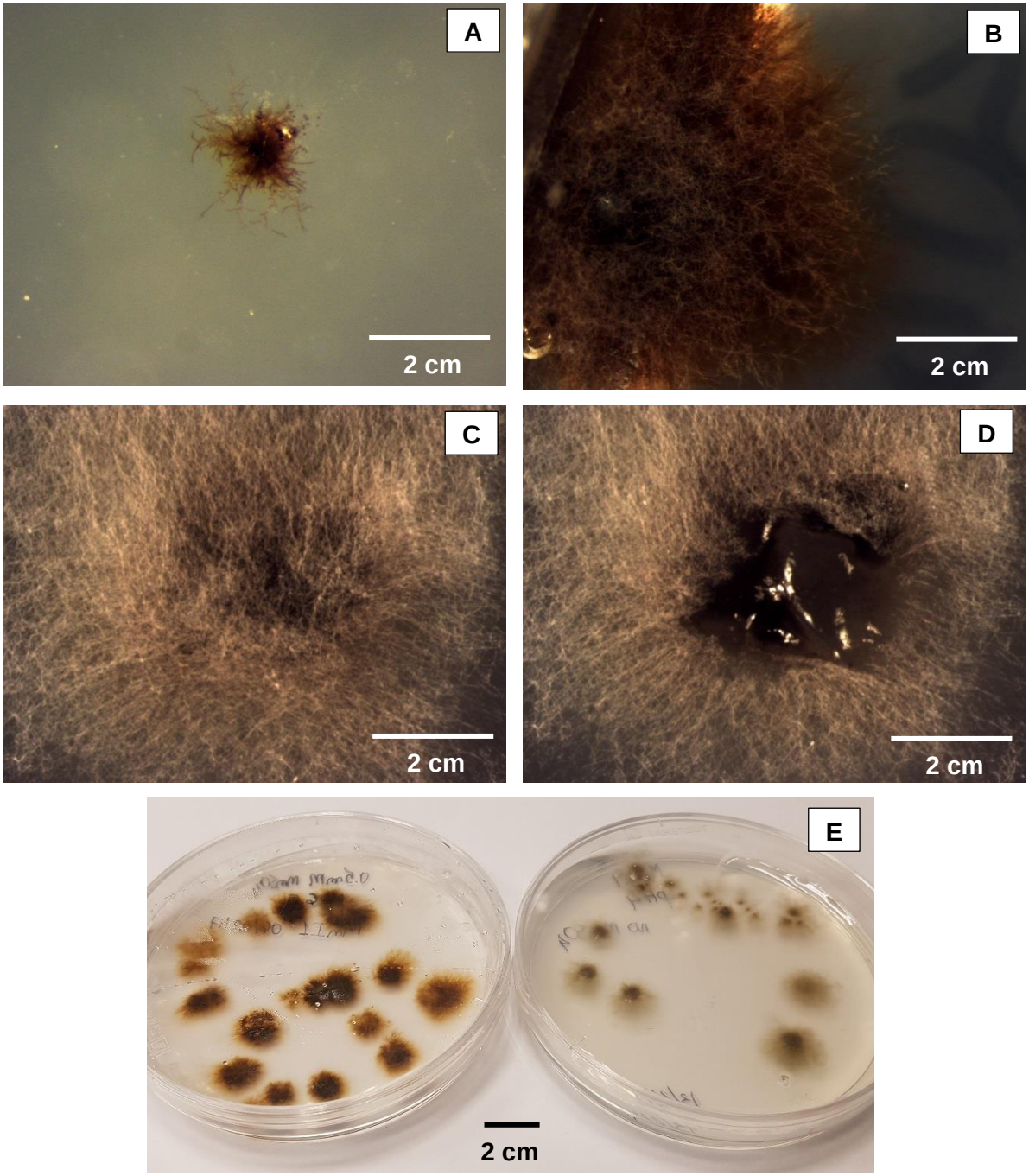


**Fig. 6.17.** Images of isolate MnI1 grown on solid media. (A and B) rhizoidal colonies on Mn-containing plates with dark brown-coloured hyphae; (C and D) colonies grown on Mn-free solid medium with dark-coloured centres and non-pigmented hyphae; (E) colonies growing on solid media at nominal pH 6.5 containing 0.5 mM Mn (II) (left) and no added Mn (II) (right).

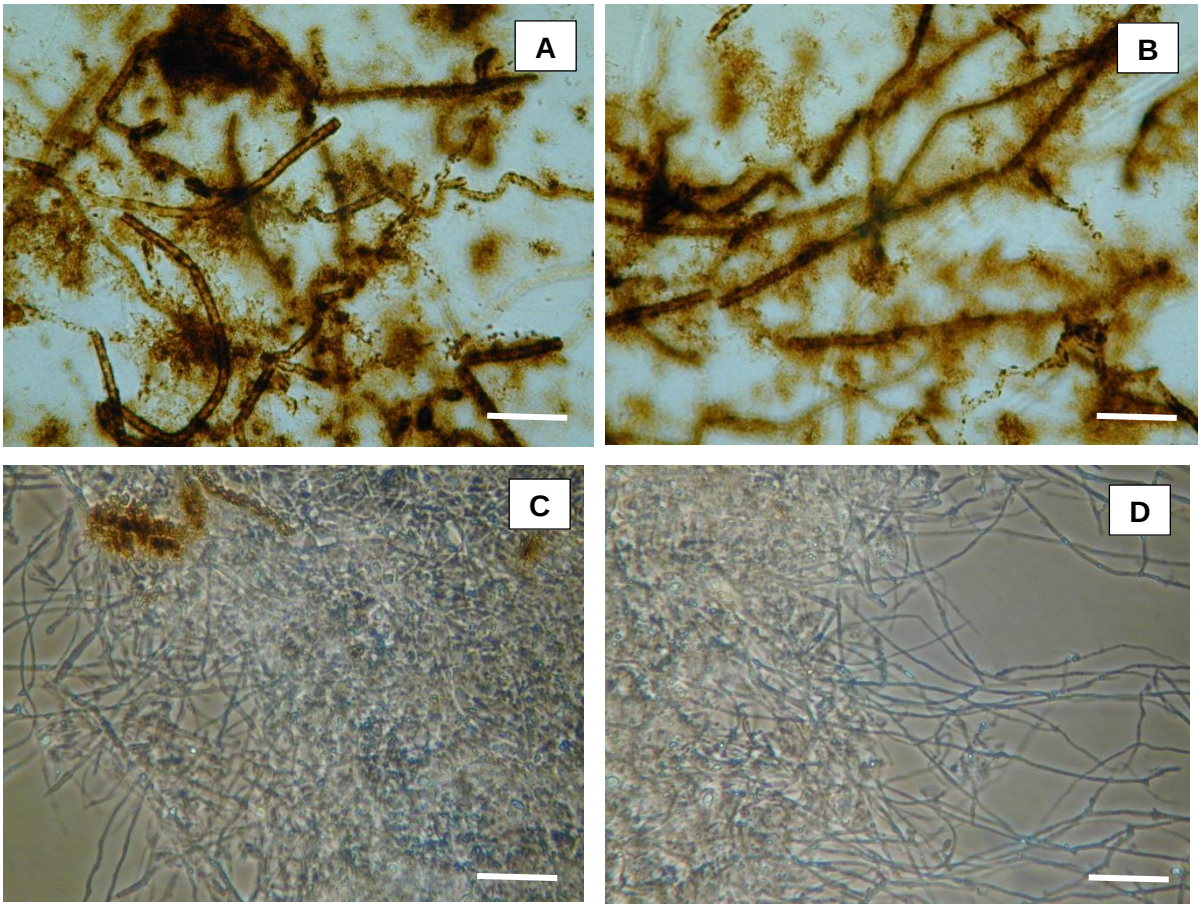


**Fig. 6.18.** Micrographs of the isolated MnI1. (A-B) potential Mn oxides deposited onto the hyphae and (C-D) growth on Mn-free plates. Bars 10 µm.

Growth was observed over a wide pH range (4.0 - 8.0) and was more pronounced between pH 4.0 - 6.5, at which the spherical mycelial growths in the flasks were uniformly pigmented dark brown/black (Table 6.8). Growth was less evident at higher pH (7.0 and 8.0) and the fungal mycelium was brown/black-coloured in the centre of the colonies but the peripheries were non-pigmented, while at pH 8.0 entire mycelium was white in colour. Table 6.8 shows initial pH values (at which liquid medium was set) and final pH (after 10 days of experiment). Lower pH values were observed at the end of the experiment in all conditions tested, therefore pH limits for grow could not be accurately determined since pH values changed throughout the experiment; nevertheless growth was observed within the range tested.

**Table 6.8.** pH limits for MnI1 growth. Key: (-) no growth observed; (+) growth observed; (++) extensive growth observed.

| Initial pH / final pH | Growth | Mycelium colour |
|---|---|---|
| **4.0 / 2.9** | ++ | Brown/black |
| **5.0 / 2.9** | ++ | Brown/black |
| **6.5 / 4.0** | ++ | Brown/black |
| **7.0 / 4.1** | + | Brown/black and white |
| **8.0 / 4.2** | + | White |

MnI1 was tested for Mn (II) oxidation at initial pH 6.5 and 25ºC; results are shown in Fig. 6.19. Concentrations of soluble manganese in non-inoculated control remained fairly constant throughout the experiment whereas in the inoculated flasks, concentrations of soluble Mn decreased gradually reaching 0.1 mM after 13 days. Parallel trends were observed with pH values. The final pH of non-inoculated control was 6.5 whereas the final pH of the inoculated flasks were ~ 4.0.

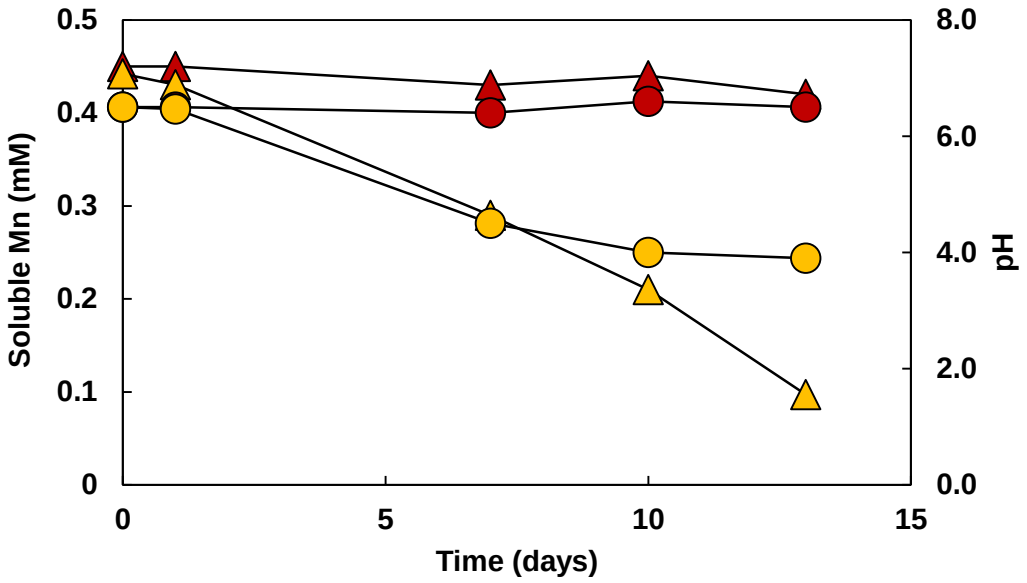


**Fig. 6.19.** Changes in soluble manganese concentrations (▲,▲) and pH (●, ●) in shake flasks cultures inoculated with isolate MnI1 (▲, ●) and non-inoculated controls (▲, ●) with isolate MnI1. The experiment was carried out in duplicate and different values between replicates are occluded by the symbols.

Results of growth tests on different organic substrates are shown in Table 6.9. Isolate MnI1 grew on a wide range of organic compounds, including hexoses, pentoses and methyl pentoses, some disaccharides and alcohols, though not on the amino acids tested.

**Table 6.9.** Utilization of organic substrates by MnI1. Key: (-) no growth observed; (+) growth observed.

| Substrate | Concentration (mM) | Growth | Mycelium colour |
|---|---|---|---|
| **Mannose** | 5 | + | White |
| **Galactose** | 5 | - | |
| **Glucose** | 5 | - | |
| **Sucrose** | 5 | + | Brown/black |
| **Fructose** | 5 | + | Brown/black |
| **Trehalose** | 5 | - | |
| **Maltose** | 5 | + | White |
| **Fucose** | 5 | - | |
| **Lactose** | 5 | + | Brown/black |
| **Arabinose** | 5 | + | Brown/black |
| **Cellobiose** | 5 | - | |
| **Ribose** | 5 | + | Brown/black |
| **Rhamnose** | 5 | + | Brown/black |
| **Xylose** | 5 | + | Brown/black |
| **Lactose** | 5 | + | Brown/black |
| **Sorbose** | 5 | - | |
| **Na-pyruvate** | 5 | + | Brown/black |
| **Mannitol** | 5 | + | Brown/black |
| **Sorbitol** | 5 | - | |
| **Glycerol** | 10 | + | Brown/black |
| **Methanol** | 20 | - | |
| **Ethanol** | 15 | + | Brown/black |
| **Benzyl Alcohol** | 5 | + | Brown/black |
| **Phenol** | 5 | - | |
| **1,3-propanodiol** | 5 | - | |
| **Glycolic Acid** | 15 | - | |
| **Citric Acid** | 5 | + | Brown/black |
| **Alanine** | 10 | - | |
| **Leucine** | 5 | - | |
| **Glycine** | 5 | - | |

6.3.4.2 Phylogenetic analysis

Phylogenetic analysis revealed that isolate MnI1 belongs to the *Ascomycota* phylum and clustered with members of the order *Pleosporales*, class *Dothideomycetes*. The 18S rRNA genes sequence from MnI1 was closely related (99% gene similarity) to those from *Ulospora bilgramii* and several other species. The phylogenetic tree (Fig. 6.20) showed MnI1 as a single member of a clade forming a branch with low bootstrap values of 47%, supporting the monophily of the clade. Based on these findings, it appears that this fungus has not been previously described. The 18S rRNA gene sequence of isolate MnI1 is shown in Appendix 1.

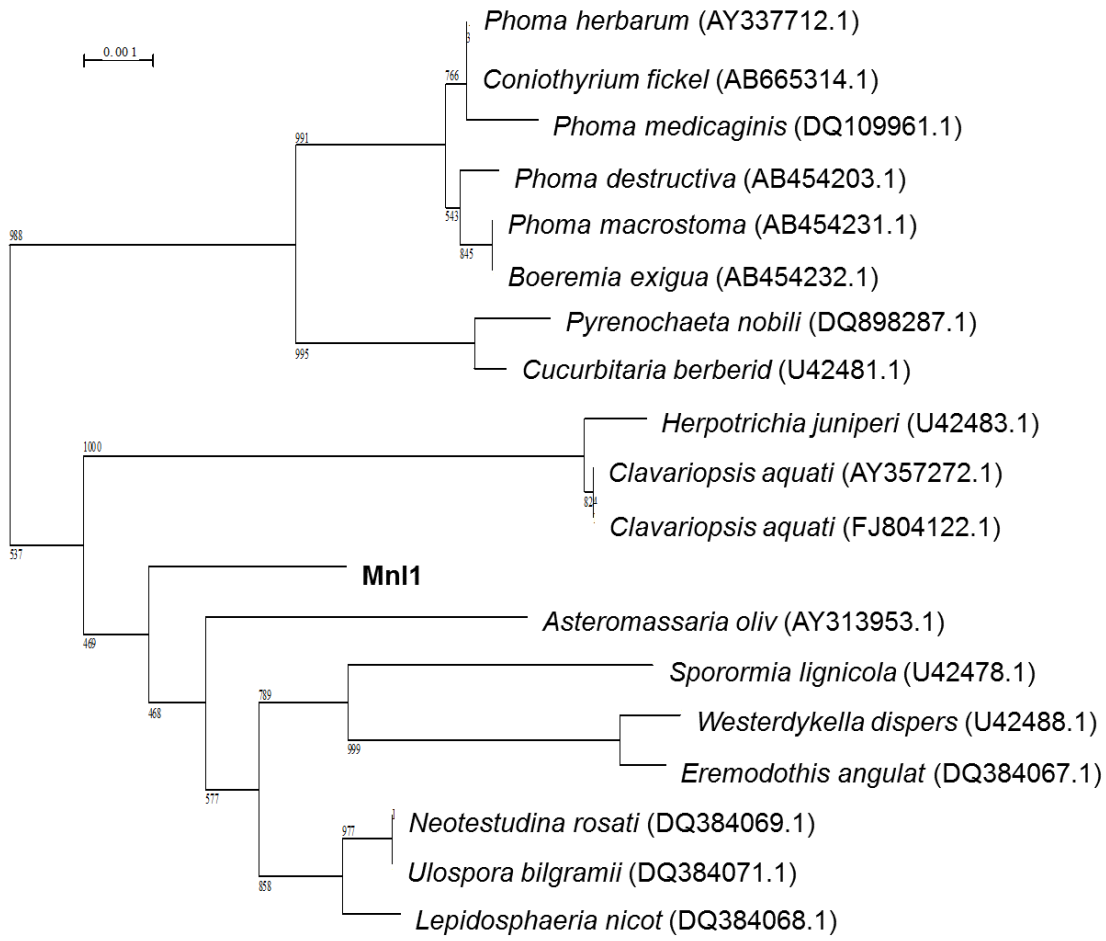


**Fig. 6.20.** Phylogenetic tree showing the relationship of the fungal isolate MnI1 to other micro-organisms based on 18S rRNA sequence homology (values in brackets are NCBI accession numbers). Scale bar is number of nucleotides substituted per base pair. Bootstrap values are given at the respective nodes. The tree was rooted with the 18S rRNA gene sequence of *Saccharomyces cerevisiae* (J01353.1).

## 6.4 Discussion

Manganese, like many other transition metals, can occur in elevated concentrations in waters draining coal and metal mines. This study focussed on Mn removal from a synthetic AMD, based on the composition of an actual mine water draining a copper mine in Brazil, using fixed bed bioreactors containing Mn (II)-oxidizing microorganisms. 'Manganese-oxidizers' are extremely diverse phylogenetically and can be isolated from very different habitats (Nealson, 2006), and these microorganisms are responsible for the global geochemical cycling of this metal and, indirectly, of some others, such as iron. The use of bioreactors containing Mn (IV) biofilm-colonised pebbles to remove Mn (II) from contaminated wastewaters was previously described by Mariner et al. (2008).

The current study developed an alternative approach to remediate Mn (II) from a synthetic mine water to that used for other metals, since manganese was not removed, as a sulfide using the sulfidogenic bioreactor, under the conditions used. Thermodynamically, Mn (II) should oxidize spontaneously to Mn (IV) in aerated, neutral pH waters, but the activation energy required is relatively high, causing the process to slow down and Mn (II) to be far more stable in non-acidic waters. This barrier can be overcome by Mn (II)-oxidizing microorganisms which catalyse the oxidation of divalent, soluble Mn (II) to insoluble Mn oxides. However, Mn (II) can be removed from solution by various mechanisms, including adsorption onto solid phase Mn (IV) oxides (Ehrlich, 2008; Hallberg and Johnson, 2005).

The Mn (IV) biofilm-colonised pebbles used in batch and bioreactor systems removed soluble Mn from the Mn-rich processed mine water very effectively in both systems tested, with over 90% Mn removal under optimised conditions. The pH values of the processed waters in batch tests were higher (~ 7.0) than the starting values (pH 5.0), even though manganese oxidation/hydrolysis is a net proton-generating process (Eq. 6.1 - Eq. 6.3). The reason for this apparent anomaly is unknown, and processed waters were found to have lower pH values that influent liquors when the colonised pebbles were used in the column bioreactor.

The MnOB was tested with feed liquors with different pH values and operated at with varying HRTs. Manganese was readily removed in the first days of operation in phase C1, but subsequently a decrease in Mn removal was observed which could be related to: (i) toxicity of trace amounts of $H_2S/HS^-$ (not measured) present in effluent waters from the aSRBR (sulfide is known to be extremely toxic to most life forms); (ii) the presence of potentially toxic transition metals (even only in trace quantities) in the feed liquor, since the effectiveness of metal sulfide precipitation in the sulfidogenic bioreactor was variable, and in some cases nickel and cobalt were ineffectively removed from solution (Chapter 4); (iii) the pH of the feed liquor used initially

(5.0), which was lower than that of the stream water (pH 6.5) from which the pebbles were taken and (iv) provision of insufficient substrate in terms of metabolisable organic carbon for the Mn (II)-oxidizing microorganisms in the MnOB. A large improvement in Mn removal was observed when the pH of the feed liquor and the HRT were increased (> 90% in phase C4) may due to the increasing of abiotic uptake of Mn (II) onto $MnO_2$ precipitates and its subsequent microbial oxidation. Manganese oxides are known for their abilities to adsorb metals and for their cation exchange capacities (Ehrlich, 2008). The former derives from negative charges of Mn (IV) oxides because of the presence of some Mn (III) or vacant sites within the mineral lattice structure (Tebo et al., 2004). Consequently, cationic transition metal as well as alkali and alkaline earth metals can be adsorbed to neutralise this negative charge. However, the polarity of the charge borne by manganese (IV) oxides is pH-dependent. Mariner et al. (2008) determined the point of zero charge ($pH_{PZC}$), i.e. the pH above which the Mn (IV) oxides is net negatively charged and below which it is net positively charged, of a similar material to that used in the present study, to be 5.5. This value correlates well with the observation that increasing the pH of the influent liquor to the MnOB resulted in improved rates of Mn (II) removal, as more negative sites would have been made available. While abiotic adsorption occurs relatively rapidly, for the process to continue the adsorbed Mn (II) requires to be oxidized to form new Mn (IV) oxides, to avoid saturation of the available sites. Manganese-oxidizing microorganisms catalyse the oxidation of Mn (II) using different mechanisms, as described by Ehrlich (2008), and some Mn-oxidizers are known to conserve the energy generated from the reaction. Figure 6.21 shows a simplified version of the model proposed by Ehrlich (2002) of oxidation of Mn (II) bound to Mn (IV) oxide ($MnO_2$) by Gram-negative bacteria that conserve energy from the reaction.

In the current work, the immediate increase in Mn removal when using a higher pH influent liquors was followed by a decline. However, addition of yeast extract to the influent liquor once again improved the removal of Mn (II). This can be interpreted as the rate-limiting step of the process ultimately being the oxidation of adsorbed Mn (II) by heterotrophic bacteria such as *Leptothrix discophora* and the fungal isolate MnI1. Insufficient metabolisable DOC was present in the effluent liquors from the aSRBR to support adequate growth of these Mn (II)-oxidizers to allow the MnOB to be effective in the long term. Ideally, the remediation process should perform in a self-sufficient way, where no further amendments would be required to the effluent liquor generated by the aSRBR. However, based on the results obtained, pH and substrate amendment (addition of yeast extract or other organic compounds) would have to be carried out in order to optimize removal of manganese. The pH of effluent liquors from the MnOB varied throughout the experiment (from 4.0 to 5.5) and was lower than the influent liquors, which was anticipated since net manganese oxidation/hydrolysis

generates hydronium ions. It is noteworthy to mention that in phase C4 (2-column system) the pH of effluents from column 1 varied within this same range, suggesting that manganese removal in column 2 occurred in pH as low as 4.0. Studies have described biological manganese oxidation at low pH (5.5) in a manganese deposit influenced by metal-rich groundwater (Bohu et al., 2016) and in low pH uranium-contaminated groundwater and soil material from a uranium mine area in Germany (Akob et al., 2014). Variations in the feed liquor pH were also observed throughout the experiment, which were probably related to microbial activity occurring in stored liquors from the aSRBR.

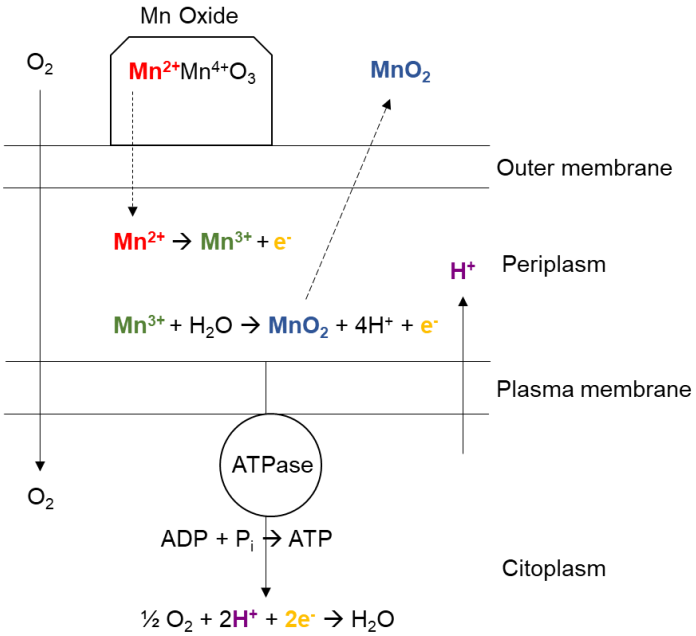


**Fig. 6.21.** Model of oxidation of Mn (II) pre-bound to Mn (IV) oxide with energy conservation by Gram-negative bacteria (modified from Ehrlich (2002)).

Variations in planktonic cell numbers in the feed liquor for the MnOB could have been caused by either ongoing tests with aSRBR or to microbial growth during the time that the feed liquor was remaining in the feed bottle (particularly when low flow rates were used). Numbers of planktonic cells in the effluent liquor from the MnOB were generally lower than those in the feed liquors, possibly due to microorganisms becoming attached to the pebbles.

Dissolved organic carbon (DOC) measured in the influent and effluent liquors from both the aSRBR and the MnOB (at end of phase C3) showed that over 99% of DOC in the influent liquor of the former was consumed in this integrated bioremediation system, with 96% of that being consumed in the aSRBR itself and the remainder in the MnOB. Average glycerol and acetate concentrations in the aSRBR effluent liquor were equivalent to 3.25 and 2.40 mg C $L^{-1}$ respectively, while the average DOC concentration was 9.10 mg $L^{-1}$. This means that

~ 3.60 mg $L^{-1}$ of other soluble carbon was also present. Some of this was potentially a residual fraction of yeast extract that was not used by the aSRB microflora (the usual concentration of yeast extract in the feed liquor was 100 mg $L^{-1}$, which is equivalent to 40 mg C $L^{-1}$ (assuming that, like glucose, yeast extract contains 40% carbon). In addition, some of the DOC not accounted for in the effluent from the aSRBR could have arisen from cell lysates and exudates. While there was some provision of DOC to the MnOB, this was clearly insufficient to sustain sufficient long-term removal of manganese, which would therefore appear to have been mediated by heterotrophic rather than autotrophic microorganisms.

Analysis of indigenous microbial populations provided evidence that Mn (II)-oxidizing microorganisms were present in pebble biofilms, including the known Mn (II)-oxidizer bacterium *Leptothrix discophora* (Boogerd and De Vrind, 1987) which was also detected by T-RFLP analysis (by calculating theoretical T-RF length). In general, T-RFLP analysis of biofilm-colonised pebbles found large numbers of different length T-RF peaks, indicating significant biodiversity. The technique would, however, have underestimated total biodiversity, since: (i) the 16S or 18S rRNA gene sequence of a microorganism can have more than one cleavage sites for the same restriction enzyme or none at all, and (ii) more than one microorganism can display the same length T-RF peak. Thus, these analyses present only a general overview of the microbial diversity of biofilms on the colonised pebbles.

A Mn (II)-oxidizing fungus was isolated from the surface of colonised pebbles from the MnOB. The isolate MnI1 belongs to the order *Pleosporales* (*Ascomycota* phylum), within which several Mn (II)-oxidizers have been described (Miyata et al., 2006; Santelli et al., 2010; Mariner et al., 2008; Sasaki et al., 2004). Isolate MnI1 was able to catalyse the removal of soluble manganese from liquid media, and accumulated brown/black-coloured precipitates on its mycelium when grown on Mn-containing plates. However, the fungal mycelium on Mn-free plates also had a dark brown pigmentation in the centre of the colonies, this pigmentation though could be from its natural coloration and microscopic images only showed deposition of Mn precipitates onto the fungal mycelium growing on Mn-containing plates.

Physiological tests carried out in liquid media showed that isolate MnI1 could grow in a relatively wide range of temperatures (15 - 30ºC) and pH (4.0 - 8.0). However, the final pH in all flasks were significantly lower than that initially set. For example, at initial pH 7.0 and 8.0, the final pH values were both ~ 4.1. Uniquely, the fungal mycelial spherical growths in media set initially at pH 8.0 were entirely white. It is not yet understood the reason why this was the case, as the final pH was much lower and similar to those where pigmentation was very obvious. Manganese oxidation was not measured in the variable pH experiment with this

isolate, though other experiments confirmed that this isolate oxidized Mn (II) and precipitated Mn (IV). Abiotic Mn oxidation occurs at pH higher than 8.0, therefore chemical oxidation was considered unlikely in the variable pH experiment.

T-RFLP analysis of amplified 18S rRNA genes (HaeIII digests) showed a high relative abundance of the 280 nt T-RF in the MnOB, especially in phase C4. The theoretical T-RF of isolate MnI1 matched this same T-RF (279 $\pm$ 2 nt), suggesting that the isolate was a dominant eukaryote in the biofilm-colonised pebbles. However, it is noteworthy to mention that other eukaryotic clones obtained from the pebble biofilm have the same T-RF length as the fungal isolate, and the high relative abundance of the 280 nt T-RF observed in T-RFLP analysis may be due to summation of 280 nt T-RFs from different organisms. A T-RF corresponding to that of isolate MnI1 was detected in the initial pebble biofilm (phase C0 of the MnOB) and also throughout the experiment. However, this isolate was not detected in T-RFLP analysis of the originally white-coloured gravel samples that were placed in the stream for up to 5 weeks.

In this study, immobilized Mn (II)-oxidizing microorganisms present in pebble biofilms facilitated the removal of soluble manganese and accumulation of a brown/black precipitates, presumed to be manganese (IV) oxides, within a column bioreactor. Mineralogical analysis of the precipitates were not performed, though previous work using a similar system identified the Mn (IV) mineral phase as birnessite (Mariner et al., 2008) which is the most common Mn (IV) bio-oxide in aquatic environments (Tebo et al., 2004). Under optimized conditions, the fixed bed bioreactor containing Mn (II)-oxidizing microorganisms was highly effective in catalysing the removal of this metal (> 99%) as a final polishing step in a series of system for removing metals (Cu, Zn, Ni, Co and Mn) from synthetic mine water based on that draining a copper mine in Northern Brazil.

# The use of alternative substrates to sustain low pH sulfidogenic bioreactors for remediating acidic and moderately acidic mine drainage

7

## 7.1 Introduction

Generation and remediation of acid mine drainage (AMD) is one of the most important problems affecting mining companies around the world. Microbial treatment of AMD by sulfate-reducing bacteria (SRB) has considerable advantages over conventional remediation strategies since the metal sulfides generated have relatively high densities, are highly insoluble and allow the metals to be recovered and recycled. Sulfate-reducing bacteria can be found in a wide range of anaerobic environments, including marine sediments, deep groundwater deposits, oil fields, mine wastes and sediments, hot springs and others. These microorganisms are responsible for the reduction of sulfate (electron acceptor) and generation of hydrogen sulfide ($H_2S$) via oxidation of organic compounds, such as carbohydrates (e.g. glucose), organic acids (acetate and propionate) and alcohols (glycerol and ethanol) as well as molecular hydrogen ($H_2$) (Chapter 1).

Studies have shown that SRB which grow at circum-neutral pH can utilize a wide range of organic substrates (Suzuki et al., 2007) and biosulfidogenesis at this pH range has been demonstrated to be relatively effective for remediating some metal-rich contaminated wastewaters. However, AMD usually contains low concentration of organic compounds which need, therefore, to be supplemented. The choice of the substrate used in each case will depend mainly on local availability and costs (Sánchez-Andrea et al., 2014). However, the potential toxicity of substrates needs to be taken into account in low pH biosulfidogenic systems.

Suitable substrates (electron donors) that are economically sustainable, locally produced, or easily transported and stored, are key factors for the feasibility of treating mine water using a SRB bioreactors (Bomberg et al., 2017). Ethanol ($CH_3CH_2OH$) is one of the substrates which can fulfil all aforementioned requirements and has successfully been applied in circum-neutral pH biosulfidogenic processes for remediating AMD (Nagpal et al., 2000; Celis et al., 2009); however little is known about its use in acidophilic sulfidogenic bioreactors.

Glycerol ($CH_2OHCHOHCH_2OH$) is an organic compound which has been used routinely as the carbon- and energy-source for acidophilic SRB in bioreactor modules used to remediate

AMD (Hedrich and Johnson, 2014; Kimura et al., 2006; Ñancucheo and Johnson, 2012; 2014). This compound can be produced either by microbial fermentation or chemical synthesis from petrochemical feedstock (da Silva et al., 2009). Crude glycerol is obtained as a co-product during transesterification of vegetable oils and animal fats with methanol ($CH_3OH$), from which biodiesel is produced. Chemical composition of crude glycerol can vary depending on catalysts used to produce biodiesel, efficiency of the transesterification process, and recovery of methanol and catalysts (Yang et al., 2012). Rehman and colleagues (2008) described a pre-treatment process for crude glycerol from sunflower oil biodiesel production to generate 1,3-propanediol, which originally contained (w/w): 30% glycerol, 50% methanol, 13% “soap”, 2% moisture, 2 - 3% salts and 2 - 3% other impurities. The presence of methanol is due to the fact that biodiesel producers use excess methanol to drive the chemical transesterification to completion, which is not recovered (Thompson and Be, 2006).

Methanol, as well as glycerol, is known to be used as an electron donor by some SRB (Braun and Stolp, 1985, Hard et al., 1997), and therefore its relatively high concentrations in crude glycerol could be potentially used as a supplementary electron donor to fuel biosulfidogenesis. Moreover, crude glycerol could be used in sulfidogenic bioreactors rather than pure glycerol (which require costly refining processes) which would ultimately reduce costs of the bioremediation process. This chapter focuses on laboratory experiments in which ethanol and methanol were used either alone or in combination with glycerol as electron donors for sulfate-reducing bacteria that grow at low pH (< 5) in a continuous flow bioreactor.

## 7.2 Materials and methods

### *7.2.1 Sulfidogenic bioreactor*

A sulfidogenic upflow biofilm reactor, described in section 2.4, populated with a mixed microbial community containing species of aSRB and non-sulfidogenic acidophilic bacteria was used in the experimental work described in this chapter. The standard feed liquor of the aSRBR contained ABS/TE (section 2.2.2.1), 2.5 mM $MgSO_4$ and 0.1 g $L^{-1}$ yeast extract, pH 2.5. Concentrations of methanol and ethanol used alone or in combination with glycerol are described below.

*7.2.2 Operational set up of the aSRBR using combined methanol and glycerol as electron donors*

The sulfidogenic bioreactor was operated in continuous flow mode for a period of 132 days. The effect of methanol, as electron donor, on the performance of the aSRBR was evaluated by combining different concentrations of methanol and glycerol in the feed liquor. The relative percentages of methanol and glycerol were based on the total amount of carbon provided to the system (methanol is a $C_1$ compound while glycerol is a $C_3$ compound, so a 3x concentration of methanol is equivalent to 1x glycerol, in terms of carbon provision).

Another way to express relative percentages when combining substrates is considering their electron donor potential by calculating the net amount of electrons available in the reaction, assuming complete oxidation to $CO_2$. For example, 1 mole glycerol has the potential to donate 14 electrons whereas ethanol and methanol donate 12 and 6 electrons, respectively. The electron donor potential for the combinations of substrates tested in this study are shown in Table 7.1 and Table 7.3.

For this experiment, the bioreactor was operated at pH 5.5 and 35ºC and fed with the standard influent liquor previously described plus different concentrations of electron donors, as shown in Table 7.1. Production of hydrogen sulfide was calculated from measuring changes in concentrations of soluble copper (section 2.5.2.1) in an attached off-line vessel containing 400 mL of 25 mM $CuSO_4$. Phases of the experiment are referred to as M0, M10, M25, M50 and M75, according to the relative percentage of methanol present in the influent liquor. No tests were made using 100% methanol in the feed liquor.

**Table 7.1.** Combinations of methanol and glycerol in the influent liquor and their combined electron donor potentials. Influent liquor containing 100% methanol was not tested.

| Methanol (relative %) | Methanol (mM) | Glycerol (mM) | Total carbon equivalent (mM) | Electron donor potential (mM) |
|---|---|---|---|---|
| **0** | 0 | 5.0 | 15 | 70 |
| **10** | 1.5 | 4.5 | 15 | 72 |
| **25** | 4.0 | 4.0 | 16 | 80 |
| **50** | 8.0 | 2.5 | 16 | 83 |
| **75** | 12.0 | 1.0 | 15 | 86 |

Samples from the aSRBR were removed at regular intervals and filtered through 0.2 µm nitro-cellulose membrane filters (Whatman, UK). Concentrations of sulfate, glycerol consumed and acetic acid produced were determined using ion chromatography (section 2.6).

Composition of planktonic bacterial population within the bioreactor vessel was assessed using semi-quantitative T-RFLP analysis (section 2.9.4). Concentrations of methanol in the influent and effluent liquors were determined using the enzymatic assay described below. Hydraulic retention times (expressed in hours), sulfate reduction rates, $H_2S$ production rates were calculated as described in Chapter 3.

7.2.2.1 Enzymatic assay for methanol determination in (moderately) acidic liquors

The principle of the method relies firstly on the conversion of methanol to formaldehyde by the alcohol oxidase (AO; Eq. 7.1), followed by conversion of formaldehyde to formic acid by formaldehyde dehydrogenase (FDH; Eq. 7.2) in presence of $NAD^+$ (Vinet, 1987).

$$CH_3OH + O_2 \xrightarrow{\textbf{AO}} HCHO + H_2O_2 \qquad \text{(Eq. 7.1)}$$

$$HCHO + H_2O + NAD^+ \xrightarrow{\textbf{FDH}} HCOOH + NADH + H^+ \qquad \text{(Eq. 7.2)}$$

Alcohol oxidase is not a specific enzyme, which means that it converts all small molecular weight alcohols to their respective aldehydes. However, formaldehyde dehydrogenase is very specific to its substrate and therefore the transformation of $NAD^+$ to NADH occurs only if methanol was originally present in the sample, since only methanol is converted to formaldehyde by the action of alcohol oxidase. The reaction is followed by the increase in absorbance due to formation of NADH which is directly related to the concentration of methanol (Vinet, 1987).

7.2.2.1.1 Reagents

Enzyme stock solutions: Alcohol oxidase (AO) from *Pichia pastoris* (Sigma-Aldrich, UK) and formaldehyde dehydrogenase (FDH) from *Pseudomonas putida* (Sigma-Aldrich, UK) were separately dissolved in 0.1 M phosphate buffer pH 7.2 containing 30% sucrose to a final concentration of 5 U $mL^{-1}$. Solutions were kept at - 20ºC until used.

$NAD^+$: ß- nicotinamide adenine dinucleotide hydrate (Sigma-Aldrich, UK) was dissolved in 0.1 M phosphate buffer pH 7.2 to a final concentration of 2.5 mM.

Enzyme reagent (ER): mixture of 1.8 mL of 2.5 mM $NAD^+$ and 0.2 mL FDH solution (5 U $mL^{-1}$). The final volume of 2 mL was enough for 10 reactions, and the reagent was stable for 24 h at 4 - 7ºC (Vinet, 1987).

Standard solutions: Methanol (HPLC grade; Fisher Scientific, UK) was used to prepare standard solutions containing the following concentrations: 0, 0.0625, 0.125, 0.25, 0.5 and 1.0 mM $CH_3OH$.

7.2.2.1.2 Assay protocol

The methanol assay involved the addition of 200 µL ER and 20 µL AO solution into a 1.5 mL centrifuge tube, which was mixed thoroughly and incubated at 30ºC for 5 mins. The total volume was transferred to a 96-well UV-star flat bottom microplate (Greiner Bio-one, UK) and 50 µL of sample (diluted with ultrapure water MiliQ® Synthesis A10, when needed) was added to the mix, and thoroughly mixed. Samples were analysed using a Multiskan™ GO Microplate Spectrophotometer (Thermo Fisher Scientific, UK). The plate reader was set up as follows: wavelength set at 340 nm, linear shaking for 5 s prior to analysis and changes in absorbance over a 20 min period (1 reading $min^{-1}$) were measured. A calibration curve was constructed based on rates of increase in absorbance (Fig. 7.1 A), which was calculated by subtracting the initial absorbance from the final (within a linear portion) and dividing it by the time interval (i.e., $\Delta A_f - \Delta A_0 / t$). In this experiment, the interval used was between 0 and 5 min. Methanol concentrations in samples were determined using the resulting linear regression equation (Fig. 7.1 B).

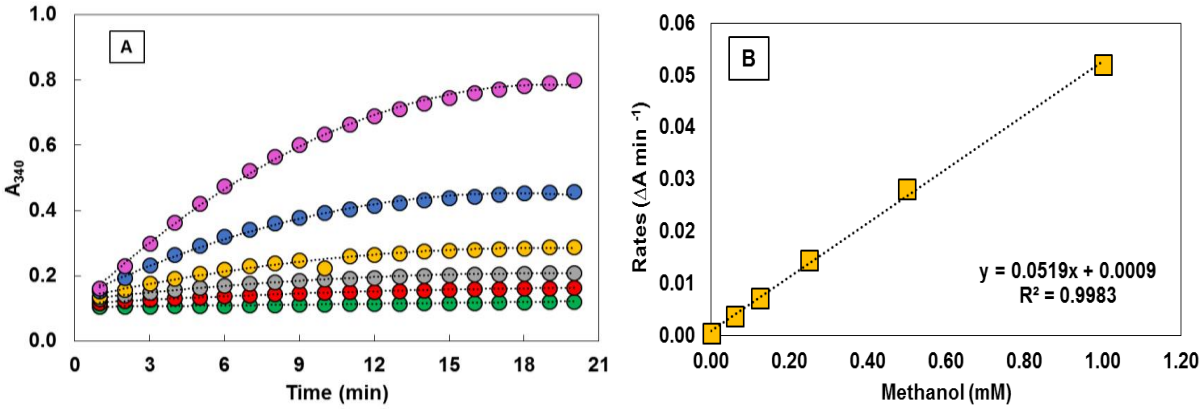


**Fig. 7.1.** Reaction progress curves for enzymatic oxidation of methanol, monitored by the production of NADH (A) and calibration curve for methanol determination (B).

The effect of acidic samples and standard medium chemical components on the determination of methanol were evaluated, as well as interference of other alcohols, such as ethanol and glycerol. Results are shown in Table 7.2.

As a circum-neutral pH value is crucial for enzymatic activity, a simple spot test was carried out using bromothymol blue in order to check whether the phosphate buffer used in the assay would resist changes in pH when acidic samples were added to the reaction mix. Bromothymol blue is a pH sensitive dye which displays a bright aquamarine colour. This reagent is yellow in acidic solutions (~ pH 2), blue in alkaline solutions (~ pH 12) and green/greenish blue in neutral solutions (pH 7 - 7.4). Solutions of ABS/TE were prepared at pH 2.0, 4.0 and 7.0, mixed to the enzymatic reagent, as described in the protocol aforementioned, and tested using 100 µL of the reagent bromothymol blue. All samples displayed a greenish blue colour, indicating circum-neutral pH values.

**Table 7.2.** Interference test of alcohols and growth medium compounds on determination of methanol in acidic samples.

| Interfering substances | Rate ($\Delta A\ min^{-1}$) |
|---|---|
| **0.5 g $L^{-1}$ yeast extract (pH 4)** | < 0.005 |
| **1 mM Glycerol** | < 0.005 |
| **1 mM Ethanol** | < 0.005 |
| **ABS/TE solution pH 4** | < 0.005 |
| **Standard SRB medium (ABS/TE, 0.1 g $L^{-1}$ yeast extract, 5 mM Glycerol) at pH 2.5** | < 0.005 |

*7.2.2.2* Clone library analysis of the planktonic bacterial population in the bioreactor

In order to assess the composition of the planktonic microbial populations present in the bioreactor at the end of the M75 phase, liquid samples were removed from above the biofilm bed, DNA extracted and bacterial 16S rRNA genes were amplified (section 2.9). A clone library was constructed in order to identify unknown organisms, as described in section 2.9.5. Theoretical T-RFs of the clones were obtained by measuring the lengths of the bacterial 16S rRNA genes fragments cleaved by the restriction enzyme HaeIII and compared to that obtained from T-RFLP analysis.

*7.2.3 Ethanol as an alternative electron donor for sustaining low pH biosulfidogenesis*

The effect of ethanol as electron donor on the performance of the aSRBR was assessed over a period of 218 days. The bioreactor was operated initially at pH 5.5 and 35ºC and fed with standard medium described earlier, plus different combinations of ethanol and glycerol in the feed liquor (Table 7.3). Concentrations of ethanol were increased and glycerol decreased progressively until ethanol was the solely electron donor in the influent liquor. Once the bioreactor performance had become relatively stable using only ethanol as electron donor, the bioreactor pH was gradually lowered from 5.5 to 4.0 in order to evaluate the effect of low pH ethanol-fuelled biosulfidogenesis. Phases of the experiment are summarised in Table 7.4. The nomenclature of each phase represents the substrate used (E; ethanol) followed by the relative percentage of this substrate (0, 10, 25, 50 or 100) and pH value at which the bioreactor was operated. For example, phase E100/4.0 refers to aSRBR operated at pH 4.0 and fed with 100% ethanol.

**Table 7.3.** Combinations of ethanol and glycerol in the influent liquor and their respective combined electron donor potential.

| Ethanol (relative %) | Ethanol (mM) | Glycerol (mM) | Total carbon equivalent (mM) | Electron donor potential (mM) |
|---|---|---|---|---|
| **0** | 0 | 5.0 | 15 | 70 |
| **10** | 1.0 | 4.5 | 16 | 75 |
| **25** | 2.5 | 3.5 | 16 | 79 |
| **50** | 5.0 | 2.5 | 16 | 95 |
| **75** | 6.5 | 1.0 | 16 | 92 |
| **100** | 8.0 | 0 | 16 | 96 |

Rates of hydrogen sulfide production were calculated from rates of copper precipitation in a connected off-line vessel (containing 400 mL of 100 mM $CuSO_4$); the stoichiometry of $H_2S$ produced to CuS generated is 1:1. Concentrations of acetic acid, sulfate and glycerol in the effluent liquor were monitored throughout the experiment, as mentioned previously. Analysis of the planktonic bacterial community was carried out using T-RFLP (section 2.9.4). Determination of ethanol was performed using an enzymatic assay, described below.

**Table 7.4.** Duration of each phase of the ethanol experiment and its respective ethanol content and bioreactor pH values.

| Phases of experiment | Ethanol content (%) | Bioreactor pH | Duration (days) |
|---|---|---|---|
| **E0** | 0 | 5.5 | 17 |
| **E10** | 10 | 5.5 | 31 |
| **E25** | 25 | 5.5 | 41 |
| **E50** | 50 | 5.5 | 10 |
| **E75** | 75 | 5.5 | 10 |
| **E100/5.5** | 100 | 5.5 | 10 |
| **E100/5** | 100 | 5.0 | 15 |
| **E100/4.5** | 100 | 4.5 | 15 |
| **E100/4** | 100 | 4.0 | 31 |

7.2.3.1 Enzymatic assay for determination of ethanol in (moderately) acidic liquors

This method for ethanol determination is based on its enzymatic oxidation and production of UV-detectable NADH at alkaline pH. The enzyme alcohol dehydrogenase (ADH) catalyses this reaction in presence of $NAD^+$ and the production of NADH is followed by absorbance measurements at 340 nm. (Eq. 7.3).

$$CH_3CH_2OH + NAD^+ \overset{ADH}{\rightleftharpoons} CH_3CHO + NADH + H^+ \qquad \text{(Eq. 7.3)}$$

This enzymatic assay for ethanol is very sensitive and relatively selective, since only certain primary and secondary aliphatic alcohols can also react, such as *n*-propanol and *n*-butanol (Bostick and Overton, 1980). It is noteworthy that the enzymatic reaction described (Eq. 7.3) is reversible and favours the oxidation of NADH at circum-neutral pH. To overcome this issue, a trapping agent is required to remove the acetaldehyde product. The most widely trapping agent used is hydrazine, which reacts with the carbonyl group generating the organic compound hydrazone (Engel and Jones, 1978).

7.2.3.1.1 Reagents

Enzyme solution: Alcohol dehydrogenase (ADH) from *Saccharomyces cerevisiae* (Sigma-Aldrich, UK) was dissolved in 0.1 M glycine-NaOH buffer pH 9 containing 30% sucrose to a final concentration of 5 U $mL^{-1}$. This solution was prepared on the day of use.

NAD$^+$: ß-nicotinamide adenine dinucleotide hydrate (Sigma-Aldrich, UK) was dissolved in 0.1 M glycine-NaOH buffer pH 9 to a final concentration of 2.5 mM.

Hydrazine solution: Hydrazine hydrate (Thermo Fisher Scientific, UK) was dissolved in ultrapure water to a final concentration of 10% (w/v).

Enzyme reagent (ER): 1.8 mL of 2.5 mM NAD$^+$ was mixed to 0.2 mL ADH solution and 15 µL of 10% hydrazine solution and thoroughly mixed. The final volume of ~ 2 mL was enough to perform 10 reactions.

Standards: Absolute ethanol (HPLC grade; Fisher Scientific, UK) was used to prepare standards containing 0, 0.0625, 0.125, 0.25, 0.5 and 1.0 mM $CH_3CH_2OH$.

7.2.3.1.2 Assay protocol

Enzyme reagent (200 µL) was added into 1.5 mL centrifuge tubes and incubated at 30ºC for 5 min. Samples were added (50 µL) and mixed thoroughly. The total volume was transferred to a 96-well UV-star flat bottom microplate (Greiner Bio-one, UK). Samples were analysed using a Multiskan™ GO Microplate Spectrophotometer (Thermo Fisher Scientific, UK). The plate reader was set up was: wavelength set at 340 nm, linear shaking for 5 s prior to analysis and changes in absorbance over a 10 min period (1 reading min$^{-1}$) were measured. A calibration curve was constructed based on maximum absorbance readings for each standard and plotted against ethanol concentrations.

## 7.3 Results

### *7.3.1 Effects of combinations of methanol and glycerol on the performance of an acidophilic sulfidogenic bioreactor*

The sulfidogenic bioreactor, which had been routinely fed with media containing 5 mM glycerol as principal electron donor, was tested using combinations of glycerol and methanol in the feed liquor. Fig. 7.2 shows changes in hydraulic retention time (HRT) during this experiment. Changing the composition of the feed liquor to 10% methanol (i.e. 1.5 mM methanol and 4.5 mM glycerol) resulted initially in an increase in HRT (from 23 h to 60 h) which was followed by a decrease on day 17, though HRTs varied greatly between 30 and 60 h during phase M10. Hydraulic retention times were lower (varying between 8 and 25 h) during

phases M25 and M50. During phase M75, HRTs increased again, reaching up to 60 h. Due to this increase in HRT and sudden decline in productivity of the bioreactor, it was decided not to test with a 100% methanol feed.

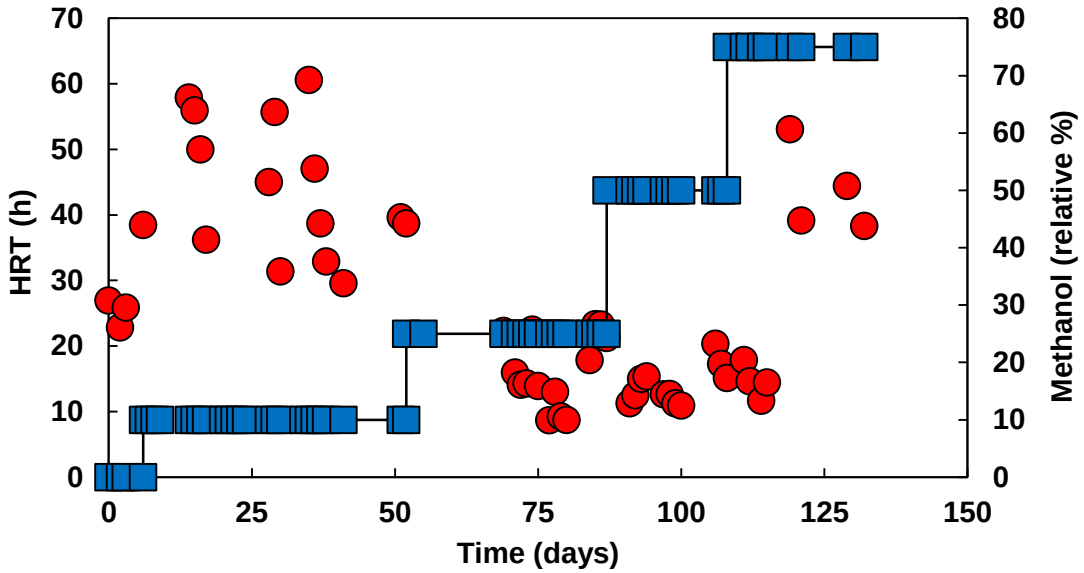


**Fig. 7.2.** Changes in HRTs (●) with varying relative percentages of methanol (■) used in the feed liquor of the aSRBR.

Figure 7.3 shows both rates of sulfate reduction and $H_2S$ generation (determined from rates of off-line copper precipitation). When the aSRBR was fed with glycerol alone (phase M0), rates of sulfate reduction were ~ 16 mmoles sulfate reduced $L^{-1}$ $day^{-1}$. This rate decreased considerably in phase M10, most likely caused by the initial addition of methanol to the system. Phases M25 and M50 showed a progressive increase in sulfate reduction rates, reaching average values of ~ 20 mmoles sulfate reduced $L^{-1}$ $day^{-1}$ during phase M50. As expected, rates of hydrogen sulfide generation followed similar pattern from that obtained for sulfate reduction rates. However, as the stoichiometry of sulfate reduced to $H_2S$ generated is 1:1, both rates should have been similar, which was frequently not the case (Fig. 7.3). Phase M75 showed a dramatic decrease in sulfate reduction, ranging between 2.0 and 3.3 mmoles sulfate reduced $L^{-1}$ $day^{-1}$. In order to maintain the bioreactor in operation and avoid stressing conditions to the microorganisms, further tests were not carried out.

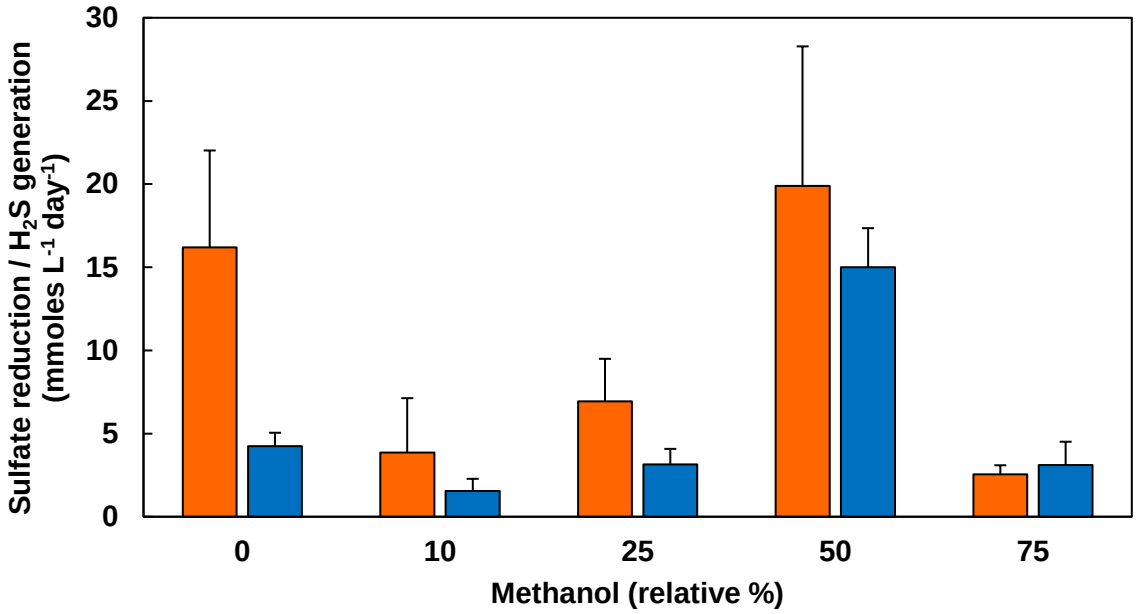


**Fig. 7.3.** Variations in rates of sulfate reduction (orange bars) and hydrogen sulfide generation (blue bars) for each combination of methanol and glycerol studied.

Concentrations of methanol were measured in the influent and effluent liquors in order to evaluate whether the microorganisms present in the bioreactor were capable of using this $C_1$ alcohol as electron donor for sulfate reduction (catabolism) or if the aSRB and/or other bacteria could use it as a carbon source (anabolism). In general, methanol did not appear to be consumed by the microbial population in the bioreactor since its concentration in the effluent liquor was similar to that present in the influent liquor (Fig. 7.4). However, there were few occasions where concentrations of methanol in the effluent liquor were slightly lower than that in the influent liquor, suggesting that there was some intermittent use of this alcohol.

On the other hand, glycerol was readily consumed within the bioreactor throughout this experiment, as shown in Fig. 7.5. Over 99% of the glycerol was consumed by the microorganisms in the bioreactor in all phases studied, suggesting that rates of sulfate reduction were coupled mostly to glycerol oxidation, since methanol was not used as electron donor. Production of acetate was observed throughout the experiment, and increased significantly in phase M10, with acetate concentrations reaching up to ~ 2.5 mM, but declined progressively during the subsequent phases. From day 120 onwards, acetate was not detected in effluent liquors.

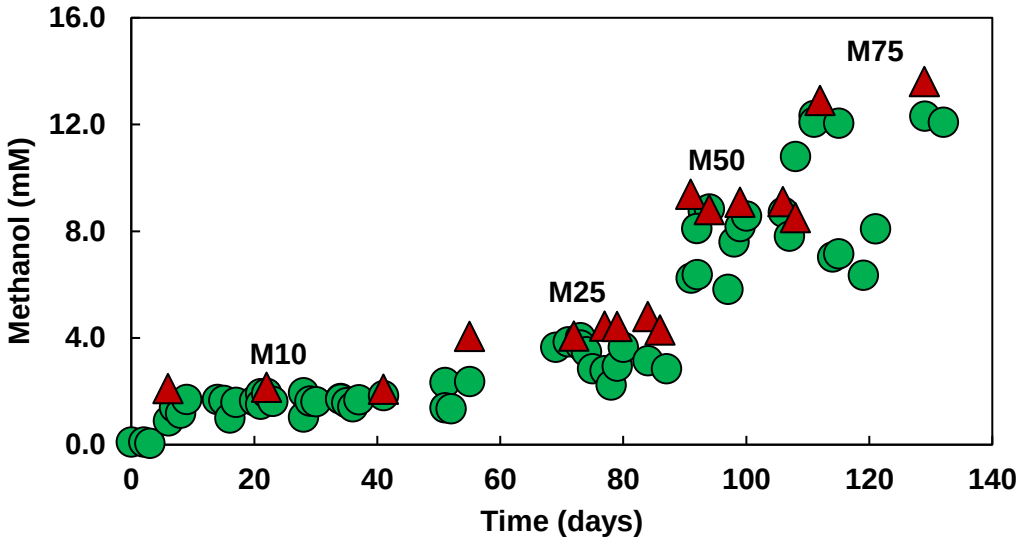


**Fig. 7.4.** Concentrations of methanol in the influent (▲) and effluent (●) liquors of the aSRBR.

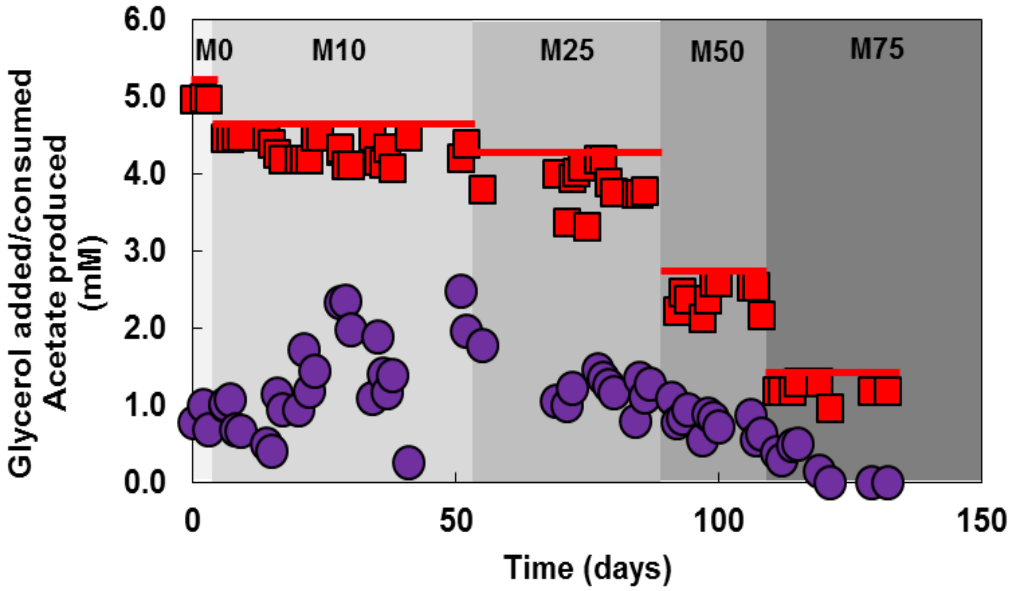


**Fig. 7.5.** Changes in concentrations of glycerol consumed (■) and acetate produced (●) in the sulfidogenic bioreactor, during tests carried out with mixtures of glycerol and methanol in the feed liquor. Concentrations of glycerol in the influent liquor in each phase are indicated by the red lines.

Figure 7.6 shows changes in relative abundance of members of the planktonic bacterial community of the aSRBR when methanol was added to the feed. In phase M0 the bacterial community was dominated by the *Actinobacterium* AR3 (230 nt; Chapter 3) which accounted for ~ 70% of the planktonic population in the bioreactor. The only sulfate-reducing bacteria detected during this phase was *D. acididurans*$^{T}$ (215 nt), which accounted for ~ 22% of the

total bacteria. The facultative anaerobic bacterium *At. ferrooxidans* (254 nt) was also detected in this phase (~ 5%), as elsewhere (Chapters 3 and 4).

Addition of methanol to the feed liquor caused major changes in the microbial population of the bioreactor (Fig. 7.6). In phase M10, two unknown T-RFs (201 nt and 266 nt, which were not present, at the time, in the Bangor acidophile database) were detected, and together accounted for almost 50% of the planktonic bacterial community. In phases M25, M50 and M75, these unknown T-RFs were again detected, plus two others (223 nt and 300 nt). Together, these accounted for 60 - 75% of the planktonic bacterial population in the bioreactor. Interestingly, the 138 nt T-RF, which corresponded to the sulfate-reducer *Peptococcaceae* CEB3 (regularly detected in previous experiments) was only detected in phase M50, at very low relative abundance (~ 2%).

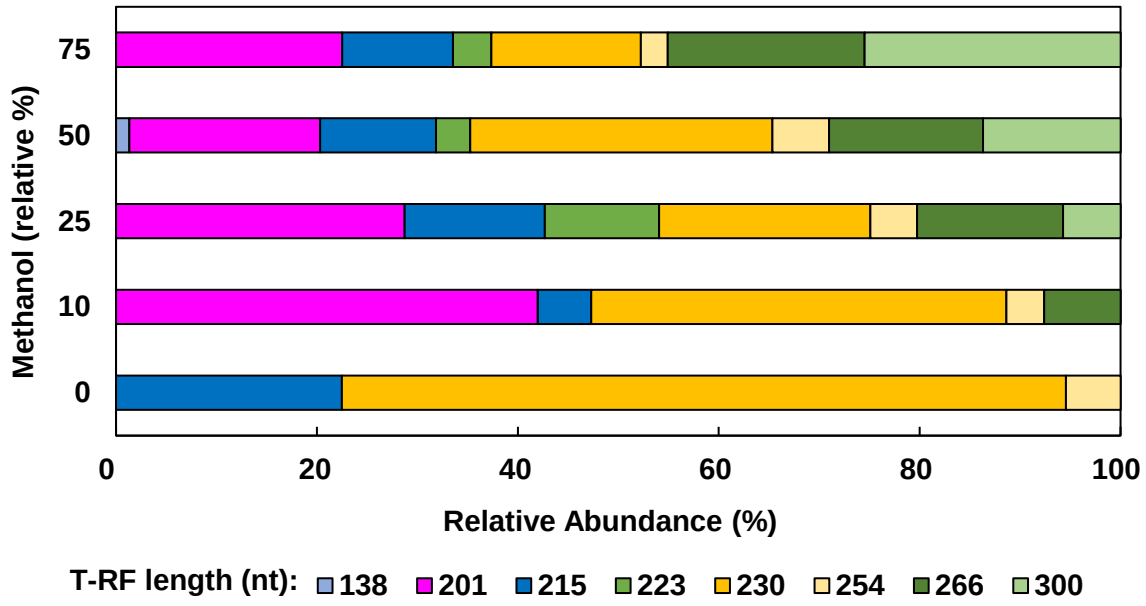


**Fig. 7.6.** Terminal restriction enzyme fragment length polymorphism (T-RFLP) analysis (HaeIII digests) of amplified 16S rRNA genes of planktonic bacterial communities in the aSRB reactor fed with different combinations of methanol and glycerol. Shades of blue represent known sulfate-reducing *Firmicutes* (138 nt, *Peptococcaceae* CEB3; 215 nt, *D. acididurans*), shades of yellow/orange represent non-sulfidogens (230 nt, *Actinobacterium* AR3; 253 nt, *At. ferrooxidans*), shades of green represent bacterial clones identified as probable non-sulfidogens, while the magenta bars represent clone SRB7, which was positively identified as a strain of the sulfate-reducer *Desulfovibrio desulfuricans*.

7.3.1.1 Clone library analysis

In order to identify the unknown T-RFs detected in the T-RFLP analysis, a clone library was constructed based on 16S rRNA genes and the identity of the clones obtained are shown in Table 7.5.

**Table 7.5.** Identity of cloned bacterial genes (16S rRNA gene) obtained from the sulfidogenic bioreactor (*n* =19).

| Clone designation | Closest Relative | % identity (16S rRNA gene) | Theoretical T-RF (HaeIII) | Reference |
|---|---|---|---|---|
| **SRB3** (*n* = 2) | *Clostridium beijerinckii* NRRL B-598 (CP011966.2) | 99 | 302 | Unpublished |
| **SRB7** (*n* = 4) | *Desulfovibrio* (*Dv.*) *desulfuricans subsp. desulfuricans* strain Essex 6 (NR_104990.1) | 99 | 201 | Loubinoux et al., 2000 |
| **SRB8** (*n* = 3) | *Bacteroides caecigallinarum* strain C13EG153 (AB861982.1) | 89 | 266 | Saputra et al., 2015 |
| **SRB11** (*n* = 5) | *Propionicimonas paludicola* strain Wd (NR_104769.1) | 99 | 223 | Akasaka et al., 2003 |
| **SRB15** (*n* = 2) | *Clostridium beijerinckii* strain BAS/B3/I/124 (CP016090.1) | 98 | 300 | Unpublished |
| **SRB19** (*n* = 3) | *Clostridium beijerinckii* isolate DSM 6423 (LN908213.1) | 99 | 300 | Unpublished |

Most of the bacterial clones obtained were closely related to organisms already described at species level, and their theoretical T-RFs matched those found in T-RFLP analysis. For example, clones SRB3, SRB15 and SRB19 were 99% related to *Clostridium beijerinckii*, a genus known to include species that ferment glycerol and other substrates in anaerobic systems (Sanguanchaipaiwong and Leksawasdi, 2017). Clone SRB7 was 99% related to *Dv. desulfuricans* which is a known neutrophilic sulfate-reducing bacterium. The presence of another SRB in the system would explain the higher rates of sulfate reduction obtained during phases M25 and M50.

*7.3.2 Effects of combinations of ethanol and glycerol on the performance of an acidophilic sulfidogenic bioreactor*

The performance of the sulfidogenic bioreactor was tested using glycerol alone and in various combinations with ethanol (Table 7.3). Changes in HRTs in each phase (E0 - E100) are shown in Fig. 7.7. Major fluctuations were observed in the first 66 days of experiment, which included phases E0, E10 and first half of E25. From day 99, HRT values remained relatively constant with minor variations (between 4 and 9 h) during phases E50, E75 and E100.

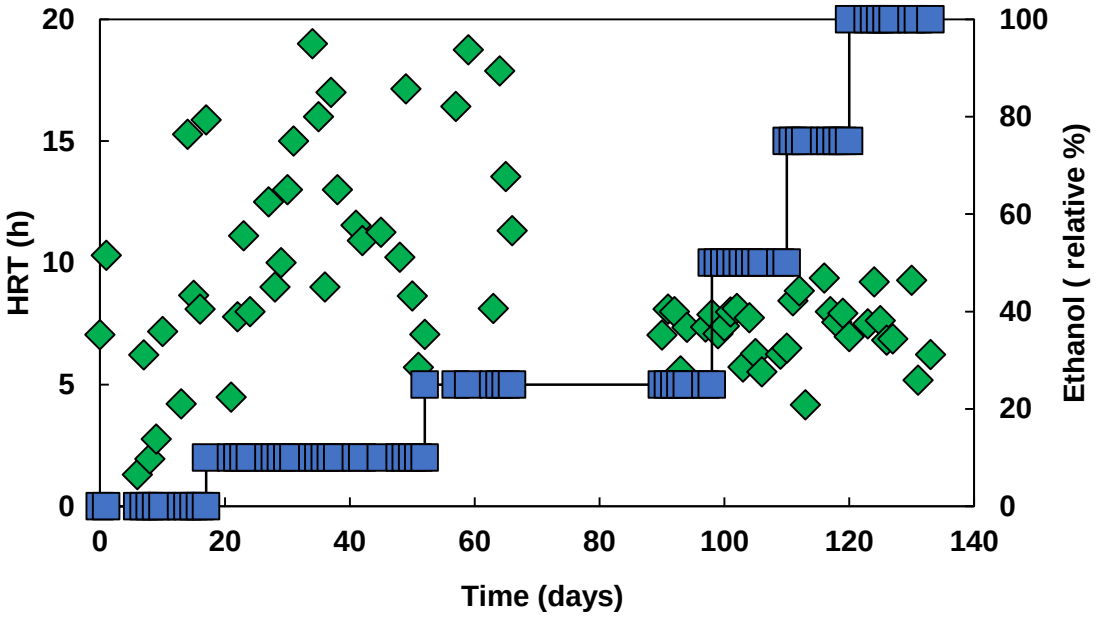


**Fig. 7.7.** Changes in HRTs (♦) with different relative percentages of ethanol (■) present in the feed liquor of the sulfidogenic bioreactor. Samples were not analysed in the interval between day 66 and day 90.

A progressive increase in mean rates of sulfate reduction and $H_2S$ production was found when relative concentrations of ethanol in the feed liquor were increased (Fig. 7.8). Average rates of sulfate reduction rates varied between 4.0 mmoles $L^{-1}$ $day^{-1}$ in phase E0 to ~ 30 mmoles $L^{-1}$ $day^{-1}$ during phase E100. Rates of $H_2S$ generation also followed a similar pattern of that observed for sulfate reduction rates and, in some cases, $H_2S$ generation rates were lower than that for sulfate reduction rates (also observed in the methanol/glycerol experiment; section 7.3.1).

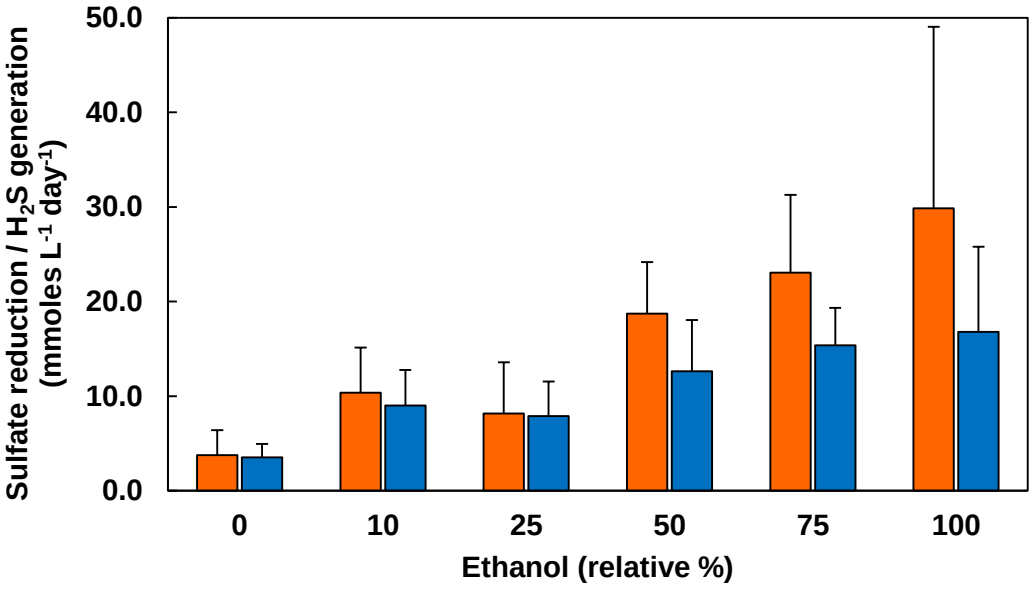


**Fig. 7.8.** Variations in rates of sulfate reduction (orange bars) and hydrogen sulfide generation (blue bars) in each combination of ethanol and glycerol studied.

Fig. 7.9 shows that acidophilic microorganisms of the aSRBR consumed over 99% of the ethanol provided in the influent liquor during all operational phases. In addition, over 99% of the glycerol provided was also consumed in the sulfidogenic bioreactor, though relatively high concentrations of acetate were produced, particularly in phase E100, where they reached up to ~ 7 mM (Fig. 7.10).

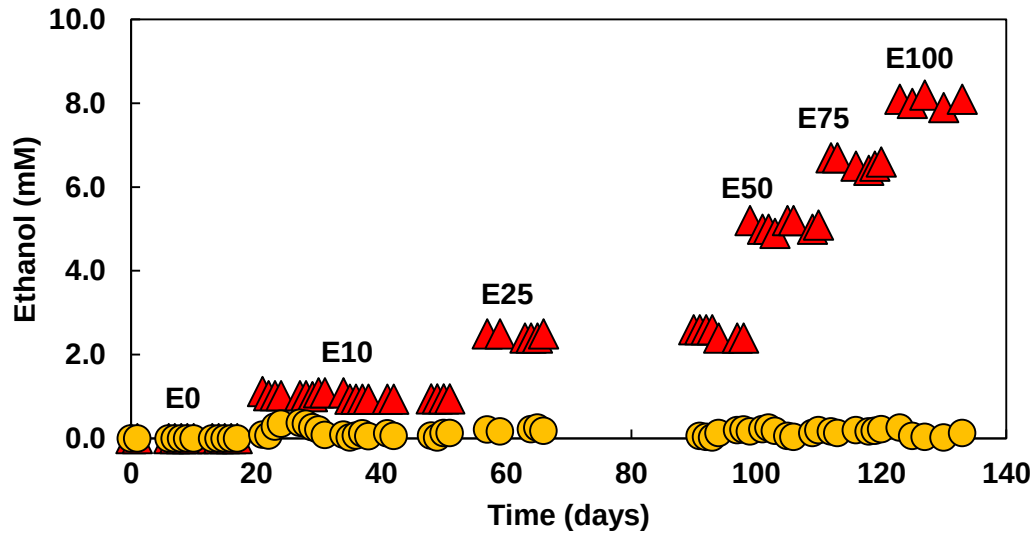


**Fig. 7.9.** Concentrations of ethanol in the influent (▲) and effluent (●) liquors of the sulfidogenic bioreactor. Samples were not analysed in the interval between day 66 and day 90.

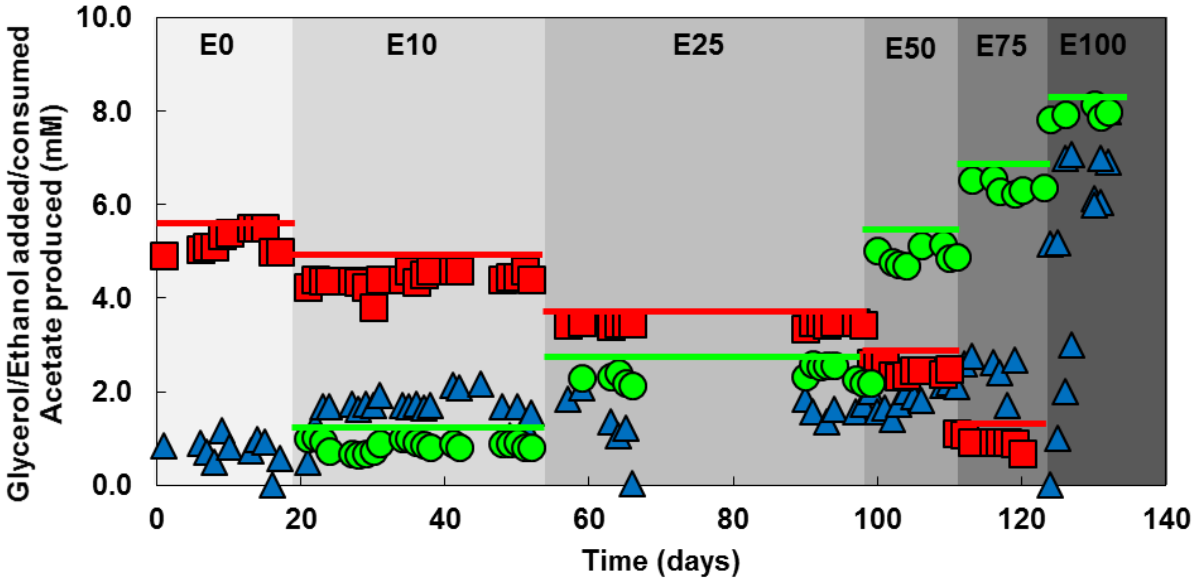


**Fig. 7.10.** Changes in concentrations of ethanol (●) and glycerol (■) consumed and acetate produced (▲) in the sulfidogenic bioreactor. Concentrations of ethanol and glycerol in the influent liquor in each phase are indicated by the green and red lines, respectively. Samples were not analysed in the interval between day 66 and day 90.

Figure 7.11 shows changes in relative abundance of members of the planktonic bacterial community of the aSRBR when ethanol was added to the feed. In phase E0, the most abundant bacterium was the *Actinobacterium* AR3 (230 nt), accounting for ~ 25% of the planktonic population in the bioreactor. The sulfate-reducing bacteria detected in this phase was *D. acididurans*$^{T}$ (215 nt) and the bacterium represented by clone SRB7 (201 nt; 99% related to *Dv. desulfuricans*) accounting for ~ 35% of the total bacteria. The facultative anaerobic bacterium *At. ferrooxidans* (254 nt) was also detected in this phase (~ 4%) plus the clones whose T-RFs matched those found in the T-RFLP analyses (Table 7.5).

Addition of ethanol to the feed liquor caused major shifts in the microbial population of the bioreactor (Fig. 7.11). Phases E10 and E25 show relatively similar profiles; however, an unknown T-RF (291 nt) was detected in low relative abundance (~ 3%). Sulfate-reducing bacteria (*D. acididurans* and *Dv. desulfuricans*) were detected in all phases with relative abundance varying between 15% (in E75) and 35% (in E50). The 416 nt T-RF (which had not been detected in previous experiments) was detected in all ethanol-containing feed liquors, though in low relative abundance. The 223 nt, 300 nt, 266 nt and 201 nt T-RFs correspond to the clones obtained from the clone library analysis described earlier (section 7.3.1.1). Two other new T-RFs were detected (291 nt and 416 nt), but no further analyses were carried out in order to identify these. The T-RFLP profile also shows a major shift from phases E0 - E50

to phases E75 - E100, where only ~ 10 - 20% of the planktonic bacterial population were sulfate-reducing bacteria.

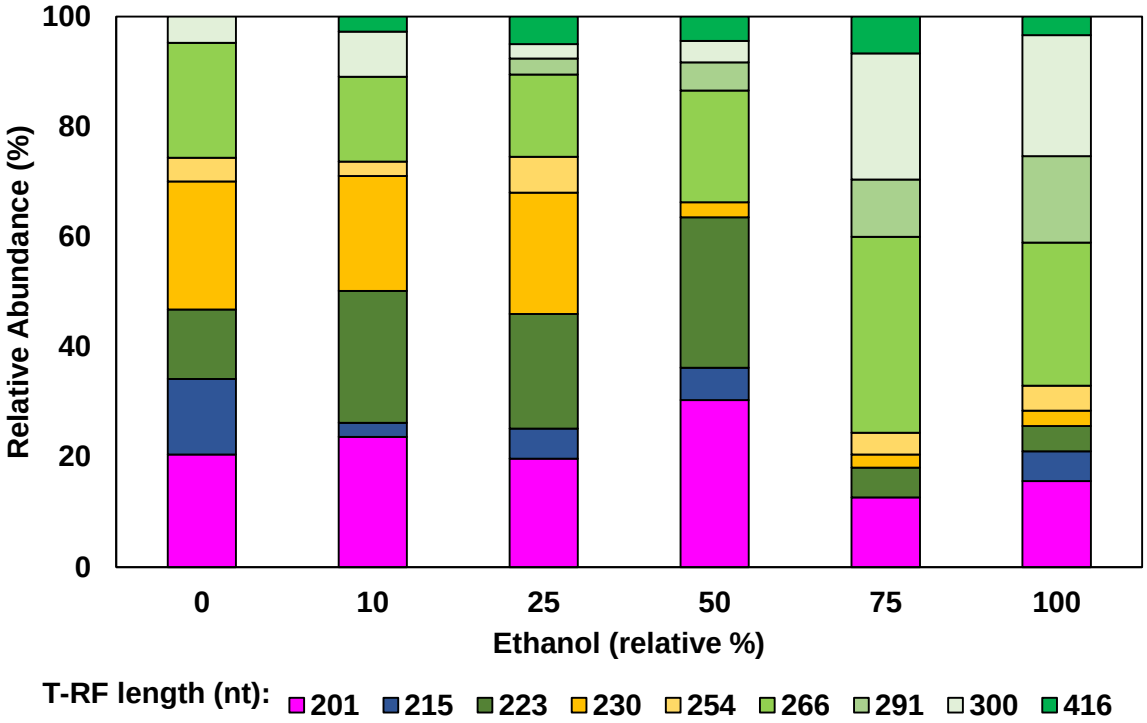


**Fig. 7.11.** Terminal restriction enzyme fragment length polymorphism (T-RFLP) analysis (HaeIII digests) of amplified 16S rRNA genes of planktonic bacterial communities in the aSRB reactor fed with different combinations of ethanol and glycerol. Shades of blue represent known sulfate-reducing *Firmicutes* (215 nt, *D. acididurans*), shades of yellow/orange represent non-sulfidogens (230 nt, *Actinobacterium* AR3; 253 nt, *At. ferrooxidans*), shades of green represent bacterial clones identified as probable non-sulfidogens and the magenta bars represent clone SRB7 (201 nt; *Dv. desulfuricans*).

*7.3.3 Ethanol as an alternative electron donor for sustaining low pH sulfidogenic bioreactors*

The performance of the aSRBR using only ethanol as electron donor was tested by progressively decreasing its operational pH value. When operated at pH 5.5, the bioreactor showed minor variations in HRT (between 5 and 9 h; Fig. 7.12). Once the pH of the bioreactor was lowered to 5.0 (day 9), an increase in HRT was observed, which was followed by a gradual decline, stabilizing at ~ 9 h. At pH 4.5, HRT increased from an average of 9 h (day 21 to day 31) up to 35 h towards the end of this phase. Major fluctuations in HRTs were observed at pH 4.0, ranging from 11 to 36 h.

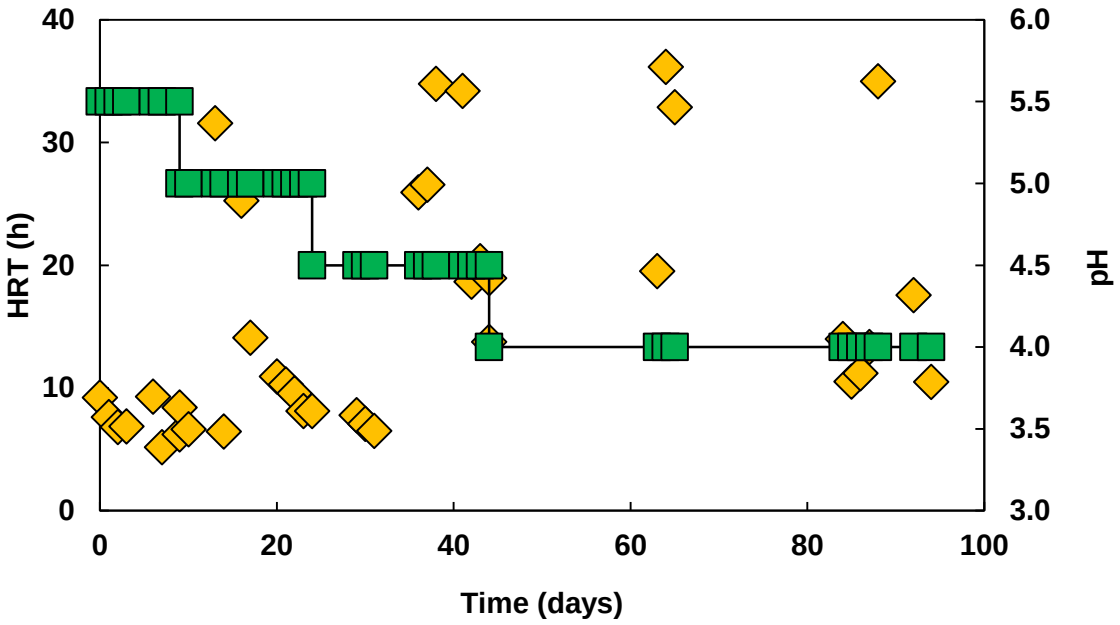


**Fig. 7.12.** Variations in HRTs (♦) at different operational pH values (■) of the sulfidogenic bioreactor.

A gradual decline in average values of rates of sulfate reduction and $H_2S$ production was found when lowering the pH of the bioreactor (Fig. 7.13). Average rates of sulfate reduction rates varied between 30 mmoles $L^{-1}$ $day^{-1}$ at pH 5.5 to ~ 12 mmoles $L^{-1}$ $day^{-1}$ at pH 4.0. Rates of $H_2S$ production (determined from rates of off-line copper precipitation) were relatively lower than that measured for sulfate reduction, though a similar trend was followed.

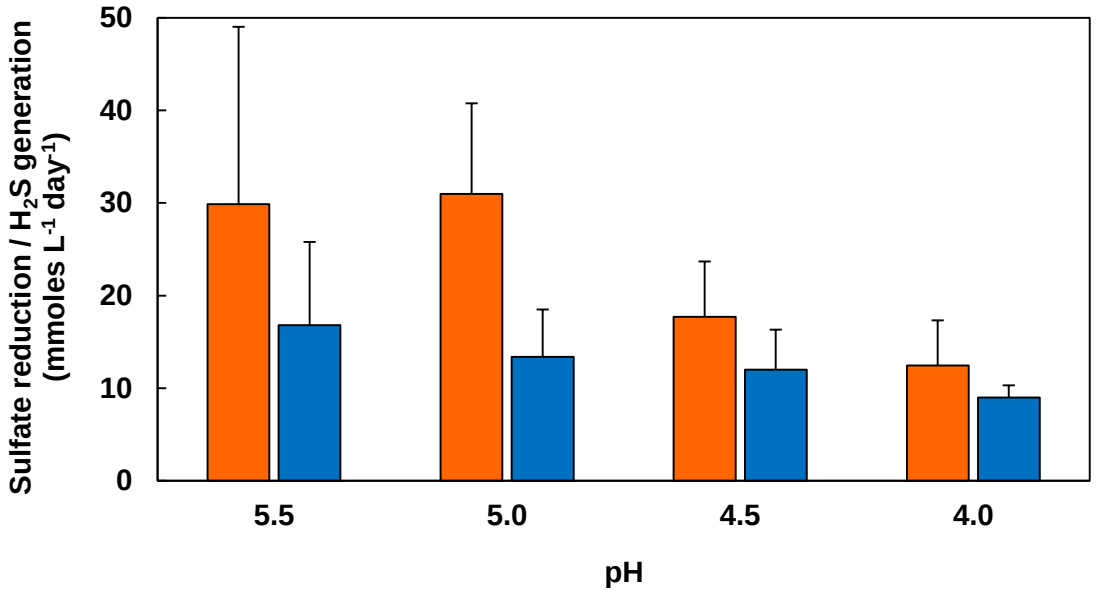


**Fig. 7.13.** Variations in rates of sulfate reduction (orange bars) and hydrogen sulfide generation (blue bars) in the aSRBR when fed with ethanol alone and varying operational pH.

Fig. 7.14 shows the consumption of ethanol throughout this experiment. The bacterial community housed in the aSRBR consumed over 99% of the ethanol provided in the influent liquor at all pH values tested.

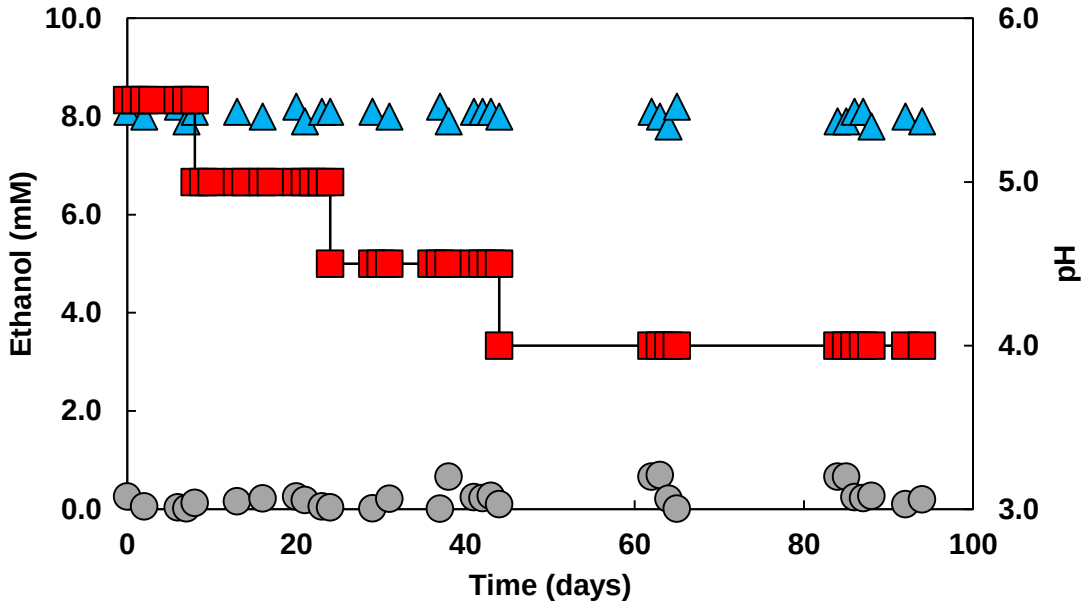


**Fig. 7.14.** Changes in pH (■) and concentrations of ethanol in the influent (▲) and effluent (●) liquors of the sulfidogenic bioreactor.

Acetate production increased progressively at pH 5.5 reaching up to ~ 8 mM, followed by a subsequent decrease (~ 5 mM) when the bioreactor pH was lowered to 5.0 which increased again reaching up to ~ 7 mM by day 21. At pH 4.5, concentrations of acetate in the effluent liquor declined and stabilized at ~ 4.5 mM. Lower concentrations of acetate were measured at pH 4.0, ranging between 3.5 and 4.5 mM (day 62 to day 85). From day 86 onwards, concentrations of acetate increased slightly, reaching up to ~ 6.0 mM.

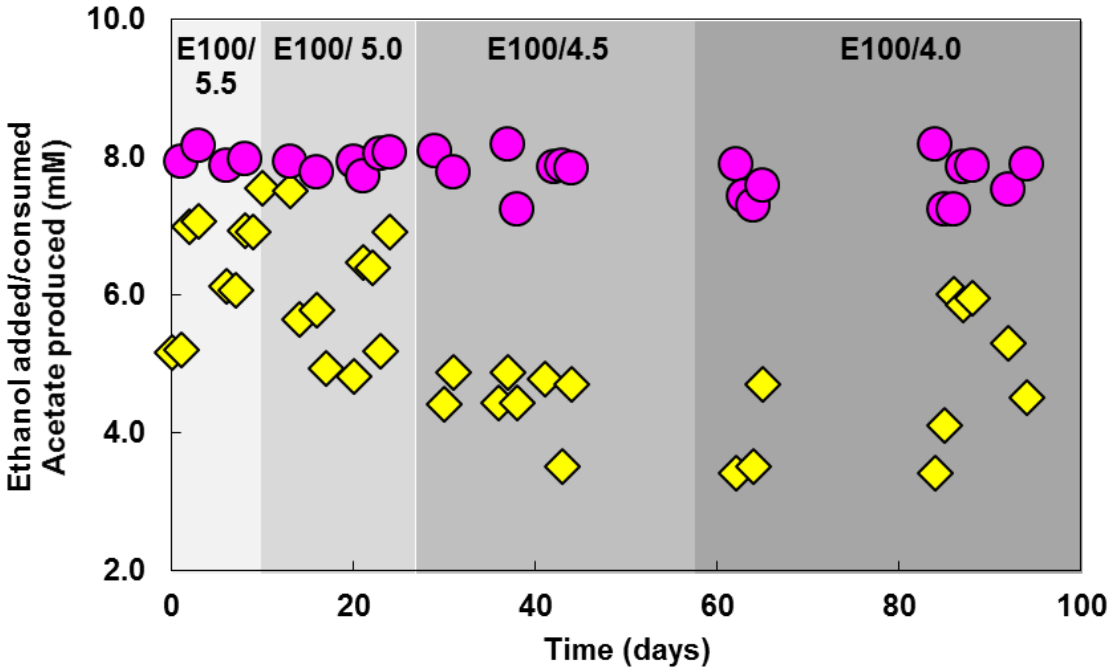


**Fig. 7.15.** Changes in concentrations of ethanol consumed (●) and acetate produced (♦) in the sulfidogenic bioreactor. The concentration of ethanol in the feed liquors remained at 8 mM throughout the experiment.

Figure 7.16 shows changes in relative abundance of the planktonic bacterial community of the aSRBR when the bioreactor pH was lowered gradually to 4.0. In phase E100/5.5 the most abundant member in bacterial community was the bacterium represented by clone SRB8 (266 nt; 89% related to *Bacteroides caecigallinarum*), which accounted for ~ 25% of the planktonic population in the bioreactor. A major shift regarding both sulfate-reducing bacteria (201 nt and 215 nt) was observed. *Desulfovibrio desulfuricans* (201 nt; clone SRB7) showed a higher relative abundance at pH 5.5 (~ 16%) which declined when the pH was lowered (~ 9% at pH 4.0). The opposite trend was observed for *D. acididurans*$^{T}$ (215 nt). An increase in the relative abundances of both *At. ferrooxidans* (254 nt) and the *Actinobacterium* AR3 (230 nt) occurred when pH was incrementally lowered. Other T-RFs did not show major differences in response to lowering the pH of the bioreactor.

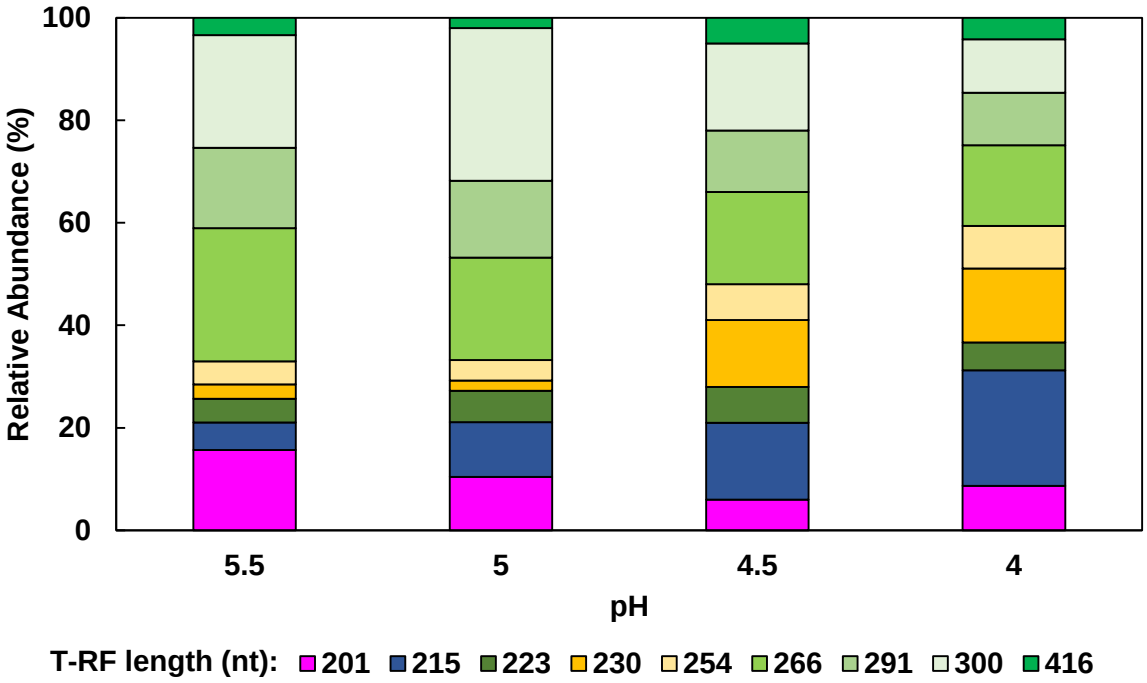


**Fig. 7.16.** Terminal restriction enzyme fragment length polymorphism (T-RFLP) analysis (HaeIII digests) of amplified 16S rRNA genes of planktonic bacterial communities in the aSRB reactor fed with 100% ethanol, at different pH values. Shades of blue represent known sulfate-reducing *Firmicutes* (215 nt, *D. acididurans*), shades of yellow/orange represent non-sulfidogens (230 nt, *Actinobacterium* AR3; 253 nt, *At. ferrooxidans*), shades of green represent bacterial clones identified as probable non-sulfidogens and the magenta bars represent clone SRB7 (201 nt; *Dv. desulfuricans*).

### *7.3.4 Visual examination of the bioreactor population and isolation of Dv. desulfuricans*

Liquid samples from the bioreactor were withdrawn regularly in order to visually examine the bacterial cells present using a phase-contrast microscope (section 2.10.2). Very motile vibrioid cells were observed in most samples, which were thought to correspond to clone SRB7 (*Dv. desulfuricans*) identified in the clone library analysis. To isolate this bacterium, modified aSRB overlay plates (pH 4.0) containing 5 mM ethanol and 2.5 mM glycerol (section 2.2.2.3) were prepared and streak inoculated with liquid samples from the aSRBR. A smear-like growth on the agar surface was obtained, but no isolated colonies. Microscopic examination of a sample of this growth again confirmed the presence of highly motile vibrioid cells. Time constraints meant that no further steps were taken at the time to purify and sequence the isolate to confirm (as seems highly likely) that it was a strain of *Dv. desulfuricans*.

## 7.4 Discussion

The application of technologies that use sulfate-reducing bacteria to remediate metal-rich contaminated wastewaters has been the focus of a large amount of research and development. These microorganisms have been isolated from a wide range of anoxic environments, in which they play important roles in the sulfur and carbon cycles (Suzuki et al., 2007). In remediation processes, the choice of substrate used to fuel biosulfidogenesis depends mainly on local availability and costs, since SRB are able to use various compounds as electron donors, such as $H_2$, alcohols, amino acids and sugars (Chapter 1).

Experimental work described in this chapter examined the effects of combining small molecular weight ($C_1$ – $C_3$) alcohols on the performance of an acidophilic sulfidogenic bioreactor used to remediate acid mine drainage. The performance of the aSRBR was initially negatively impacted by the addition of 10% methanol (1.5 mM) to the feed liquor, with rates of sulfate reduction rates (SRR) being 75% lower than that obtained using glycerol alone. This was possibly caused by partial inhibition of aSRB activity when first exposed to methanol. The aSRBR recovered with time (probably as a result of adaptation) and an increase in SRR were observed in the following phases (M25 and M50), though in phase M75 a dramatic decline in SRR was observed, suggesting that, at this concentration (12 mM), methanol may have a more toxic effect on the microbial population. Standard deviations were large in some cases, which reflected, in part, the time taken for the system to reach equilibrium after varying the concentration of glycerol and methanol in the feed liquor. Analysis of methanol concentrations in the effluent liquor showed that the microbial community did not appear to have consumed this alcohol, since these were similar in the effluent liquor to those present in the feed liquor. Sulfate reduction obtained in this experiment was therefore coupled mostly to glycerol oxidation (with a possible small contribution from some components of yeast extract), concentrations of which were incrementally lowered as the experiment continued.

Comparison between SRR and $H_2S$ production (determined from rates of off-line copper precipitation) showed that there were large discrepancies in most cases, with SRR often being much greater than rates of $H_2S$ production. Possible reasons for this include: (i) the sulfidogenic system may have not been fully sealed, allowing hydrogen sulfide to leak through other compartments which were not connected to the off-line vessel and (ii) partial chemical re-oxidation of $H_2S$ (possibly to elemental sulfur) may have occurred within the bioreactor due to the presence of trace amounts of oxygen in the system.

Glycerol was readily consumed by the microbial population throughout the experiment, though it may not have been all used for sulfate reduction, since some members of the bacterial population in the bioreactor are known to ferment glycerol (Chapter 4). Acetate was

detected in most phases of this experiment, particularly in M10, reaching up to 3 mM, as a consequence of incomplete oxidation of glycerol (Chapter 3 and 4). Concentrations of acetate fell in M75 (to ~ 0.5 mM) as SRR declined.

Analyses of the bacterial community by T-RFLP showed a major change in terms both of microorganisms present and their relative abundance occurred when methanol-containing feed liquors were introduced to the system. Two new T-RFs were detected in phase M10 and two more in phases M25, M50 and M75. All four were identified from clone library analysis. These were: a sulfate-reducing bacterium (SRB7: *Dv. desulfuricans*); a strictly anaerobic bacterium (SRB3, SRB8 and SRB9: *Clostridium beijerinckii*) which ferments glycerol to acetate (Sanguanchaipaiwong and Leksawasdi, 2017); a facultatively anaerobic, Gram-positive bacterium (SRB11: *Propionicimonas paludicola*, strain Wd), which also ferments glycerol to acetate but does not utilize methanol or ethanol (Akasaka et al., 2003). The closest relative to clone SRB15 was *Bacteroides caecigallinarum* strain C13EG153 (89% gene sequence similarity), an anaerobic Gram-negative rod-shaped bacterium which does not ferment glycerol (Saputra et al., 2015). Utilization of methanol or ethanol by this bacterium has not been reported, but since it is only very distantly related to clone SRB15 (and probably a different genus) nothing definite can be inferred about the physiology of this clone.

The consortium of microorganisms used in the aSRBR contained pure cultures of aSRB plus an enrichment culture of an anaerobic streamer mat from the abandoned Cantareras copper mine in Spain (Chapter 2). Even though T-RFLP analyses had failed to detect these "new" T-RFs in previous experiments, it is highly likely that this original enrichment culture contained these organisms, which in turn were present in the bioreactor, though in very low abundance up until the time that the experiments described in this chapter were initiated. Interestingly, their relative abundance was detected only when methanol was added to the system, even though they do not appear to metabolise this compound. *Acidocella* (*Ac.*) *aromatica* PFBC, an acidophilic heterotrophic bacterium that grows in co-culture with acid-tolerant sulfidogenic bacteria by metabolising acetate generated from the incomplete oxidation of glycerol (Kimura et al., 2006) was added to the aSRBR consortium in previous experiments (Chapter 4). In this experiment, which was carried out at pH 5.5, *Ac. aromatica* was not detected in the bioreactor, which is thought why concentrations of acetate increased to ~ 3.0 mM. The pH is the most likely reason for that, since *Ac. aromatica* has an optimum pH of 3.8 and grows between pH 2.5 and 5.0 (Jones et al., 2013).

The combined use of glycerol and methanol for sulfate reduction showed that, even though methanol was not metabolised by the microorganisms, sulfate reduction occurred at relatively high rates, and that methanol concentrations of up to 12 mM did not inhibited

sulfidogenesis, suggesting that crude glycerol (by-product of biodiesel production that contains methanol) could be used directly without costly refining processes.

In contrast to results using combined methanol and glycerol, the addition of both ethanol and glycerol as electron donors in the influent liquor resulted in a progressive increase in terms of SRR, even when the aSRBR was being fed only with ethanol (8 mM). Average sulfate reduction rates in this phase (E100 at pH 5.5) were ~ 8-fold greater than that using glycerol alone (E0 at pH 5.5). Large discrepancies in terms of SRR and $H_2S$ production rates were also observed in this experiment, possibly for the same reasons described earlier. Analysis of the effluent liquor showed that over 99% ethanol present in the feed liquor was consumed by the microbial community of the bioreactor throughout the experiment, particularly in phase E100/5.5 in which ethanol was the sole electron donor (together with possible minor contributions from some components of yeast extract) confirming that ethanol was used as electron donor to fuel sulfate reduction.

Both glycerol and ethanol were readily metabolised by the bacterial population in the bioreactor in all phases of this experiment. Concentrations of acetate in the effluent liquor increased as both ethanol concentrations in the feed liquor and SRR increased, reaching up to 8 mM in phase E100 at pH 5.5. This was considered to be mainly caused by incomplete oxidation and fermentation of both glycerol and ethanol. Both *D. acididurans* and *Dv. desulfuricans* are known for incomplete oxidation of glycerol and ethanol, respectively (Sen and Johnson, 1999; Mechalas and Rittenburg, 1960). The generation of organic acids, such as acetic acid, in sulfidogenic systems are potentially toxic to the microbial community depending on their concentration and dissociation constants. Since the pH of the aSRBR was set to 5.5 and the p$K_a$ of acetic acid is 4.75, which infers that ~ 85 % of the total acetic acid/acetate in the effluent was present as anionic acetate and only ~ 15 % as non-dissociated acetic acid, the performance of the bioreactor was not negatively impacted by the potential toxicity of acetic acid.

Analyses of the bacterial community in the planktonic phase showed that *Dv. desulfuricans*, which can metabolise both glycerol (Alico and Liegey, 1966) and ethanol (Nagpal et al., 2000), was the most abundant SRB detected in the bioreactor throughout this experiment. The relative abundance of *D. acididurans* declined as glycerol concentrations in the feed liquor were lowered. *D. acididurans* has been reported not to use ethanol as electron donor (Sánchez-Andrea et al., 2015), though the situation with strain M1 is more ambiguous (Sen, 2001). One possible reason for the dominance of *Dv. desulfuricans* is that this SRB grows more rapidly than *D. acididurans* on ethanol, particularly at higher pH values.

Unidentified T-RFs were also detected when most ethanol-containing feed liquors were used (291 nt and 416 nt) and further investigations are needed in order to identify these bacteria. In phases E75 and E100/5.5, the relative abundance of known SRB (*D. acididurans* and *Dv. desulfuricans*) in the bioreactor was relatively low (~ 20%) even though high SRR were obtained at these times.

Several studies have reported ethanol utilization by sulfate-reducing bacteria at circum-neutral pH (Bryant et al., 1977; Widdel, 1988; Nagpal et al., 2000; Suzuki et al., 2007) and the use of this alcohol to fuel biosulfidogenesis (at pH 6 - 9) for remediating acid mine drainage (Barnes et al., 1991; Zaguty et al. 2006). Though, little is known about sulfate-reducing bacteria utilizing ethanol at low pH and, therefore, the performance of the sulfidogenic bioreactor, fed with ethanol, was tested by incrementally lowering its pH.

Sulfate reduction rates at pH 4.0 declined by ~ 60% to that obtained at pH 5.5, even though 99% ethanol was consumed in all phases. The reason could be that ethanol was being consumed at slower rates, causing HRTs to increase, which, in turn, negatively impacted SRR. Concentrations of acetate also declined slightly, corroborating the low SRR obtained at lower pH, since its generation is co-dependent of incomplete oxidation of ethanol. As the bioreactor pH was lowered, the relative concentration of acetic acid would have increased (due to its dissociation equilibrium) and, at pH 4.0, ~ 85% of the total acetic acid/acetate in the effluent would have been present as non-dissociated acetic acid, which would have negatively impacted microorganisms present in the aSRBR, and possibly some species more so than others. The microbial community analyses of this experiment mainly showed that the relative abundance of *Dv. desulfuricans* declined at lower pH. This species has been reported to grow optimally at pH 7.8 (Alico and Liegey, 1966). On the other hand, the relative abundance of *D. acididurans* increases at lower pH, possibly for the same reason, since this bacterium has been reported to show relatively high growth rates at pH 4.0 (Sánchez-Andrea et al., 2015).

In conclusion, combinations of glycerol and ethanol and ethanol alone showed high rates of sulfate reduction, but slightly lower rates with ethanol alone at lower pH. These results suggest the possibility of using different small molecular weight alcohols (either alone or in combination) as electron donors for low pH biosulfidogenesis systems used to remediate metal-rich wastewaters.

# Characterisation of two acidophilic microalgae and their potential use as feedstock for sulfidogenic bioreactors

8

## 8.1 Introduction

Microbial treatment of acid mine drainage (AMD) by sulfate-reducing bacteria (SRB) has considerable advantages over conventional remediation strategies since the solid-phase metal sulfides generated can be recovered and recycled. However, most acidic mine waters contain relatively low concentrations (< 20 mg $L^{-1}$) of dissolved organic carbon (DOC), and to accentuate the activities of heterotrophic microorganisms (such as SRB) in these oligotrophic environments organic carbon compounds need to be supplemented.

Primary production in AMD sites that receive sunlight is mediated by both phototrophic and chemolithotrophic acidophiles (Johnson and Aguilera, 2015). The majority of acidophilic phototrophs are eukaryotic microalgae (filamentous and unicellular forms and diatoms). Aguilera et al. (2007) listed microalgal phyla that have been found to be metabolically active in highly-acidic metal-rich environments. These included *Chlorophyta* (e.g. *Chlamydomonas acidophila* and *Dunaliella acidophila*), *Chrysophyta* (e.g. *Ochromonas* sp.) and *Euglenophyta* (e.g. *Euglena mutabilis*). Macroscopic growths of acidophilic algae have been reported in various streams and rivers, for example, the Iberian Pyrite Belt (IPB) in South-western Spain. Rowe et al. (2007) described an open drainage channel receiving AMD at an abandoned copper mine (Cantareras) in the IPB. This channel contained a stratified (~12 cm thick) microbial mat, the surface of which was populated with acidophilic algae and lower zones dominated by heterotrophic acidophiles, including species of ferric iron- and sulfate-reducing bacteria, suggesting that acidophilic algae can provide organic materials (e.g. monosaccharides) that are metabolised by iron- and sulfate-reducing heterotrophic acidophiles in natural and man-made acidic environments.

Ñancucheo and Johnson (2012b) reported that strains of two species of acidophilic algae, *Chlorella protothecoides* var. *acidicola* and *Euglena mutabilis*, which had been isolated from abandoned copper mines in Spain and Wales, produced small molecular weight organic compounds (including glycolic acid, fructose and glucose) that were rapidly consumed by acidophilic iron-reducing heterotrophic bacteria, such as *Acidiphilium* and *Acidobacterium* spp.. Elsewhere, Ñancucheo and Johnson (2011) showed that sulfidogenesis was far more

pronounced in mineral tailings mesocosms that were inoculated with the same two acidophilic algal cultures and aSRB, than in those inoculated with aSRB alone.

The low pH sulfidogenic bioreactors developed at Bangor University are usually operated using glycerol as primary carbon- and energy-source. The effect of alternative substrates, such as methanol and ethanol, on rates of sulfate reduction in low pH bioreactor modules was evaluated as part of this thesis (Chapter 7). However, little is known regarding the use of algal biomass and its exudates to fuel sulfate reduction in bioreactor systems. This chapter describes two species of acidophilic microalgae isolated from mine sites and their potential use for providing suitable electron donors for biosulfidogenesis at low pH.

## 8.2 Physiological characterisation of acidophilic algal isolates AC1 and ITV

### *8.2.1 Materials and methods*

#### 8.2.1.1 Isolation and cultivation of the algal cultures

Strains AC1 and ITV were isolated, respectively, from a metal mine pit lake in South-west Spain (by Dr. Carmen Falagán, Bangor University, UK) and a copper mine stream in Northern Brazil (by colleagues at the Vale Technological Institute, state of Pará, Brazil). Isolate AC1 was purified as an axenic algal culture by repeated single colony isolation on an acidic basal salts (ABS) and trace elements (TE) solid medium at pH 3.0, supplemented with ferrous sulfate (0.5 mM final concentration). Isolate ITV was provided as a pure culture (confirmed as such at Bangor University). Purity of both isolates was tested by extracting DNA, amplifying the 18S rRNA genes using EukF and EukR primers (section 2.9.2) and analysing with both T-RFLP (section 2.9.4) and sequencing (section 2.9.5.4). Amplification of bacterial and archaeal 16S rRNA genes were also carried out to confirm purity of the algal cultures (section 2.9.2).

Both acidophilic microalgae were grown in axenic cultures and sub-cultured routinely in basal salts and trace elements liquid medium (section 2.2.2.1), amended with ferrous sulfate solution at a final concentration of 100 µM. The liquid medium pH was adjusted to 3.0 with sulfuric acid for strain AC1 and to 2.5 for strain ITV cultures. Shake flasks were incubated at 25°C in an illuminated shaking incubator at 50 rpm (Innova® 43, New Brunswick Scientific, UK).

8.2.1.2 Effects of pH and temperature on growth rates of the algal isolates

Strains AC1 and ITV were grown in ABS/TE liquid medium in a 2 L (working volume) FerMac 200 modular bioreactor shrouded in an LED-light unit set at 25% maximum light intensity, under constant illumination (ElectroLab Biotech, UK), as shown in Fig. 8.1. The bioreactor was fitted with pH and temperature control and stirred at 100 rpm. To determine the effects of pH on the growth of each isolate, cultures were grown at a fixed temperature of 25°C and varying pH (2.5 - 5.5 for isolate AC1, and 1.5 - 3.0 for isolate ITV). Samples were withdrawn at regular intervals and algal cells enumerated using a Thoma counting chamber and viewed with a Leitz Labolux phase contrast microscope (section 2.10.2.1).

Once the optima growth pH had been determined, the effect of temperature was evaluated by maintaining the bioreactor pH at the optima values for the two microalgae (by automated addition of 0.1 M $H_2SO_4$ or 0.1 M NaOH) and the set temperature varied between 17 and 30ºC for isolate AC1, and between 17 and 25ºC for isolate ITV. Culture doubling times were determined from semi-logarithmic plots of number of cells against time. After each experimental run algal biomass was collected, harvested by centrifugation (6,000 x *g* for 40 min at 4ºC) and stored at - 20ºC.

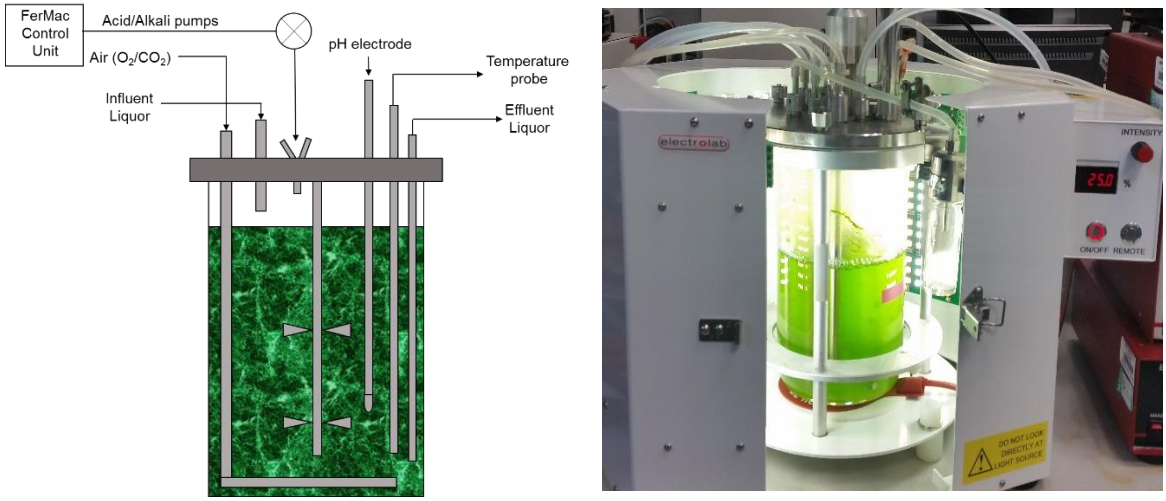


**Fig. 8.1.** Schematic representation of the acidophilic algae bioreactor (left) and image of the actual system (right). Arrows indicate the direction of liquid/gas flow.

8.2.1.3 Determination of tolerance to transition metals, aluminium and sodium chloride

The ability of the isolates to tolerate elevated concentrations of some transition metals and aluminium was tested by adding different concentrations of the metals (as their sulfate salts) to the growth medium (ABS/TE at pH 4.0 for isolate AC1 and at pH 2.5 for isolate ITV),

inoculated with 5% (v/v) active culture of each alga and incubated in shaker for one week at 25ºC under constant illumination. Metal-free control cultures were set up in parallel for both algal isolates. Numbers of cells were enumerated using a Thoma counting chamber, as described previously. Similarly, salt (NaCl) tolerance was tested by supplementing ABS/TE medium with different concentrations of sodium chloride. Parallel controls were carried out without addition of NaCl.

8.2.1.4 Effect of osmotic stress on growth rates of isolates AC1 and ITV and assessment of osmo-protectant production

Algal cultures were grown in a 2 L (working volume) bioreactor under constant illumination (Fig. 8.1). The liquid medium contained ABS/TE solution, ferrous iron at a final concentration of 100 µM, and different concentrations of magnesium sulfate (0 - 600 mM). The effect of osmotic stress on growth rates of both algal isolates was determined under optimum growth conditions of pH and temperature (pH 4.0 and 25ºC for isolate AC1 and pH 2.5 and 22.5ºC for isolate ITV). Samples were withdrawn at regular intervals and algal cells enumerated using a Thoma counting chamber and viewed with a Leitz Labolux phase contrast microscope (section 2.10.2.1). Culture doubling times were determined from semi-logarithmic plots of cell numbers against time. After each experimental run algal biomass was collected, harvested by centrifugation (6,000 x *g* for 40 min at 4ºC) and stored at - 20ºC.

To get an approximate assessment of the production and accumulation of small molecular weight osmo-protectants, produced as a result of osmotic stress, a hypo-osmotic shock approach was used (Galleguillos et al., 2018). Algal biomass grown under osmotic stress (i.e. in the presence of elevated concentrations of $MgSO_4$) and harvested by centrifugation as described previously, was re-suspended in sterile ultrapure water at pH 4.0 for AC1 and pH 2.5 for ITV. This approach was devised to induce cells to expel small molecular weight osmo-protectants in response to them being immersed in low osmotic strength solutions. Algal biomass slurries were maintained at room temperature without agitation for 3 hours. Samples from the algal biomass slurries (1 mL) were collected aseptically at regular intervals, filtered through 0.2 µm pore size membrane filters and concentrations of dissolved organic carbon determined (section 2.8).

8.2.1.5 Identification and phylogenetic analysis of algal isolates AC1 and ITV

Active algal cultures were filtered (~20 mL) through 0.2 µm pore size nitro-cellulose membrane filters. The filtrates were discarded and membranes containing trapped cells used

for DNA extraction (section 2.9.1.2). The 18S rRNA genes of the isolates were amplified using the primers Euk F and EUk R (section 2.9.2), sequenced and compared with those in the GenBank database (section 2.9.5.4). Phylogenetic tree was generated using neighbour-joining analysis, as described in section 2.9.6.

*8.2.2 Results*

Both algal isolates grew in liquid medium producing cultures with a bright green colour. Morphological examination showed that AC1 formed elongated ovoid shape (~1-3 µm wide and ~4-7 µm long), non-motile cells, while those of ITV cells were spherical (~3-7 µm diameter) with single parietal chloroplast and also non-motile (Fig. 8.2).

The effects of pH and temperature on the growth rates of strains AC1 and ITV are shown in Fig. 8.3. Isolate AC1 grew between 17ºC and 30ºC, and optimally at 25ºC. This isolate grew between pH 2.5 and 5.5, and optimally at pH 4.0; no growth was obtained at pH 2.0, and growth above pH 5.5 was not tested. Under optimum growth conditions, this acidophilic alga had a culture doubling time of 21 h. Isolate ITV grew within a temperature range of 20ºC and 25ºC and optimally at ~ 22.5ºC. No growth was obtained at 30ºC, and growth below 20ºC was not tested due to time constraints. This isolate grew between pH 1.8 and 3.0, and optimally at pH 2.5; growth rates below pH 1.8 and above 3.0 were not tested. Under optimum growth conditions, isolate ITV had a culture doubling time of 18 h.

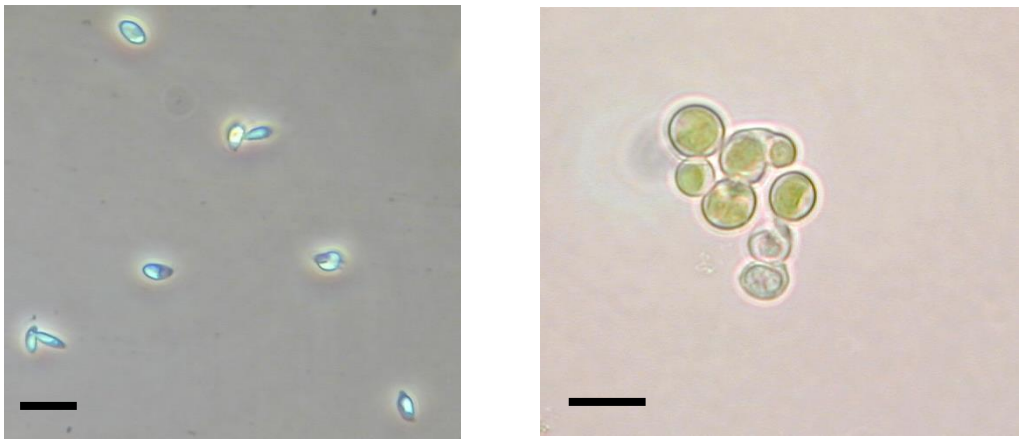

**Fig. 8.2.** Phase contrast microscopy of isolates AC1 (left) and ITV (right). The scale bar represents 10 µm in both images.

Microscopic examination showed that bacterial cells, as well as eukaryotic cells, were present in cultures of AC1, confirming that it was originally a mixed culture rather than a pure algal culture. T-RFLP analysis of amplified bacterial 16S rRNA genes showed a single restriction fragment, corresponding to *Acidiphilium cryptum*, based on the Bangor database.

Concentrations of dissolved organic carbon (DOC) in the mixed culture were very small (0.86 mg $L^{-1}$) and analysis failed to detect any identifiable organic compounds. This was presumably due to the fact that readily-metabolised DOC derived from the alga as exudates or lysates had been utilised by the heterotrophic bacteria present. A pure culture of isolate AC1 was successfully obtained by repeated single colony isolation, confirmed by microscopic examination and attempts to amplify bacterial and archaeal 16S rRNA genes in the algal culture were proved negative.

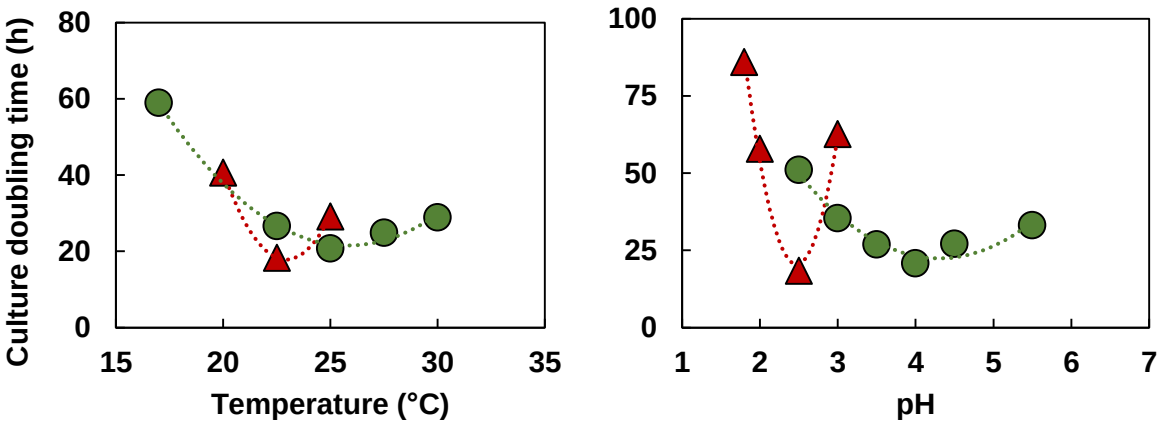


**Fig. 8.3.** Effect of temperature (left) and pH (right) on culture doubling times of algal isolates AC1 (●) and ITV (▲) in a bioreactor. The line shown is the best fit based on polynomial analysis of the data.

Table 8.1 shows the minimum inhibitory concentrations (MIC) of some metals on the growth of both algal isolates. Isolate AC1 grew in media containing 10 mM of either aluminium or nickel (MIC = 50 mM). It was more tolerant of zinc (MIC = 100 mM), though more sensitive to copper (MIC = 25 mM at pH 4). In terms of salt tolerance, isolate AC1 grew in media supplemented with 300 mM NaCl, though it was inhibited by 500 mM NaCl. Isolate ITV showed greater tolerance to nickel, zinc and aluminium (Table 8.1) but was more sensitive to NaCl (MIC = 200 mM at pH 4) than isolate AC1.

It has been reported that metal and salt tolerance in acidophilic microorganisms are pH-dependent (Falagán and Johnson, 2018). To test this hypothesis, liquid media were prepared at both pH 2 and 4 and supplemented with either copper (II) sulfate or sodium chloride. Table 8.1 shows that the isolate ITV grew in much higher concentration of copper (II) at pH 2 (50 mM) than that at pH 4 (5 mM) and the opposite trend was observed for NaCl, where the isolate showed greater tolerance to sodium chloride at higher pH (MIC = 200 mM).

Shake flasks experiments showed that isolate AC1 grew in medium supplemented with 600 mM $MgSO_4$, though it was totally inhibited by 800 mM $MgSO_4$, whereas isolate ITV grew

in medium containing 200 mM $MgSO_4$, but it was partially inhibited by 400 mM $MgSO_4$. Culture doubling times of strains AC1 and ITV increased considerably when concentrations of magnesium sulfate were also increased (Fig. 8.4). Concentrations higher than 600 mM for AC1 and 200 mM for ITV were not tested, since these were determined to be the highest concentration at which growth was observed for each culture. Isolate AC1 had a culture doubling time of ~ 20 h in medium without additional $MgSO_4$ and ~ 50 h in medium containing 600 mM $MgSO_4$. The culture doubling time for isolate ITV in medium without additional $MgSO_4$ was ~ 19 h and 60 h in medium containing 200 mM $MgSO_4$.

**Table 8.1.** Minimum inhibitory concentrations (MICs) of some metals and sodium chloride on the growth of the isolates AC1 and ITV. Numbers in parentheses are the highest concentrations at which growth of the isolates was observed. Concentrations are expressed in mM.

| Metals / Salts | AC1 | ITV |
|---|---|---|
| **Cu (II) pH 2** | n.d. | 100 (50) |
| **Cu (II) pH 4** | 25 (5) | 10 (5) |
| **Ni (II)** | 50 (10) | 100 (50) |
| **Zn (II)** | 100 (50) | 150 (50) |
| **Al (III)** | 50 (10) | 100 (25) |
| **NaCl pH 2** | n.d. | 10 (5) |
| **NaCl pH 4** | 500 (300) | 200 (100) |

n.d. not determined.

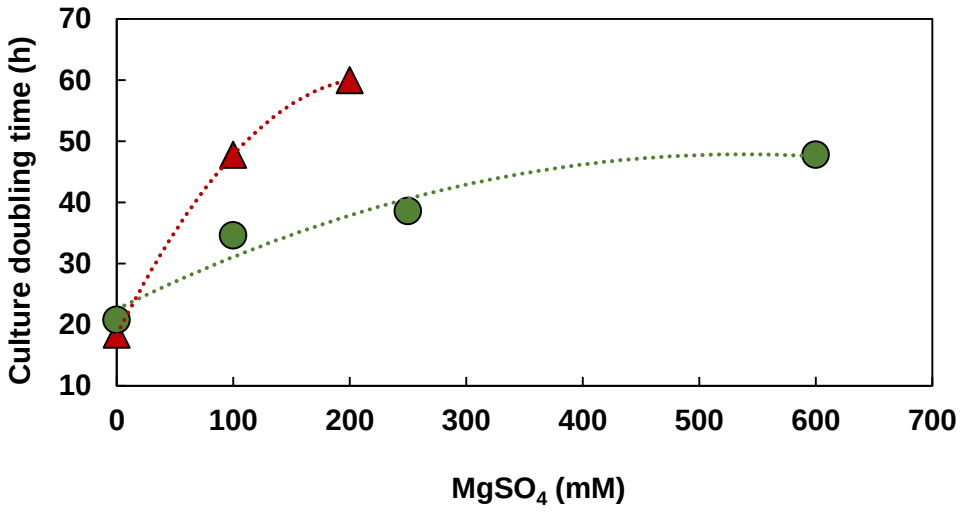


**Fig. 8.4.** Effect of presence of magnesium sulfate on culture doubling times of algal isolates AC1 (●) and ITV (▲) grown in temperature- and pH-controlled bioreactors. The line shown is the best fit based on polynomial analysis of the data.

Changes in concentrations of dissolved organic carbon in harvested biomass suspensions of both algal isolates (grown in medium with and without additional $MgSO_4$) suspended in ultrapure water are shown in Fig. 8.5. A gradual increase in DOC concentrations was observed in the first 2 hours of experiment in both AC1 and ITV biomass slurries. After 2 hours, DOC concentrations appeared to have reached a plateau and remained fairly constant until the end of the experiment. The biomass slurry AC1 reached ~ 1,600 mg DOC $L^{-1}$ whereas ITV biomass reached ~ 600 mg DOC $L^{-1}$. The control experiment (algal biomass grown without additional $MgSO_4$) displayed a much lower concentration of DOC for both algal biomass (~ 150 mg $L^{-1}$).

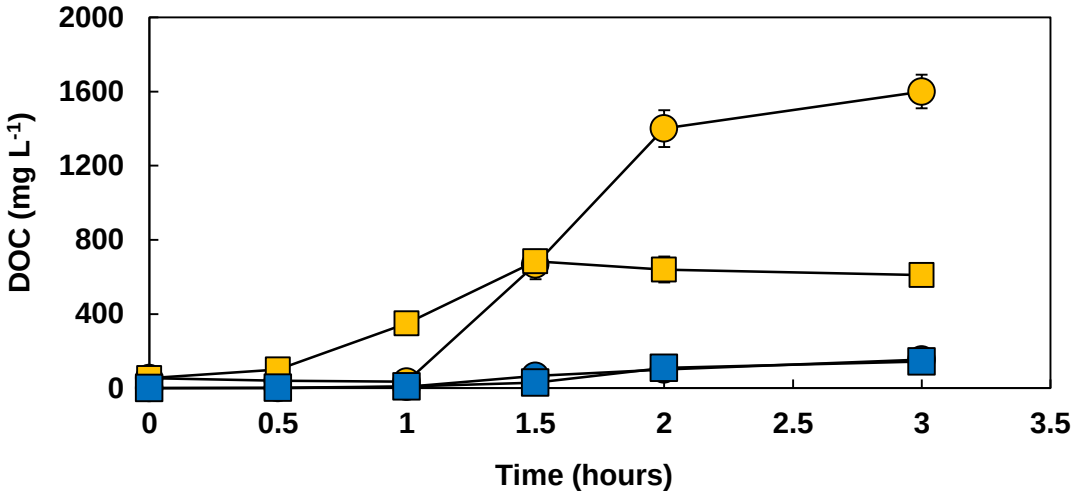


**Fig. 8.5.** Changes in concentrations of dissolved organic carbon in harvested biomass suspended in ultrapure water of algae grown in medium with (● AC1; ■ ITV) and without (● AC1; ■ ITV) additional 600 mM $MgSO_4$ for isolate AC1 and 200 mM $MgSO_4$ for isolate ITV. Data points depict mean values and error bars standard deviations of triplicated analyses of each sample.

Phylogenetic analysis of the 18S rRNA gene sequences of the algal isolates showed that isolate AC1 belonged to the class *Trebouxiophyceae* in the phylum *Chlorophyta* with 99% gene similarity to *Coccomyxa onubensis* strain SAG 2510 (which was isolated from acidic waters of the Tinto River in Spain; Fuentes et al., 2016). Isolate ITV also belonged to the class *Trebouxiophyceae* and the closest relative at species level was *Heterochlorella luteoviridis* strain SAG 2133 (98% gene similarity) which was detected (but not isolated) in an air-exposed artificial substrate from the suburban area of Göttingen in Germany (Hallmann et al., 2016). The phylogenetic tree in Fig. 8.6 shows ITV as a single member of a clade forming a branch on its own, supporting the monophily of the clade. Based on these findings, it appears that this isolate has not been described previously. The 18S rRNA gene sequences of isolates ITV and AC1 are shown in Appendix 1.

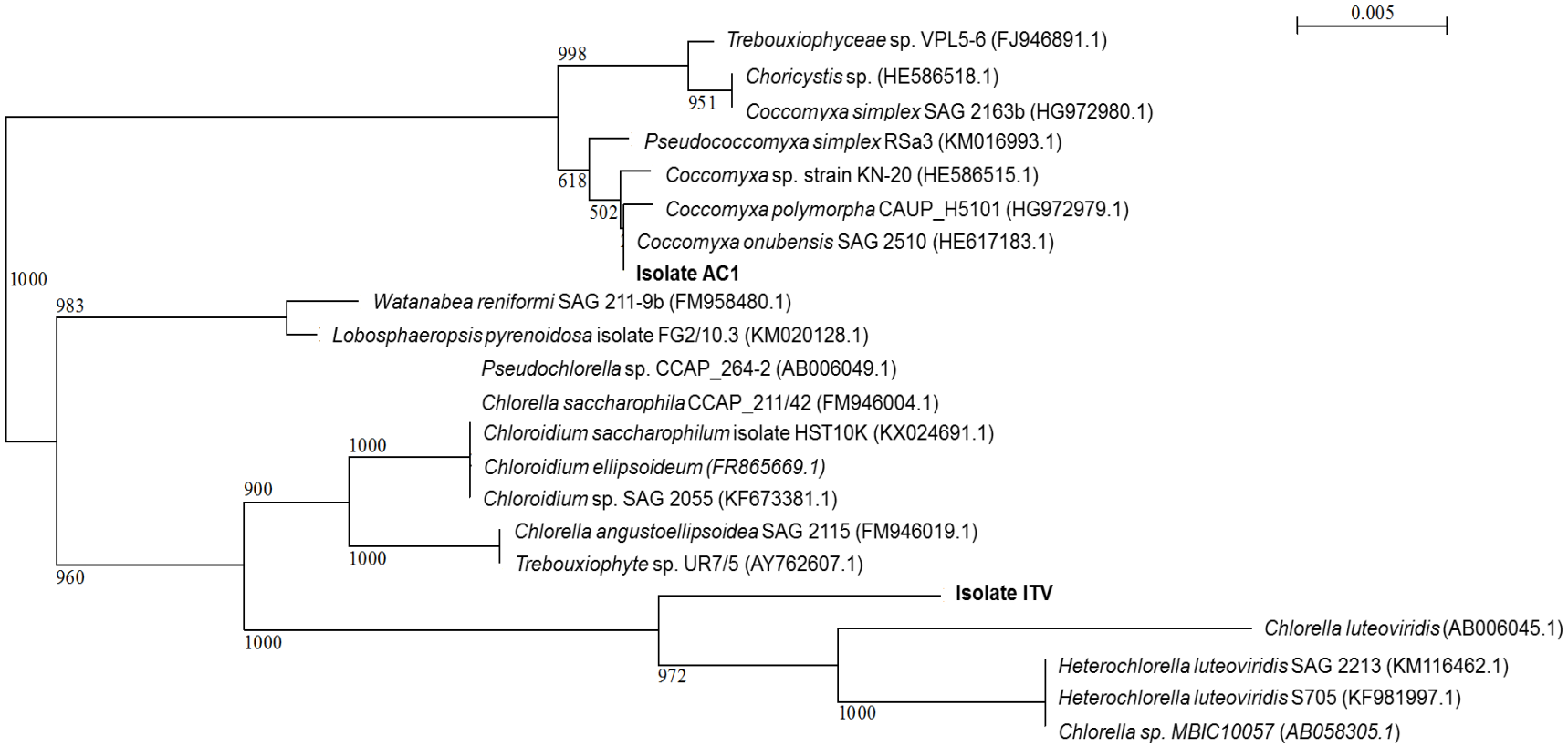


**Fig. 8.6.** Phylogenetic tree showing the relationship of algal isolates AC1 and ITV to other green algae based on 18S rRNA sequence homology (values in brackets are NCBI accession numbers). The scale bar is the number of nucleotides substituted per base pair. Bootstrap values are given at the respective nodes. The tree was rooted with the 18S rRNA gene sequence of *Ulospora bilgramii* (DQ384071.1).

## 8.3 Preliminary tests on low pH biosulfidogenesis sustained by algal biomass

### *8.3.1 Materials and methods*

To test the hypothesis that algal biomass could provide suitable electron donors to support biosulfidogenesis at low pH, a preliminary experiment was set up using either bioreactor-grown AC1 and ITV biomass, harvested and re-suspended in 25 mL of sterile pH 4.0 basal salts solution. Four species of acidophilic sulfate-reducing bacteria (aSRB), were used in the experiment: *Desulfosporosinus* (*D.*) *acididurans* M1$^T$, *Peptococcaceae* CEB3, "*Desulfobacillus* (*Db*.) *acidavidus"* CL4 and *Firmicute* C5 (section 2.1). The culture medium for these sulfate-reducing bacteria is described in section 2.2.2.2. Number of cells in aSRB inocula ranged between 2.5 - 6.0 x $10^7$ cells $mL^{-1}$.

Serum bottles (50 mL) were filled to near capacity (40 mL) with a sterile solution containing ABS, TE and 4 mM zinc sulfate, adjusted to pH 4.0. These were sparged with a stream of oxygen-free nitrogen (OFN) for 40 min to remove dissolved oxygen. Table 8.2 shows the three conditions tested: (i) "positive controls" (2.5 mM glycerol and 0.1 g $L^{-1}$ yeast extract, final concentrations + 2.5 mL active cultures of aSRB), (ii) algae/aSRB (2.5 mL of either AC1 or ITV biomass and 2.5 mL active cultures of aSRB), and (iii) "negative controls" (2.5 mL of either AC1 or ITV biomass, with no aSRB). The algae/aSRB test was carried out in duplicate whereas the positive (glycerol and YE) and negative (aSRB-free) controls were carried out using single serum bottles for each aSRB.

**Table 8.2.** Conditions tested in the experiment. The presence or absence of each component is indicated by plus or minus, respectively.

| Conditions | Algal biomass (2.5 mL) | 2.5 mM Glycerol and 0.1 g $L^{-1}$ yeast extract | aSRB (2.5 mL) |
|---|---|---|---|
| **Positive controls (Glycerol and YE)** | - | + | + |
| **Algae/aSRB** | + | - | + |
| **Negative controls (aSRB-free)** | + | - | - |

Serum bottles were sealed with rubber septa and metal caps, re-flushed with OFN for 10 mins and incubated, unshaken, at 30°C for four weeks (Fig. 8.7). Samples were withdrawn using aseptic needles at the start of the experiment and at weekly intervals thereafter, to determine concentrations of soluble zinc (section 2.6.3). At the end of the experiment, pH,

concentrations of dissolved organic carbon (section 2.8) and of soluble zinc present were determined. Individual small molecular weight organic compounds (SMWOC) were identified based on the retention times of standard solution chromatograms carried out in parallel. (section 2.6.2). The range of standard solutions analysed in this experiment was based on previous studies which described production of compatible solutes in response to osmotic stress in acidophilic bacteria (Galleguillos et al., 2018) and of other acidophilic microalgae (Ñancucheo and Johnson, 2012b).

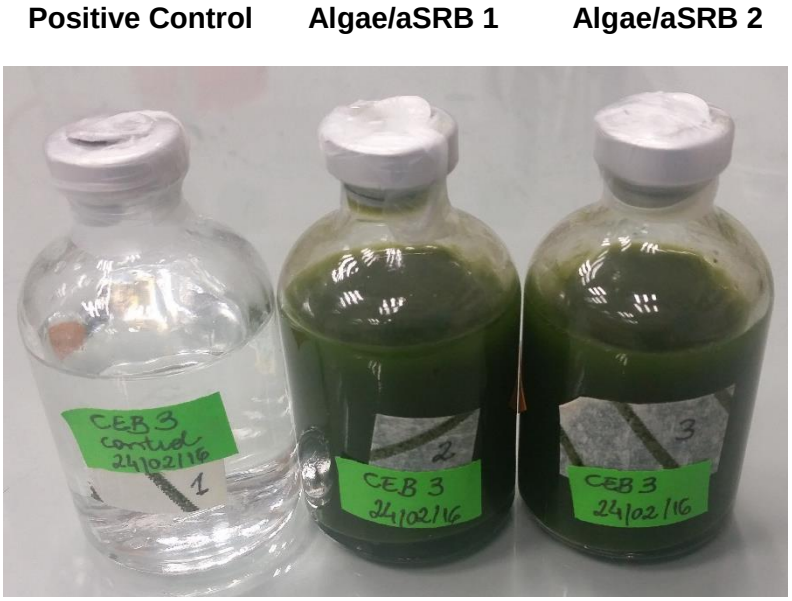


**Fig. 8.7.** Image of the experiment set up using the sulfate-reducer *Peptococcaceae* CEB3. Positive control bottle (glycerol and YE; left) and algae/aSRB bottles in duplicate (centre and right). The negative control bottle is not shown.

*8.3.2 Results*

The rationale of using whole algal biomass to fuel biosulfidogenesis is that the algal cells would rapidly become non-viable in the anoxic mesocosms, inducing cell lysis, and that some of the organic compounds released would act as electron donors for sulfate reduction. Figure 8.8 shows that biomass of both algal species was able to fuel the reduction of sulfate to hydrogen sulfide in pure cultures of aSRB, as evidenced by reductions in concentrations of soluble zinc over time. In addition, the characteristic smell of $H_2S$ and the formation of off-white precipitates (inferred to be ZnS) precipitates attached to the glass of the bottles confirmed that biosulfidogenesis had occurred. This was observed in cultures of all four aSRB used though to different extents, with *D. acididurans* being the most effective with both algal biomass. Additional evidence in support of biosulfidogenesis was that pH values increased in all anaerobic cultures that had been inoculated with aSRB (Table 8.3) whereas the pH in the

negative control (aSRB-free) increased very little (to 4.08 for isolate AC1 and 4.03 for isolate ITV) over the time course of the experiment.

In all positive control bottles (aSRB cultures amended with glycerol and yeast extract), the concentrations of glycerol declined from 2.5 mM to < 0.1 mM, and the concentrations of soluble zinc declined from 4 mM to < 0.5 mM (except "*Db. acidavidus*" CL4 with 0.8 mM soluble zinc remaining at the end of the experiment) over the time course of the experiment, indicating that aSRB were metabolically active and precipitation of ZnS was coupled to glycerol oxidation (Fig. 8.8). No precipitation of ZnS occurred in serum bottles to which algal biomass (AC1 or ITV) but no aSRB were added, confirming that the latter were responsible for removing soluble zinc in this experiment.

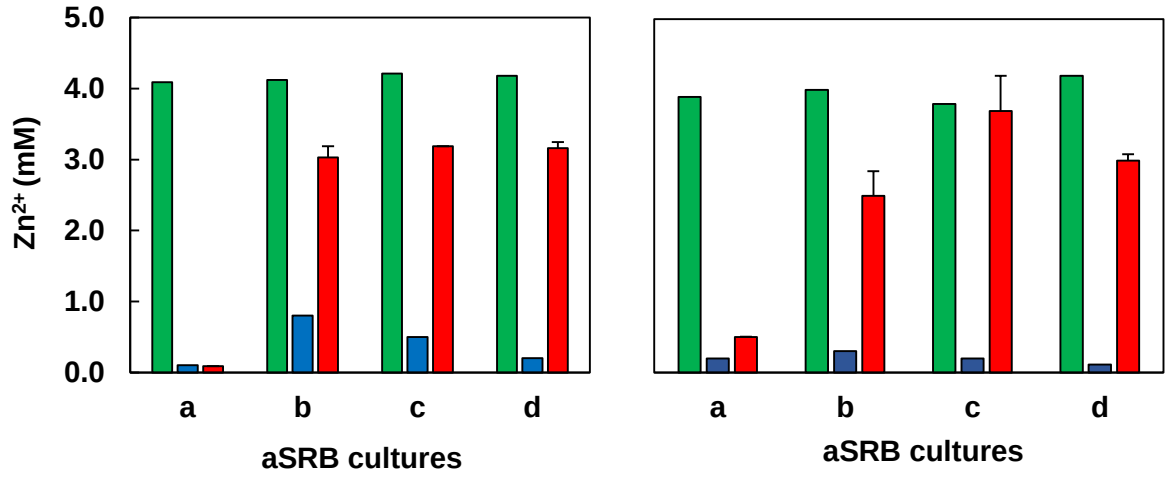


**Fig. 8.8.** Changes in concentrations of zinc in anaerobic serum bottles containing different species of aSRB, (a) *D. acididurans*$^{T}$; (b) "*Db. acidavidus*" CL4, (c) *Peptococcaceae* CEB3, (d) *Firmicute* C5, and amended with either AC1 biomass (left) or ITV biomass (right). Key: Negative control (green bars); positive control (blue bars); algae/aSRB (red bars). The bars depict mean values and the error bars the range between replicate samples (*n* = 2).

**Table 8.3.** Values of pH measured at the end of the four weeks of the experiment. The pH of all suspensions at the start of the experiment was 4.0.

| | Positive control (glycerol + YE) | AC1 biomass | ITV biomass |
|---|---|---|---|
| *D. acididurans* | 5.52 | 5.20 | 5.34 |
| "*Db. acidavidus*" CL4 | 5.27 | 5.17 | 5.21 |
| *Peptococcaceae* CEB3 | 5.28 | 5.08 | 4.92 |
| *Firmicute* C5 | 5.43 | 5.03 | 5.12 |
| Negative control (aSRB-free) | | 4.08 | 4.03 |

There were several strands of evidence that supported the hypothesis that algal cells rapidly lost viability and released DOC when put into the anoxic serum bottles. The initial bright green colour of these cultures, which is characteristic of these algae species grown aerobically, changed over time to a dark green/brown colour, and microscopic examination showed that algal cells had lysed. Also, at the end of the experiment DOC in the cell-free liquor of each system tested were detected.

Table 8.4 shows concentrations of dissolved organic carbon (DOC) measured 2 hours after the experiment had been set up. Concentrations of DOC were significantly higher than the total concentration of the identified small molecular weight organic compounds (calculated as mg C $L^{-1}$) in each system. The apparent discrepancy between "total" and "calculated" DOC concentrations in the positive control is due to presence of yeast extract.

**Table 8.4.** Comparison of total DOC concentrations and those of the combined small molecular weight organic compounds identified in the mesocosms. Samples were analysed 2 hours after the experiment had been set up.

| | | **Total DOC** | | **Identified organic compounds** | |
|---|---|---|---|---|---|
| | | **mg C $L^{-1}$** | | | |
| **Positive Control (Glycerol/YE)** | *D. acididurans* | 136 | | 96 | |
| | *Peptococcaceae* CEB3 | 123 | | 83 | |
| | "*Db. acidavidus"* CL4 | 133 | | 93 | |
| | *Firmicute* C5 | 132 | | 92 | |
| | | **+AC1 biomass** | **+ITV biomass** | **+AC1 biomass** | **+ITV biomass** |
| **Algae/aSRB** | *D. acididurans* | 410 | 300 | 119 | 145 |
| | *Peptococcaceae* CEB3 | 401 | 300 | 109 | 150 |
| | "*Db. acidavidus"* CL4 | 411 | 312 | 135 | 156 |
| | *Firmicute* C5 | 420 | 306 | 117 | 137 |
| **Negative control (aSRB-free)** | | 418 | 348 | 150 | 145 |

Figure 8.9 shows data of DOC concentrations at the start (2 hours after setting up) and at the end of the experiment (4 weeks). Dissolved organic carbon was effectively metabolised in all positive control bottles (glycerol and YE) with only 20-35% DOC remaining after 4 weeks of the experiment. Concentrations of DOC in mesocosms containing algal biomass (AC1 or

ITV) were considerably higher than that in the positive control mesocosms, though only 12-40% of DOC had been metabolised by the aSRB. Negative control serum bottles (aSRB-free) did not show a significant difference between DOC concentrations at the start and end of the experiment with > 98% of total DOC remaining after 4 weeks with both algal biomass.

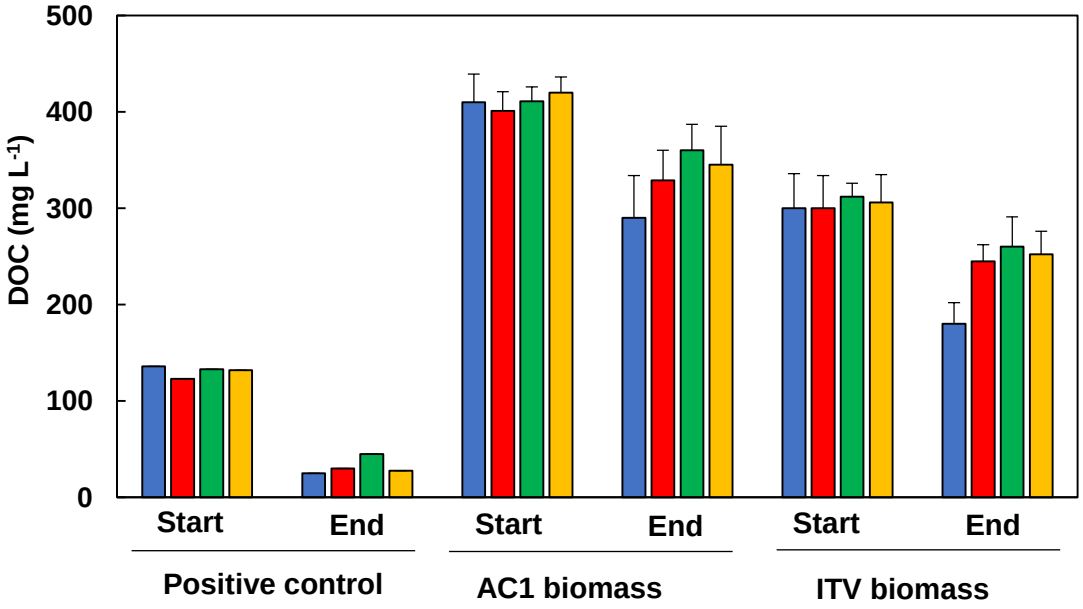


**Fig. 8.9.** Comparison between DOC concentrations at the start (2 h after setting up) and end of the experiment. Key: *D. acididurans*$^{T}$ (blue bars), *Peptococcaceae* CEB3 (red bars), "*Db. acidavidus*" CL4 (green bars) and *Firmicute* C5 (yellow bars). Bars indicate mean values and the error bars the range between replicate samples (*n* = 2).

Concentrations of the identified small molecular weight organic compounds (SMWOC) in the cell-free liquors of serum bottles containing AC1 and ITV biomass are shown in Table 8.5 and Table 8.6, respectively. Glycerol was the only compound identified in the positive control (which initially contained glycerol and yeast extract) while glycerol and a few others organic compounds were identified in both negative controls and mesocosms containing algae/aSRB of either AC1 or ITV biomass. Overall, concentrations of individual SMWOC were slightly higher in systems amended with AC1 biomass than those with ITV biomass. Total DOC concentrations in negative (aSRB-free) controls were used to assess the maximum amounts of organic compounds potentially available to fuel sulfidogenesis in the mesocosms, and assumed that: (i) algal biomass was equally distributed across all systems and (ii) the potential electron donors were not metabolised in the negative controls. Tables 8.5 and 8.6 show that, in most cases, DOC concentrations in serum bottles inoculated with pure cultures of aSRB were lower than those in their respective negative controls, suggesting that they had been metabolised by the aSRB.

**Table 8.5.** Mean concentrations (in mM) of small molecular weight organic compounds identified at the end of the experiment in duplicate AC1 biomass mesocosms. Values of the negative controls are from single mesocosms in each case.

| aSRB | AC1 biomass | | | | |
|---|---|---|---|---|---|
| | **Glycerol** | **Trehalose** | **Glycolic acid** | **Glucose** | **Galactose** |
| *D. acididurans* | 0.53 | <0.01 | <0.01 | <0.01 | <0.01 |
| *Peptococcaceae* CEB3 | 0.64 | 0.28 | 0.21 | 0.41 | 0.16 |
| "*Db. acidavidus"* CL4 | 0.54 | 0.36 | 0.30 | 0.61 | 0.25 |
| *Firmicute* C5 | 0.49 | 0.30 | 0.23 | 0.52 | 0.18 |
| Negative (aSRB-free) control | 0.84 | 0.37 | 0.25 | 0.58 | 0.20 |

**Table 8.6.** Mean concentrations (in mM) of small molecular weight organic compounds identified at the end of the experiment in duplicate ITV biomass mesocosms. Values of the negative controls are from single mesocosms in each case.

| aSRB | ITV biomass | | | | |
|---|---|---|---|---|---|
| | **Glycerol** | **Trehalose** | **Glycolic acid** | **Mannitol** | **Fructose** |
| *D. acididurans* | 0.32 | 0.11 | 0.03 | 0.17 | 0.08 |
| *Peptococcaceae* CEB3 | 0.41 | 0.11 | 0.07 | 0.18 | 0.06 |
| "*Db. acidavidus"* CL4 | 0.43 | 0.14 | 0.08 | 0.19 | 0.07 |
| *Firmicute* C5 | 0.33 | 0.08 | 0.02 | 0.14 | 0.05 |
| Negative (aSRB-free) control | 0.44 | 0.15 | 0.09 | 0.20 | 0.09 |

Figure 8.10 shows the percentage of the SMWOC identified in each system (positive and negative controls) calculated based on their concentrations and equivalent DOC concentrations. The positive control contained initially only glycerol (90 mg $L^{-1}$ carbon equivalent) and yeast extract (which was estimated at 40 mg C $L^{-1}$, assuming that 40% of its dry weight was carbon). The negative controls (aSRB-free) from AC1 and ITV biomass showed a range of organic compounds which were identified using ion chromatography. However, when compared to the total DOC concentrations, the combined organic compounds identified represent only ~ 30% of the total for AC1 biomass and ~ 20% of the ITV biomass.

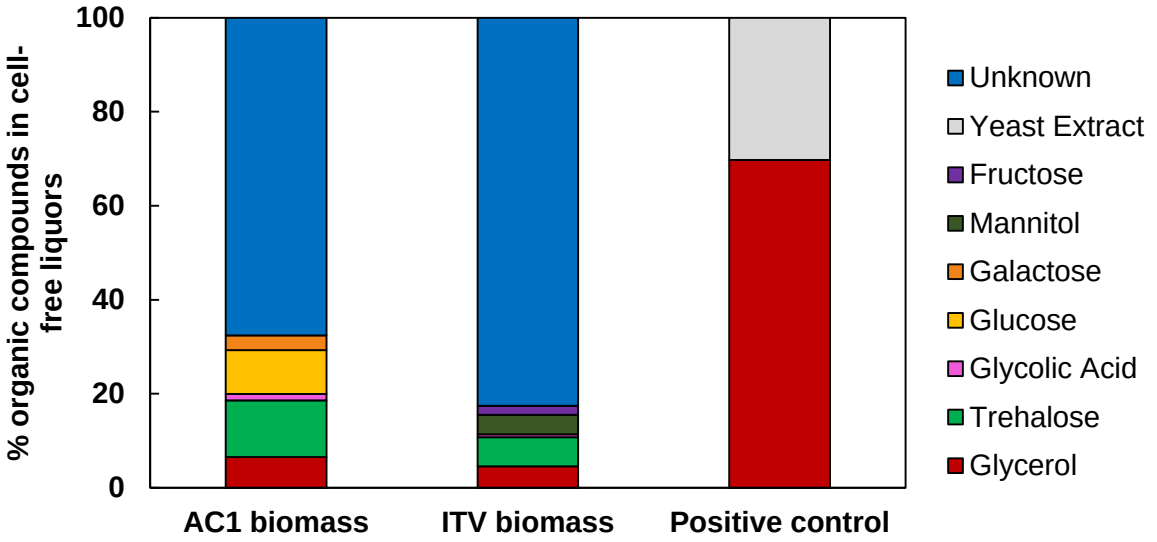


**Fig. 8.10.** Percentage of small molecular weight organic carbon compounds in cell-free liquors of positive (glycerol and YE) and negative controls (AC1 and ITV biomass alone) 2 hours after the start of the experiment.

## 8.4. Potential use of algal biomass to fuel sulfidogenesis in bioreactor systems at low pH

### *8.4.1 Materials and methods*

#### 8.4.1.1 Preparation of the algal biomass slurry

Isolate AC1 biomass from bioreactor-grown cultures was re-suspended in sterile pH 4.0 ABS/TE solution (section 2.2.2.1). Two algal biomass slurries were obtained using AC1 biomass (AC1a and AC1b). Biomass slurry AC1a had a final volume of 100 mL and contained algal biomass which was grown in a low osmotic strength (no additional $MgSO_4$), whereas slurry AC1b contained algal biomass which were grown in media both with and without additional $MgSO_4$ and had a final volume of 400 mL. Both biomass slurries were thoroughly homogenised and aliquoted in 10 mL and 20 mL aliquots, which were stored at 4ºC in sterile universal bottles. For determination of approximate estimates of DOC concentrations in lysed algal suspensions, algal cells (5 mL of each biomass slurry) were disputed using a high frequency ultrasonic bath at room temperature for 1 h (VWR International, UK). Cell debris was removed by filtering through a 0.2 µm pore size membrane filter and DOC was determined in the filtrates (section 2.8). Differences in cell numbers and total DOC concentrations between biomass slurries AC1a and AC1b are shown in Table 8.7. Algal biomass from isolate ITV was not tested in bioreactor systems.

**Table 8.7.** Differences between slurries AC1a and AC1b.

| | AC1a | AC1b |
|---|---|---|
| **Slurry final volume (mL)** | 100 | 400 |
| **Cell numbers in the slurry ($mL^{-1}$)** | $9.2 \times 10^9$ | $3.4 \times 10^{11}$ |
| **DOC in lysed cell suspensions ($mg\ L^{-1}$)** | 150 | 1,580 |

8.4.1.2 Commissioning and operation of the sulfidogenic bioreactor

An acidophilic sulfate-reducing bacteria reactor (aSRBR) populated with a mixed microbial community (section 2.4) was used in experimental work. In brief, the bioreactor had a working volume of 2.0 L and was coupled to a FerMac 310/60 unit to control pH (pH 4.0), temperature (35°C) and agitation (50 rpm). Oxygen-free nitrogen (OFN) was bubbled through the bioreactor at 150 mL $min^{-1}$ in order to promote anoxic conditions within the vessel and to act as a carrier for the excess of $H_2S$ generated by aSRB. Automated flow into the bioreactor vessel was controlled by a pump linked to the pH unit of the control module. The experiment was carried out in three different phases. In phase 1, 5 mM glycerol and 0.1 g $L^{-1}$ yeast extract were used as electron donors for 14 days, and rates of hydrogen sulfide production were monitored by off-line precipitation of CuS. Prior to changing to algal biomass (AC1a; phase 2), 4.0 L of organic carbon-free feed liquor at pH 4.0 was pumped through the reactor continuously in order to remove residual traces of glycerol and yeast extract from phase 1. The algal biomass slurries (AC1a; phase 2 and AC1b; phase 3) were aseptically introduced to the bioreactor system through an open-ended tube extended to the bottom of the bioreactor vessel, in order to promote homogeneous percolation through the biofilm bed (Fig. 8.11). The biomass was injected using an external pressure generated by a sterile nitrogen flow into the bottle connected to the open-ended tube causing the algal concentrate to be directed to the bioreactor vessel. An organic carbon-free feed liquor, containing ABS/TE and 25 mM $MgSO_4$ at pH 2.5 was pumped into the bioreactor to compensate for pH increases induced by microbial sulfidogenesis.

The first algal injection contained 20 mL of slurry AC1a and subsequent injections (10 mL) were carried out every two days for 20 days. In order to avoid algal cells being flushed out of the reactor before they lysed and released their cytoplasmic organic compounds, pumps were switched off for 2 - 4 h after each injection. After 20 days of the experiment, a second AC1 biomass slurry (AC1b; phase 3) was prepared, as described previously, and 20 mL injections were carried out every other day for 5 days. Subsequently, 200 mL of algal biomass slurry was injected and the bioreactor monitored for a further 10 days, followed by a final 80 mL injection, and the bioreactor was monitored for further 25 days.

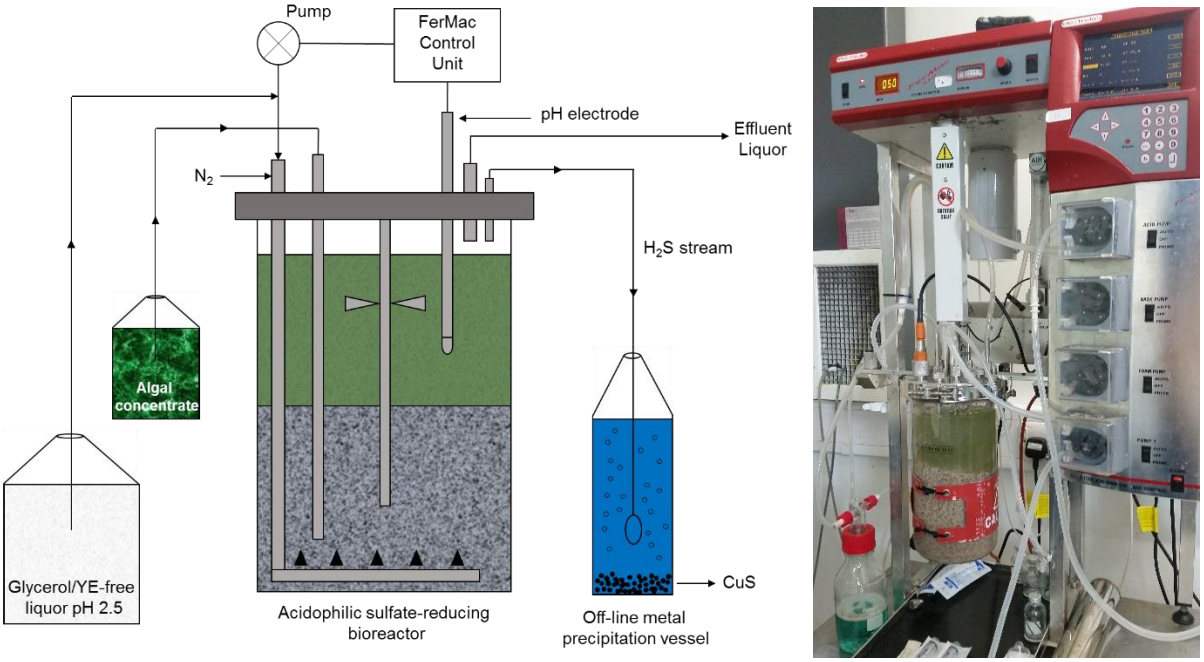


**Fig. 8.11.** Schematic representation of the biosulfidogenic reactor showing the algal injection system (left) and image of the actual bioreactor (right).

Hydraulic retention times were determined in cases where the aSRBR was operating in continuous flow mode. Concentrations of sulfate in the influent and effluent liquors were monitored throughout the experiment using ion chromatography (section 2.6.1). Dissolved organic carbon concentrations and those of individual SMWOC were determined using a Protoc DOC analyser (section 2.8) and using ion chromatography (section 2.6.2). Analysis of the planktonic bacterial community of the aSRBR was carried out using T-RFLP, as described in section 2.9.4.

*8.4.2 Results*

The sulfidogenic bioreactor was operated in three phases: (phase 1) glycerol + yeast extract, (phase 2) algal biomass slurry AC1a and (phase 3) algal biomass slurry AC1b. Between phases 1 and 2, 4 L of organic carbon-free feed liquor at pH 4.0 was pumped through the bioreactor at a rate of ~ 17 mL $min^{-1}$ causing the concentration of glycerol to fall to < 0.01 mM. Hydraulic retention times (HRTs) increased considerably when algal biomass replaced glycerol/yeast extract, ranging between 23 and 255 h compared to an average of 11 h when using glycerol and yeast extract (Fig. 8.12). Addition of algal biomass slurry AC1a was evaluated from day 15 to day 40 and generation of effluent liquor was observed only during the first 4 days of the experiment. Between day 21 and day 40 there was no pH increase and the addition of the pH 2.5 organic carbon-free feed liquor for pH adjustment was not required,

therefore effluent liquor was not generated, indicating that sulfidogenesis was not occurring. A more concentrated algal biomass slurry (AC1b) was then introduced to the system (phase 3), which resulted in a delayed increase of the bioreactor pH and generation of effluent liquor. Hydraulic retention times at this stage fluctuated between 23 and 255 h.

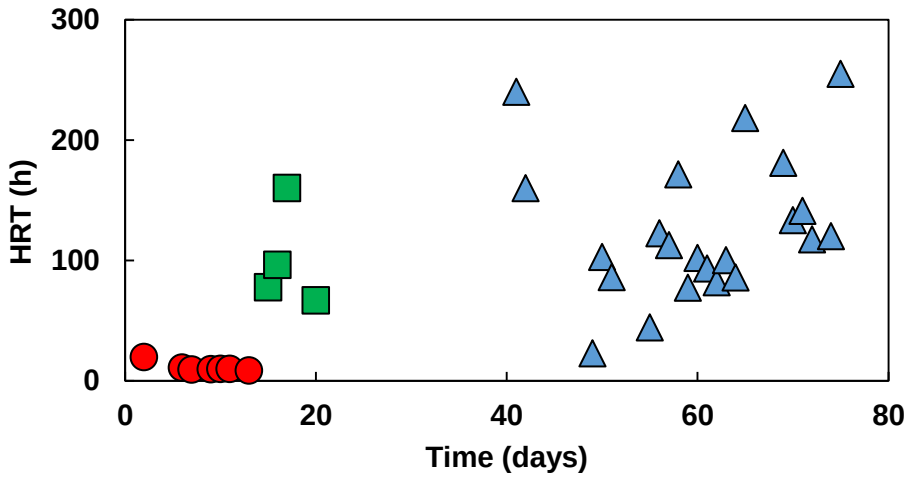


**Fig. 8.12.** Changes in hydraulic retention times (HRT) of the aSRBR during the three phases of the experiment: bioreactor fed with 5 mM glycerol + 0.1 g $L^{-1}$ yeast extract (●) (phase 1); algal biomass slurry AC1a (■) (phase 2), and algal biomass slurry AC1b (▲) (phase 3). Between days 20 and 40 the aSRBR did not generate effluent liquor and therefore HRTs were not recorded.

Rates of $H_2S$ production, varied greatly within the three phases (Fig. 8.13). When using glycerol and yeast extract, the average rate was 500 µmoles $H_2S$ $L^{-1}$ $day^{-1}$ compared to 20 and 30 µmoles $H_2S$ $L^{-1}$ $day^{-1}$ when using algal biomass slurries AC1a and AC1b, respectively. To circumvent this impasse, a greater volume (200 mL) of the more concentrated algal biomass (AC1b) was injected into the system. This resulted in the bioreactor pH increasing and copper sulfide formation in the external gas bottle, both as a result of biosulfidogenesis.

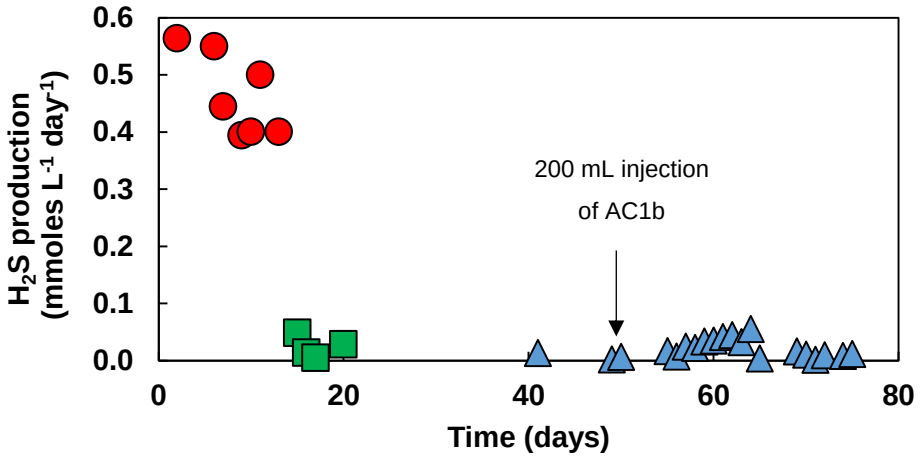


**Fig. 8.13.** Changes in rates of hydrogen sulfide production of the aSRBR during the three phases of the experiment: bioreactor fed with 5 mM glycerol + 0.1 g $L^{-1}$ yeast extract (●) (phase 1); algal biomass slurry AC1a (■) (phase 2), and algal biomass slurry AC1b (▲) (phase 3). The time interval between day 20 and day 40 represent the period where the aSRBR did not generate effluent liquor. The arrow indicates the time at which 200 mL of AC1b biomass slurry was injected.

The initial bright green colour of the algal biomass slurry changed over time to a dark green/brown colour in the aSRBR, and microscopic examination revealed that algal cells had lysed. Figure 8.14 shows changes in concentrations of DOC in the cell-free bioreactor liquor before and after each injection of algal biomass. Each injection of algal slurry AC1a throughout phase 1 had a volume of 10 mL, apart from the first injection which was 20 mL. Algal slurry AC1b injected to the aSRBR (phase 3) had a volume of 20 mL on day 2 and 7, followed by 200 mL on day 10 and 80 mL on day 21.

Glycerol and glucose (3.0 and 1.5 mM, respectively) were identified as major components of the cell-free bioreactor liquor when using AC1b biomass slurries; smaller concentrations of trehalose, glycolic acid and galactose (~ 0.5 mM each) were also detected.

The bacterial community within the bioreactor was monitored at the end of each phase of the experiment (Fig. 8.15). The results show that the relative abundance of sulfate-reducing bacteria fell dramatically when the feed organic material was switched to the algal biomass slurries. Over 75% of the planktonic bacterial community was represented by aSRB (*Peptococcaceae* CEB3 and *Desulfosporosinus acididurans*) with glycerol/yeast extract, compared to less than 25% when using algal concentrates, and an *Actinobacterium* AR3, which had previously been identified as a member of the bioreactor community (Chapter 3) became much more relatively abundant (accounting for between 65 and 68% of the summated T-RFs).

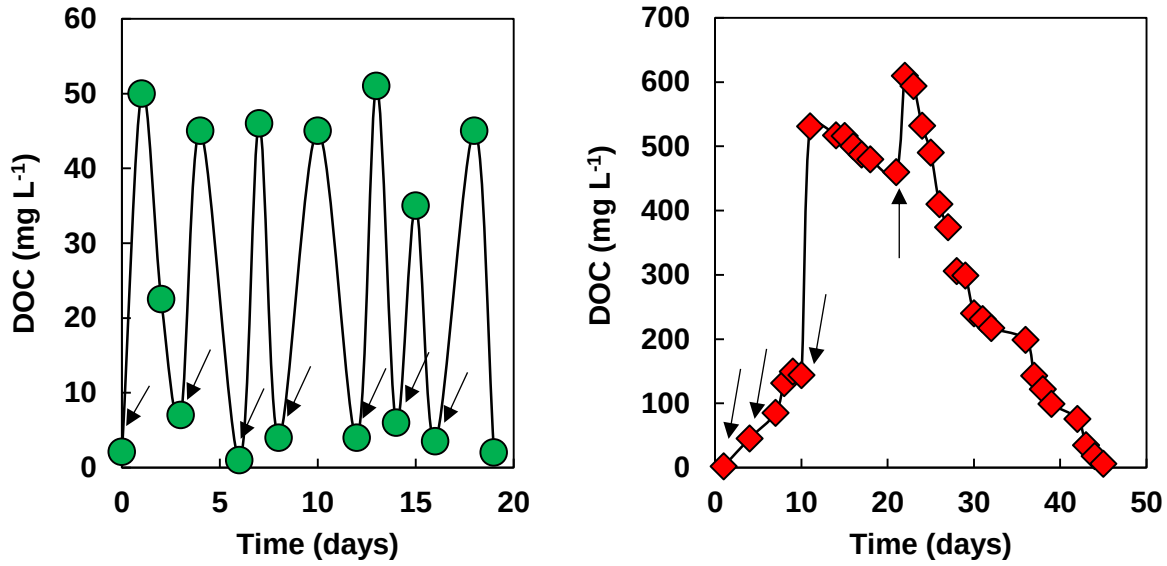


**Fig. 8.14.** Changes in concentrations of DOC for AC1a (phase 2; left) and AC1b (phase 3; right) biomass slurries. Arrows indicate the times of each injection. The first injection of AC1a biomass had a volume of 20 mL while all others were 10 mL. Algal slurry AC1b injected to the aSRBR had a volume of 20 mL on days 2 and 7, followed by 200 mL on day 10 and 80 mL on day 21. DOC was measured 2 - 4 h after each injection of biomass.

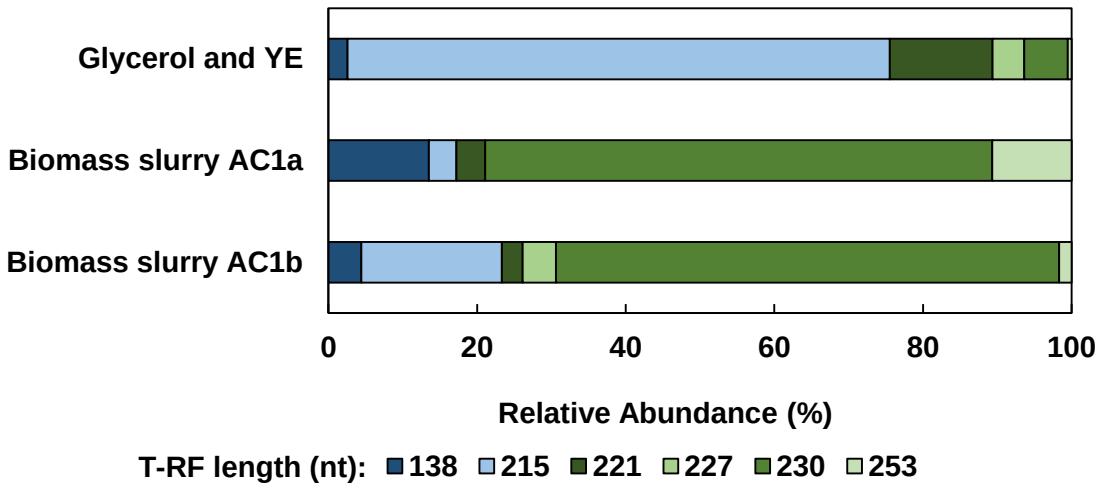


**Fig. 8.15.** Terminal restriction enzyme fragment length polymorphism (T-RFLP) analysis (HaeIII digests of amplified 16S rRNA genes) of planktonic bacterial communities in the aSRB reactor operated using different feed stocks. Shades of blue represent sulfate-reducing bacteria (138 nt, *Peptococcaceae* CEB3; 215 nt, *D. acididurans*), shades of green represent non-sulfidogens (221 nt, *Clostridium* sp.; 230 nt, *Actinobacterium* AR3; 253 nt, *At. ferrooxidans*).

## 8.5 Discussion

The process which converts light energy into chemical energy used by plants and other photosynthetic organisms such as microalgae, has been used in a variety of industrial applications, using the production of different metabolites usually stored in carbohydrate molecules (e.g. sugars). In the context of the bioremediation of metal-contaminated wastewaters, various approaches for using algal biomass as carbon sources and electron donors for sulfate-reducing bacteria have been described. A study developed by Rose et al. (1998) described a treatment for acidic metal-rich wastewaters from tanneries using an integrated algal sulfate reducing ponding process. Elsewhere, Boshoff et al. (2004) provided insights based on experimental studies into how to establish this process using an anaerobic digestor to remediate metal- and sulfate-rich wastewaters, also from tanneries.

This current study described two acidophilic microalgae that had been isolated from mining-impacted areas and evaluated their potential to provide suitable electron donors for biosulfidogenesis at low pH. In terms of their gross physiologies isolate AC1 was categorised as mesophilic (optimum growth at 25ºC) and moderately acidophilic (optimum growth at pH 4.0 and unable to grow at pH values below 2.0), while isolate ITV was categorised also as a mesophile (optimum growth at 22.5ºC) but as a more extreme acidophile (growth observed at pH 1.8 - 3.0, though its optimum was 2.5). In general, isolate ITV showed greater tolerance to transition metals and aluminium than isolate AC1, but it was more sensitive to NaCl.

Falagán and Johnson (2018) reported that both salt and metal tolerance in acidophilic bacteria was pH dependent, due to variations in membrane potential ($\Delta\Psi$; the charge difference between either side of the cell membrane) which varies with external pH. When growing in very acidic liquors, these bacteria accumulate inorganic cations (e.g. potassium) intracellularly, causing the membrane potentials to be positive and counterbalancing the pH gradients ($\Delta$pH; between intra and extracellular sides of the membrane). The trans-membrane proton electrochemical potential ($\Delta\rho$, or proton motive force) derives from the combination of membrane potential and pH gradient ($\Delta\rho = \Delta\Psi - 59 \cdot \Delta pH$). Being positively charged, the membrane of acidophiles is more susceptible to the influx of permeable anions, such as chloride ($Cl^-$), potentially causing a collapse of the membrane potential. The current study tested this same hypothesis by growing isolate ITV in liquid medium containing copper sulfate and sodium chloride at either pH 4 or 2. At low pH liquors, acidophiles have a “more positively charged” membrane potential which can preclude the influx of permeable cations (e.g. $Cu^{2+}$) however it can facilitate the influx of anions (e.g. $Cl^-$) and tolerance to anions (other than sulfate) decreases as the pH liquor decreases. On the other hand, in higher pH liquors the sensitivity to cations increases. The trend observed in the current test using an acidophilic

eukaryotic microalga corroborated the findings with prokaryotes obtained by Falagán and Johnson (2018).

Several studies have reported the synthesis of compatible solutes in response to osmotic stress in halotolerant and halophilic prokaryotes and eukaryotes (e.g. Kempf and Brenner, 1998; Welsh, 2000; Roberts, 2005; Gustav et al., 2010; Yin et al., 2015). In most prokaryotes microorganisms, the adaptation mechanisms to prevent NaCl from diffusing into the cells involve the accumulation of $K^+$ ions to counteract the external osmotic pressure. In contrast, most halophilic bacteria and eukaryotes increase their intracellular solute pool by accumulating water soluble organic compounds of low molecular weight, referred to as compatible solutes or osmo-protectants. The accumulation of these compounds helps to maintain turgor pressure, cell volume and concentration of electrolytes (Roberts, 2005). Cells grown in high osmotic strength media tend to synthetize or uptake osmolytes in order to balance the differential between internal and external osmotic potentials. The type of compatible solutes (organic compounds) synthetized by the cells can include polyols (e.g. glycerol and arabitol), sugars (mono and disaccharides), amino acids (e.g. proline), amino compounds, etc. (Welsh, 2000). Many of these small molecular weight compounds are potential substrates for sulfate-reducing bacteria (Sánchez-Andrea et al., 2014; Suzuki et al., 2007).

The hypo-osmotic shock approach described in this chapter involved growing isolates AC1 and ITV in elevated osmotic strength media and re-suspending cells in a low osmotic strength medium which caused the osmolytes to be rapidly exuded by the cells. This experiment showed that in response to osmotic stress (caused by addition of $MgSO_4$ to the liquid medium), both algal isolates could synthesize and retain putative osmo-protectants intracellularly as an adaptive strategy to survive on high-osmolality environment. However, when cells were suspended in lower osmotic pressure solution (ultrapure water), these organic compounds were released from the inside of the cells into the solution. Only a small percentage of the total SMWOC were identified in the algal biomass slurries, since most of the analysis were based on small molecular weight sugars and polyols. Further investigation is needed in order to identify other long chain sugars, alcohols and organic acids (such as ectoines) as well as betaines, amino acids and derivatives, which are also known to be synthesized by prokaryotes and eukaryotes under osmotic stress (Welsh, 2000).

The production of DOC by algal cells was thought as an alternative to glycerol and yeast extract which have been used as electron donors to fuel biosulfidogenesis at Bangor University for many years. The advantages of this novel approach include: (i) easy access to

indigenous algal community (most acidophilic algae have been found in natural and mine-impacted waters which hold high metal content and/or salinity), (ii) DOC originated from photosynthetic primary producers has been reported to sustain biological sulfate reduction in mine-impacted areas (Rowe et al., 2007), and (iii) a possible more cost-effective approach, since the need for continuous inputs of extraneous organic compounds would be avoided.

Overall, the experiments in this chapter have shown that algal biomass was able to provide DOC as electron donors for the dissimilatory reduction of sulfate to hydrogen sulfide at low pH. In the mesocosms experiment, several strands of evidence confirmed that alga-sustained biosulfidogenesis occurred: (i) decrease in soluble zinc concentrations ($Zn^{2+} + H_2S \rightarrow ZnS + 2\ H^+$) followed by off-white precipitates attached onto the glass of the bottle, (ii) pH values increased in all aSRB cultures (sulfate reduction at low pH is a proton-consuming reaction, though in the presence of soluble zinc this is counter-balanced by the formation of zinc sulfide), (iii) concentrations of identified SMWOC in the algae/aSRB liquors were lower than that containing algal biomass alone (aSRB-free), suggesting that they had been metabolised by the aSRB, and (iv) the characteristic smell of $H_2S$ released from the bottles while sampling. The sulfate-reducer *D. acididurans* showed to be the most effective with both algal biomass (AC1 and ITV), and it was thought that the aSRBR could harness of that effectiveness, since this sulfate-reducer was previously the most abundant organism within the bioreactor population.

In the bioreactor system, alga-sustained biosulfidogenesis did occur, as evidenced by pH increase and off-line precipitation of CuS, though rates of $H_2S$ production were much lower than when using glycerol/yeast extract as electron donors. The use of a more concentrated AC1 biomass slurry (AC1b), which also contained algal cells grown under osmotic stress (therefore higher total DOC) did not show a significant improvement in terms of $H_2S$ production rates even though DOC was being metabolised by the bacterial community in the aSRBR.

Analysis of the planktonic microbial community in the aSRBR showed a major shift when the bioreactor was fed with algal biomass. The relative abundance of sulfate-reducing bacteria in the first stage (glycerol and YE) accounted for over 75%, and dropped drastically to ~ 25% when algal biomass was introduced. In contrast, the relative abundance of non-sulfidogens increased to ~ 75% when using algal biomass, with *Actinobacterium* AR3 accounting for ~ 68% of the bacterial population in the bioreactor. The reason for the change in the bioreactor microbial community is not known but probably reflects the greater ability of *Actinobacterium* AR3 to grow on a wider range of organic materials present in the algal biomass than the aSRB. The change does, however, help explain the low $H_2S$ production with algal biomass as this organism is not known to reduce sulfate to hydrogen sulfide (R. Holanda and D.B. Johnson, Bangor University, unpublished data).

While the commensal relationship between acidophilic algae and aSRB could be used as the basis of an eco-friendly engineering strategy for remediating acidic mine waters which avoided the requirement for extraneous organic compounds, clearly this needs to be significantly improved and optimised, for example by increasing the concentrations of organic compounds present in algal biomass that can be used by SRB. Using algae in a metal mining context would also have benefit in terms of carbon footprint, as these are autotrophic ($CO_2$-fixing) microorganisms.

# 9 General discussion

The research described in this thesis has sought to develop an integrated system to simultaneously recover potentially valuable metals from and remediate a moderately acidic waste water draining a copper mine in Northern Brazil. The Sossego mine has been in operation since 2004 and consists of two main copper-gold ore bodies (Sossego and Sequeirinho). At Sossego, the ore is processed and copper is extracted using froth flotation and sold as a concentrate. As a consequence of mining activity (exposure of sulfide minerals to water and oxygen), a moderately acidic copper-rich stream has been generated and the drainage flows continuously from the ore body to a run-off area. Currently, the process used at the mine to remediate the potential pollution of this stream involves the addition of limestone ($CaCO_3$), causing the pH to rise and metals to precipitate as carbonates. As discussed, this chemical process is expensive and precludes metal recovery and recycling. In addition, the metal-rich slurry generated requires appropriate disposal since metal remobilisation can occur in the long-term.

Using a single acidophilic sulfidogenic bioreactor (aSRBR) populated with a consortium of sulfate-reducing bacteria and other acidophiles to remediate a synthetic mine water based on the chemical composition of the mine water draining Sossego copper mine was highly effective in terms of promoting biomineralisation of metal sulfides. The different scales of concentrations of copper and the other transition metals (Zn, Ni, Co and Mn) present in the synthetic mine water meant that the former could be readily removed and recovered as a sulfide phase while other metals needed to be concentrated ahead of being recovered. Removal of copper (> 99%) was achieved off-line using excess $H_2S$ generated by the aSRBR. The large generation of acidity that accompanied the formation of copper sulfide precluded the formation of other metal sulfides (the remaining transition metals have larger solubility products for their sulfide phases and do not form below pH 3) and allowed the partly-processed water to be suitable for use as feed liquor for the aSRBR. At this stage, the aSRBR was operating at pH 4.0 and 30ºC in which over 99% of the zinc present was removed in the in-line precipitation, together with 85% nickel and 75% cobalt. Manganese was not removed since formation of MnS only occurs at pH well above 7.0. The planktonic microbial community

in the bioreactor changed considerably when the partly-processed mine water was introduced in the system as feed liquor, with the sulfate-reducing bacteria (*Desulfosporosinus acididurans* and *Peptococcaceae* CEB3) accounting for 72% of the planktonic microbial population.

The effect of pH and temperature on the kinetics of the aSRBR showed large variations in terms of rates of sulfate reduction at each condition tested, though it was possible to operate over a wide range of temperatures (30 - 45°C) at pH 4.0 to 5.0. The sulfate reduction rates obtained throughout this experiment were closely related to the microbial community in the bioreactor. Sulfate-reducing bacteria appeared to dominate (from T-RFLP analysis) at pH 5.0 and 4.5 than at pH 4.0; this reflected the amount of $H_2S$ generated which increased with pH (at 30ºC). One of the two major aSRB detected in the bioreactor, *Peptococcaceae* CEB3 appeared to thrive at lower pH and higher temperature environments than *D. acididurans*. However, due to difference of the solubility products of the sulfide phases of the four transition metals in the influent liquor (Ni, Co, Zn and Mn), operating conditions that showed maximum metal precipitation removal (> 99% at pH 5.0 and 35ºC) were different to those where maximum $H_2S$ production rates were observed (~ 20 mmoles $H_2S$ $L^{-1}$ $day^{-1}$ at pH 5.0 and 35ºC and ~ 30 mmoles $H_2S$ $L^{-1}$ $day^{-1}$ at pH 5.0 and 40ºC). Changes in temperature or pH with the ranges tested had only short-term impact on the performance of the bioreactor, and bacteria that are more suitable to the new conditions rapidly emerged in greater abundance. However, changes in chemical composition of the feed liquor (tested with different concentration of yeast extract and NaCl) caused a longer-term and, in some cases, an apparent irreversible impact on the sulfidogenic bioreactor.

Previous reports of the low pH sulfidogenic bioreactors developed at Bangor University have reported only the microbial composition of the liquid phase above the bead bed (i.e. planktonic bacteria) (Ñancucheo and Johnson, 2012a; Hedrich and Johnson, 2014) while work carried out in the present study also examined populations attached to the beads themselves as well as those in interstitial liquids at different depths on the bioreactor. Analysis on the biofilm bed revealed both depth-related changes in pH in the colonised bead layer, and variations in the composition of the immobilised bacterial communities. The pH gradient generated was due to low pH feed liquor percolating upward through the biofilm bed of the bioreactor within which proton-consuming sulfidogenesis occurred. Most of the total acidity was neutralised and glycerol metabolised at the bottom layer of the biofilm bed, implying that most of the sulfidogenic activity in the aSRBR took place within a relatively shallow depth of the biofilm layer.

All of transition metals (Cu, Ni, Zn and Co) present in the synthetic AMD were effectively removed under optimised conditions, either using the off-line or in-line precipitation approaches, with the notable exception of manganese, which required an alternative approach for its removal from the effluent liquor generated by the aSRBR. This system was based on previous research carried out at Bangor University (Mariner, 2008) on the biological oxidation of soluble Mn (II) to Mn (IV) and the subsequent precipitation of solid phase Mn (IV) oxides. The fixed bed bioreactor containing Mn (IV)-coated pebbles colonised by Mn (II)-oxidizing microorganisms operating at pH 6.5 was highly effective in catalysing the removal of this metal (> 99%). However, variations in manganese removal were obtained even under optimised conditions. Addition of yeast extract in the influent liquor was able to mitigate this problem by providing energy and carbon source to the heterotroph Mn (II)-oxidizing microorganisms present in the bioreactor. Ideally, this remediation step should perform in a self-sufficient way, where no further amendments would be required to the effluent liquor generated by the aSRBR. However, pH and substrate amendment (addition of yeast extract or other organic compounds) would have to be carried out in order to optimize manganese removal. A Mn (II)-oxidizing fungus (isolate MnI1) affiliated to the order *Pleosporales* (*Ascomycota* phylum) was isolated from the surface of the colonised pebbles from the MnOB. Isolate MnI1 was able to catalyse the removal of soluble manganese in liquid media, and accumulated brown/black-coloured precipitates on its mycelium when grown on Mn-containing plates. Mineralogical analysis of the precipitates in the bioreactor or on plates were not performed, though previous work using a similar system identified the Mn (IV) mineral phase as birnessite (Mariner et al., 2008). This manganese remediating system could be applied as a final polishing step in a system for removing metals (Cu, Zn, Ni, Co and Mn) from a variety of mine waters.

The use of a single low pH anaerobic sulfidogenic bioreactor and an aerobic manganese-oxidizing bioreactor as an integrated system for remediating this synthetic mine water was successful in generating a processed water that fell within the legal discharge levels for industrial waste according to Brazilian regulations Act nº430/2011 (Industrial Effluent Discharge Act, 2011).

The metal sulfides (mainly CoS, NiS and ZnS) that accumulated in the aSRBR over a two-year period when the bioreactor was operated were subsequently re-solubilised using an oxidative (bio)leaching protocol at very low pH (1.5). The percentages of metals leached at this stage were 77% of the accumulated nickel, 61% of cobalt and 81% of zinc. Using a second phase (bio)leaching at low pH, the total percentage of metals leached increased to approximately 99% zinc, 98% nickel and 92% cobalt. Whether the bacteria introduced to accelerate sulfide mineral dissolution had any impact was not proven and appeared to be

tenuous, since they only appeared to have a transient existence in the systems (possibly being killed by the large amount of $H_2S$ generated from acid dissolution of the minerals).

The effects of using combinations of glycerol and methanol, and of glycerol and ethanol, on the performance of the aSRBR was examined, since: (i) methanol is a component (along with glycerol) of crude glycerol, and (ii) ethanol is produced in vast amounts as a fermentation product, particularly in countries like Brazil. The combined use of glycerol and methanol for sulfate reduction showed that, even though methanol was not metabolised by the microorganisms, sulfate reduction occurred at relatively high rates, and that methanol concentrations of up to 12 mM did not inhibit sulfidogenesis. In contrast, the addition of both ethanol and glycerol as electron donors in the influent liquor resulted in a progressive increase in terms of sulfate reduction rates, even when the aSRBR was being fed only with ethanol. Over 99% of the ethanol present in the feed liquor was consumed by the microbial community of the bioreactor, confirming that this alcohol was used as electron donor to fuel sulfate reduction at low pH. Major changes in terms of microorganisms present and their relative abundance occurred when methanol- and ethanol-containing feed liquors were introduced to the sulfidogenic bioreactor, including the appearance of a "new" SRB (*Desulfovibrio desulfuricans*) which was assumed to have been present in the bioreactor from the outset but only in non-detectable numbers up to that point. Overall, these results suggest the possibility of using methanol and ethanol (either alone or in combination with glycerol) as electron donors for low pH biosulfidogenesis systems used to remediate metal-rich wastewaters.

Two acidophilic micro-algae that had been isolated from mining-impacted areas were evaluated as potential providers of electron donors for biosulfidogenesis at low pH. Isolates AC1 and ITV were characterised in terms of their gross physiologies: the former was categorised as mesophilic and moderately acidophilic microalga while isolate ITV was categorised as a mesophile and an extreme acidophile. Several studies have reported the use of algal biomass and exudates as feedstock to heterotrophic microorganisms in the "natural" environment and laboratory experiments (Russel et al., 2003; Bolshoff et al., 2004; Rowe et al., 2007). This present study was based on the synthesis of organic compounds by the microalgae that could potentially be used by the aSRB. While the experiments showed that algal biomass was able to provide suitable DOC to act as electron donors for the dissimilatory reduction of sulfate to hydrogen sulfide at low pH, much lower rates of sulfide generation were obtained than when using defined organic compounds (glycerol and ethanol). Analysis of the planktonic microbial community in the aSRBR showed a major shift when the bioreactor was fed with algal biomass, with the abundance of sulfate-reducing bacteria declining dramatically

from > 75% to ~ 25%. In contrast, the relative abundance of non-sulfidogens increased to ~ 75%. Although the combined use of acidophilic algae and aSRB has the potential to be the basis of an eco-friendly engineering strategy for remediating acidic mine waters, this needs to be significantly improved and optimised to achieve greater sulfate reduction rates in mixed culture bioreactors.

The research described in this thesis provides a firm foundation for upscaling a low maintenance active bio-system that could be used to remediate mine waters and to recover valuable metals from them. Future work could include:

- Detailed characterisation of *Actinobacterium* AR3, one of the main players in the sulfidogenic bioreactor, in order to understand more fully its role in the microbial community.
- Evaluation of the effects of a shallower biofilm bed on the performance of the sulfidogenic bioreactor since it was suggested that the sulfidogenic activity in the aSRBR occurs within a relatively shallow depth of the biofilm layer.
- Further investigations of the re-solubilisation of metal sulfides that accumulate within the low pH sulfidogenic bioreactor, particularly looking at facilitating active bioleaching of these sulfides, for example using the concept of indirect bioleaching, in which ferric iron is generated by iron-oxidizing microorganisms in a separate vessel from that where the actual leaching process is occurring. In this case, exposure of the microorganisms to high concentrations of hydrogen sulfide would be avoided.
- Selective precipitation of the re-solubilised metals using techniques such as solvent extraction/electrowinning (SX/EW) and ion exchange.
- Further characterisation of the fungal isolate including sequencing and taxonomic analysis as well as optimisation of Mn (II) oxidation rates.
- Metagenomic analysis of the Mn (IV)-coated pebbles used in the Mn (II)-oxidizing bioreactor for a better understanding of the microbial population which was limited by the techniques used in this current study.
- Further analysis of the microbial community of the aSRBR when fed with ethanol in order to identify the “new” microorganisms in the bioreactor community as well as full characterisation of the SRB isolate (*Desulfovibrio desulfuricans*).
- Optimisation of sulfate reduction rates using mixed culture bioreactors fed with algal biomass, for example by growing it in media containing high concentration of salt, which would increase the contents of osmolytes that could be used by aSRB.

- Complete identification of the small molecular weight organic carbon compounds produced by the microalgae.

In conclusion, this work provided baseline data that could be used to develop pilot- and full-scale bioreactors as a more environmentally benign and cost-effective approach to remediate acid mine drainage. The design of the integrated system based on the remediation process developed for synthetic mine water draining an active copper mine in Brazil and the metal solubilisation process for recovery of the metals accumulated in the sulfidogenic bioreactor is shown in Fig. 9.1.

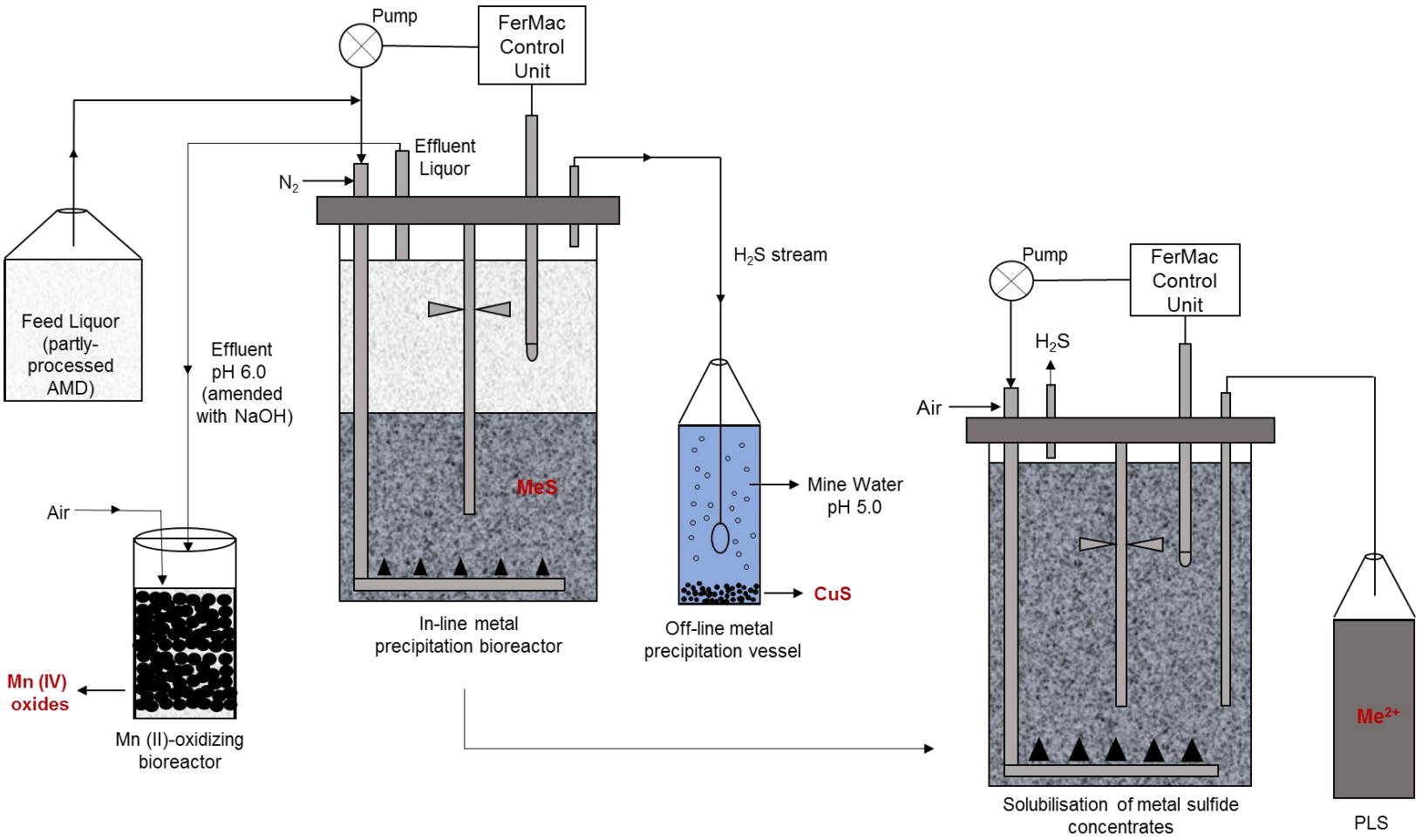


**Fig. 9.1.** Summary of the integrated system protocol developed in the current research project. The synthetic AMD remediation process involves: (a) biosulfidogenesis, as (i) off-line precipitation of copper and recovery of CuS, (ii) in-line precipitation and accumulation of most other transition metals ($Me^{2+}$) within the bioreactor, and (b) aerobic oxidation of soluble Mn (II) to Mn (IV) and precipitation of solid-phase Mn (IV) oxides. Subsequently, metal sulfides are re-solubilised, facilitating the downstream recovery of these metals.

# References


Aguilera, A., Souza-Egipsy, V., Gómez, F., Amils, R. (2007) Development and structure of eukaryotic biofilms in an extreme acidic environment, Rio Tinto (SW, Spain). *Microb. Ecol.* 53:294-305.

Akasaka, H., Ueki, A., Hanada, S., Kamagata, Y., Ueki, K. (2003) *Propionicimonas paludicola* gen. nov., sp. nov., a novel facultatively anaerobic, Gram-positive, propionate-producing bacterium isolated from plant residue in irrigated rice-field soil. *Int. J. Syst. Evol. Microbiol.* 53(6):1991-1998.

Akob, D.M., Bohu, T., Beyer, A., Schäffner, F., Händel, M., Johnson, C.A. (2014) Identification of Mn(II)-oxidizing bacteria from a low-pH contaminated former uranium mine. *Appl. Environ. Microbiol.* 80:5086–5097.

Akpor, O.B., Muchie, M. (2010) Remediation of heavy metals in drinking water and wastewater treatment systems: processes and applications. *Int. J. Phys. Sci.* 5(12):1807-1817.

Alazard, D., Joseph, M., Battaglia-Brunet F., Cayol, J.L., Ollivier, B. (2010) *Desulfosporosinus acidiphilus* sp. nov.: a moderately acidophilic sulfate-reducing bacterium isolated from acid mining drainage sediments. *Extremophiles.* 14(3):305–312.

Alico, R.K., Liegey, F.W. (1966) Growth of *Desulfovibrio desulfuricans* under heterotrophic and anaerobic conditions. *J. Bacteriol.* 91(3):1112-1114.

Alldredge, A.L., Cohen, Y. (1987) Can microscale chemical patches persist in the sea? Microelectrode study of marine snow, fecal pellets. *Science.* 235(4789):689-691.

Altschul, S.F., Gish, W., Miller, W., Myers, E.W., Lipman, D.J. (1990) Basic local alignment search tool. J. Mol. Biol. 215(3):403-410.

Amaral, Z.L.A., Gómez, F., Zettler, E., Keenan, B.G., Amils, R., Sogin, M.L. (2002) Eukaryotic diversity in Spain's River of Fire. *Nature.* 417:137.

Anwar, M.A., Iqbal, M., Qamar, M.A., Rehman, M., Khalid A.M. (2000) Technical communication: Determination of cuprous ions in bacterial leachates and for environmental monitoring. *World J. Microbiol. Biotechnol*. 16:135.

Ashe, N.L., McLean, I., Nodwell, M. (2008) Review of operations of the biosulphide process plant at the copper Queen mine, Bisbee, Arizona. In: Young, C.A., Taylor, P.R., Anderson, C.G., Choi, Y. (eds.). *Hydrometallurgy 2008: Proceedings of the 6th International Symposium on Hydrometallurgy.* Phoenix, Arizona: Society for Mining, Metallurgy and Exploration, Inc. pp. 98-107.

Auguet, J.C., Nomokonova, N., Camarero, L., Casamayor, E.O. (2011) Seasonal changes of freshwater ammonia-oxidizing archaeal assemblages and nitrogen species in oligotrophic alpine lakes. *Appl. Environ. Microbiol.* 77(6):1937-1945.

Ayora, C., Macías, F., Torres, E., Lozano, A., Carrero, S., Nieto, J.M., Pérez-López, R., Fernández-Martínez, A., Castillo-Michel H. (2016) Recovery of rare earth elements and yttrium from passive-remediation systems of acid mine drainage. *Environ. Sci. Technol.* 50:8255-8262.

Banks, D., Younger, P., Arnesen, R.T., Iversen E.R., Banks, S.B. (1997) Mine-water chemistry: the good, the bad and the ugly. *Environ. Geol.* 32:157-174.

Barnes, L.J., Janssen, F.J., Sherren, J., Versteegh, J.H., Koch, R.O., Scheeren P.J.H. (1991) A new process for the microbial removal of sulphate and heavy metals from contaminated waters extracted by a geohydrological control system. *Trans. I. Chem. E.* 69:184-186.

Bayer, B., Vojvoda, J., Offre, P., Alves, R.J., Elisabeth, N.H., Garcia, J.A., Volland, J.M., Srivastava, A., Schleper, C., Herndl, G.J. (2016) Physiological and genomic characterization of two novel marine thaumarchaeal strains indicates niche differentiation. *ISME J.* 10(5):1051-1063.

Bender, J., Gould, J.P., Vatcharapijarn, Y., Young, J.S., Phillips, P. (1994) Removal of zinc and manganese from contaminated water with cyanobacteria mats. *Water Environ. Res.* 66(5):679-683.

Ben-Dov, E., Brenner, A., Kushmaro, A. (2007) Quantification of sulfate-reducing bacteria in industrial wastewater by real-time polymerase chain reaction (PCR) using *dsr*A and *aps*A genes. *Microb. Ecol.* 54:439-451.

Bijmans, M.F.M, Dopson, M., Ennin, F., Lens, P.N., Buisman, C.J. (2008) Effect of sulfide removal on sulfate reduction at pH 5 in a hydrogen fed gas-lift bioreactor. *Microbiol. Biotechnol.* 18:1809-1818.

Bijmans, M.F.M. (2008) Sulfate reduction under acidic conditions for selective metals recovery. PhD thesis. The Netherlands: Wageningen University & Research.

Bijmans, M.F.M., de Vries, E., Yang, C.H., Buisman, C.J.N., Lens, P.N.L. (2010) Sulfate reduction at pH 4.0 for treatment of process and wastewaters. *Biotechnol Progr.* 26(4):1029-1037.

Bijmans, M.F.M., van Helvoort, P.J., Buisman, C.J.N., Lens, P.N.L. (2009) Effect of the sulfide concentration on zinc bio-precipitation in a single stage sulfidogenic bioreactor at pH 5.5. *Sep. Purif. Technol.* 69(3):243-248.

Blowes, D.W., Ptacek, C.J., Jambor, J.L., Weisener, C.G., Paktunc, D., Gould, W.D., Johnson, D.B. (2014) The Geochemistry of Acid Mine Drainage. *Treatise Geochem*. doi:10.1016/B978-0-08-095975-7.00905-0.

Bohu, T., Akob, D.M., Abratis, M., Lazar, C.S., Kusel, K. (2016) Biological low-pH Mn(II) oxidation in a manganese deposit influenced by metal-rich groundwater. *Appl. Environ. Microbiol.* 82:3009-3021.

Bohu, T., Santelli, C.M., Akob, D.M., Neu, T.R., Ciobota, V., Rosch, P., Popp, J., Nietzsche, S., Kusel, K. (2015) Characterization of pH dependent Mn(II) oxidation strategies and formation of a bixbyite-like phase by *Mesorhizobium australicum* T-G1. *Front. Microbiol.* 6:734.

Bomberg, M., Mäkinen, J., Salo, M., Arnold M. (2017) Microbial community structure and functions in ethanol-fed sulfate removal bioreactors for treatment of mine water. *Microorganisms*. doi:10.3390/microorganisms5030061.

Boogerd, F.C., de Vrind, J.P.M. (1987) Manganese oxidation by *Leptothrix discophora. J. Bacteriol.* 169(2):489-494.

Boonstra, J., van Lier, R., Janssen, G., Dijkman, H., Buisman, C.J.N. (1999) Biological treatment of acid mine drainage. *Process Metallurgy.* 9:559-567.

Borichewski, R.M. (1967) Keto acids as growth-limiting factors in autotrophic growth of *Thiobacillus thiooxidans*. *J. Bacteriol.* 93:597-599.

Bortnikova, S.B., Smolyakov, B.S., Sidenko, N.V., Kolonin, G.R., Bessonova, E.P., Androsova, N.V. (2001) Geochemical consequences of acid mine drainage into a natural reservoir: inorganic precipitation and effects on plankton activity. *J. Geochem. Explor.* 74:127-139.

Boshoff, G., Duncan, J., Rose, P.D. (2004) The use of micro-algal biomass as a carbon source for biological sulfate reducing systems. *Water Res.* 38:2659-2666.

Bostick, W.D., Overton, J.B. (1980) Modified kit procedure for the kinetic assay of ethanol. *Biotechnol. Bioeng.* 22(11):2383-2392.

Bottcher, M.E., Thamdrup, B., Gehre, M., Theune, A. (2005) S34/S32 and O18/O16 fractionation during sulphur disproportionation by *Desulfobulbus propionicus*. *J. Geomicrobiol.* 22:219–226.

Bradley, A., Leavitt, W., Johnston, D. (2011) Revisiting the dissimilatory sulfate reduction pathway. *Geobiology.* 9(5):446-457.

Braun, M., Stolp H. (1985) Degradation of methanol by a sulfate reducing bacterium. *Arch. Microbiol.* 142:77-80.

Brix, H. (1997) Do macrophytes play a role in constructed treatment wetlands?. *Water Sci. Tech.* 35(5):11-17.

Broady, P.A. (1987) The morphology, distribution and ecology of *Pseudococcomyxa simplex* (Mainx) Fott (*Chlorophyta*, *Chlorellaceae*), a widespread terrestrial Antarctic alga. *Polar Biol.* 7:25-30.

Brüser, T., Lens, P.N.L., Trüper, H.G. (2000) The biological sulfur cycle. In: Lens, P., Hulshoff-Pol, L. (eds.). *Environmental technologies to treat sulfur pollution: Principles and Engineering*. London: IWA Publishing. pp. 47-85.

Bryant, M.P., Campbell, L.L., Reddy, C.A., Crabill, M.R. (1977) Growth of *Desulfovibrio* in lactate or ethanol media low in sulfate in association with $H_2$-utilizing methanogenic bacteria. *Appl. Environ. Microbiol.* 33(5):1162-1169.

Carranza, F., Iglesias, N., Romero, R. (1993) Kinetics improvement of high-grade sulfides bioleaching by effects separations. *FEMS Microbiol. Rev.* 11:129-138.

Cavalier-Smith, T., Chao, E.E., Stechmann, A., Oates, B., Nikolaev, S. (2008) *Planomonadida* ord. nov. (Apusozoa): ultrastructural affinity with *Micronuclearia podoventralis* and deep divergences within *Planomonas* gen. nov. *Protist.* 159(4):535-562.

Celis, L.B., Villa-Gómez, D., Alpuche-Solis, A.G., Ortega-Morales, B.O., Razo-Flores, E. (2009) Characterization of sulfate-reducing bacteria dominated surface communities during start-up of a down-flow fluidized bed reactor. *J. Ind. Microbiol. Biotechnol.* 36:111-121.

Chen, T., Yana, B., Lei, C., Xiao, X. (2014) Pollution control and metal resource recovery for acid mine drainage. *Hydrometallurgy*. 147-148:112-119.

Cheng, S., Dempsey, B.A., Logan, B.E. (2007) Electricity generation from synthetic acid mine drainage (AMD) water using fuel cell technologies. *Environ. Sci. Technol.* 41(23):8149–8153.

Cheng, S., Je-Hu, J., Dempsey, B.A., Logan, B.E. (2011) Efficient recovery of nanosized iron oxide particles from synthetic acid-mine drainage (AMD) water using fuel cell technologies. *Water Res.* 45:303-307.

Chin, K., Lukow, T., Stubner, S., Conrad, R. (1999) Structure and function of the methanogenic archaeal community in stable cellulose-degrading enrichment cultures at two different temperatures (15 and 30 degrees C). *FEMS Microbiol. Ecol.* 30(4):313-326.

Chirwa, E.M.N., Molokwane, P.E. (2011) Biological Cr(VI) reduction: Microbial diversity, kinetics and biotechnological solutions to pollution. Available at https://www.intechopen.com/books/biodiversity/biological-cr-vi-reduction-microbial-diversity-

kinetics-and-biotechnological-solutions-to-pollution. Accessed July 2018.

Coci, M., Odermatt, N., Salcher, M.M., Pernthaler, J., Corno, G. (2015) Ecology and distribution of *Thaumarchaea* in the deep hypolimnion of Lake Maggiore. *Archaea.* doi: 10.1155/2015/590434.

Cravo-Laureau, C., Matheron, R., Cayol, J.L., Joulian, C., Hirschler-Réa, A. (2004) *Desulfatibacillum aliphaticivorans* gen. nov., spec. nov., and n−alkane and n−alkene−degrading, sulphate-reducing bacterium. *Int. J. Syst. Evol. Microbiol.* 54:77-83.

Cruz-Martinez, K., Suttle, K.B., Brodie, E.L., Power, M.E., Andersen, G.L., Banfield, J.F. (2009) Despite strong seasonal responses, soil microbial consortia are more resilient to long-term changes in rainfall than overlying grassland. *ISME J.* 3(6):738-744.

da Silva, G.P., Mack, M., Contiero, J. (2009) Glycerol: A promising and abundant carbon source for industrial microbiology. *Biotechnol. Adv.* 27:30-39.

Dalsgaard, T., Bak, F. (1994) Nitrate reduction in a sulfate-reducing bacterium, *Desulfovibrio desulfuricans*, isolated from rice paddy soil: sulphide inhibition, kinetics, and regulation. *Appl. Environ. Microbiol.* 60:291-297.

Das, B.K., Roy, A., Koschorreck, M., Mandal, S.M., Wendt-Potthoff, K., Bhattacharya, J. (2009) Occurrence and role of algae and fungi in acid mine drainage environment with special reference to metals and sulfate immobilization. *Water Res.* 43:883-894.

Dilling, W., Cypionka, H. (1990) Aerobic respiration in sulfate-reducing bacteria. *FEMS Microbiol Lett.* 71(112):123-128.

Dold, B. (2010) Basic concepts in environmental geochemistry of sulfidic mine-waste management. In: Sunil Kumar, E. (ed.) *Waste Management*. Croatia: InTech. pp. 173-198.

Dopson, M. (2016) Physiological and phylogenetic diversity of acidophilic bacteria. In: Quatrini, R., Johnson, D.B. (eds.). *Acidophiles: Life in extreme acidic environments*. Norfolk, UK: Caister Academic Press. pp. 79-91.

Dopson, M., Johnson, D.B. (2012) Biodiversity, metabolism and applications of acidophilic sulfur- metabolizing micro-organisms. *Environ. Microbiol*. 14:2620-2631.

Dove, P. M., De Yoreo, J. J., Weiner, S. (2003). *Biomineralization: Reviews in mineralogy and geochemistry*. Washington, DC: Mineralogical Society of America.

Duckworth, O.W., Holmström, S.J.M., Peña, J., Sposito, G. (2009) Biogeochemistry of iron oxidation in a circum-neutral freshwater habitat. *Chem. Geol.* 260(3-4):149-158.

Egiebor, N.O., Oni, B. (2007) Acid rock drainage formation and treatment: a review. *Asia Pacific J. Chem. Eng.* 2:47-62.

Ehrlich, H.L. (1996) *Geomicrobiology*. 3rd edition. New York: Marcel Dekker.

Ehrlich, H.L. (2002) *Geomicrobiology*. 4th edition. New York: Marcel Dekker.

Ehrlich, H.L., Newman, D.K. (2008) Geomicrobiology of manganese. In: Ehrlich, H.L., Newman, D.K. (eds.). Geomicrobiology. 5th edition. Boca Raton, FL: CRC Press. pp. 347–420.

El-Nadi, Y.A. (2016) Solvent extraction and its applications on ore processing and recovery of metals: classical approach. *Sep. Purif. Rev.* 46(3):195-215.

Engel, P.C., Jones, J.B. (1978) Causes and elimination of erratic blanks in enzymatic metabolite assays involving the use of $NAD^+$ in alkaline hydrazine buffers: Improved conditions for the assay of L-Glutamate, L-Lactate, and other metabolites. *Anal. Biochem.* 88:475-484.

Falagán, C. (2015) *Geomicrobiology of meromictic, metal-mine pit lakes in the Iberian Pyrite Belt and biotechnological applications*. PhD thesis. Bilbao: Universidad del País Vasco.

Falagán, C., Grail, B.M., Johnson, D.B. (2017) New approaches for extracting and recovering metals from mine tailings. *Miner. Eng.* 106:71-78.

Falagán, C., Johnson, D.B. (2016) *Acidithiobacillus ferriphilus* sp. nov., a facultatively anaerobic iron- and sulfur-metabolizing extreme acidophile. *Int. J. Syst. Evol. Microbiol.* 66:206-211.

Falagán, C., Johnson, D.B. (2018) The significance of pH in dictating the relative toxicities of chloride and copper to acidophilic bacteria. *Res. Microbiol.* doi: 10.1016/j.resmic.2018.07.004.

Falagán, C., Sánchez-Espana, J., Johnson, D.B. (2014) New insights into the biogeochemistry of extremely acidic environments revealed by a combined cultivation-based and culture-independent study of two stratified pit lakes. *FEMS Microbiol. Ecol.* 87:231-243.

Falayi, T., Ntuli, F. (2014) Removal of heavy metals and neutralisation of acid mine drainage with un-activated attapulgite. *J. Ind. Eng. Chem.* 20:1285-1292.

Fauque, G., Ollivier, B. (2004) Anaerobes: the sulfate-reducing bacteria as an example of metabolic diversity. In: Bull, A.T. (ed.) *Microbial diversity and bioprospecting*. Washington, DC: ASM Press. pp. 169-176.

Flores, R.G., Andersen, S.L.F., Maia, L.K.K., José, H.J., Moreira, R.F.P.M. (2012) Recovery of iron oxides from acid mine drainage and their application as adsorbent or catalyst. *J. Environ. Manag.* 111:53-60.

Ford, K. L. (2003) Passive treatment systems for acid mine drainage. *U.S. Bureau of Land Management Papers*. Available at http://digitalcommons.unl.edu/usblmpub/19. Accessed July 2018.

Fuentes, J.L., Huss, V.A.R., Montero, Z., Torronteras, R., Cuaresma, M., Garbayo, I., Vilchez, C. (2016) Phylogenetic characterization and morphological and physiological aspects of novel acidotolerant and halotolerant microalga *Coccomyxa onubensis* (*Chlorophyta*, *Trebouxiophyceae*). *J. Appl. Phycol.* 28:3269-3279.

Fujii, K., Kikuchi, S., Satomi, M., Ushio-Sata, N., Morita, N. (2002) Degradation of 17 beta-estradiol by a Gram-negative bacterium isolated from activated sludge in a sewage treatment plant in Tokyo, Japan. *Appl. Environ. Microbiol.* 68(4):2057-2060.

Gadd, G.M. (1993) Interactions of fungi with toxic metals. *New Phytol.* 124:25-60.

Gadd, G.M. (2010) Metals, minerals and microbes: geomicrobiology and bioremediation. *Microbiology.* 156:609-643.

Gadd, G.M., Griffiths, A.J. (1978) Microorganisms and heavy metal toxicity. *Microb. Ecol.* 4:303-317.

Galleguillos Perez, P.A. (2011) *Biodiversity and stress response of extremophilic prokaryotes isolated from the Escondida copper mine, Chile*. PhD thesis. Bangor: Bangor University.

Galleguillos, P.A., Grail, B.M., Hallberg, K.B., Demergasso, C.S., Johnson, D.B. (2018) Identification of trehalose as a compatible solute in different species of acidophilic bacteria. *J. Microbiol.* submitted.

Gammons, C.H., Seward, T.M. (1996) Stability of manganese (II) chloride complexes from 25 to 300°C. *Geochim. Cosmochim. Acta.* 60(22):4295-4311.

Gardeatorresdey, J.L., Peraltavidea, J.R., Delarosa, G.D., Parsons, J.G. (2005) Phytoremediation of heavy metals and study of the metal coordination by X-ray absorption spectroscopy. *Coordinat. Chem. Rev.* 249:1797-1810.

Geets, J., Borremans, B., Diels, L., Springael, D., Vangronsveld, J., van der Lelie, D., Vanbroekhoven, K. (2006) DsrB gene-based DGGE for community and diversity surveys of sulphate-reducing bacteria. *J. Microbiol. Methods* 66:194-205.

Golyshina, O.V., Ferrer, M., Golyshin, P.N. (2016) Diversity and physiologies of acidophilic archaea. In: Quatrini, R., Johnson, D.B. (eds.). *Acidophiles: Life in extreme acidic environments*. Norfolk, UK: Caister Academic Press. pp. 79-91.

Gray, N.F. (1996) Field assessment of acid mine drainage contamination in surface and ground water. *Environ. Geol.* 27:358-361.

Gross, S., Robbins, E.I. (2000) Acidophilic and acid-tolerant fungi and yeasts. *Hydrobiologia.* 433:91-109.

Gustavs, L., Eggert, A., Michalik, D., Karsten, U. (2010) Physiological and biochemical responses of green microalgae from different habitats to osmotic and matric stress *Protoplasma*. 243:3-14.

Gyure, R.A., Konopka, A., Brooks, A., Doemel, W. (1987). Algal and bacterial activities in acidic (pH 3) strip mine lakes. *Appl. Environ. Microbiol.* 53:2069-2076.

Gyure, R.A., Konopka, A., Brooks, A., Doemel, W. (1990) Microbial sulfate reduction in acidic (pH 3) stripmine lakes. *FEMS Microbiol. Ecol.* 73:193-202.

Halcomb, M., Fare, D. (2002) Soil pH explained. Agricultural Extension Service. The University of Tennessee. Available at http://www.utextension.utk.edu/mtnpi/handouts/Fertility/Soil_pH_Explained.pdf. Accessed June 2018.

Hallberg, K.B., Johnson, D.B. (2005) Biological manganese removal from acid mine drainage in constructed wetlands and prototype bioreactors. *Sci. Total Environ.* 338(1-2):115-124.

Hallmann, C., Hoppert, M., Mudimu, O., Friedl, T. (2016) Biodiversity of green algae covering artificial hard substrate surfaces in a suburban environment: a case study using molecular approaches. *J. Phycol.* 52:732-744.

Hamsher, S.E., Casamatta, D.A., Filkin, N.R., McClintic, A.S., Chiasson, W.B., Verb, G.R., Vis, M.L. (2003) A new method for studying nutrient limitation of *Periphyton*: a case study from acid mine drainage streams. *J. Phycol.* 38(1):15.

Hansel, C.M., Zeiner, C.A., Santelli C.M., Webb, S.M. (2012) Mn(II) oxidation by an ascomycete fungus is linked to superoxide production during asexual reproduction. *Proc. Natl. Acad. Sci.* 109(31):12621-12625.

Hard, B.C., Babel, F.W. (1997) Bioremediation of acid mine water using facultatively methylotrophic metal-tolerant sulfate-reducing bacteria. *Microbiol. Res.* 152:65-73.

Hartman, H.L., Mutmansky, J.M. (eds.) (2002) *Introductory mining engineering*. New Jersey: John Wiley and Sons, Inc.

Hedin, R.S., Watzlaf, G.R., Nairn, R.W. (1994) Passive treatment of acid mine drainage with limestone. *J. Environ. Qual.* 23:1338-1345.

Hedrich, S., Johnson, D.B. (2012) A modular continuous flow reactor system for the selective bio-oxidation of iron and precipitation of schwertmannite from mine-impacted waters. *Bioresour. Technol*. 106:44-49.

Hedrich, S., Johnson, D.B. (2014) Remediation and selective recovery of metals from acidic mine waters using novel modular bioreactors. *Environ. Sci. Technol.* 48:12206-12212.

Hussain, A., Hasan, A., Javid, A., Qazi, J.I. (2016) Exploited application of sulfate-reducing bacteria for concomitant treatment of metallic and non-metallic wastes: a mini review. *3 Biotech.* doi: 10.1007/s13205-016-0437-3.

Industrial Effluent Discharge Act 2011 (nº 430/2011) Brasília: Conselho Nacional do Meio Ambiente. Available at http://www.mma.gov.br/port/conama/legiabre.cfm?codlegi=646. Accessed Jan 2015.

Ito, T., Nielsen, J.L., Okabe, S., Watanabe, Y., Nielsen, P.H. (2002) Phylogenetic identification and substrate uptake patterns of sulfate-reducing bacteria inhabiting an oxic–anoxic sewer biofilm determined by combining microautoradiography and fluorescence in situ hybridization. *Appl. Environ. Microbiol.* 68:356-364.

Jameson, E., Rowe, O.F., Hallberg, K.B., Johnson, D.B. (2010) Sulfidogenesis and selective precipitation of metals at low pH mediated by Acidithiobacillus spp. and acidophilic sulfate-reducing bacteria. *Hydrometallurgy.* 104(3-4):488-493.

Johnson, D.B. (1995) Selective solid media for isolating and enumerating acidophilic bacteria. *J. Microbiol. Methods* 23:205-218.

Johnson, D.B. (1998) Biodiversity and ecology of acidophilic microorganisms. *FEMS Microbiol. Ecol.* 27:307-317.

Johnson, D.B. (2003) Chemical and microbiological characteristics of mineral spoils and drainage waters at abandoned coal and metal mines. *Water Air Soil Pollut.* 3:47-66.

Johnson, D.B. (2012a) Geomicrobiology of extremely acidic subsurface environments. *FEMS Microbiol. Ecol.* 81:2-12.

Johnson, D.B. (2012b) Reductive dissolution of minerals and selective recovery of metals using acidophilic iron- and sulfate-reducing acidophiles. *Hydrometallurgy* 127-128:172-177.

Johnson, D.B. (2014) Recent developments in microbiological approaches for securing mine wastes and for recovering metals from mine waters. *Minerals.* 4:279-292.

Johnson, D.B., Aguilera, A. (2015) The Microbiology of Extremely Acidic Environments. In: Yates, M., Nakatsu, C., Miller, R., Pillai, S. (eds.) *Manual of Environmental Microbiology.* 4th edition. Washington, DC: ASM Press. pp. 4.3.1-1 - 4.3.1-24.

Johnson, D.B., Hallberg, K.B. (2003) The microbiology of acidic mine waters. *Res. Microbiol.* 154:466-473.

Johnson, D.B., Hallberg, K.B. (2005) Acid mine drainage: remediation options. *Sci. Total. Environ.* 338:3-14.

Johnson, D.B., Hallberg, K.B. (2009) Carbon, iron and sulfur metabolism in acidophilic micro-organisms. *Adv. Microb. Physiol.* 54:202-256.

Johnson, D.B., Hedrich, S., Pakostova, E. (2017) Indirect redox transformations of iron, copper, and chromium catalyzed by extremely acidophilic bacteria. *Front. Microbiol*. doi: 10.3389/fmicb.2017.00211.

Johnson, D.B., Jameson, E., Rowe, O.F., Wakeman, K., Hallberg, K.B. (2009) Sulfidogenesis at low pH by acidophilic bacteria and its potential for the selective recovery of transition metals from mine waters*. Adv. Mat. Res.* 71-73:693-696.

Johnson, D.B., Kanao, T., Hedrich, S. (2012) Redox transformations of iron at extremely low pH: fundamental and applied aspects. *Front. Microbiol.* doi:10.3389/fmicb.2012.00096.

Johnson, D.B., Kelso, W.I., Jenkins, D.A. (1979) Bacterial streamer growth in a disused pyrite mine. *Environ. Pollut.* 18:107-118.

Johnson, D.B., Yajie, L., Okibe, N. (2008) “Bioshrouding” - a novel approach for securing reactive mineral tailings. *Biotechnol. Lett.* 30(3):445-449.

Jones, R.M., Hedrich, S., Johnson, D.B. (2013) *Acidocella aromatica* sp. nov.: an acidophilic heterotrophic alphaproteobacterium with unusual phenotypic traits. *Extremophiles.* 17:841−850.

Jones, R.M., Johnson, D.B. (2016) Iron Kinetics and Evolution of Microbial Populations in Low-pH, Ferrous Iron-Oxidizing Bioreactors. *Environ. Sci. Technol.* 50(15):8239–8245.

Jonkers, H.M., van der Maarel, M.J.E.C., van Gemerden, H., Hansen, T.A. (1996) Dimethylsulfoxide reduction by marine sulphate-reducing bacteria. *FEMS Microbiol. Lett.* 136-283–287.

Jung, M.Y., Park, S.J., Min, D., Kim, J.S., Rijpstra, W.I., Sinninghe-Damste, J.S., Kim, G.J., Madsen, E.L., Rhee, S.K. (2011) Enrichment and characterization of an autotrophic ammonia-oxidizing archaeon of mesophilic crenarchaeal group I.1a from an agricultural soil. *Appl. Environ. Microbiol.* 77(24):8635-8647.

Kanneby, T., Todaro, M.A., Jondelius, U. (2013) Phylogeny of *Chaetonotidae* and other *Paucitubulatina* (Gastrotricha: Chaetonotida) and the colonization of aquatic ecosystems. *Zool. Scr.* 42(1):88-105.

Kay, C.M., Rowe, O.F., Rocchetti, L., Coupland K., Hallberg K.B., Johnson D.B. (2013) Evolution of microbial “streamer” growths in an acidic metal-contaminated stream draining an abandoned underground copper mine. *Life* 3:189-211.

Kefeni, K., Msagati, T., Mamba B. (2017) Acid mine drainage: Prevention, treatment options, and resource recovery: A review. *J. Clean. Prod.* 151:475-493.

Kempf, B., Bremer, E. (1998) Uptake and synthesis of compatible solutes as microbial stress responses to high-osmolality environments. *Arch. Microbiol.* 170(5):319-30.

Khayatzadeh, J., Abbasi, E. (2010) The effects of heavy metals on aquatic animals. *The 1st International Applied Geological Congress*. Department of Geology, Islamic Azad University – Mashhad Branch, 26th - 28th April. Mashhad, Iran. Available at http://conference.khuisf.ac.ir/DorsaPax/userfiles/file/pazhohesh/zamin%20mashad/125.pdf Accessed June 2018.

Kimura, S., Hallberg, K.B., Johnson, D.B. (2006) Sulfidogenesis in low pH (3.8 – 4.2) media by a mixed population of acidophilic bacteria. *Biodegradation.* 17:57-65.

Kleinmann, R.L.P., Hedin, R.S., Nairn, R.W. (1998) Treatment of mine drainage by anoxic limestone drains and constructed wetlands. In: Geller, A., Klapper, H., Salomons, W. (eds.). *Acidic Mining Lakes: acid mine drainage, limnology and reclamation*. Berlin: Springer. pp. 303-319.

Kobayashi, K., Tachibana, S., Ishimoto, M. (1969) Intermediary formation of trithionate in sulfite reduction by a sulfate-reducing bacterium. *J. Biochem.* 65:155-157.

Koschorreck, M. Microbial sulphate reduction at a low pH. *FEMS Microbiol. Ecol.* 64:329-342.

Koschorreck, M., Wendt-Potthoff, K., Geller W. (2003) Microbial sulfate reduction at low pH in sediments of an acidic lake in Argentina. *Environ. Sci. Technol.* 37(6):1159-1162.

Krekeler, D., Cypionka, H. (1995) The preferred electron acceptor of *Desulfovibrio desulfuricans* CSN. *FEMS Microbiol. Ecol.* 17(4):271–277.

Küsel K. (2003). Microbial cycling of iron and sulfur in acidic coal mining lake sediments. *Water Air Soil Pollut.* 3(1):67-90.

Labrenz, M., Druschel, G.K., Thomsen-Ebert, T., Gilbert, B., Welch, S.A., Kemner, K.M., Logan, G.A., Summons, R.E., de Stasio, G., Bond, P.L., Lai, B., Kelly, S.D., Banfield, J.F. (2000) Formation of sphalerite (ZnS) deposits in natural biofilms of sulfate-reducing bacteria. *Science.* 290(5497):1744-1747.

Lane, D.J. (1991) 16S/23S rRNA sequencing. In: Stackebrandt E., Goodfellow M. (eds.). *Nucleic acid techniques in bacterial systematics.* Chichester: John Wiley & Sons. pp. 115-175.

Larkin, M.A., Blackshields, G., Brown, N.P., Chenna, R., McGettigan, P.A., McWilliam, H., Valentin, F., Wallace, I.M., Wilm, A., Lopez, R., Thompson, J.D., Gibson, T.J., Higgins, D.G. (2007) Clustal W and Clustal X version 2.0. *Bioinformatics*. 23(21):2947-2948.

Lens, P.N., Kuenen, J.G. (2001) The biological sulfur cycle: novel opportunities for environmental biotechnology. *Water Sci. Technol.* 44(8):57-66.

Lesaulnier, C., Papamichail, D., McCorkle, S., Ollivier, B., Skiena, S., Taghavi, S., Zak, D., van der Lelie, D. (2008) Elevated atmospheric $CO_2$ affects soil microbial diversity associated with trembling aspen. *Environ. Microbiol.* 10(4):926-941.

Lewis, A.E. (2010) Review in metal sulfides. *Hydrometallurgy.* 104:222-234.

Lewis, M.E., Clark, M.L. (1997) *How does streamflow affect metals in the upper Arkansas River?* Denver, CO: US Geological Survey. Available at https://pubs.usgs.gov/fs/1996/0226/report.pdf. Accessed July 2018.

Loubinoux, J., Mory, F., Pereira, I.A., Le Faou, A.E. (2000) Bacteremia caused by a strain of *Desulfovibrio* related to the provisionally named *Desulfovibrio fairfieldensis*. *J. Clin. Microbiol.* 38(2):931-934.

Lovley, D.R., Klug, M.J. (1983) Sulfate reducers can outcompete methanogens at freshwater sulfate concentrations. *Appl. Environ. Microbiol.* 45(1):187-192.

Macingova, E., Luptakova, A. (2012) Recovery of metals from acid mine drainage. *Chem. Eng. Trans.* 28:109-114.

Madigan, R.T. (1981) *Of minerals and man*. Parkville, Australia: Australasian Institute of Mining and Metallurgy. 138 pp.

Marchesi, J.R., Sato T., Weightman A.J., Martin T.A., Fry J.C., Hiom J., Wade W.G. (1998) Design and evaluation of useful bacterium-specidic PCR primers that amplify genes coding for bacterial 16S rRNA. *Appl. Environ. Microbiol* 64:795-799.

Mariner, R., Johnson, D.B., Hallberg, K.B. (2007) Development of a novel biological system for removing manganese from contaminated waters. *Adv. Mater. Res.* 20-21:267-270.

Mariner, R., Johnson, D.B., Hallberg, K.B. (2008) Characterisation of an attenuation system for the remediation of Mn (II) contaminated waters. *Hydrometallurgy.* 94:100-104.

Mariner, R.C. (2008) Development of a biological system for removing manganese from contaminated waters. PhD thesis. Bangor: Bangor University.

Masukume, M., Onyango, M.S., Maree J.P. (2014) Sea shell derived adsorbent and its potential for treating acid mine drainage. *Int. J. Min. Process.* 133:52-59.

Mechalas, B.J., Rittenberg, S.C. (1960) Energy coupling in *Desulfovibrio desulfuricans*. *J. Bacteriol.* 80(4):501-507.

Meybeck, M. (1982) Carbon, nitrogen, and phosphorus transport by world rivers. *Am. J. Sci.* 282:401-450.

Middelburg, J.J. (2000) The geochemical sulfur cycle. In: Lens, P., Hulshoff-Pol, L. (eds.). *Environmental technologies to treat sulfur pollution: Principles and Engineering*. London: IWA Publishing. pp. 33-46.

Miller, D.M., Dew, D.W., Norton, A.E., Cole, P.M., Benetis, G. (1997) The BioNIC process: description of the process and presentation of results. In: Cooper, W.C., Mihaylov, I. (eds.). *Proceedings of the Nickel-Cobalt 97th International Symposium*, volume I, 17th - 20th August 1997. Sudbury, Canada: The Metallurgical Society of CIM. pp. 97-110.

Mine Environment Neutral Drainage Program (MEND) (2001). Prevention and Control. Volume 4. Manual 5.4.2d. G.A. Tremblay and C.M. Hogan (eds.), CANMET.

Miyata, N., Maruo, K., Tani, Y., Tsuno, H., Seyama, H., Soma, M., Iwahori, K. (2006) Production of biogenic manganese oxides by anamorphic Ascomycete fungi isolated from streambed pebbles. *J. Geomicrobiol.* 23(2):63-73.

Miyata, N., Tani, Y., Iwahori, K., Soma, M. (2004) Enzymatic formation of manganese oxides by an *Acremonium*-like hyphomycete fungus, strain KR21-2. *FEMS Microbiol. Ecol*. 47:101-109.

Miyata, N., Tani, Y., Sakata, M., Iwahori, K. (2007) Microbial manganese oxide formation and interaction with toxic metal ions. *J. Biosci. Bioeng.* 104:1-8.

Molwantwa, J.B., Molipane, N.P., Rose, P.D. (2000) Biological sulfate reduction utilizing algal extracellular products as a carbon source. In: *WISA 2000 Biennial Conference*, Sun City, South Africa.

Monachese, M., Burton, J.P., Reid, G. (2012) Bioremediation and tolerance of humans to heavy metals through microbial processes: a potential role for probiotics?. *Appl. Environ. Microbiol.* 78(18):6397-6404.

Monhemius, A.J. (1977) Precipitation diagrams for metal hydroxides, sulfides, arsenates and phosphates. *Trans. Inst. Min. Metall*. 86:C202-C206.

Moskalyk, R.R., Alfantazi, A.M. (2002). Nickel laterite processing and electrowinning practice. *Miner. Eng.* 15(8):593–605.

Muyzer, G., Stams, A.J.M. (2008) The ecology and biotechnology of sulphate-reducing bacteria. *Nat. Rev. Microbiol.* 6:441-454.

Nagpal, S., Chuichulcherm, S., Livingston, A., Peeva, L. (2000) Ethanol Utilization by Sulfate-Reducing Bacteria: An Experimental and Modeling Study. *Biotechnol. Bioeng.* 70:532-543.

Ñancucheo, I. (2011) Acidophilic consortia involved in securing mineral wastes and remediating mine waters. PhD thesis. Bangor: Bangor University.

Ñancucheo, I., Bitencourt, J.A.P., Sahoo, P.K., Alves, J.O., Siqueira, J.O., Oliveira, G. (2017) Recent developments for remediating acidic mine waters using sulfidogenic bacteria. *BioMed Res. Int.* doi:10.1155/2017/7256582.

Ñancucheo, I., Hedrich, S., Johnson, D.B. (2012) New microbiological strategies that enable the selective recovery and recycling of metals from acid mine drainage and mine process waters. *Mineral. Mag.* 76:2683-2692.

Ñancucheo, I., Johnson, D.B. (2010) Production of glycolic acid by chemolithotrophic iron- and sulfur-oxidizing bacteria and its role in delineating and sustaining acidophilic sulfide mineral-oxidizing consortia. *Appl. Environ. Microbiol.* 76(2):461-467.

Ñancucheo, I., Johnson, D.B. (2011) Safeguarding reactive mine tailings by ecological engineering: The significance of microbial communities and interactions. *Appl. Environ. Microbiol.* 77:8201-8208.

Ñancucheo, I., Johnson, D.B. (2012a) Selective removal of transition metals from acidic mine waters by novel consortia of acidophilic sulfidogenic bacteria. *Microb. Biotechnol.* 5:34-44.

Ñancucheo, I., Johnson, D.B. (2012b) Acidophilic algae isolated from mine-impacted environments and their roles in sustaining heterotrophic acidophiles. *Front. Microbiol.* 3:1-8.

Ñancucheo, I., Johnson, D.B. (2014) Removal of sulfate from extremely acidic mine waters using low pH sulfidogenic bioreactors. *Hydrometallurgy.* 150:222-226.

Ñancucheo, I., Rowe, O. F., Hedrich, S., Johnson, D.B. (2016) Solid and liquid media for isolating and cultivating acidophilic and acid-tolerant sulfate-reducing bacteria. *FEMS Microbiol. Lett.* 363(10):1-6.

Ndlovu, S., Simate, G.S., Seepe, L., Shemi, A., Sibanda, V., van Dyk, L. (2013) The removal of $Co^{2+}$, $V^{3+}$ and $Cr^{3+}$ from waste effluents using cassava waste, South African. *J. Chem. Eng.* 18(1):1-19.

Nealson, K.H. (2006) “The manganese-oxidizing bacteria”. In: Falkow, S., Rosenberg, E., Schleifer, K.H., Stackebrandt E. (eds.). *The Prokaryotes*. New York: Springer. pp. 222-231.

Nleya, Y., Simate, G.S., Ndlovu S. (2015) Sustainability assessment of the recovery and utilisation of acid from acid mine drainage. *J. Clean. Prod.* 6959:17-27.

Nordstrom, D.K. (1982) Aqueous pyrite oxidation and the consequent formation of secondary iron minerals. In: Kittrick, J.A., Fanning, D.S. (eds.) *Acid sulfate weathering*. Madison, WI: Soil Science Society of America. pp. 37-56.

Nordstrom, D.K., Blowes, D.W. and Ptacek, C.J. (2015) Hydrogeochemistry and microbiology of mine drainage: an update. *Appl. Geochem.* 57:3-16.

Novis, P.M., Harding, J.S. (2007) Extreme acidophiles: freshwater algae associated with acid mine drainage. In: Seckbach, J. (ed.). *Algae and cyanobacteria in extreme environment*. The Netherlands: Springer. pp. 443-463.

O'Flahert, V., Colleran, E. Sulfur problems in anaerobic digestion. In: Lens, P., Hulshoff-Pol, L. (eds.). *Environmental technologies to treat sulfur pollution: Principles and Engineering*. London: IWA Publishing. pp.476-482.

Okibe, N., Gericke, M., Hallberg, K.B., Johnson, D.B. (2003) Enumeration and characterization of acidophilic microorganisms isolated from a pilot plant stirred tank bioleaching operation. *Appl. Environ. Microbiol.* 69:1936-1943.

Olds, W., Weber, P., Pizey M. (2012) Alkalinity producing covers for minimisation of acid mine drainage generation in waste rock dumps. In: Miller, H., Preuss L. (eds.) *Proceedings of the 8th Australian workshop on acid and metalliferous drainage*. pp. 253-262.

Oleoline Ltd. (2017) *Glycerine Market Report*.. Available at http://www.hbint.com/datas/media/590204fd077a6e381ef1a252/sample-quarterly-glycerine.pdf. Accessed Jan 2018.

Oliveira, T.F., Vonrhein, C., Matias, P.M., Venceslau, S.S., Pereira, .IA.C., Archer, M. (2008) The crystal structure of *Desulfovibrio vulgaris* dissimilatory sulfite reductase bound to DsrC provides novel insights into the mechanism of sulfate respiration. *J. Biol. Chem.* 28:34141-34149.

Orandi, S., Yaghubpur, A., Sahraei, H. (2007) Influence of AMD on aquatic life at Sarcheshmeh copper mine. In: *Proceedings of the 17th Goldschmidt Conference*. 19th-24th August 2007. Cologne, Germany: Cambridge Publications. pp. A742.

Otsuka, S., Suenaga, T., Vu, H.T., Ueda, H., Yokota, A., Senoo, K. (2013) *Brevifollis gellanilyticus* gen. nov., sp. nov., a gellan-gum-degrading bacterium of the phylum *Verrucomicrobia*. *Int. J. Syst. Evol. Microbiol.* 63(8):3075-3078.

Pakostova, E., Grail, B.M., Johnson, D.B. (2017) Column bioleaching of a saline, calcareous copper sulfide ore. *Solid State Phenom.* 262:7-11.

Pant, D., van Bogaert, G., Diels, L., Vanbroekhoven K. (2010) A review of the substrates used in microbial fuel cells (MFCs) for sustainable energy production. *Bioresour. Technol.* 101:1533-1543.

Passamaneck, Y.J., Schander, C., Halanych, K.M. (2004) Investigation of molluscan phylogeny using large-subunit and small-subunit nuclear rRNA sequences. *Mol. Phylogenet. Evol.* 32(1):25-38.

Peck, H.D., Legall, J. (1982) Biochemistry of dissimilatory sulphate reduction. *Philos. Trans. R. Soc. Lon. B. Biol. Sci.* 298:443-466.

Pereira L.B., Vicentini R., Ottoboni L.M.M. (2014) Changes in the bacterial community of soil from a neutral mine drainage channel. *PLOS One* 9(5):1-10.

Phillips, P., Bender, J., Simms, R., Rodriguez-Eaton, S., Britt, C. (1995) Manganese removal from acid coal-mine drainage by a pond containing green algae and microbial mat. *Water Sci. Technol.* 31:161-170.

Pinto, E., Sigaud-Kutner, T.C.S., Leitao, M.A.S., Okamoto, O.K., Morse, D., Colepicolo, P. (2003) Heavy metal-induced oxidative stress in algae. *J. Phycol.* 39:1008-1018.

Praharaj, T., Fortin, D. (2004) Indicators of microbial sulfate reduction in acidic sulfide-rich mine tailings. *J. Geomicrob.* 21:457-467.

Prasad, M.S., Kenyen, V.P., Assar, D.N. (2007) Development of SX-EW Process for Copper Recovery - An Overview. *Miner. Process. Extr. Metall. Rev.* 8(1-4):95-118.

Rastogi, G., Sani, R.K., Peyton, B.M., Moberly, J.G., Ginn, T.R. (2009) Molecular studies on the microbial diversity associated with mining-impacted Coeur d'Alene River sediments. *Microb. Ecol.* 58(1):129-139.

Rawlings, D.E., Johnson, D.B. (2007) The microbiology of biomining: development and optimization of mineral-oxidizing microbial consortia. *Microbiology.* 153:315-324.

Reed, R.H., Gadd, G.M. (1990). Metal tolerance in eukaryotic and prokaryotic algae. In: Shaw, A.J. (ed.) *Heavy Metal Tolerance in Plants: Evolutionary Aspects*. Boca Raton, Florida: CRC Press. pp. 105-118.

Rees, C. (1973) A steady-state model for sulphur isotope fractionation in bacterial reduction processes. *Geochim. Cosmochim. Acta.* 37:1141-1162.

Rehman, A., Saman, W.R.G., Nomura, N., Sato, S., Matsumura, M. (2008) Pre-treatment and utilization of raw glycerol from sunflower oil biodiesel for growth and 1,3-propanediol production by *Clostridium butyricum*. *J. Chem. Technol. Biotechnol.* 83:1072-1080.

Roberts, M.F. (2005) Organic compatible solutes of halotolerant and halophilic microorganisms. *Saline Syst.* doi:10.1186/1746-1448-1-5.

Rose, P.D., Boshoff, G.A., van Hille, R.P., Wallace, L.C.M., Dunn, K.M., Duncan, J.R. (1998) An integrated algal sulphate reducing high rate ponding process for the treatment of acid mine drainage wastewaters. *Biodegradation*. 9:247-257.

Rowe, O. F., Sánchez-España, J., Hallberg, K.B., Johnson, D.B. (2007) Microbial communities and geochemical dynamics in an extremely acidic, metal-rich stream at an abandoned sulfide mine (Huelva,Spain) underpinned by two functional primary production systems. *Environ. Microbiol.* 9:1761-1771.

Russell, R.A. Holden, P.J. Wilde, K.L. Neilan, B.A. (2003) Demonstration of the use of *Scenedesmus* and *Carteria* biomass to drive bacterial sulfate reduction by *Desulfovibrio alcoholovorans* isolated from an artificial wetland. *Hydrometallurgy.* 71(1-2):227-234.

Sáez-Navarrete, C., Zamorano, A., Ferrada, C., Rodríguez, L. (2009) Sulphate reduction and biomass growth rates for *Desulfobacterium autotrophicum* in yeast extract - Supplemented media at 38ºC. *Desalination*. 248:377-383.

Sampaio, R.M.M., Timmers, R.A., Xu, Y., Keesman, K.J., Lens, P.N.L. (2009) Selective precipitation of Cu from Zn in a pS controlled continuously stirred tank reactor. *J. Hazard. Mater.* 165:256–265.

Sánchez-Andrea, I., Sanz, J.L., Bijmans, M.F.M., Stams, A.J.M. (2014) Sulfate reduction at low pH to remediate acid mine drainage. *J. Hazard. Mater*. 269:98-109.

Sánchez-Andrea, I., Stams, A.J.M., Hedrich, S., Ñancucheo, I., Johnson, D.B. (2015) *Desulfosporosinus acididurans* sp. nov., an acidophilic sulfate-reducing bacterium isolated from acidic sediments. *Extremophiles.* 19:39-47.

Sanguanchaipaiwong, V., Leksawasdi, N. (2017) Using glycerol as a sole carbon source for *Clostridium beijerinckii* fermentation. *Energy Procedia*. 138:1105-1109.

Santelli, C.M., Pfister, D.H., Lazarus, D., Sun, L., Burgos, W.D., Hansel, C.M. (2010) Promotion of Mn(II) oxidation and remediation of coal mine drainage in passive treatment systems by diverse fungal and bacterial communities. *Appl. Environ. Microbiol.* 76:4871–4875.

Santos, A.L., Johnson, D.B. (2015) Combined recovery of copper and mitigation of pollution potential of a synthetic metal-rich stream draining a copper mine in Brazil. *Adv. Mat. Res.* 1130:606-609.

Santos, A.L., Johnson, D.B. (2017) The effects of temperature and pH on the kinetics of an acidophilic sulfidogenic bioreactor and indigenous microbial communities. *Hydrometallurgy.* 168:116-120.

Sanz, J.L., Köchling, T. (2007) Molecular biology techniques used in wastewater treatment: an overview. *Process. Biochem.* 42(2):119-133.

Saputra, S., Irisawa, T., Sakamoto, M., Kitahara, M., Sulistiani, Yulinery, T., Ohkuma, M., Dinoto, A. *Bacteroides caecigallinarum* sp. nov., isolated from caecum of an Indonesian chicken. *Int. J. Syst. Evol. Microbiol.* 65(12):4341-4346.

Sasaki, K., Konno, H., Endo, M., Takano, K. (2004) Removal of Mn(II) ions from aqueous neutral media by manganese-oxidizing fungus in the presence of carbon fiber. *Biotechnol. Bioeng.* 85(5):489-96.

Sauder, L.A., Albertsen, M., Engel, K., Schwarz, J., Nielsen, P.H., Wagner, M., Neufeld, J.D. (2017) Cultivation and characterization of *Candidatus Nitrosocosmicus exaquare*, an ammonia-oxidizing archaeon from a municipal wastewater treatment system. *ISME J.* 11(5):1142-1157.

Schippers, A., Hedrich, S., Vasters, J., Drobe, M., Sand, W., Willscher, S. (2014) Biomining: metal recovery from ores with microorganisms. *Adv. Biochem. Eng. Biotechnol.* 141:1-47.

Schnaitman, C., Lundgren, D.G. (1965) Organic compounds in the spent medium of *Ferrobacillus ferrooxidans*. *Can. J. Microbiol*. 11:23-27.

Segerer, A.H., Langworthy, T.A., Stetter, K.O. (1988) *Thermoplasma acidophilum* and *Thermoplasma volcanium* sp. nov. from solfatara fields. *Syst. Appl. Microbiol.* 10:161-171.

Sen, A.M., Johnson, D.B. (1999) Acidophilic sulphate-reducing bacteria: candidates for bioremediation of acid mine drainage. *Process Metallurgy.* 9:709-718.

Siering, P.L., Ghiorse, W.C. (1996) Phylogeny of the *Sphaerotilus-Leptothrix* group inferred from morphological comparisons, genomic fingerprinting, and 16S ribosomal DNA sequence analyses. *Int. J. Syst. Bacteriol.* 46(1):173-182.

Simate, G.S., Ndlovu, S. (2014) Acid mine drainage: Challenges and opportunities. *J. Environ. Chem. Eng.* 2(3):1785-1803.

Singh, G. (1987) Mine water quality deterioration due to acid mine drainage. *Int. J. Mine Water*. 6(1):49-61.

Singh, R., Gautam, N., Mishra, A., Gupta, R. (2011) Heavy metals and living systems: an overview. *Ind. J. Pharmacol.* 43 (3) 246-253.

Skou, E., Jacobsen, T., van der Hoeven, W., Atlung, S. (1977) On the Zinc-Chloride complex formation. *Electrochim. Acta* 22:169-174.

Skousen, J., Rose, A., Geidel, G., Foreman, J., Evans, R., Hellier, W. (1998) *Handbook of technologies for avoidance and remediation of acid mine drainage*. Morgantown, West Virginia: The National Mine Land Reclamation Centre at West Virginia University.

Smith, R.L., Buckwalter, S.P., Repert, D.A., Miller D.N. (2005) Small-scale, hydrogen-oxidizing-denitrifying bioreactor for treatment of nitrate-contaminated drinking water. *Water Res.* 39(10):2014-2023.

Sole, K.C., Mooiman, M.B., Hardwick, E. (2018) Ion exchange in hydrometallurgical processing: an overview and selected applications. *Sep. Purif. Rev.* 47(2):159-178.

Solomon F. (2008) Impacts of Metals on Aquatic Ecosystems and Human Health. Available at http://www.infomine.com/library/publications/docs/Mining.com/Apr2008c.pdf. Accessed June 2018.

Steudel, R. (2000) The chemical sulfur cycle. In: Lens, P., Hulshoff-Pol, L. (eds.). *Environmental technologies to treat sulfur pollution: Principles and Engineering*. London: IWA Publishing. pp. 1-31.

Stieglmeier, M., Klingl, A., Alves, R.J., Rittmann, S.K., Melcher, M., Leisch, N., Schleper, C. (2014) *Nitrososphaera viennensis* gen. nov., sp. nov., an aerobic and mesophilic, ammonia-oxidizing archaeon from soil and a member of the archaeal phylum *Thaumarchaeota*. *Int. J. Syst. Evol. Microbiol.* 64(8):2738-2752.

Stookey, L.L. (1970) Ferrozine - A new spectrophotometric reagent for iron. *Anal. Chem.* 42(7):779-781.

Stumm, W., Morgan, J.J. (1981) *Aquatic chemistry: An introduction emphasizing chemical equilibria in natural waters.* New York: Wiley Interscience.

Sun, M., Ru, X.R., Zhai, L.F. (2015) In-situ fabrication of supported iron oxides from synthetic acid mine drainage: high catalytic activities and good stabilities towards electro-Fenton reaction. *Appl. Catal. B. Environ.* 165:103-110.

Suzuki, D., Ueki, A., Amaishi, A., Ueki, K. (2007) Diversity of substrate utilization and growth characteristics of sulfate-reducing bacteria isolated from estuarine sediment in Japan. *J. Gen. Appl. Microbiol.* 53:119-132.

Tabak, H.H., Govind, R. (2003) Advances in biotreatment of acid mine drainage and biorecovery of metals: 2. Membrane bioreactor system for sulfate reduction. *Biodegradation.* 14(6):437-452.

Tebo, B.M., Bargar, J.R., Clement, B.G., Dick, G.J., Murray, K.J., Parker, D., Verity, R., Webb, S.M. (2004) Biogenic Manganese Oxides: Properties and Mechanisms of Formation. *Annu. Rev. Earth Planet. Sci.* 32:287-328.

Tebo, B.M., Johnson, H.A., McCarthy, J.K., Templeton, A.S. (2005) Geomicrobiology of manganese(II) oxidation. *Trends in Microbiol.* 13(9):421-428.

Tekerlekopoulou, A.G., Pavlou, S., Vayenas, D.V. (2013) Removal of ammonium, iron and manganese from potable water in biofiltration units: a review. *J. Chem. Technol. Biotechnol.* 88:751-773.

Thauer, R.K., Jungermann, K., Decker, K. (1977) Energy conservation in chemotrophic anaerobic bacteria. *Bacteriol. Rev.* 41:100-180.

Thompson, J.C., He B.B. Characterization of Crude Glycerol from Biodiesel Production from Multiple Feedstocks. *Appl. Eng. Agric.* 22(2):261-265.

Thoreau H.D. (2002) Effects of acid rain on aquatic species. Available at http://www.rst2.edu/ties/acidrain/PDF/3effects/ef6.pdf. Accessed June 2018.
Thornton, F.C. (1995) Manganese removal from water using limestone-filled tanks. *Ecol. Eng.* 4:11-18.

Todaro, M.A., Telford, M.J., Lockyer, A.E., Littlewood, D.T.J. (2006) Interrelationships of the Gastrotricha and their place among the Metazoa inferred from 18S rRNA genes. *Zool. Scr.* 35(3):251-259.

Tuttle, J.H., Dugan, P.R., Randles, C.I. (1969) Microbial sulfate reduction and its potential utility as an acid mine water pollution abatement procedure. *Appl. Microbiol.* 17(2):297-302.

Uchimiya, M., Lima, I.M., Klasson, K.T., Chang, S., Wartelle, L.H., Rodgers J.E. (2010) Immobilization of heavy metal ions (Cu II, Cd II, Ni II, and Pb II) by broiler litter-derived biochars in water and soil. *Agric. Food Chem.* 58:5538-5544.

VALE S.A. (2017). ANNUAL REPORT FORM - 20F. Rio de Janeiro. Available at http://www.vale.com/EN/investors/information-market/annual-reports/20f/20FDocs/Vale_20F_2017_i.PDF. Accessed May 2018.

Vasconcelos, Y. (2012) Microbes that mine. *Pesquisa FAPESP*. Available at revistapesquisa.fapesp.br/en/2012/10/19/microbes-that-mine/. Accessed Dec 2017.

Veloso, R.W., Glasauer, S., Mello, J.W.V., Cardoso, L.P. (2012) Comparison between two sequential extraction procedures to assess Arsenic mobility. *Annual Activity Report* 2011-2012 INTC-Acqua 1: 88-89.

Vera, M., Schippers, A., Sand, W. (2013) Progress in bioleaching: Fundamentals and mechanisms of bacterial metal sulfide oxidation - Part A. *Appl. Microbiol. Biotechnol.* 97:7529-7541.

Vinet, B. (1987) An enzymic assay for the specific determination of methanol in serum. *Clin. Chem.* 33(12):2204-2208.

Wagner, M., Loy, A., Klein, M., Lee, N., Ramsing, N.B., Stahl, D.A., Friedrich, M.W. (2005) Functional marker genes for identification of sulfate-reducing prokaryotes. *Methods Enzymol.* 397:469-489.

Watten, B.J., Sibrell, P.L., Schwartz M.F. (2005) Acid neutralization within limestone sand reactors receiving coal mine drainage. *Environ. Pollut.* 137:295-304.

Webster, G., Watt, L.C., Rinna, J., Fry, J.C., Evershed, R.P., Parkes, R.J., Weightman, A.J. (2006) A comparison of stable isotope probing of DNA and phospholipids fatty acids to study prokaryotic functional diversity in sulfate-reducing marine sediment enrichment slurries. *Environ. Microbiol.* 8:1575-1589.

Weiland, P. (2010) Biogas production: current state and perspectives. *Appl. Microbiol. Biotechnol.* 85(4):849-860.

Welsh, D.T. (2000) Ecological significance of compatible solute accumulation by micro-organisms: from single cells to global climate. *FEMS Microbiol. Rev.* 24:263-290.

Widdel, F. (1988) Microbiology and ecology of sulfate- and sulfur-reducing bacteria. In: Zehnder, A.J.B. (ed.). *Biology of Anaerobic Microorganisms*. New York: Wiley Interscience. pp. 469-586.

Yadav, S.K. (2010) Heavy metals toxicity in plants: an overview on the role of glutathione and phytochelatins in heavy metal stress tolerance of plants. *South Afr. J. Bot.* 76:167-179.

Yang, F., Hanna, M.A., Sun, R. (2012) Value-added uses for crude glycerol–a byproduct of biodiesel production. *Biotechnol. Biofuels.* doi:10.1186/1754-6834-5-13.

Yin, J., Chen, J.C., Wu, Q., Chen, G.Q. (2015) Halophiles, coming stars for industrial biotechnology. *Biotechnol. Adv.* 33:1433–1442.

Younger, P.L., Banwart, S.A. and Hedin, R.S. (2002) *Mine water: hydrology, pollution, remediation*. The Netherlands: Springer.

Zagury, G.J., Kulnieks, V.I., Neculita, C.M. (2006) Characterization and reactivity assessment of organic substrates for sulphate-reducing bacteria in acid mine drainage treatment. *Chemosphere*. 64:944-954.

Zinck, J., Fiset, J.F., Griffith, W. (2010) Stability of treatment sludge in various disposal environments: a multi-year leaching study. In: *International Mine Water Association: Mine water and Innovative thinking*. 5th-9th September 2010. Sydney, Nova Scotia: Cape Breton University. pp. 527-530.

Zou, S., Li, Q., Kong, L. (2011) Additional gene data and increased sampling give new insights into the phylogenetic relationships of *Neogastropoda*, within the caenogastropod phylogenetic framework. *Mol. Phylogenet. Evol.* 61(2):425-435.

# Appendix 1

18S rRNA gene sequences of eukaryotes characterised as part of this study.

(i) **Fungal isolate MnI1** - isolated from the surface of colonised pebbles from the Mn (II)-oxidizing bioreactor.

TGCATGTCTAAGTATAAGCAATTATACCGTGAAACTGCGAATGGCTCATTAAATCAGTTA
TCGTTTATTTGATAGTACCTTACTACTTGGATAACCGTGGTAATTCTAGAGCTAATACAT
GCTAAAAACCCCAACTTCGGGAGGGGTGTATTTATTAGATAAAAAACCAATGCCCTTCG
GGGCTCTTTGGTGATTCATGATAACTTAACGGATCGCATGGCCTTGCGCCGGCGACGG
TTCATTCAAATTTCTGCCCTATCAACTTTCGATGGTAAGGTATTGGCTTACCATGGTTTC
AACGGGTAACGGGGAATTAGGGTTCGATTCCGGAGAGGGAGCCTGAGAAACGGCTAC
CACATCCAAGGAAGGCAGCAGGCGCGCAAATTACCCAATCCCGACACGGGGAGGTAG
TGACAATAAATACTGATACAGGGCTCTTTTGGGTCTTGTAATTGGAATGAGTACAATTTA
AACCCCTTAACGAGGAACAATTGGAGGGCAAGTCTGGTGCCAGCAGCCGCGGTAATTC
CAGCTCCAATAGCGTATATTAAAGTTGTTGCAGTTAAAAAGCTCGTAGTTGAAACTTGG
GCCTGGCTGTCTGGTCCGCCTCACCGCGTGTACTGGTTCGGCCGGGCCTTTCCTTCTG
GAGAGCCTCATGCCCTTCACTGGGTGTGTTGGGGAACCAGGACTTTTACTTTGAAAAAA
TTAGAGTGTTCAAAGCAGGCCTTTGCTCGAATACGTTAGCATGGAATAATAGAATAGGA
CGTGCGATCCTATTTTGTTGGTTTCTAGGACCGCCGTAATGATTAATAGGGATAGTCGG
GGGCATCAGTATTCAATTGTCAGAGGTGAAATTCTTGGATTTATTGAAGACTAACTACTG
CGAAAGCATTTGCCAAGGATGTTTTCATTAATCAGTGAACGAAAGTTAGGGGATCGAAG
ACGATCAGATACCGTCGTAGTCTTAACCGTAAACTATGCCGACTAGGGATCGGGCGAT
GTTATTATTTTGACTCGCTCGGCACCTTACGAGAAATCAAAGTTTTTGGGTTCTGGGGG
GAGTATGGTCGCAAGGCTGAAACTTAAAGAAATTGACGGAAGGGCACCACCAGGCGTG
GAGCCTGCGGCTTAATTTGACTCAACACGGGGAAACTCACCAGGTCCAGATGAAATAA
GGATTGACAGATTGAGAGCTCTTTCTTGATTTTTCAGGTGGTGGTGCATGGCCGTTCTT
AGTTGGTGGAGTGATTTGTCTGCTTAATTGCGATAACGAACGAGACCTTAACCTGCTAA
ATAGCCAGGCTAGCTTTGGCTGGTCGCCGGCTTCTTAGAGGGACTATCGGCTCAAGCC
GATGGAAGTTTGAGGCAATAACAGGTCTGTGATGCCCTTAGATGTTCTGGGCCGCACG
CGCGCTACACTGACAGAGCCAACGAGTTCATCACCTTGGCCGGAAGGTCTGGGTAATC
TTGTTAAACTCTGTCGTGCTGGGGATAGAGCATTGCAATTATTGCTCTTCAACGAGGAA
TGCCTAGTAAGCGCATGTCATCAGCATGCGTTGATTACGTCCCTGCCCTTTGTACACAC
CGCCCGTCGCTACTACCGATTGAATGGCTCAGTGAGGCCTTCGGACTGGCTTAGGGAG
GTTGGCAACGACCACCCCGAGCCGGAAAGTTCGTCAAACTCGGTCATTAGAGAAGT

(ii) **Algal isolate AC1** – isolated from a metal mine pit lake in South-west Spain (by Dr. Carmen Falagán, Bangor University, UK).

ACCTGGTTGATCCTGCCAGTAGTCATATGCTTGTCTCAAAGATTAAGCCATGCATGTCT
AAGTATAAACTGCTTTATACTGTGAAACTGCGAATGGCTCATTAAATCAGTTATAGTTTAT
TTGATGGTACCTTGCTACTCGGATAACCGTAGTAATTCTAGAGCTAATACGTGCGTAAAT
CCCGACTTCTGGAAGGGACGTATTTATTAGATAAAAGGCCGACCGGACTCTGTCCGAC
TCGCGGTGAATCATGATAACTCCACGGATCGCATGGCCTCGTGCCGGCGATGTTTCAT
TCAAATTTCTGCCCTATCAACTTTCGACGGTAAGGTATTGGCTTACCGTGGTGGTAACG
GGTGACGGAGGATTAGGGTTCGATTCCGGAGAGGGAGCCTGAGAAACGGCTACCACA
TCCAAGGAAGGCAGCAGGCGCGCAAATTACCCAATCTTGACACAAGGAGGTAGTGACA
ATAAATAACAATACCGGGGTTTTTCAACTCTGGTAATTGGAATGAGTACAATCTAAACCC
CTTAACGAGGATCAATTGGAGGGCAAGTCTGGTGCCAGCAGCCGCGGTAATTCCAGCT
CCAATAGCGTATATTTAAGTTGTTGCAGTTAAAAAGCTCGTAGTTGGATTTCGGGCGGG
CTCGGCTGGTCCGCCTATCGGTGTGCACTGACCGAGCCCGTCTTGTTGCCGGGGACG
GGCTCCTGGGCTTAACTGTCCGGGACTCGGAGTCGGCGAGGTTACTTTGAGTAAATTA
GAGTGTTCAAAGCAGGCCTACGCTCTGAATACATTAGCATGGAATAACACGATAGGACT
CTGGCCTATCTTGTTGGTCTGTGGGACCGGAGTAATGATTAAGAGGGACAGTCGGGGGG
CATTCGTATTTCATTGTCAGAGGTGAAATTCTTGGATTTATGAAAGACGAACTACTGCGA
AAGCATTTGCCAAGGATGTTTTCATTAATCAAGAACGAAAGTTGGGGGCTCGAAGACGA
TTAGATACCGTCCTAGTCTCAACCATAAACGATGCCGACTAGGGATTGGCGGGCGTTCT
TTTGATGACCTCGCCAGCACCTTATGAGAAATCAAAGTTTTTGGGTTCCGGGGGGAGTA
TGGTCGCAAGGCTGAAACTTAAAGGAATTGACGGAAGGGCACCACCAGGCGTGGAGC
CTGCGGCTTAATTTGACTCAACACGGGAAAACTTACCAGGTCCAGACATAGTGAGGATT
GACAGATTGAGAGCTCTTTCTTGATTCTATGGGTGGTGGTGCATGGCCGTTCTTAGTTG
GTGGGTTGCCTTGTCAGGTTGATTCCGGTAACGAACGAGACCTCAGCCTGCTAACTAG
TCACGGTTGGTTTTTCCAGCCGGCCGACTTCTTAGAGGGACTATTGGCGACTAGCCAAT
GGAAGTGTGAGGCAATAACAGGTCTGTGATGCCCTTAGATGTTCTGGGCCGCACGCGC
GCTACACTGATGCAATCAACGAGCCTAGCCTTGGCCGAGAGGTCCGGGTAATCTTTGA
AACTGCATCGTGATGGGGATAGATTATTGCAATTATTAATCTTCAACGAGGAATGCCTA
GTAAGCGCGAGTCATCAGCTCGCGTT

(iii) **Algal isolate ITV** – isolated from a copper mine stream in Northern Brazil (by colleagues at the Vale Technological Institute, state of Pará, Brazil).

ACCTGGAGTCGACGACGTCACTTTGAGTAAATTAGAGTGTTCAAAGCAAGCCTACGCTC
TGAATACGTTAGCATGGAATGACACGATAGGACTCTGGCTTATCCTGTTGGTCTGTGAG
ACCGGAGTAATGATTAAGAGGGACAGTCGGGGGCATTCGTATTTCATTGTCAGAGGTG
AAATTCTTGGATTTATGAAAGACGAACTTCTGCGAAAGCATTTGCCAAGGATGTTTTCAT
TAATCAAGAACGAAAGTTGGGGGCTCGAAGACGATTAGATACCGTCCTAGTCTCAACCA
TAAACGATGCCGACTAGGGATCGGCGGGTGTTCATCAATGACCCCGCCGGCACCTTAC
GAGAAATCAAAGTCTTTGGGTTCCGGGGGGAGTATGGTCGCAAGGCTGAAACTTAAAG
GAATTGACGGAAGGGCACCACCAGGCGTGGAGCCTGCGGCTTAATTTGACTCAACACG
GGAAAACTTACCAGGTCCAGACATAGTGAGGATTGACAGATTGAAAGCTCTTTCTTGAT
TCTATGGGTGGTGGTGCATGGCCGTTCTTAGTTGGTGGGTTGCCTTGTCAGGTTGATTC
CGGTAACGAACGAGACCTCAGCCTGCTAAATAGTCGCGATCAGCTTTTGCTGGTCAGC
GTGCTTCTTAGAGGGACTATCGGCGACTAGCCGATGGAAGTGTGAGGCAATAACAGGT
CTGTGATGCCCTTAGATGTTCTGGGCCGCACGCGCGCTACACTGATGCAATCAACGAG
CCCAGCCTTGGTCGAGAGACCCGGGTAATCTTGTAAACTGCATCGTGATGGGGCTAGA
CTCTTGCAATTATTAGTCTTCAACGAGGAATGCCTAGTAAGCGCAAGTCATCAGCTTGC
GTTGATTACGTCCCTGCCCTTTGTACACACCGCCCGTCGCTCCTACCGATTGGATGTGC
TGGTGAAGCGTTCGGACTGGCTGCATGCGGTGGTTCTCCGCCGTTAGCAGCC

# Appendix 2

## List of publications and presentations

### Publications

Santos, A.L., Johnson, D.B. (2018) Design and application of a pow pH upflow biofilm sulfidogenic bioreactor for recovering transition metals from synthetic waste water at a Brazilian copper mine. *Front. Microbiol.* doi: 10.3389/fmicb.2018.02051

Santos, A.L., Johnson, D.B. (2017) The effects of temperature and pH on the kinetics of an acidophilic sulfidogenic bioreactor and indigenous microbial communities. *Hydrometallurgy* 168:116-120.

Santos, A.L., Johnson, D.B. (2017) The use of algal biomass to sustain sulfidogenic bioreactors for remediating acidic metal-rich wastewaters. *Solid State Phenom.* 262:577-581.

Santos, A.L., Johnson, D.B. (2015) Combined recovery of copper and mitigation of pollution potential of a synthetic metal-rich stream draining a copper mine in Brazil. *Adv. Mat. Res.* 1130:606-609.

### Presentations

Santos, A.L., Johnson, D.B. (2018) Characterisation of two acidophilic algal species and theirpotential to fuel biosulfidogenesis for remediating metal-rich wastewaters. 12th International Conference of Extremophiles. Ischia, Italy.

Santos, A.L., Johnson, D.B. (2018) Assessing the potential of methanol and ethanol to fuel biosulfidogenesis for remediating acidic metal-rich waste waters. 5th International Symposium on Microbial Sulfur Metabolism. Vienna, Austria.

Santos, A.L., Johnson, D.B. (2017) The use of algal biomass to sustain sulfidogenic bioreactors for remediating acidic metal-rich waste waters. 22nd International Biohydrometallurgy Symposium. Freiberg, Germany.

Santos, A.L., Johnson, D.B. (2017) Removal of Mn (II) from metal-contaminated waters as part of an integrated bioremediation process. EMG & Geomicrobiology Network: Research in Progress Meeting. Manchester, UK.

Santos, A.L., Johnson, D.B. (2016) Remediation of acidic metal-rich waste waters using sulfidogenic bioreactor sustained by algal biomass. 8th International Symposium on Biohydrometallurgy. Cornwall, UK.

Santos, A.L., Johnson, D.B. (2015) Combined Recovery of Copper and Mitigation of Pollution Potential of a Synthetic Metal-Rich Stream Draining a Copper Mine in Brazil. 21th International Biohydrometallurgy Symposium. Bali, Indonesia.

Santos, A.L., Johnson, D.B. (2015) Application of an acidophilic sulfidogenic bioreactor for combining the selective recovery of metals, amelioration of pH and partial removal of sulfate from a metal-rich stream draining a copper mine in Brazil. Society for General Microbiology. Focused Meeting: Industrial applications of metal-microbe interactions. London, UK.

Santos, A.L., Johnson, D.B. (2015) Development and application of sulfidogenic bioreactors for combined selective recovery of copper and mitigation of an acidic waste water from a copper mine in Brazil. EMG & Geomicrobiology Network: Research in Progress Meeting. Leeds, UK.